

f



Solid State Physics

Peter E. Blöchl

Caution! This is an unfinished draft version
Errors are unavoidable!

Institute of Theoretical Physics; Clausthal University of Technology;
D-38678 Clausthal Zellerfeld; Germany;
<http://www.pt.tu-clausthal.de/atp/>

© Peter Blöchl, 2000-May 9, 2012

Source: <http://orion.pt.tu-clausthal.de/atp/phix.html>

Permission to make digital or hard copies of this work or portions thereof for personal or classroom use is granted provided that copies are not made or distributed for profit or commercial advantage and that copies bear this notice and the full citation. To copy otherwise requires prior specific permission by the author.

1

¹To the title page: What is the meaning of ΦSX ? Firstly, it reads like "Physics". Secondly the symbols stand for the three main pillars of theoretical physics: "X" is the symbol for the coordinate of a particle and represents Classical Mechanics. " Φ " is the symbol for the wave function and represents Quantum Mechanics and "S" is the symbol for the Entropy and represents Statistical Physics.

Contents

1	Syllabus	7
I	Lecture notes	9
2	The covalent bond	11
2.1	Linear combination of atomic orbitals (LCAO)	11
2.2	From non-orthonormal to orthonormal basis functions	12
2.3	The two-center bond	13
2.4	Bonds and occupations	18
2.5	Three-center bond	19
2.6	Chains and rings	20
2.6.1	Chains	20
2.6.2	Rings	24
2.6.3	Exercise: eigenstates of aromatic ring systems	27
3	The use of symmetry	29
3.1	Introduction	29
3.2	Symmetry and quantum mechanics	29
3.3	Symmetry eigenstates of the hydrogen molecule	32
3.4	Symmetry eigenstates of a main group dimer	33
3.4.1	Approximate diagonalization	36
3.4.2	σ bonds and antibonds	37
3.4.3	π bonds and antibonds	38
3.5	Parameterized Hamiltonian of the main group dimer	39
3.5.1	Notion of σ , π , δ -states	39
3.5.2	Slater-Koster tables	39
3.5.3	Hopping matrix elements of Harrison	39
3.5.4	Parameterized Hamiltonian of the main group dimer	40
3.5.5	Diagonalize the sub-blocks	42
3.6	Stability of main group dimers	43
3.7	Bond types	43
3.8	Worked example: orbitals of the ethene	44
3.9	Worked example: orbitals of the methane	48
3.10	Worked example: orbitals of the allyl ion	50
3.11	Exercise: sketch orbitals	53

4	From bonds to bands	55
4.1	The Jellium model	55
4.2	Density of States	56
4.2.1	Motivation	56
4.2.2	Density of States for extended systems	58
4.2.3	Free particle density of states with mass	60
4.2.4	Free particle density of states without mass	61
4.3	Real and reciprocal lattice	62
4.3.1	Real and reciprocal lattice: One-dimensional example	62
4.3.2	Real and reciprocal lattice in three dimensions	63
4.4	Bloch Theorem	66
4.5	Reduced zone scheme	68
4.6	Bands and orbitals	70
4.7	Calculating band structures in the tight-binding model	71
5	From atoms to solids	75
5.1	The Atom	75
5.1.1	The generalized hydrogen atom	75
5.1.2	Lifting the ℓ -degeneracy: Aufbau principle	76
5.2	From atoms to ions	78
5.2.1	Ionization potential and electron affinity	78
5.2.2	Oxidation states and electron count	79
5.2.3	Transition metals	80
5.3	Prototypical density of states	81
5.4	Canonical band structures	82
5.5	Van Hove Singularities	84
5.5.1	Dimensionality	84
6	The Standard model of solid-state physics	85
7	Spin orbitals	89
8	Many-Particle wave functions	95
8.1	Mathematical Preparation: The Levi-Civita Symbol or the fully antisymmetric tensor	95
8.2	Symmetry and quantum mechanics	96
8.3	Slater determinants	98
9	The Hartree-Fock approximation	103
9.1	One-electron and two-particle operators	103
9.2	Expectation values of Slater determinants	105
9.2.1	Expectation value of a one-particle operator	105
9.2.2	Expectation value of a two-particle operator	108
9.3	Hartree energy	109
9.4	Exchange energy	110
9.5	Hartree-Fock equations	112
9.6	Hartree-Fock of the free-electron gas	114
9.7	Beyond the Hartree Fock Theory: Correlations	116

9.7.1	Left-right and in-out correlation	116
9.7.2	In-out correlation	117
9.7.3	Spin contamination	117
9.7.4	Dynamic and static correlation	117
10	Density functional theory	119
10.1	Introduction	119
10.2	Basics of density-functional theory	120
10.3	Adiabatic connection	128
10.4	Jacob's ladder of density functionals	130
10.5	X_α method	130
10.6	Benchmarks, successes and failures	136
10.7	Appendix to chapter DFT	137
10.7.1	Model exchange-correlation energy	137
10.7.2	Large-gradient limit of the enhancement factor	137
11	Electronic structure methods and the PAW method	139
11.1	Introduction	139
11.2	Augmented wave methods	141
11.3	Pseudopotentials	143
11.4	Projector augmented-wave method	146
12	Born-Oppenheimer approximation and Classical Limit	157
12.1	Separation of electronic and nuclear degrees of freedom	157
12.2	Born-Oppenheimer approximation	161
12.3	Classical approximation	162
12.3.1	Classical approximation in the Born-Oppenheimer approximation	162
12.4	Nonadiabatic correction	162
12.4.1	Derivative couplings	162
12.4.2	Crossing of Born-Oppenheimer surfaces	163
12.4.3	Landau-Zener Formula	163
12.4.4	Phase relations	166
II	Appendices	169
A	Notation for spin indices	171
B	Time-inversion symmetry	173
B.1	Schrödinger equation	173
B.2	Pauli equation	174
C	Slater determinants for parallel and antiparallel spins	177
C.0.1	Spatial symmetry for parallel and antiparallel spins	178
C.0.2	An intuitive analogy for particle with spin	180
D	Hartree-Fock of the free-electron gas	181
D.1	Exchange potential as non-local potential	181

D.2	Energy level shifts by the Exchange potential	183
E	Slater-Condon rules	187
E.1	Matrix elements between identical Slater determinants	187
E.2	Matrix element of a one-particle operator with Slater determinants differing by 1 one-particle orbital	187
E.3	Matrix element of a two-particle operator with Slater determinants differing by one one-particle orbital	188
E.4	Matrix element of a one-particle operator with Slater determinants differing by 2 one-particle orbitals	189
E.5	Matrix element of a two-particle operator with Slater determinants differing by 2 one-particle orbitals	190
E.6	Matrix elements between Slater determinants differing by more than two one-particle orbitals	190
F	Non-adiabatic effects	191
F.1	The off-diagonal terms of the first-derivative couplings $\vec{A}_{n,m,j}$	191
G	Non-crossing rule	193

Chapter 1

Syllabus

- two-center bond, three-center bond, chains and rings:
(Two-center bond demonstrates perturbation theory. Relation of degenerate levels to Jahn Teller effect, Peierls distortion and nesting. Three-center bond and non-bonding orbitals. Chains and multilayer structures. rings and periodic boundary conditions.)
- Symmetry
- Periodic boundary conditions, Density of states, Reciprocal lattice, Bloch theorem, meaning of band structures, band structures as general concept, relation to Boltzmann equation. Excitations, Quasi-particles
- Estimation of density of states for solids.
- Density functional theory
- Born-Oppenheimer approximation, Frank Condon, conical intersections. Force fields, phonons.

Part I

Lecture notes

Chapter 2

The covalent bond

Chapter 2 of P. Blöchl, Φ SX: Chemical bond

2.1 Linear combination of atomic orbitals (LCAO)

The LCAO method has been proposed first by Bloch[1]. Slater and Koster[2] showed how the matrix elements can be evaluated from a small number of parameters.

Already the states of electrons in most molecules cannot be solved exactly. The problem is related to the interaction. One approximation is to assume that the electrons are not interacting. A sound theoretical justification for this approximation is given by **density functional theory (DFT)**, which maps the interacting electrons onto non-interacting electrons in an effective potential. However, density functional theory introduces additional terms in the total energy that we will not consider at this point.

We still need to determine the electronic wave functions for a complicated potential. That is we need to solve the Schrödinger equation

$$\left[\frac{-\hbar^2}{2m_e} \vec{\nabla}^2 + v(\vec{r}) - \epsilon_n \right] \psi_n(\vec{r}) = 0$$

which, in bra-ket notation has the form

$$\left[\frac{\hat{p}^2}{2m_e} + \hat{v} - \epsilon_n \right] |\psi_n\rangle = 0 \quad (2.1)$$

with $\hat{v} = \int d^3r |\vec{r}\rangle v(\vec{r}) \langle \vec{r}|$. One way to tackle this problem is to define a basis set so that we can write the one-particle wave functions $|\psi_n\rangle$ as superposition of basis functions $|\chi_{R,\ell,m,\sigma,i}\rangle$. Let us at the moment consider the wave functions of the isolated atoms as basis functions. The index R denotes a given atomic site, ℓ is the angular momentum quantum number, m the magnetic quantum number and σ is the spin quantum number. i is the principal quantum number of the atom. In the following we will use a shorthand for the indices so that $\alpha = (R, \ell, m, \sigma, i)$. Thus we represent the one-particle wave functions as

$$|\psi_n\rangle = \sum_{\alpha} |\chi_{\alpha}\rangle c_{\alpha,n} \quad (2.2)$$

We insert the ansatz Eq. 2.2 into the Schrödinger equation Eq. 2.1, and multiply the equation from the left with $\langle \chi_{\beta}|$. This leads to a generalized eigenvalue problem¹ for matrices

$$\sum_{\alpha} (H_{\beta,\alpha} - \epsilon_n O_{\beta,\alpha}) c_{\alpha,n} = 0 \quad (2.3)$$

¹An eigenvalue problem is called generalized if it has an overlap matrix that differs from the unity matrix

where the Hamilton matrix $H_{\alpha,\beta}$ and the overlap matrix $O_{\alpha,\beta}$ are defined by

$$H_{\alpha,\beta} = \langle \chi_\alpha | \frac{\hat{p}^2}{2m_e} + \hat{v} | \chi_\beta \rangle$$

$$O_{\alpha,\beta} = \langle \chi_\alpha | \chi_\beta \rangle$$

A **generalized eigenvalue problem**, can be solved numerically using the **LAPACK** library[?]. The generalized eigenvalue problem yields the eigenvalues ϵ_n and the **eigenvectors** \vec{c}_n with elements $c_{\alpha,n}$.

The generalized eigenvalue problem does not yet determine the norm of the eigenvectors. The normalization condition is

$$\langle \psi_n | \psi_m \rangle = \sum_{\alpha,\beta} c_{\alpha,n}^* O_{\alpha,\beta} c_{\beta,m} = \delta_{n,m}$$

2.2 From non-orthonormal to orthonormal basis functions

We consider here only one orbital on each atom as, for example, in the hydrogen molecule. We will see that the concept can be generalized to most chemical bonds. The resulting eigenvalue equation is

$$\sum_{\beta=1}^2 H_{\alpha,\beta} c_{\beta,n} = \sum_{\beta=1}^2 O_{\alpha,\beta} c_{\beta,n} \epsilon_n$$

where **H** is the Hamilton matrix and **O** is called the overlap matrix. The diagonal elements are approximated by the atomic eigenvalues $\bar{\epsilon}_1$ and $\bar{\epsilon}_2$ of the two atoms and the diagonal elements of the overlap matrix are unity, if we start from normalized eigenvalues. We rename $H_{12} = t$ and $O_{12} = \Delta$ so that

$$\mathbf{H} = \begin{pmatrix} \bar{\epsilon}_1 & t \\ t^* & \bar{\epsilon}_2 \end{pmatrix} \quad \text{and} \quad \mathbf{O} = \begin{pmatrix} 1 & \Delta \\ \Delta^* & 1 \end{pmatrix} \quad (2.4)$$

The parameter t is called **hopping matrix element**.²

Approximate orthonormalization

Below, we will work with orthonormal basissets, even though the overlap is not negligible. For a non-orthonormal basis set the first step is an orthonormalization.

The Schrödinger equation $(\mathbf{H} - \epsilon_n \mathbf{O}) \vec{c}_n = 0$ can be rewritten by multiplication from the left with $\mathbf{O}^{-\frac{1}{2}}$.

$$\begin{aligned} & (\mathbf{H} - \epsilon_n \mathbf{O}) \vec{c}_n = 0 \\ \Rightarrow & \mathbf{O}^{-\frac{1}{2}} (\mathbf{H} - \epsilon_n \mathbf{O}) \underbrace{\mathbf{O}^{-\frac{1}{2}} \mathbf{O}^{\frac{1}{2}}}_{=1} \vec{c}_n = 0 \\ \Rightarrow & \left(\underbrace{\mathbf{O}^{-\frac{1}{2}} \mathbf{H} \mathbf{O}^{-\frac{1}{2}}}_{\mathbf{H}'} - \epsilon_n \right) \underbrace{\mathbf{O}^{\frac{1}{2}} \vec{c}_n}_{\vec{c}'} = 0 \end{aligned}$$

A function of an operator, such as the inverse square root, is defined via its Taylor expansion. The Taylor expansion of $f(x) = (1+x)^{-\frac{1}{2}}$ is $f(x) = 1 - \frac{1}{2}x + O(x^2)$. Thus the inverse square root of the overlap operator is

$$\begin{pmatrix} 1 & \Delta \\ \Delta^* & 1 \end{pmatrix}^{-\frac{1}{2}} = \begin{pmatrix} 1 & -\frac{1}{2}\Delta \\ -\frac{1}{2}\Delta^* & 1 \end{pmatrix} + O(|\Delta|^2)$$

²The name results from the picture of an electron hopping from site to site. This transport is larger if the hopping matrix element is larger. It is often used in the context of orthonormal orbitals.

This gives us the transformed Hamiltonian in the form

$$\mathbf{H}' = \begin{pmatrix} \bar{\epsilon}_1 - \text{Re}[\Delta^* t] & t + \Delta \frac{\bar{\epsilon}_1 + \bar{\epsilon}_2}{2} \\ t^* + \Delta^* \frac{\bar{\epsilon}_1 + \bar{\epsilon}_2}{2} & \bar{\epsilon}_2 - \text{Re}[\Delta^* t] \end{pmatrix} + O(|\Delta|^2)$$

Normally the hopping matrix element t is negative and the overlap matrix element Δ is positive. We then observe that the diagonal elements are shifted upwards in energy. This effect is called **Pauli repulsion**: If two atoms come close, their atomic orbitals overlap. When orthogonality is restored, the energy levels shift up. A simple argument goes as follows: As two atoms overlap, the electrons repel each other due to the Pauli principle. The atoms become effectively compressed. As a consequence, via Heisenberg's uncertainty principle³, the kinetic energy is increased and energy is shifted up.

Wolfsberg-Helmholtz Formula

We may use a simple empirical relation for the hopping matrix elements, namely the **Wolfsberg-Helmholtz formula**[3], which says

$$t = k \frac{\bar{\epsilon}_1 + \bar{\epsilon}_2}{2} \Delta \quad (2.5)$$

where $k \approx 1.75$ is an empirical constant. Values for k depend somewhat on the type of the bond and vary between 1.6 and 2.0. For a motivation of the Wolfsberg formula see App. ?? on p. ??.

One can now orthonormalize the orbitals. Using the Wolfsberg-Helmholtz formula Eq. 2.5 we obtain a Hamiltonian to first order in Δ which has the form

$$\mathbf{H}' = \begin{pmatrix} \bar{\epsilon}_1 & (k-1) \frac{\bar{\epsilon}_1 + \bar{\epsilon}_2}{2} \Delta \\ (k-1) \frac{\bar{\epsilon}_1 + \bar{\epsilon}_2}{2} \Delta^* & \bar{\epsilon}_2 \end{pmatrix} \quad \text{and} \quad \mathbf{O}' = \begin{pmatrix} 1 & 0 \\ 0 & 1 \end{pmatrix}$$

The derivation is given in App. ??.

The main difference to the general Hamilton matrix given in Eq. 2.4 is a renormalization of the hopping matrix element.

Complete neglect of overlap (CNO)

Since we want to approach the problem in small steps, we go back to Eq. 2.4 and ignore the off-diagonal elements of the overlap matrix. Thus, in the following we consider instead

$$\mathbf{H} = \begin{pmatrix} \bar{\epsilon}_1 & t \\ t^* & \bar{\epsilon}_2 \end{pmatrix} \quad \text{and} \quad \mathbf{O} = \begin{pmatrix} 1 & 0 \\ 0 & 1 \end{pmatrix} \quad (2.6)$$

For our discussion it is important that $t < 0$, which is usually fulfilled. This approximation is called **Complete Neglect of Overlap** (CNO).

2.3 The two-center bond

. We consider now the simple case of a system with two orbitals. The typical example is a hydrogen molecule. However the findings will be more general and will be applicable in most cases where two atoms form a bond.

The model Hamiltonian, we investigate, is

$$\mathbf{H} = \begin{pmatrix} \bar{\epsilon}_1 & t \\ t^* & \bar{\epsilon}_2 \end{pmatrix} \quad \text{and} \quad \mathbf{O} = \mathbf{1} = \begin{pmatrix} 1 & 0 \\ 0 & 1 \end{pmatrix}$$

³Heisenberg's uncertainty principle says that the variation of position and momentum is equal or larger than $\frac{1}{2}\hbar$, that is $\Delta x \Delta p \geq \frac{1}{2}\hbar$. This suggests that the momentum of a confined particle should be larger than about $p > \frac{\hbar}{2\Delta x}$. Hence the energy would be about $E_{kin} > \frac{\hbar^2}{m(2\Delta x)^2}$. This says that the kinetic energy rises with confinement.

Eigenvalues

We diagonalize the Hamiltonian by finding the zeros of the determinant of $\mathbf{H} - \epsilon \mathbf{1}$.⁴ The zero's of the characteristic polynomial determine the eigenvalues

$$0 = (\bar{\epsilon}_1 - \epsilon)(\bar{\epsilon}_2 - \epsilon) - |t|^2$$

EIGENVALUES OF THE TWO-CENTER BOND

$$\epsilon_{\pm} = \frac{\bar{\epsilon}_1 + \bar{\epsilon}_2}{2} \pm \sqrt{\left(\frac{\bar{\epsilon}_1 - \bar{\epsilon}_2}{2}\right)^2 + |t|^2} \quad (2.7)$$

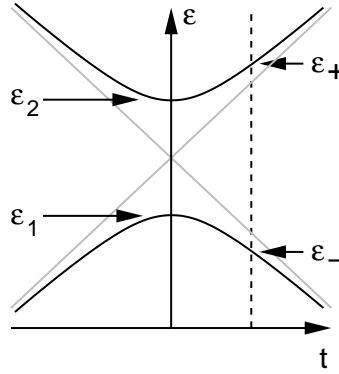


Fig. 2.1: Energy levels of the two-center bond as function of the hopping parameter t .

The result of Eq. 2.7 is shown in Fig. 2.1. If the hopping parameter t vanishes, the eigenvalues are, naturally, just the diagonal elements of the Hamiltonian, the “atomic energy levels” ϵ_1 and ϵ_2 . With increasing hopping parameter the splitting of the energy levels grows. It never becomes smaller!

- for a large hopping parameter t , i.e. for $|t| \gg |\bar{\epsilon}_2 - \bar{\epsilon}_1|$, we obtain approximately

$$\epsilon_{\pm} \approx \frac{\bar{\epsilon}_1 + \bar{\epsilon}_2}{2} \pm |t| \quad (2.8)$$

If the hopping parameter becomes much larger than the initial energy level splitting $\epsilon_2 - \epsilon_1$, the energy levels deviate approximately linearly with t from the mean value.

- for a small hopping parameter t , i.e. for $|t| \ll |\epsilon_2 - \epsilon_1|$, we obtain approximately

$$\epsilon_- \approx \bar{\epsilon}_1 - \frac{|t|^2}{|\epsilon_2 - \epsilon_1|} \quad (2.9)$$

$$\epsilon_+ \approx \bar{\epsilon}_2 + \frac{|t|^2}{|\epsilon_2 - \epsilon_1|} \quad (2.10)$$

For small t the energy levels deviate approximately quadratic with t from their $t = 0$ values. The level shift is larger if the energy levels lie close initially.

⁴The condition that the determinant vanishes, that is $\det[\mathbf{H} - \epsilon \mathbf{O}] = 0$ determines the eigenvalues of the system. We need to determine the zeroes of a polynomial of the energy. This polynomial is called the **characteristic polynomial**

Diagonalization conserves the trace

Note, that the mean value of the eigenvalues remains always the same, if basisset is orthonormal. This is a consequence of the fact that the trace of a matrix is invariant under unitary transformation.

The normalized eigenvectors \vec{c}_n of a hermitean matrix \mathbf{H} form a unitary matrix \mathbf{U} with $U_{\alpha,n} = c_{\alpha,n}$. Thus the eigenvalue equation has the form

$$\mathbf{H}\mathbf{U} = \mathbf{U}\mathbf{h}$$

where \mathbf{h} is a diagonal matrix with the eigenvalues ϵ_n on the main diagonal and \mathbf{U} is unitary, that is $\mathbf{U}\mathbf{U}^\dagger = \mathbf{1}$. Then we can show

$$\sum_{\alpha} H_{\alpha,\alpha} = \text{Tr}[\mathbf{H}] = \text{Tr}[\mathbf{H}\mathbf{U}\mathbf{U}^\dagger] = \text{Tr}[\mathbf{U}\mathbf{h}\mathbf{U}^\dagger] = \text{Tr}[\mathbf{U}^\dagger\mathbf{U}\mathbf{h}] = \text{Tr}[\mathbf{h}] = \sum_n \epsilon_n$$

which proves that the sum of eigenvalues is identical to the sum of diagonal elements of the Hamiltonian.

This statement is important because it says that the stabilizing effect of a bond is exactly canceled by the destabilizing effect of the corresponding antibond.

This statement is however only true for an orthonormal basis set. If the overlap matrix is not unity, there is the Pauli repulsion shifting the orbitals upward. The statement of the trace conservation however says that only the overlap matrix is able to shift the mean value of the energies.

Eigenvectors

The two eigenvectors \vec{c}_n with $n \in \{+, -\}$ are obtained from $(\mathbf{H} - \epsilon_n \mathbf{1})\vec{c}_n = 0$, that is alternatively from the equation

$$(\bar{\epsilon}_1 - \epsilon_{\pm})c_{1,\pm} + tc_{2,\pm} = 0 \quad (2.11)$$

or from

$$t^*c_{1,\pm} + (\bar{\epsilon}_2 - \epsilon_{\pm})c_{2,\pm} = 0 \quad (2.12)$$

Both equations lead to the same result.

In our two-dimensional case we can solve the equations simply by looking for an orthogonal vector to the coefficients⁵ and to normalize it. Because the results will have a more transparent form, we choose the second equation Eq. 2.12 for the lower, bonding eigenstate

$$c_{1,-} = \frac{\bar{\epsilon}_2 - \epsilon_-}{\sqrt{(\bar{\epsilon}_2 - \epsilon_-)^2 + |t|^2}} \quad \text{and} \quad c_{2,-} = \frac{-t^*}{\sqrt{(\bar{\epsilon}_2 - \epsilon_-)^2 + |t|^2}} \quad (2.13)$$

and the first equation Eq. 2.11 for the higher, antibonding state

$$c_{1,+} = \frac{t}{\sqrt{(\bar{\epsilon}_1 - \epsilon_+)^2 + |t|^2}} \quad \text{and} \quad c_{2,+} = \frac{-(\bar{\epsilon}_1 - \epsilon_+)}{\sqrt{(\bar{\epsilon}_1 - \epsilon_+)^2 + |t|^2}} \quad (2.14)$$

Both results can be combined into

EIGENVECTORS OF THE TWO-CENTER BOND

$$\vec{c}_- = \begin{pmatrix} 1 \\ \frac{-t^*}{\bar{\epsilon}_2 - \epsilon_-} \end{pmatrix} \left(1 + \frac{|t|^2}{(\bar{\epsilon}_2 - \epsilon_-)^2}\right)^{-\frac{1}{2}} \quad \text{and} \quad \vec{c}_+ = \begin{pmatrix} \frac{t}{\bar{\epsilon}_1 - \epsilon_+} \\ 1 \end{pmatrix} \left(1 + \frac{|t|^2}{(\bar{\epsilon}_1 - \epsilon_+)^2}\right)^{-\frac{1}{2}} \quad (2.15)$$

The eigenvalues ϵ_{\pm} are given in Eq. 2.7.

In order to make the qualitatively relevant results more evident, we distinguish the degenerate limit, i.e. $(\epsilon_2 - \epsilon_1) \ll |t|$ from the non-degenerate case $(\epsilon_2 - \epsilon_1) \gg |t|$.

⁵A complex 2-dimensional vector \vec{b} orthogonal to a vector \vec{a} can be found simply as $b_1 = a_2$ and $b_2 = -a_1$

Degenerate case

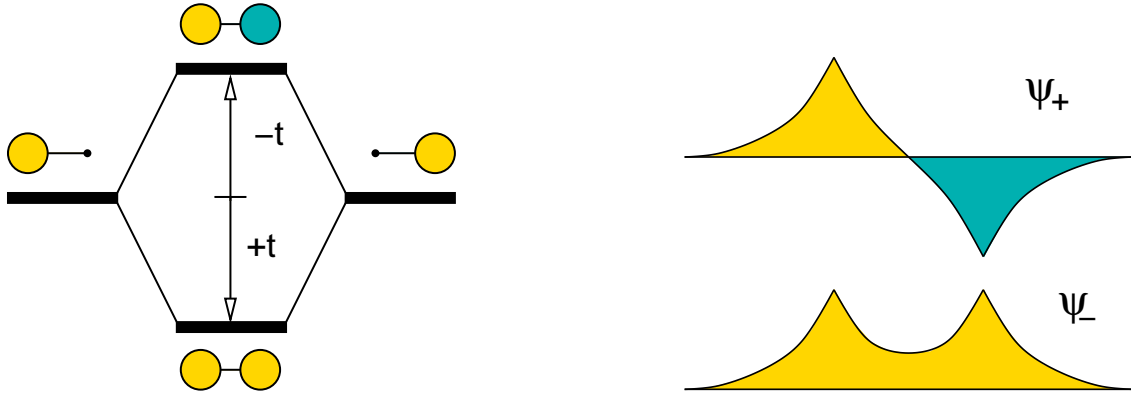
In the degenerate limit the two “atomic levels” are identical, i.e. $\bar{\epsilon}_1 = \bar{\epsilon}_2 =: \bar{\epsilon}$. The degenerate case describes the bonding of two symmetric orbitals, such as the orbitals of a hydrogen molecule.

From Eq. 2.7 we can directly determine the energy eigenvalues as

EIGENVALUES OF THE DEGENERATE TWO-CENTER BOND

$$\epsilon_{\pm} = \bar{\epsilon} \pm |t| \quad (2.16)$$

The lower wave function with energy ϵ_- is the **bonding state** and the upper wave function with energy ϵ_+ is called the **anti-bonding state**.



Let us consider the binding between two atoms with one electron each. Before the bond is formed, the atoms are far apart and the hopping matrix element t vanishes. Once the bond has formed, both electrons can move into the lower, bonding orbital. The energy gained is $2|t|$. If there are two electrons in each orbital or if there are no electrons the sum of occupied energy eigenvalues remains identical. Occupying the anti-bonding orbital (at $\bar{\epsilon} + |t|$) costs energy.

We can look up the eigenvectors from Eq. 2.15, but they are easily obtained directly⁶:

$$\begin{pmatrix} \bar{\epsilon} - \epsilon_{\pm} & t \\ t^* & \bar{\epsilon} - \epsilon_{\pm} \end{pmatrix} \begin{pmatrix} c_{1,\pm} \\ c_{2,\pm} \end{pmatrix} = \begin{pmatrix} \mp|t| & t \\ t^* & \mp|t| \end{pmatrix} \begin{pmatrix} c_{1,\pm} \\ c_{2,\pm} \end{pmatrix} = 0 \quad \Rightarrow \quad c_{2,\pm} = \pm \frac{t}{|t|} c_{1,\pm}$$

If the hopping parameter t is real and negative, we obtain the eigenstates

$$\begin{aligned} |\Psi_{-}\rangle &= (|\chi_1\rangle + |\chi_2\rangle) \frac{1}{\sqrt{2}} \\ |\Psi_{+}\rangle &= (|\chi_1\rangle - |\chi_2\rangle) \frac{1}{\sqrt{2}} \end{aligned}$$

The state $|\Psi_{-}\rangle$ with lower energy is the bonding state and the state $|\Psi_{+}\rangle$ is the anti-bonding state.

The anti-bonding wave function has one node-plane, while the bonding wave function has none. A **node plane** is that surface, where the wave function changes its sign.

The bonding wave function is stabilized, because the electron can spread over two sites: According to Heisenberg’s uncertainty principle⁷, this spreading out leads to a lower kinetic energy.⁸

⁶Personally, I prefer the direct calculation, because the steps are easier to memorize than a formula

⁷Heisenberg’s uncertainty principle says in a specialized version, that $\Delta x \Delta p \geq \frac{\hbar}{2}$.

⁸The reader may argue that the antibonding orbital is spread out over an even larger volume but has a higher

The fact that the anti-bonding wave function has a node, indicates that it has a higher kinetic energy than the bonding state. Kinetic energy can be looked upon as a measure for the mean square curvature of the wave function. This curvature becomes larger nodes are introduced.

We can now estimate the bond energy as function of the number of electrons. For each electron in the bonding orbital we gain an energy t and for each electron in the anti-bonding orbital we lose an energy t . Thus every electron in an anti-bonding orbital cancels the stabilization of an electron in the bonding orbital.

Non-degenerate case

Let us now consider the non-degenerate state. We use Eq. 2.7 with the choice $\epsilon_1 < \epsilon_2$ and truncate the Taylor expansion of the result in t after the second order. $|t|$.

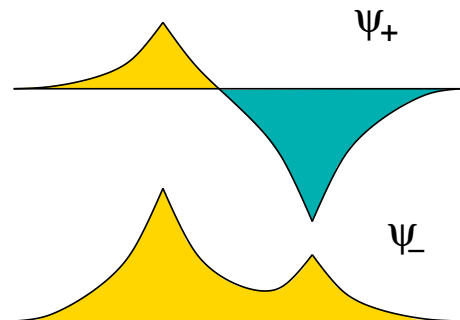
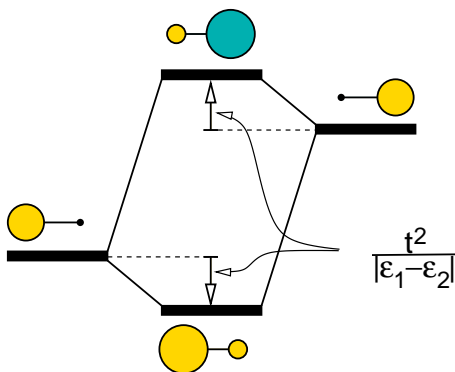
$$\epsilon_{\pm} = \frac{\bar{\epsilon}_1 + \bar{\epsilon}_2}{2} \pm \sqrt{\left(\frac{\bar{\epsilon}_2 - \bar{\epsilon}_1}{2}\right)^2 + |t|^2} = \frac{\bar{\epsilon}_1 + \bar{\epsilon}_2}{2} \pm \left[\frac{\bar{\epsilon}_2 - \bar{\epsilon}_1}{2} + \frac{|t|^2}{\bar{\epsilon}_2 - \bar{\epsilon}_1} + O(|t|^4) \right]$$

APPROXIMATE EIGENVALUES OF THE NON-DEGENERATE TWO-CENTER BOND

$$\epsilon_- = \bar{\epsilon}_1 - \frac{|t|^2}{\bar{\epsilon}_2 - \bar{\epsilon}_1} + O(|t|^4) \quad (2.17)$$

$$\epsilon_+ = \bar{\epsilon}_2 + \frac{|t|^2}{\bar{\epsilon}_2 - \bar{\epsilon}_1} + O(|t|^4) \quad (2.18)$$

If we start from one electron in each orbital, the energy gain consists of two parts. First we gain an amount $\bar{\epsilon}_2 - \bar{\epsilon}_1$ by transferring the electron from the upper orbital at $\bar{\epsilon}_2$ to the lower orbital at $\bar{\epsilon}_1$. This is the ionic contribution, because a cation and an anion are formed. Secondly the lower orbital is lowered through “hybridization” with the higher orbital and we gain $\frac{2|t|^2}{\bar{\epsilon}_2 - \bar{\epsilon}_1}$ for the electron pair. This covalent contribution becomes smaller the larger the initial energy separation. Thus if the ionic contribution is large, the covalent contribution is usually small.



The eigenvectors can be obtained from Eq. 2.15, but approximate eigenstates are easily obtained

energy. Extending the argument based on Heisenberg's uncertainty principle to antibonding states can be done, but it appears a bit artificial: Consider a particle in a box. In that case the atomic case corresponds to a box only half as large. Thus the volume for the electron becomes larger in the molecule, that is the larger box. The node-plane restricts the “effectively accessible volume”. Thus the antibonding state has higher energy. In a real molecule the electron can avoid some of this penalty by moving into a region with higher potential, but this can be considered a secondary effect.

directly by inserting the approximate eigenvalues into

$$\begin{pmatrix} \bar{\epsilon}_1 - \epsilon_{\pm} & t \\ t^* & \bar{\epsilon}_2 - \epsilon_{\pm} \end{pmatrix} \begin{pmatrix} c_{1,\pm} \\ c_{2,\pm} \end{pmatrix} = 0$$

We use the upper row for the lower eigenvalue ϵ_- and insert the approximate value from Eq. 2.18.

$$\frac{|t|^2}{\bar{\epsilon}_2 - \bar{\epsilon}_1} c_1 + t c_2 = 0 \quad \Rightarrow \quad c_2 = \frac{-t^*}{\bar{\epsilon}_2 - \bar{\epsilon}_1} c_1$$

Analogously, we obtain the eigenstate for the upper eigenvalue from the second row of the matrix equation. The normalization only enters in second order of $|t|$, and will be neglected. The result can be compared to the Taylor expansion of Eq. 2.15.

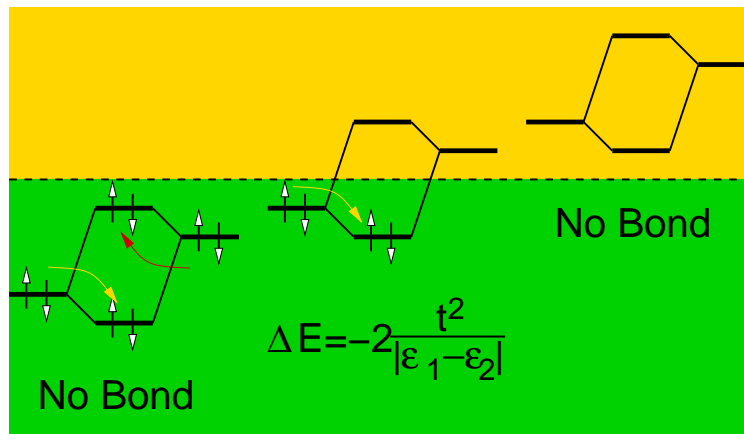
Let us now consider the eigenstates

$$\begin{aligned} |\Psi_- \rangle &\approx |\chi_1 \rangle + |\chi_2 \rangle \frac{-t^*}{\bar{\epsilon}_2 - \bar{\epsilon}_1} \\ |\Psi_+ \rangle &\approx |\chi_2 \rangle - |\chi_1 \rangle \frac{-t}{\bar{\epsilon}_2 - \bar{\epsilon}_1} \end{aligned}$$

The bonding state is mostly localized on the atom with lower energy, but both orbitals contribute with the same sign. The anti-bonding state is localized mostly on the atom with higher energy and, as in the degenerate case there is a node plane between the atoms.

2.4 Bonds and occupations

We find that the destabilization of the anti-bonding orbital is identical to the stabilization of the bonding orbital. The underlying reason can be traced to the fact that the trace of a matrix is invariant under unitary transformation. As we diagonalize the Hamiltonian, we perform a unitary transformation from the original basis set to the eigenstates of the Hamiltonian. Thus the sum of the eigenvalues is equal to the sum of the Hamilton expectation values of all basis functions. However, the observation that the stabilization of the bonding state and the destabilization of the anti-bonding state compensate each other exactly is only true for orthonormal basis sets.



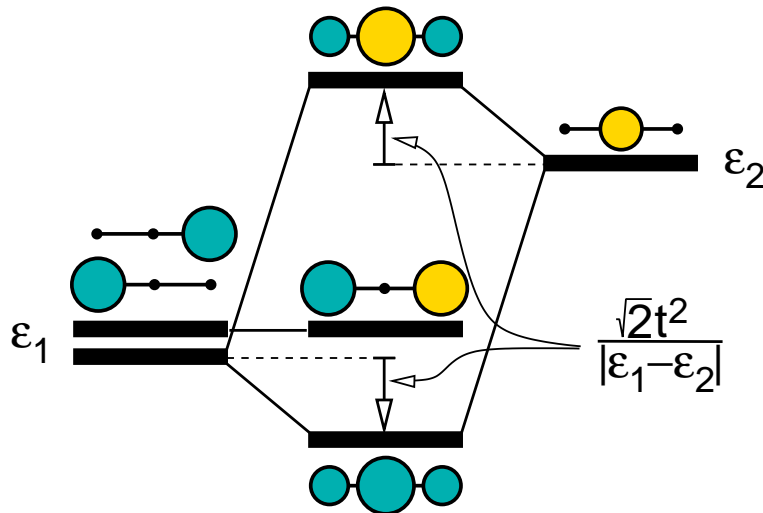
Thus we gain energy only if the orbitals are partially occupied. This statement has important consequences:

- Orbitals that lie far from the **Fermi-level** do not contribute to bonding. This explains why the role of core states to binding can be ignored. The interaction of core states from different atoms is negligible because bonding and anti-bonding orbitals are occupied.

- Molecules with unpaired electrons are very reactive because they have an orbital close to the Fermi level, that can interact with both, filled and empty, orbitals. Such molecules are called **radicals**. An example for a radical is the hydroxyl radical OH . Because radicals are so reactive they are very rare. Nevertheless they often play an important role as intermediate in chain reactions. Thus most orbitals exhibit paired electrons
- Molecules with an empty orbital just above the Fermi level are called an **electrophile**. Molecules with a filled orbital just below the Fermi level are called a **nucleophile**. An electrophile can only form a bond with a radical or a nucleophile. If two electrophile come together no bond can be formed because both orbitals are empty. If two nucleophiles come together, they cannot form a bond because a bond would result in occupied bonding as well as anti-bonding states, so that the net stabilization would vanish. The name electrophile indicates that the molecule "likes electrons", namely those of the nucleophile.
- Molecules can exhibit electrophilic and nucleophilic behavior at the same time. The electrophilic and nucleophilic orbitals are called **frontier orbitals**[4]. These are the orbitals that control the reactivity of a molecule. Usually these frontier orbitals are the **highest occupied molecular orbital (HOMO)** and the **lowest unoccupied molecular orbital (LUMO)**.
- Molecules with a large band gap between occupied and unoccupied states tend to be very stable, while molecules with orbitals near the Fermi level tend to be reactive.

2.5 Three-center bond

While most bonds can be characterized as two-center bonds, one often encounters bonds between three centers. Let us consider a central atom with two ligands on either side.



The Hamiltonian has the form

$$\mathbf{H} = \begin{pmatrix} \epsilon_1 & t & 0 \\ t^* & \epsilon_2 & t \\ 0 & t^* & \epsilon_1 \end{pmatrix}$$

The characteristic equation $\det[\mathbf{H} - \epsilon \mathbf{1}] = 0$ is

$$\begin{aligned} (\epsilon_1 - \epsilon) [(\epsilon_2 - \epsilon)(\epsilon_1 - \epsilon) - |t|^2] - t^2(\epsilon_1 - \epsilon) &= 0 \\ (\epsilon_1 - \epsilon) [(\epsilon_2 - \epsilon)(\epsilon_1 - \epsilon) - 2|t|^2] &= 0 \end{aligned}$$

We can see that there are three states: a bonding state, a non-bonding state and an anti-bonding state. Due to symmetry, the non-bonding state cannot interact with the orbital on the central atom.

The bond strength of a three-center bond is intermediate between one and two two-center bonds. The second bond contributes about one-half of a full bond.

Characteristic for a three center bond is that it maintains its full bond strength for two, three and four electrons, because the electrons enter into the non-bonding orbital, which does not contribute to the bond-strength.

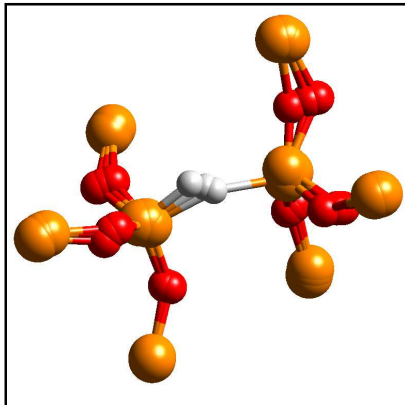


Fig. 2.2: The hydrogen complex with an oxygen vacancy in silica is responsible for stress-induced leakage currents in transistors. Because the electrons tunnel through a non-bonding orbital of the three-center bond Si-H-Si, electrons are not trapped. Red balls are oxygen atoms, yellow balls are silicon atoms and the white ball is a hydrogen atom. Structures for the three charge states $+ / 0 / -$ are superimposed. Only the relevant atoms out of the infinite crystal are shown. From [5, 6].

2.6 Chains and rings

Let us now extend our description from a three-center bond to a chain and ring structures of many atoms.

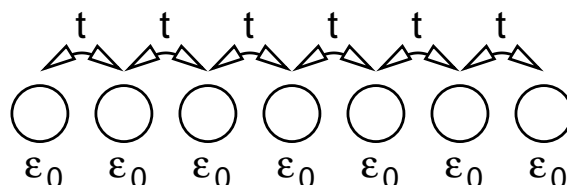
A chain is a model for a polymer, such as polyacetylene⁹ It is also a model for a finite cluster. It is also a model for a state in a semiconductor heterojunction, which is within the conduction of one material, but in the band gap of the two neighboring materials.

A ring is a model for example for aromatic molecules such as benzene.

Chains and rings will later be important for the description of solids. For the description we will use **periodic boundary conditions**, two describe an infinite crystal. In one dimension, this construction corresponds directly to a ring structure. Similarly, the chain is a one-dimensional model for a solid with surfaces.

2.6.1 Chains

We assume that all atoms are identical.



Here and in the following we assume that the hopping parameter t is a real number

⁹Polyacetylene $(CH)_n$ dimerizes. The chain may describe the π orbitals for the undimerized polyacetylene. For the dimerized system the antibonding orbitals of a dimer may play the role of one orbital in our model

The Hamiltonian of the linear chain has the following form

$$\mathbf{H} = \begin{pmatrix} \epsilon_0 & t & 0 & 0 & \cdots \\ t & \epsilon_0 & t & 0 & \cdots \\ 0 & t & \epsilon_0 & t & \cdots \\ 0 & 0 & t & \epsilon_0 & \cdots \\ \vdots & \vdots & & & \ddots \end{pmatrix} \quad \text{with } \text{Im}[t] = 0$$

The Schrödinger equation $(\mathbf{H} - \epsilon \mathbf{1})\vec{c} = 0$ can be written line-by-line as

$$(\epsilon_0 - \epsilon)c_1 + tc_2 = 0 \quad (2.19)$$

$$tc_{i-1} + (\epsilon_0 - \epsilon)c_i + tc_{i+1} = 0 \quad \text{for } 2 < i < N-1 \quad (2.20)$$

$$tc_{N-1} + (\epsilon_0 - \epsilon)c_N = 0 \quad (2.21)$$

Let us make a little detour, before we continue: Eq. 2.20 has similarities with a differential equation. Introducing a small spacing Δ , it can be written in the form

$$t\Delta^2 \underbrace{\frac{c_{i-1} - 2c_i + c_{i+1}}{\Delta^2}}_{\approx \partial_x^2 f(x)} + (\epsilon_0 + 2t)c_i - \epsilon c_i = 0$$

If we consider a function $f(x)$ with values $f(j\Delta) = c_j$, we can look at the above equation as a discretized version of the following differential equation for $f(x)$

$$[t\Delta^2 \partial_x^2 + (\epsilon_0 + 2t) - \epsilon] f(x) = 0$$

This equation is analogous to the one-dimensional Schrödinger equation for a constant potential. The solutions of this problem are plane waves, which we can exploit to find a solution for the original problem.

Dispersion relation

After this intermezzo let us continue with the equation for the orbital coefficients. The translational symmetry suggests that we use an exponential ansatz for Eq. 2.20.

$$c_j = e^{ik\Delta j} \quad (2.22)$$

We have inserted here the spacing Δ between the sites, so that the parameter k has the usual meaning and units of a wave vector.

Insertion of this ansatz into Eq. 2.20 yields

$$\begin{aligned} te^{-ik\Delta} + (\epsilon_0 - \epsilon) + te^{ik\Delta} &\stackrel{\text{Eqs. 2.20, 2.22}}{=} 0 \\ \Rightarrow 2t \cos(k\Delta) + (\epsilon_0 - \epsilon) &= 0 \\ \Rightarrow \epsilon(k) &= \epsilon_0 + 2t \cos(k\Delta) \end{aligned} \quad (2.23)$$

This is the **dispersion relation** $\epsilon(k)$ for the linear chain, shown in Fig. 2.3.

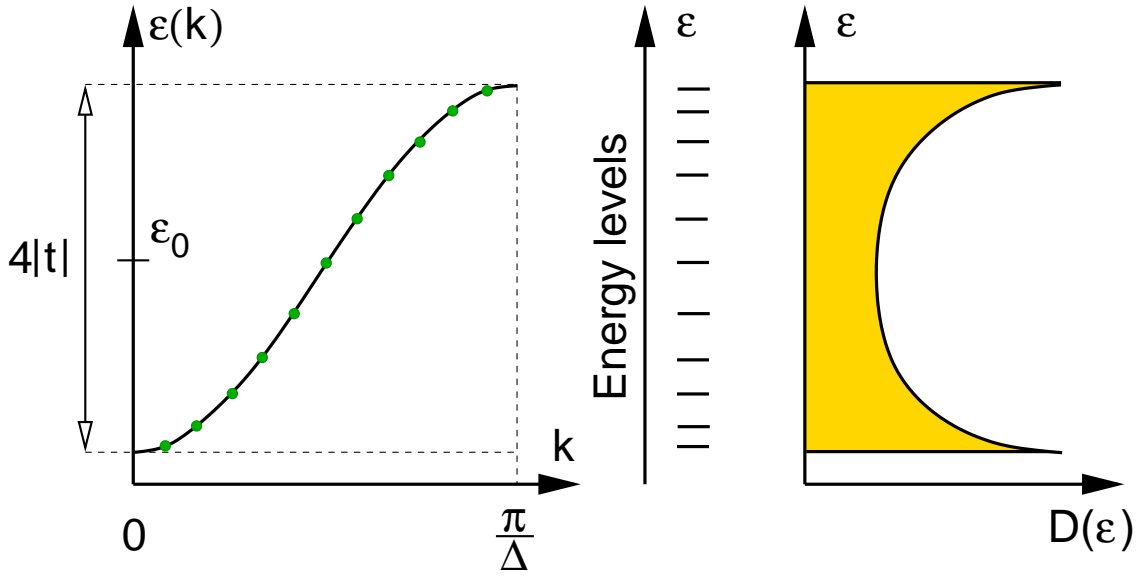


Fig. 2.3: Dispersion relation of the linear chain. The green points correspond to the energy levels of a chain with 11 atoms. In the middle figure we show the energy levels, and on the right the schematic density of states $D(\epsilon)$ for the infinite chain.

While it is common for small molecules to investigate the energy levels individually. However, for complex molecules or crystals, the energy levels are positioned so close in energy that such a representation is no more useful. Therefore one chooses a different representation, namely the **Density of States**. As the name says the density of states is the density of energy levels as function of energy. For a molecule with discrete energies, the density of states would be a sum of δ -functions, one for each energy level. For our chain, we will see below that the allowed k -values are equi-spaced on the k -axis. Using the dispersion relation $\epsilon(k)$, we can determine the spacing of energy levels on the energy axis.

$$\Delta\epsilon = \underbrace{\frac{d\epsilon}{dk}}_{v_g} \Delta k$$

which gives us the density of states as

$$D(\epsilon) = \frac{1}{\Delta\epsilon} = \left(\frac{d\epsilon}{dk} \right)^{-1} \frac{1}{\Delta k}$$

Thus the density of states of a one-dimensional system is proportional to the inverse slope of the dispersion relation. The shape of the density of states shown in Fig. 2.3 is characteristic for a one-dimensional problem. For two or three dimensional problems the density of states would not diverge at the band edges, but start with a step in two dimensions or like the square root of the energy relative to the band edge in three dimensions.

Boundary conditions

We still need to enforce the boundary conditions Eqs. 2.19, 2.21. We can bring the boundary conditions into the form of the central condition Eq. 2.20.

$$tc_{i-1} + (\epsilon_0 - \epsilon)c_i + tc_{i+1} = 0 \quad \text{for } 1 < i < N \text{ and } c_0 = c_{N+1} = 0 \quad (2.24)$$

Note that the values $i = 1$ and $i = N$ were not allowed for Eq. 2.20. I like this form, because it is now analogous to the particle-in-a-box problem. The only difference is the discrete nature of this problem.

For a given energy we obtain two linear independent solutions, which we superimpose to form a general ansatz.

$$c_j = Ae^{ik\Delta j} + Be^{-ik\Delta j} \quad (2.25)$$

The boundary conditions, now in the form $c_0 = c_{N+1} = 0$, determine the allowed values for k and $\frac{B}{A}$.

- The first boundary condition

$$0 = c_0 \stackrel{\text{Eq. 2.25}}{=} A + B \quad \Rightarrow \quad B = -A$$

restricts the Ansatz Eq. 2.25 for the wave function to pure sine functions, i.e.

$$c_j = 2iA \sin(k\Delta j) \quad (2.26)$$

- the second boundary condition

$$0 = c_{N+1} = 2iA \sin(k\Delta(N+1))$$

restricts the wave vectors k to the discrete values

$$k_n = \frac{\pi}{\Delta(N+1)} n \quad \text{for integer } n$$

Exclude trivial quantum numbers

Many solutions with different quantum number n are actually identical. This can be seen as follows: Consider the orbital coefficients in Eq. 2.27.

- periodicity of the sine function

$$\begin{aligned} \sin(k_n \Delta j) &= \sin(k_n \Delta j + 2\pi j) = \sin\left(\left[k_n + \frac{2\pi}{\Delta}\right] \Delta j\right) \stackrel{\text{Eq. 2.29}}{=} \sin\left(\left[\frac{\pi}{\Delta(N+1)} n + \frac{\pi}{\Delta(N+1)} 2(N+1)\right] \Delta j\right) \\ &= \sin\left(\frac{\pi}{\Delta(N+1)} [n + 2(N+1)]\right) = \sin(k_{n+2(N+1)} \Delta j) \end{aligned}$$

This shows that the adding $2(N+1)$ to a quantum number n does not produce a new state. Thus we can limit the quantum numbers N to the interval $-N, \dots, N+1$

- antisymmetry of the sine function

$$\sin(k_n \Delta j) = -\sin(-k_n \Delta j) \stackrel{\text{Eq. 2.29}}{=} -\sin(k_{-n} \Delta j)$$

Thus we can exclude all negative quantum numbers, that is all from $-N$ to -1 .

We are left with quantum numbers $0, 1, \dots, N+1$.

Two of the $N+2$ quantum numbers produce a wave function that is zero, namely $n = 0$ and $n = N+1$. For this reason we limit the quantum numbers to the range from 1 to N .

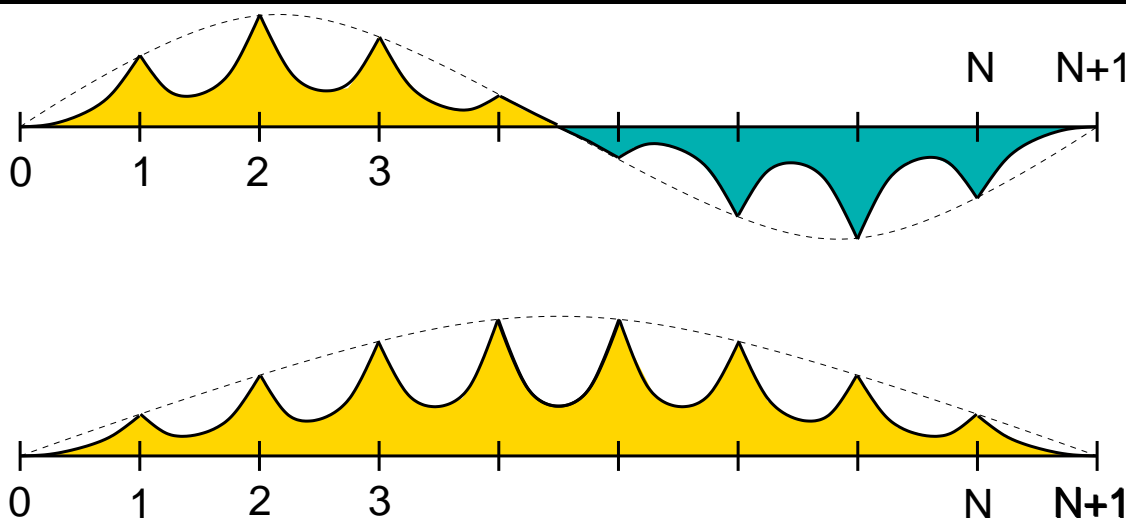
STATES OF THE LINEAR CHAIN

Thus the wave functions and energies are

$$|\psi_n\rangle = \sum_j |\chi_j\rangle \sin(k_n \Delta j) \sqrt{\frac{2}{N+1}} \quad (2.27)$$

$$\epsilon_n = \epsilon_0 + 2t \cos(k_n \Delta) \quad (2.28)$$

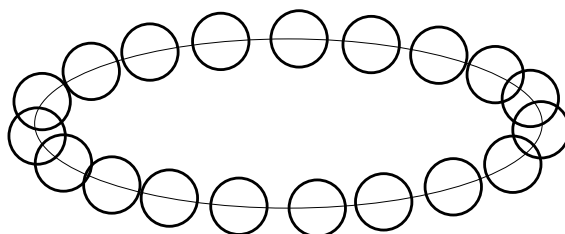
$$k_n = \frac{\pi}{\Delta(N+1)} n \quad \text{with} \quad n = 1, 2, \dots, N \quad (2.29)$$



Note that the envelope of the wave function corresponds directly to the states of a particle in a box. This is a direct consequence of the analogy of Eq. 2.20 with a particle in a constant potential discussed before.

Note that the three center bond is a simple example for a linear chain. It is instructive to compare the general results obtained here for chains with those obtained previously for the three-center bond.

2.6.2 Rings



The Hamiltonian looks very similar to that of a linear chain. The only difference is that the first atom in the ring is connected to the last one. Thus there is an addition hopping parameter in the

upper right and the lower left corner of the matrix.

$$\mathbf{H} = \begin{pmatrix} \epsilon_0 & t & 0 & 0 & \cdots & t \\ t & \epsilon_0 & t & 0 & \cdots & 0 \\ 0 & t & \epsilon_0 & t & \cdots & 0 \\ 0 & 0 & t & \epsilon_0 & \cdots & 0 \\ \vdots & \vdots & & & & \\ t & 0 & \cdots & 0 & t & \epsilon_0 \end{pmatrix}$$

Boundary conditions

In contrast to the linear chain, the ring has full translational symmetry, which is not even destroyed by the boundaries. The boundary conditions can again be expressed by the first and the last line of the Schrödinger equation. However, we can also treat the ring as an infinite chain with the requirement, that the wave function is periodic, that is $c_{N+1} = c_1$. We use the ansatz

$$c_j = e^{ik\Delta j}$$

The boundary condition $c_{N+1} = c_1$ requires that

$$\begin{aligned} c_{N+1} = e^{ik\Delta(N+1)} = c_1 = e^{ik\Delta} &\Rightarrow e^{ik\Delta N} = 1 \Rightarrow k_n \Delta N = 2\pi n \\ \Rightarrow k_n = \frac{2\pi}{N\Delta} n &\end{aligned} \quad (2.30)$$

Exclude trivial quantum numbers

Two wave functions for two quantum numbers n and n' are identical, if

$$\begin{aligned} e^{ik_n \Delta j} &= e^{ik_{n'} \Delta j} \quad \text{for all integer } j \\ \Rightarrow e^{i(k_n - k_{n'}) \Delta j} &= 1 \quad \text{for all integer } j \\ \Rightarrow k_{n'} &= k_n + \frac{2\pi}{\Delta} q \quad \text{with integer } q \\ \Rightarrow n' &= n + qN \end{aligned}$$

States with quantum numbers that differ by N are identical. Therefore we limit wave vectors k_n to the interval $]-\frac{\pi}{2}, \frac{\pi}{2}]$. Only one of the values at the boundaries may be included.

STATES OF A RING

Thus we obtain the wave functions and the energy eigenvalues as

$$\begin{aligned} |\psi_n\rangle &= \sum_j |\chi_j\rangle e^{ik_n \Delta j} \frac{1}{\sqrt{N}} \\ \epsilon_n &= \epsilon_0 + 2t \cos(k_n \Delta) \\ k_n &= \frac{2\pi}{N\Delta} n \quad \text{with} \quad n = -\frac{N}{2} + 1, \dots, \frac{N}{2} \end{aligned}$$

The resulting k -values lie in the interval $]\frac{\pi}{\Delta}, \frac{\pi}{\Delta}]$.

The spacing in k -space is approximately twice as large as in the linear chain with the same number of beads, but values with positive and negative k_n are allowed.

Each pair of degenerate wave functions can be transformed into a pair of real wave functions, of which one is a sinus and the other is a cosinus.

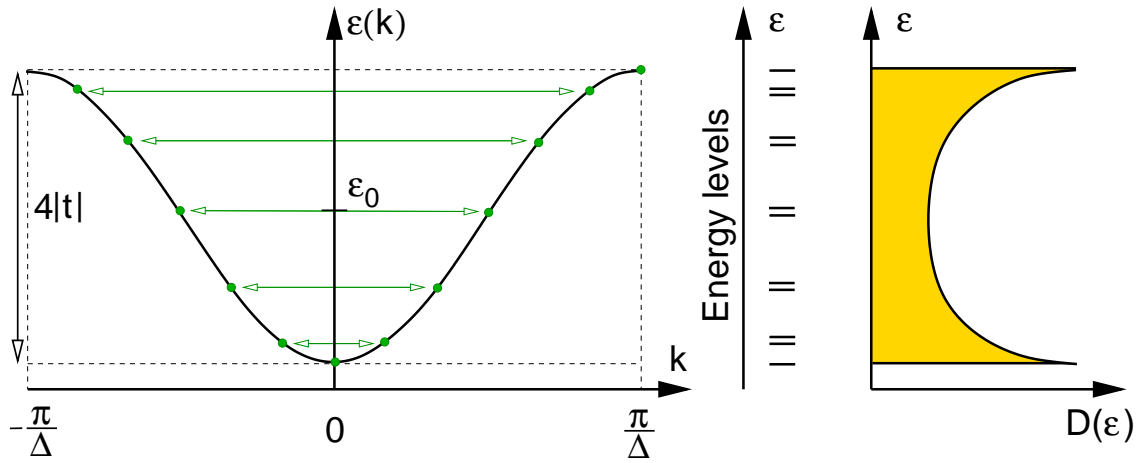


Fig. 2.4: Dispersion relation of the ring. The green points correspond to the energy levels of a ring with 14 atoms. In the middle figure we show the energy levels, and on the right the schematic density of states $D(\epsilon)$ for the infinite chain.

Geometrical construction of the eigenstates

There is an interesting and easy way to memorize construction for the energy levels of a ring. The construction is demonstrated in Fig. 2.5. If one inscribes an equilateral polygon corresponding to the ring structure into a sphere, one can easily obtain the energy levels of the ring structure as vertical position of the corners.

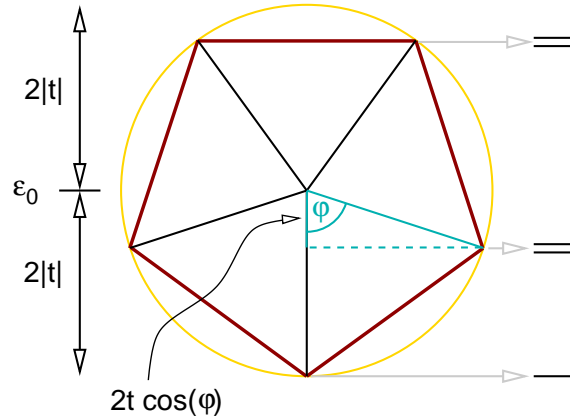


Fig. 2.5: Geometrical construction for the energy levels of a symmetric ring structure with n corners. The angles are $\phi = k_n \Delta = \frac{2\pi n}{N}$. Note that t is assumed to be negative.. With this assumption, the polygon stands on its top. The vertical position of the sphere center is at ϵ_0 , and the radius is $2|t|$. The vertical positions of the corners are at the energy level positions $\epsilon_0 + 2t \cos(k_n \Delta)$

The construction follows directly from the quantization condition

$$k_n = \frac{2\pi}{N\Delta} n \quad \text{for} \quad n = 0, 1, 2, \dots, N$$

and the dispersion relation

$$\epsilon(k) = \epsilon_0 + 2t \cos(k\Delta)$$

Let us interpret $\phi := k\Delta$ as an angle. The allowed values of the angle are $\phi_n = \frac{2\pi}{N}n$ and the allowed energy values are

$$\epsilon_n = \epsilon_0 + 2t \cos(\phi_n)$$

The cosine is the ratio of the adjacent leg¹⁰ to the hypotenuse of a rectangular triangle¹¹. Thus if the adjacent leg points from a point at height ϵ_0 straight down (because t is negative), the end point is the projection of the hypotenuse on the vertical axis. The hypotenuse shall have the length $2|t|$ and the end points lie on a circle with radius $2|t|$. Since the allowed values of the angles, are equispaced, and $\phi = 0$ is an allowed angle, the end-points of the hypotenuses form the corners of an equilateral polygon inscribed into the circle. The projection of the corners on the vertical axis gives us the allowed eigenvalues.

2.6.3 Exercise: eigenstates of aromatic ring systems

- Draw the eigenstates of the π system of p orbitals on benzene. Benzene C_6H_6 is a symmetric ring structure.
- Argue why cyclopentadiene C_5H_5 is found as an anion.

¹⁰adjacent leg is called "Ankathete" in german.

¹¹A rectangular triangle is called "rechtwinkliges Dreieck" in german

Chapter 3

The use of symmetry

Chapter 3 of P. Blöchl, Φ SX: Chemical bond

3.1 Introduction

Exploiting the symmetry allows one to break down a large eigenvalue problem into many smaller ones. The complexity of a matrix diagonalization grows with the third power of the matrix dimension. Therefore, it is much easier to diagonalize many smaller matrices than one big one, that is composed of the smaller ones. If one manages to break down the problem into ones with only one, two or three orbitals, we may use the techniques from the previous chapter to diagonalize the Hamiltonian. This often allows one to obtain an educated guess of the wave functions without much computation.

As shown below, the eigenstates of the Hamiltonian are also eigenstates of the symmetry operator, if the Hamiltonian has a certain symmetry. (For degenerate states this is not automatically so, but a transformation can bring them into the desired form.) Furthermore, we will show the following statement, which will be central to this section:

BLOCK DIAGONALIZATION BY SYMMETRY

The Hamilton matrix elements between eigenstates of a symmetry operator with different eigenvalues vanish.

In other words:

In a basis of symmetry eigenstates, the Hamiltonian is **block diagonal**. All states in a given block agree in all symmetry eigenvalues.

3.2 Symmetry and quantum mechanics

Here, I will revisit the main **symmetry** arguments discussed in Φ SX:Quantum Physics. This is a series of arguments that is good to keep in mind.

1. Definition of a **transformation operator**. An operator \hat{S} can be called a transformation, if it conserves the norm for every state.

$$\forall_{|\psi\rangle} \quad \langle\psi|\psi\rangle \stackrel{|\phi\rangle=\hat{S}|\psi\rangle}{=} \langle\phi|\phi\rangle \quad (3.1)$$

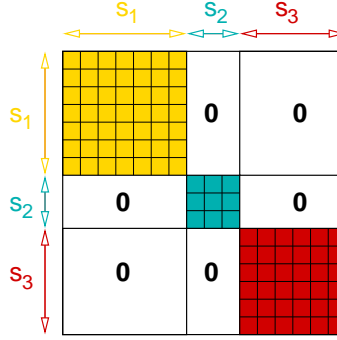


Fig. 3.1: Block form of a Hamiltonian by using symmetry eigenstates with symmetry eigenvalues s_1, s_2, s_3 .

2. Every transformation operator is unitary, that is $\hat{S}^\dagger \hat{S} = 1$

$$\forall_{|\psi\rangle} \quad \langle \psi | \hat{S}^\dagger \hat{S} | \psi \rangle = \langle \psi | \psi \rangle \quad \Rightarrow \quad \hat{S}^\dagger \hat{S} = 1 \quad (3.2)$$

3. Definition of a **symmetry**: A system is symmetric under the transformation \hat{S} , if, for any solution $|\Psi\rangle$ of the Schrödinger equation describing that system, also $\hat{S}|\Psi\rangle$ is a solution of the same Schrödinger equation. That is, if

$$\left(i\hbar \partial_t |\Psi\rangle = \hat{H} |\Psi\rangle \right) \xrightarrow{|\Phi\rangle := \hat{S} |\Psi\rangle} \left(i\hbar \partial_t |\Phi\rangle = \hat{H} |\Phi\rangle \right) \quad (3.3)$$

4. A unitary operator \hat{S} is a symmetry operator of the system, if

$$[\hat{H}, \hat{S}]_- = 0 \quad (3.4)$$

Proof: Let $|\Psi\rangle$ be a solution of the Schrödinger equation and let $|\Phi\rangle = \hat{S}|\Psi\rangle$ be the result of a symmetry transformation.

$$\begin{aligned} i\hbar \partial_t |\Phi\rangle &= \hat{H} |\Phi\rangle \\ |\Phi\rangle &\stackrel{|\Phi\rangle := \hat{S} |\Psi\rangle}{\Rightarrow} i\hbar \partial_t \hat{S} |\Psi\rangle = \hat{H} \hat{S} |\Psi\rangle \\ \partial_t \hat{S} &\stackrel{\partial_t \hat{S} = 0}{\Rightarrow} i\hbar \partial_t |\Psi\rangle = \hat{S}^{-1} \hat{H} \hat{S} |\Psi\rangle \\ i\hbar \partial_t |\Psi\rangle &\stackrel{i\hbar \partial_t |\Psi\rangle = \hat{H} |\Psi\rangle}{\Rightarrow} \hat{H} |\Psi\rangle = \hat{S}^{-1} \hat{H} \hat{S} |\Psi\rangle \\ \underbrace{(\hat{H} \hat{S} - \hat{S} \hat{H})}_{[\hat{H}, \hat{S}]_-} |\Psi\rangle &= 0 \end{aligned}$$

Because this equation holds for any solution of the Schrödinger equation, it holds for any wave function, because any function can be written as superposition of solutions of the Schrödinger equation. (The latter form a complete set of functions.) Therefore

$$[\hat{H}, \hat{S}]_- = 0$$

Thus, one usually identifies a symmetry by working out the commutator with the Hamiltonian.

5. The matrix elements of the Hamilton operator between two eigenstates of the symmetry operator with different eigenvalues vanish. That is

$$\left(\hat{S} |\Psi_s\rangle = |\Psi_s\rangle s \quad \wedge \quad \hat{S} |\Psi_{s'}\rangle = |\Psi_{s'}\rangle s' \quad \wedge \quad s \neq s' \right) \Rightarrow \langle \Psi_s | \hat{H} | \Psi_{s'} \rangle = 0 \quad (3.5)$$

Proof: In the following we will need an expression for $\langle \psi_s | \hat{S}$, which we will work out first:

- We start showing that the absolute value of an eigenvalue of a unitary operator is equal to one, that is $s = e^{i\phi}$ where ϕ is real. With an eigenstate $|\psi_s\rangle$ of \hat{S} with eigenvalue s , we obtain

$$s^* \langle \psi_s | \psi_s \rangle s \stackrel{\hat{S}|\psi_s\rangle = |\psi_s\rangle s}{=} \langle \hat{S}\psi_s | \hat{S}\psi_s \rangle = \langle \psi_s | \underbrace{\hat{S}^\dagger \hat{S}}_{\hat{1}} | \psi_s \rangle = \langle \psi_s | \psi_s \rangle$$

$$\Rightarrow |s| = 1 \quad (3.6)$$

- Next we show that the eigenvalues of the hermitian conjugate operator \hat{S}^\dagger of a unitary operator \hat{S} are the complex conjugates of the eigenvalues of \hat{S} .

$$\hat{S}^\dagger |\psi\rangle \stackrel{\hat{S}^\dagger \hat{S} = 1}{=} \hat{S}^{-1} |\psi_s\rangle \stackrel{\hat{S}|\psi_s\rangle = |\psi_s\rangle s}{=} |\psi_s\rangle s^{-1} = |\psi_s\rangle \frac{s^*}{s s^*} \stackrel{|s|=1}{=} |\psi_s\rangle s^* \quad (3.7)$$

- Now, we are ready to show that the matrix elements of the Hamilton operator between two eigenstates of the symmetry operator with different eigenvalues vanish.

We will use

$$\langle \psi_s | \hat{S} = s \langle \psi_s | \quad (3.8)$$

which directly follows from Eq. 3.7.

$$\begin{aligned} 0 & \stackrel{[\hat{H}, \hat{S}] = 0}{=} \langle \psi_s | [\hat{H}, \hat{S}] | \psi_{s'} \rangle = \langle \psi_s | \hat{H} \hat{S} | \psi_{s'} \rangle - \langle \psi_s | \hat{S} \hat{H} | \psi_{s'} \rangle \\ & \stackrel{\hat{S}|\psi_s\rangle = |\psi_s\rangle s, \text{ Eq. 3.8}}{=} \langle \psi_s | \hat{H} | \psi_{s'} \rangle s' - s \langle \psi_s | \hat{H} | \psi_{s'} \rangle = \langle \psi_s | \hat{H} | \psi_{s'} \rangle (s' - s) \\ & \stackrel{s \neq s'}{\Rightarrow} \langle \psi_s | \hat{H} | \psi_{s'} \rangle = 0 \end{aligned} \quad (3.9)$$

6.

CONSTRUCTION OF SYMMETRY EIGENSTATES

Eigenstates of a symmetry operator with a finite symmetry group, that is $\hat{S}^N = \hat{1}$ for a given eigenvalue s_α can be constructed from an arbitrary state $|\chi\rangle$ by superposition.

$$|\Psi_\alpha\rangle = \sum_{n=0}^{N-1} \hat{S}^n |\chi\rangle s_\alpha^{-n} \quad (3.10)$$

The eigenvalues s_α of the symmetry operator \hat{S} are

$$s_\alpha = e^{i \frac{2\pi}{N} \alpha}, \quad (3.11)$$

which follows from $|s_\alpha| = 1$ (Eq. 3.6) and $s_\alpha^N = 1$. The operation in Eq. 3.10 acts like a filter, that projects out all contributions from eigenvalues other than the chosen one. Therefore, the result may vanish.

Proof:

$$\begin{aligned} \hat{S} |\Psi_\alpha\rangle &= \hat{S} \sum_{n=0}^{N-1} \hat{S}^n |\chi\rangle s_\alpha^{-n} = \left[\sum_{n=0}^{N-1} \hat{S}^{n+1} |\chi\rangle s_\alpha^{-(n+1)} \right] s_\alpha \\ &\stackrel{\hat{S}^N = \hat{1}; s_\alpha^N = 1}{=} \left[\sum_{n=0}^{N-1} \hat{S}^n |\chi\rangle s_\alpha^{-n} \right] s_\alpha = |\Psi_\alpha\rangle s_\alpha \end{aligned}$$

With what has been discussed above, we have shown that the Hamilton operator is block diagonal in a representation of eigenstates of its symmetry operators. The eigenstates of the Hamilton operator can be obtained for each block individually. For us, it is more important that a wave function that starts out as an eigenstate of a symmetry operator to a given eigenvalue, will always remain an eigenstate to the same eigenvalue. In other words the eigenvalue of the symmetry operator is a conserved quantity. (Note, that symmetry operators usually have complex eigenvalues)

The eigenvalues of the symmetry operators are the **quantum numbers**.

3.3 Symmetry eigenstates of the hydrogen molecule

Let us consider the hydrogen molecule and let us only consider the two s-orbitals. The hydrogen molecule is symmetric with respect to a mirror plane in the bond center.

We orient the hydrogen molecule in z-direction and place the bond-center into the origin. The mirror operation \hat{S} about the bond center has the form

$$\hat{S}\psi(x, y, z) = \psi(x, y, -z)$$

or in bra-ket notation

$$\langle x, y, z | \hat{S} | \psi \rangle = \langle x, y, -z | \psi \rangle$$

If we apply the mirror operation twice, we obtain the original result. Therefore, $\hat{S}^2 = \hat{1}$ is the identity. For an eigenstate

$$\hat{S}|\psi\rangle = |\psi\rangle s$$

we obtain

$$\hat{S}^2|\psi\rangle = |\psi\rangle s^2 \stackrel{\hat{S}^2=\hat{1}}{=} |\psi\rangle 1$$

Hence we obtain $s^2 = 1$ which has two solutions, namely $s = 1$ and $s = -1$.

We can now construct symmetrized orbitals out of our basis functions:

- for the eigenvalue $s = +1$ we obtain the symmetric state, namely

$$|\chi'_1\rangle = \frac{1}{\sqrt{2}} (|\chi_1\rangle + |\chi_2\rangle)$$

- for the eigenvalue $s = -1$ we obtain the anti-symmetric state, namely

$$|\chi'_2\rangle = \frac{1}{\sqrt{2}} (|\chi_1\rangle - |\chi_2\rangle)$$

The factor $\frac{1}{\sqrt{2}}$ has been added to ensure that also the new orbitals are orthonormal.

In matrix-vector notation we may write¹

$$\begin{pmatrix} |\chi'_1\rangle \\ |\chi'_2\rangle \end{pmatrix} = \begin{pmatrix} |\chi_1\rangle \\ |\chi_2\rangle \end{pmatrix} \frac{1}{\sqrt{2}} \begin{pmatrix} 1 & 1 \\ 1 & -1 \end{pmatrix}$$

¹In the following expression one usually write the matrix to the left and the vector to the right. I use the convention that, in an expression that is a ket-vector, the ket stands always on the left side and the matrix, on the right side. From one notation to the other, it is necessary to transpose the matrix accordingly. For bra-expression the bra-vector stands on the right side, and the matrix on the left. My notation has the advantage that the order of the individual terms remains unchanged, when a bra and a ket is combined to a matrix element (bra-ket).

Now we can transform the Hamiltonian into the new basis set. In terms of the atomic orbitals the Hamilton matrix is

$$\mathbf{H} = \begin{pmatrix} \bar{\epsilon} & t \\ t & \bar{\epsilon} \end{pmatrix}$$

The Hamiltonian in the basis of the new orbitals is

$$\mathbf{H}' = \begin{pmatrix} \langle \chi'_1 | \hat{H} | \chi'_1 \rangle & \langle \chi'_1 | \hat{H} | \chi'_2 \rangle \\ \langle \chi'_2 | \hat{H} | \chi'_1 \rangle & \langle \chi'_2 | \hat{H} | \chi'_2 \rangle \end{pmatrix} = \mathbf{U}^\dagger \mathbf{H} \mathbf{U} = \begin{pmatrix} \bar{\epsilon} + t & 0 \\ 0 & \bar{\epsilon} - t \end{pmatrix}$$

In this case we have already diagonalized the matrix. By introducing a basis set made of symmetrized orbitals the Hamiltonian became block diagonal with two 1×1 blocks.

3.4 Symmetry eigenstates of a main group dimer

Let us now consider the dimeric main group dimers. In addition to the two s-orbitals used for hydrogen, we need to include also the p orbitals in the basis. The main group dimer is, in a way, the prototype for a bond between two main group atoms.

As for the hydrogen molecule we will follow a sequence of steps:

1. choose a basis set
2. determine the symmetry of the molecule
3. select a subset of symmetry operations. Preferably, one selects operations that do not commute with each other. In that case they can be treated as independent.
4. For each set of eigenvalues of the symmetry operators, form the corresponding symmetrized orbitals from the basis orbitals.

This procedure produces groups of orbitals, that block diagonalize the Hamiltonian. This is all one can do with symmetry operations. What remains to be done is to diagonalize the remaining sub-blocks of the Hamiltonian. This can be done in several ways, short of doing an ab-initio calculation.

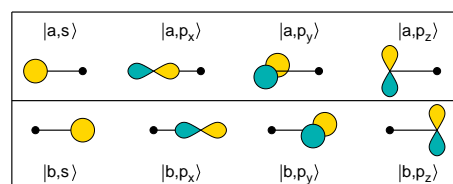
- One can set up a parameterized Hamiltonian for the subblocks and diagonalize them. If the subgroups only contain less than three orbitals, they can be diagonalized directly. If more orbitals are involved, one better uses the computer.
- One can do the first steps of an iterative diagonalization by hand. This gives only approximate answers, but often provides most insight.

Choose a basis

The first step is to choose a set of basis states. We start out here with atom-centered orbitals on the two sites, denoted by a (the left one) and b (the right one).

The angular dependence is characterized by a “real” spherical harmonic ($s, p_x, p_y, p_z, d_{x^2-y^2}, \dots$). The first few have the form

$$Y_s(\vec{r}) = \frac{1}{\sqrt{4\pi}} \quad ; \quad Y_{p_x}(\vec{r}) = \sqrt{\frac{3}{4\pi}} \frac{x}{|\vec{r}|} \quad ; \quad Y_{p_y}(\vec{r}) = \sqrt{\frac{3}{4\pi}} \frac{y}{|\vec{r}|} \quad ; \quad Y_{p_z}(\vec{r}) = \sqrt{\frac{3}{4\pi}} \frac{z}{|\vec{r}|}$$



The angular dependence is illustrated as lobes which are a schematic drawing of the polar-coordinate representation of the real spherical harmonics.

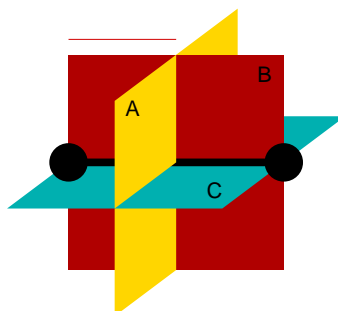
The fat dot represents an atom for which none of its atomic orbitals contribute to the wave function.

Symmetry operations of the molecule

We again by determining the symmetry of the molecule.

- mirror plane perpendicular to the bond through the bond center
- mirror planes with the bond in the mirror plane
- continuous rotational symmetry about the bond
- two fold rotational symmetry about any axis perpendicular to the bond, with the axis passing through the bond center
- point inversion about the bond center

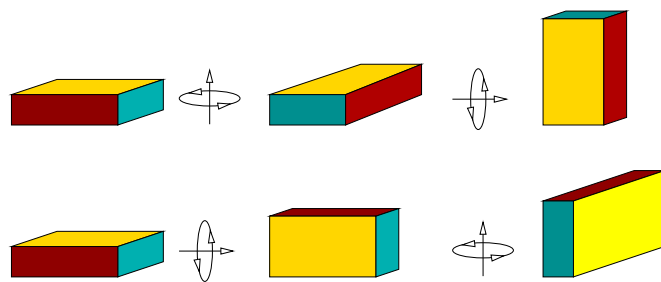
We only need to pick out a few. Since we are already familiar with mirror operations, let us pick the three mirror planes.



One should select a subset of symmetry operations that commute with each other. Symmetry operations commute, if the order in which they are performed on a general object does not affect the final state.

Example for non-commutating operations

An example for two operations that do not commute is given in Fig. 3.2 on p. 35.

$$\underbrace{\begin{pmatrix} 0 & -1 & 0 \\ 1 & 0 & 0 \\ 0 & 0 & 1 \end{pmatrix}}_{R_z(90^\circ)} \underbrace{\begin{pmatrix} 1 & 0 & 0 \\ 0 & 0 & -1 \\ 0 & 1 & 0 \end{pmatrix}}_{R_x(90^\circ)} = \underbrace{\begin{pmatrix} 0 & 0 & 1 \\ 1 & 0 & 0 \\ 0 & 1 & 0 \end{pmatrix}}_{R_{(111)}(90^\circ)}$$


$$\underbrace{\begin{pmatrix} 1 & 0 & 0 \\ 0 & 0 & -1 \\ 0 & 1 & 0 \end{pmatrix}}_{R_x(90^\circ)} \underbrace{\begin{pmatrix} 0 & -1 & 0 \\ 1 & 0 & 0 \\ 0 & 0 & 1 \end{pmatrix}}_{R_z(90^\circ)} = \underbrace{\begin{pmatrix} 0 & -1 & 0 \\ 0 & 0 & -1 \\ 1 & 0 & 0 \end{pmatrix}}_{R_{(1\bar{1}1)}(90^\circ)}$$

Fig. 3.2: Demonstration of two non-commutative rotations. The result (top) of a 90° rotation about the z -axis (vertical) followed by a 90° about the x -axis (horizontal, in the paper plane) differs from the result (bottom) obtained when the same operations are performed in reversed order. $R_{(111)}(90^\circ)$ denotes a 90° rotation about the diagonal pointing along $(1, 1, 1)$. $R_{(1\bar{1}1)}(90^\circ)$ denotes a 90° rotation about the $(1, -1, 1)$ axis

Eigenstates of the symmetry operators

Our basis orbitals are an s -orbital on each atom and three p -orbitals on each atom. We now group them according to the eigenvalues for the three mirror planes A, B, C .

We begin by grouping them according to the eigenvalues of B and C , because the orbitals we have chosen are already eigenstates of these operations. The $B+$ indicates the states that are symmetric with respect to the mirror plane B and $B-$ indicates the states that are antisymmetric with respect to the mirror plane B . We use the analogous notation for the mirror plane C . On the right hand side we list those orbitals that have the corresponding behavior with respect to the two mirror planes.

$B+$	$C+$	$ a,s\rangle$ $ b,s\rangle$ $ a,p_x\rangle$ $ a,p_x\rangle$
$B+$	$C-$	$ a,p_z\rangle$ $ b,p_z\rangle$
$B-$	$C+$	$ b,p_y\rangle$ $ b,p_y\rangle$
$B-$	$C-$	

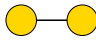
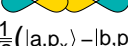


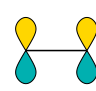
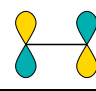
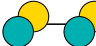
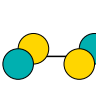
Now we form the symmetrized states with respect to A using Eq. 3.10 from p. 31. Note that we need not consider any mixing between states from sets with different symmetry eigenvalues.

$$|\psi_\alpha\rangle \stackrel{\text{Eq. 3.10}}{=} \sum_{n=1}^{N-1} \hat{S}^n |\chi\rangle s_\alpha^{-n} \quad (3.12)$$

We start with $|a, s\rangle$ and form $\hat{S}_A |a, s\rangle = |b, s\rangle$. Thus the symmetric state with respect to the mirror plane A is $\frac{1}{\sqrt{2}}(|a, s\rangle + |b, s\rangle)$ and the antisymmetric state is $\frac{1}{\sqrt{2}}(|a, s\rangle - |b, s\rangle)$. Starting from the

state $|b, s\rangle$ gives the same states. The state $|a, p_x\rangle$ transforms into $\hat{S}_A|a, p_x\rangle = -|b, p_x\rangle$. Therefore the symmetric state is $\frac{1}{\sqrt{2}}(|a, p_x\rangle - |b, p_x\rangle)$ and the antisymmetric state is $\frac{1}{\sqrt{2}}(|a, p_x\rangle + |b, p_x\rangle)$. Note, that a state with a positive sign is not automatically a symmetric state. Now new states are obtained starting from $|b, p_x\rangle$.

An important cross check is to verify that the number of orbitals in each group is the same before and after symmetrization.

A+	B+	C+	$\frac{1}{\sqrt{2}}(a, s\rangle + b, s\rangle)$  $\frac{1}{\sqrt{2}}(a, p_x\rangle - b, p_x\rangle)$ 
A-	B+	C+	$\frac{1}{\sqrt{2}}(a, s\rangle - b, s\rangle)$  $\frac{1}{\sqrt{2}}(a, p_x\rangle + b, p_x\rangle)$ 
A+	B+	C-	$\frac{1}{\sqrt{2}}(a, p_z\rangle + b, p_z\rangle)$ 
A-	B+	C-	$\frac{1}{\sqrt{2}}(a, p_z\rangle - b, p_z\rangle)$ 
A+	B-	C+	$\frac{1}{\sqrt{2}}(a, p_y\rangle + b, p_y\rangle)$ 
A-	B-	C+	$\frac{1}{\sqrt{2}}(a, p_y\rangle - b, p_y\rangle)$ 
A+	B-	C-	
A-	B-	C-	

Instead of solving a 8-dimensional eigenvalue problem, we only need to determine two 2-dimensional eigenvalue problems, a tremendous simplification.

The two-dimensional problem can be estimated graphically. They correspond to the non-degenerate problem of the two-center bond, discussed in section 2.3.

3.4.1 Approximate diagonalization

Up to now we have done all that can be done for the main-group dimer using symmetry alone. Now we need to diagonalize the remaining sub-blocks of the symmetry eigenstates. Here, I will show how one can get an idea of the eigenstates graphically, that is without any calculation. The results will be approximate. Later we will see how to set up a parameterized Hamiltonian, and do the calculation for a simple **tight-binding model**.

There are two problems to be solved:

- diagonalize the remaining sub-blocks containing more than one orbital
- determine the relative position of the orbitals

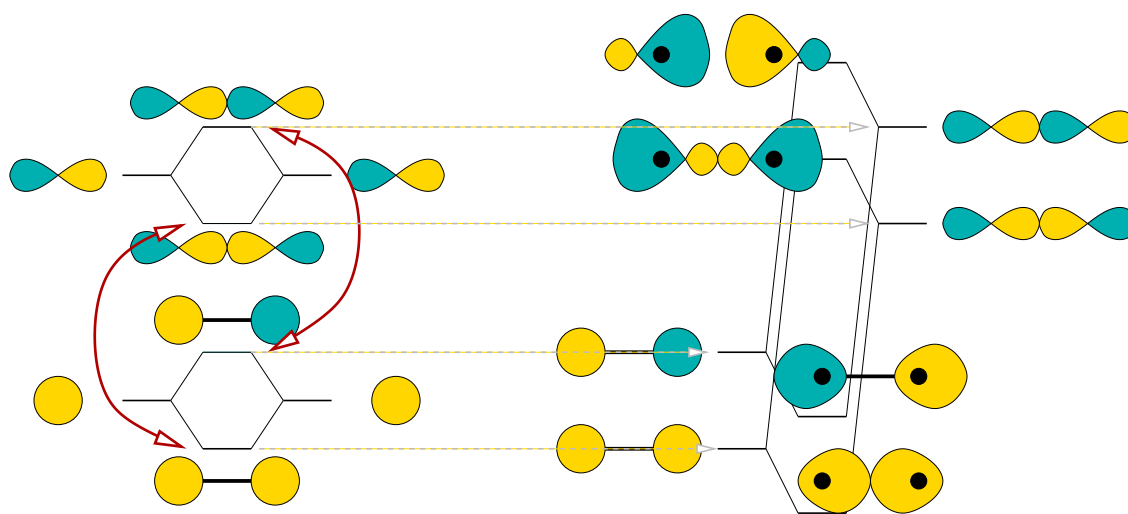


Fig. 3.3: Schematic drawing of the hybridization of the σ states of a dimeric molecule. The vertical axis corresponds to the energy of the orbitals

3.4.2 σ bonds and antibonds

The terms σ and π bond will be explained below. The σ bonds and antibonds result from the 2×2 blocks with orbitals that have cylinder symmetry.

Let us consider once the s orbitals on both atoms. As known from the section on the two-center bond, they form a bonding and an antibonding orbital. The bonding orbital is symmetric with respect to mirror operation at the bond-center plane, and the antibonding orbital is antisymmetric. This is the information we know also from the symmetry consideration, but now we also know that the energy levels are centered at the “atomic s orbital energy”.

Similarly we form the bonding and antibonding p-orbitals, that again form a symmetric (bonding) and an antisymmetric (antibonding) state.

From our symmetry considerations we know that only the bonding orbitals interact with each other and the two antibonding orbitals interact with each other. This is indicated by the red arrows in figure 3.3. Because they belong to different symmetry eigenvalues, the bonding orbitals do not interact with the antibonding orbitals.

The hybridization of the two bonding orbitals is analogous to the two-center bond in the non-degenerate case. Note that the model of a two center bond gave us a general recipe on diagonalizing 2×2 Hamiltonians. The two states need not be orbitals on the two bonding partners.

The lower bonding level will have mostly s-character and it will lie even below the energy the pure s-type orbital. The bonding p-orbital mixes into the s-type bond orbital so as to enhance the orbital weight in the center of the bond, and to attenuate the wave function in the back bond. (pointing away from the neighbor). This mixing of s and p-orbital forms so-called hybrid orbitals that will be discussed later.

The higher bonding orbital will lie above the p-type bonding orbital, and it will have predominantly p-type character. However the s-type bonding orbital mixes in, but now in the opposite compared to the bond orbital discussed above. Now the orbital in the middle of the bond is attenuated and enhanced in the back bond. This weakening of the bond explains that the p-type bond orbital shifts up in energy.

Similarly we can analyze the interaction between the two antibonding orbitals. Only here the s-type antibond is weakened, so that it shifts towards lower energy and the p-type antibond is made stronger, shifting it further up in energy.

3.4.3 π bonds and antibonds

The 1×1 blocks form the π bonds and antibonds shown in Fig. 3.4. Using what we learned from the symmetric two-center bond, we know that bonding and antibonding orbitals are centered around the “atomic p-level”. From the rotational symmetry of the bond, we can infer that the two bonding orbitals are degenerate and that the two antibonding orbitals are degenerate, too.

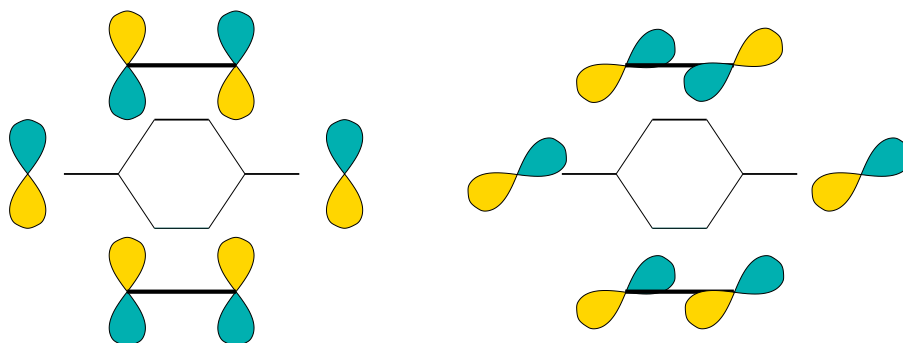


Fig. 3.4: Schematic drawing of the hybridization of the π -states of a dimeric molecule. The vertical axis corresponds to the energy of the orbitals

Finally we can place the orbitals into one diagram shown in Fig.3.5. The center of the π orbitals will lie below the two upper σ bonds, because the latter have been shifted up by the hybridization with the s orbitals.

The splitting between the π orbitals will be smaller than that of the σ orbitals, because the latter point towards each other and therefore have a larger overlap and Hamilton matrix element.

The order of the orbitals is not completely unique and, in particular, the σ -p-bond and π -bond can interchange as one goes through a period in the periodic table.

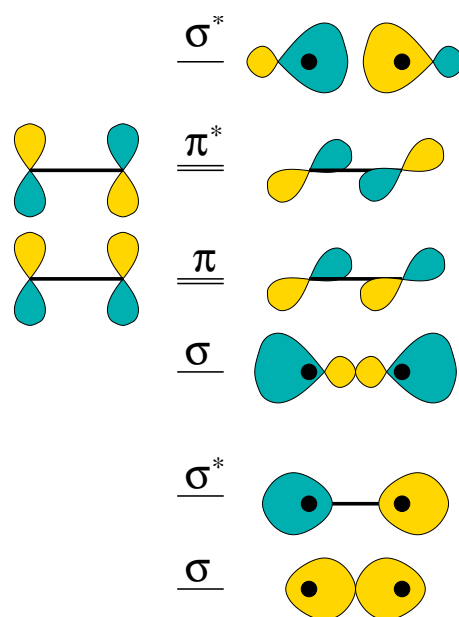


Fig. 3.5: Schematic energy level diagram of a main group dimer

3.5 Parameterized Hamiltonian of the main group dimer

In the following I will demonstrate the consequences of these steps on a parameterized Hamiltonian. Such a Hamiltonian in its symmetrized form allows us to diagonalize the remaining blocks of the Hamiltonian.

3.5.1 Notion of σ , π , δ -states

The states of a dimer are classified according to σ and π states. This notation is analogous to the naming convention of atomic orbitals as s , p , d , f -states. The notation defines the main angular momentum. The σ , π , δ notation refers to the angular momentum about the bond axis.

- A state that is rotationally symmetric is called a σ -state. A sigma state has the angular momentum quantum number is $m = 0$ for rotation about the bond axis.
- A state that changes its sign twice when moving in a circle about the bond axis is a π state. A π -state has the angular momentum quantum number is $m = 1$ for rotation about the bond axis.
- A state that changes its sign two times, when moving in a circle about the bond axis, is a δ -state. A δ -state has the angular momentum quantum number is $m = 2$ for rotation about the bond axis.

The notation carries a meaning beyond that of symmetry. σ bonds and anti-bonds are typically the strongest. The π -bonds are weaker and the δ -bonds are nearly negligible.

Antibonding orbitals are distinguished from the bond-orbitals by a star such as σ^* , pronounced “sigma-star”. The best is to inspect figure 3.5.

3.5.2 Slater-Koster tables

Slater and Koster[2] have formed the basis of today’s **empirical tight-binding methods**². They showed that if one knows the matrix elements of Hamilton and overlap matrix for certain symmetric combinations along a bond, the Hamiltonian and overlap matrix can be built up easily using their **Slater-Koster tables**[2]. If the matrix elements are furthermore known as function of distance one can also investigate the changes of the electronic structure, respectively estimate the forces.

3.5.3 Hopping matrix elements of Harrison

Harrison (“*The physics of solid state chemistry*”, Walter A. Harrison, Advances in Solid state Physics 17, p135)[?] has shown that the matrix elements can be reasonably fit by simple expressions. He has chosen the orbital energies equal to the atomic energy levels obtained with the Hartree Fock approximation. For the hopping matrix elements he found the following expressions, where d is the interatomic distance.

$$\begin{aligned} t_{ss\sigma} &= 1.40 \frac{\hbar^2}{md^2} \\ t_{sp\sigma} &= -1.84 \frac{\hbar^2}{md^2} \\ t_{pp\sigma} &= -3.24 \frac{\hbar^2}{md^2} \\ t_{pp\pi} &= 0.81 \frac{\hbar^2}{md^2} \end{aligned}$$

²The kind of empirical models, where only nearest neighbor matrix elements of Hamiltonian are considered, and overlap is set to unity is called tight binding models. However the definition is not clear cut and there are many variants and extensions that run with the same name.

h!

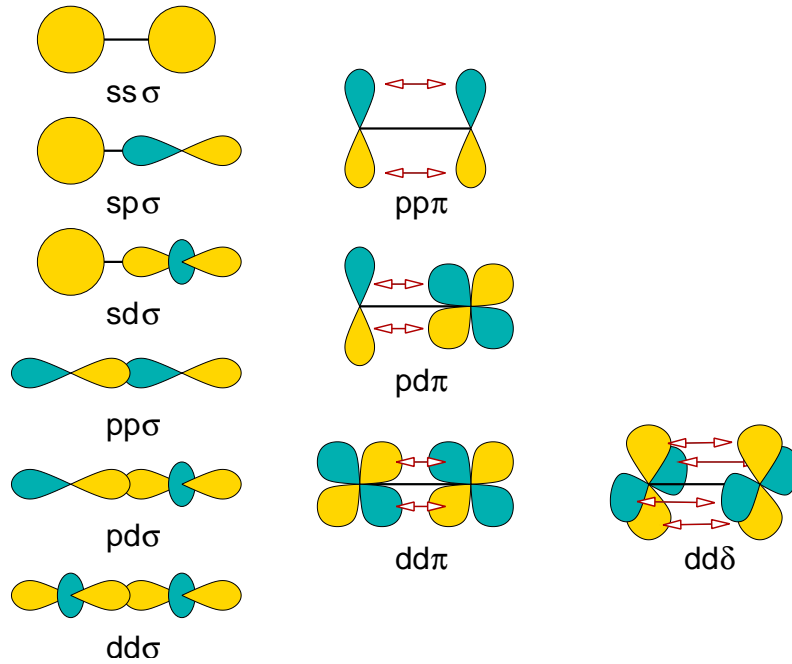


Fig. 3.6: Non-vanishing tight-binding matrix elements along a bond and their naming.

The parameters can be derived by fitting the free electron bands with tight-binding matrix elements,[7]. The constants are structure dependent.

Further reading can be found in [8, 9].

3.5.4 Parameterized Hamiltonian of the main group dimer

I will demonstrate how to parameterize a Hamiltonian and how to work out the energy levels in terms of these parameters. I will use the example of a dimeric molecule as an example.

Let us first consider the energies of the orbitals

$$\begin{aligned}\bar{\epsilon}_s &= \langle a, s | \hat{H} | a, s \rangle = \langle b, s | \hat{H} | b, s \rangle \\ \bar{\epsilon}_p &= \langle a, p_x | \hat{H} | a, p_x \rangle = \langle a, p_y | \hat{H} | a, p_y \rangle = \langle a, p_z | \hat{H} | a, p_z \rangle \\ &= \langle b, p_x | \hat{H} | b, p_x \rangle = \langle b, p_y | \hat{H} | b, p_y \rangle = \langle b, p_z | \hat{H} | b, p_z \rangle\end{aligned}$$

Usually one thinks here of the atomic orbitals.

For the off-site terms, we will use the, admittedly rather crude, approximations of choosing the Hamilton matrix elements proportional to the overlap matrix elements and then to ignore the deviations from orthonormality. Due to the rotational symmetry about the molecular axis, only certain matrix elements are nonzero. This rotational symmetry is another simplifying assumption.

$$\begin{aligned}t_{ss\sigma} &= \langle a, s | \hat{H} | b, s \rangle \\ t_{sp\sigma} &= \langle a, s | \hat{H} | b, p_x \rangle \\ t_{pp\sigma} &= \langle a, p_x | \hat{H} | b, p_x \rangle \\ t_{pp\pi} &= \langle a, p_y | \hat{H} | b, p_y \rangle = \langle a, p_z | \hat{H} | b, p_z \rangle\end{aligned}$$

If we describe the states as a vector with basisstates in the order ($|a, s\rangle$, $|a, p_x\rangle$, $|a, p_y\rangle$, $|a, p_z\rangle$, $|b, s\rangle$, $|b, p_x\rangle$, $|b, p_y\rangle$, $|b, p_z\rangle$), the Hamilton matrix has the form

$$H \hat{=} \begin{pmatrix} \epsilon_s & 0 & 0 & 0 & t_{ss\sigma} & t_{sp\sigma} & 0 & 0 \\ 0 & \epsilon_p & 0 & 0 & -t_{sp\sigma} & t_{pp\sigma} & 0 & 0 \\ 0 & 0 & \epsilon_p & 0 & 0 & 0 & t_{pp\pi} & 0 \\ 0 & 0 & 0 & \epsilon_p & 0 & 0 & 0 & t_{pp\pi} \\ t_{ss\sigma} & -t_{sp\sigma} & 0 & 0 & \epsilon_s & 0 & 0 & 0 \\ t_{sp\sigma} & t_{pp\sigma} & 0 & 0 & 0 & \epsilon_p & 0 & 0 \\ 0 & 0 & t_{pp\pi} & 0 & 0 & 0 & \epsilon_p & 0 \\ 0 & 0 & 0 & t_{pp\pi} & 0 & 0 & 0 & \epsilon_p \end{pmatrix} \quad (3.13)$$

Now we can work out the Hamiltonian in the basis of eigenstates of the three symmetry planes, namely

$$\begin{pmatrix} |\phi_1\rangle \\ |\phi_2\rangle \\ |\phi_3\rangle \\ |\phi_4\rangle \\ |\phi_5\rangle \\ |\phi_6\rangle \\ |\phi_7\rangle \\ |\phi_8\rangle \end{pmatrix} = \begin{pmatrix} \frac{1}{\sqrt{2}}(|a, s\rangle + |b, s\rangle) \\ \frac{1}{\sqrt{2}}(|a, p_x\rangle - |b, p_x\rangle) \\ \frac{1}{\sqrt{2}}(|a, s\rangle - |b, s\rangle) \\ \frac{1}{\sqrt{2}}(|a, p_x\rangle + |b, p_x\rangle) \\ \frac{1}{\sqrt{2}}(|a, p_z\rangle + |b, p_z\rangle) \\ \frac{1}{\sqrt{2}}(|a, p_z\rangle - |b, p_z\rangle) \\ \frac{1}{\sqrt{2}}(|a, p_y\rangle + |b, p_y\rangle) \\ \frac{1}{\sqrt{2}}(|a, p_y\rangle - |b, p_y\rangle) \end{pmatrix} \quad (3.14)$$

This can be done in two ways, which I demonstrate for one example, namely the matrix element between $\langle\phi_1| := \frac{1}{\sqrt{2}}(\langle a, s| + \langle b, s|)$ and $|\phi_2\rangle := \frac{1}{\sqrt{2}}(|a, p_x\rangle - |b, p_x\rangle)$

- We can represent the bra by a vector $\vec{c}_1 = (1, 0, 0, 0, 1, 0, 0, 0)\frac{1}{\sqrt{2}}$ and the ket by the vector $\vec{c}_2 = (0, 1, 0, 0, 0, -1, 0, 0)\frac{1}{\sqrt{2}}$, so that

$$\begin{aligned} \langle\phi_1| &= \sum_{i=1}^8 \langle\phi_1|\chi_i\rangle\langle\chi_i| = \sum_{i=1}^8 c_{i,1}^* \langle\chi_i| \\ |\phi_2\rangle &= \sum_{i=1}^8 |\chi_i\rangle\langle\chi_i|\phi_2\rangle = \sum_{i=1}^8 |\chi_i\rangle c_{i,2} \end{aligned}$$

Now we multiply the Hamilton matrix from Eq. 3.13, which has elements $\langle\chi_i|\hat{H}|\chi_j\rangle$, with \vec{c}_1^* from the left and with \vec{c}_2 from the right, which yields

$$\langle\phi_1|\hat{H}|\phi_2\rangle = \frac{1}{2}(-t_{sp\sigma} - t_{sp\sigma}) = -t_{sp\sigma}$$

- As an alternative we can also directly decompose the matrix elements of the symmetrized states into those of the original (not symmetrized) basis orbitals.

$$\begin{aligned} & \left[\frac{1}{\sqrt{2}} (\langle a, s| + \langle b, s|) \right] \hat{H} \left[\frac{1}{\sqrt{2}} (|a, p_x\rangle - |b, p_x\rangle) \right] \\ &= \frac{1}{2} \left(\underbrace{\langle a, s|\hat{H}|a, p_x\rangle}_0 - \underbrace{\langle a, s|\hat{H}|b, p_x\rangle}_{t_{sp\sigma}} + \underbrace{\langle b, s|\hat{H}|a, p_x\rangle}_{-t_{sp\sigma}} - \underbrace{\langle b, s|\hat{H}|b, p_x\rangle}_0 \right) \\ &= -t_{sp\sigma} \end{aligned}$$

In the basis of symmetry eigenstates from Eq. 3.14, the Hamiltonian obtains its block-diagonal form with two 2×2 blocks and six eigenstates. The elements of this Hamilton matrix are $\langle \phi_i | \hat{H} | \phi_j \rangle$.

$$\hat{H} \hat{=} \begin{pmatrix} \epsilon_s + t_{ss\sigma} & -t_{sp\sigma} & 0 & 0 & 0 & 0 & 0 & 0 \\ -t_{sp\sigma} & \epsilon_p + t_{pp\sigma} & 0 & 0 & 0 & 0 & 0 & 0 \\ \hline 0 & 0 & \epsilon_s - t_{ss\sigma} & t_{sp\sigma} & 0 & 0 & 0 & 0 \\ 0 & 0 & t_{sp\sigma} & \epsilon_p - t_{pp\sigma} & 0 & 0 & 0 & 0 \\ \hline 0 & 0 & 0 & 0 & \epsilon_p + t_{pp\pi} & 0 & 0 & 0 \\ 0 & 0 & 0 & 0 & 0 & \epsilon_p - t_{pp\pi} & 0 & 0 \\ \hline 0 & 0 & 0 & 0 & 0 & 0 & \epsilon_p + t_{pp\pi} & 0 \\ 0 & 0 & 0 & 0 & 0 & 0 & 0 & \epsilon_p - t_{pp\pi} \end{pmatrix}$$

Note that the Hamilton matrix here differs from the one given previously, because it is represented in a different basis namely the symmetrized orbitals ϕ_j as opposed to the original basis states $|\chi_\alpha\rangle$. The basis set plays the role of a coordinate system. Like the components of a vector, also the matrix elements of a tensor depend on the choice of the coordinate system.

3.5.5 Diagonalize the sub-blocks

The subblocks can be diagonalized. We use the approximate expression Eq. 2.18 for the non-degenerate two-center bond with $|t| < |\epsilon_1 - \epsilon_2|$. The modifications of the orbitals are demonstrated in Fig. 3.3 on p. 37.

- For the first block containing the $ss\sigma$ and $pp\sigma$ bonding orbitals we obtain the energies

$$\begin{aligned} \epsilon_- &\approx \epsilon_s + t_{ss\sigma} - \frac{|t_{sp\sigma}|^2}{\epsilon_p - \epsilon_s + t_{pp\sigma} - t_{ss\sigma}} \\ \epsilon_+ &\approx \epsilon_p + t_{pp\sigma} + \frac{|t_{sp\sigma}|^2}{\epsilon_p - \epsilon_s + t_{pp\sigma} - t_{ss\sigma}} \end{aligned}$$

- The lower of the two states will have a character of a $ss\sigma$ bond, however with a contribution from the $pp\sigma$ bond mixed in such that the electrons are further localized in the bond.
- The higher lying state will have a character of a $pp\sigma$ bond, but now the $ss\sigma$ orbital is mixed in such that the electron density in the bond is depleted.

- For the second block containing the $ss\sigma$ and $pp\sigma$ antibonding orbitals we obtain the energies

$$\begin{aligned} \epsilon_- &\approx \epsilon_s - t_{ss\sigma} - \frac{|t_{sp\sigma}|^2}{\epsilon_p - \epsilon_s + t_{pp\sigma} - t_{ss\sigma}} \\ \epsilon_+ &\approx \epsilon_p - t_{pp\sigma} + \frac{|t_{sp\sigma}|^2}{\epsilon_p - \epsilon_s + t_{pp\sigma} - t_{ss\sigma}} \end{aligned}$$

- The lower of the two states will have a character of a $ss\sigma$ antibond, however with a contribution from the $pp\sigma$ antibond mixed in such that the electrons are less localized in the bond. The state becomes less antibonding, which lowers its energy.
- The higher lying state will have a character of a $pp\sigma$ antibond, but the $ss\sigma$ orbital is mixed in such that the electron density in the bond is enhanced, making the state more antibonding, which shifts it up in energy.

The π type orbitals are already eigenstates, namely the bonding and antibonding states shown in Fig. 3.4.

3.6 Stability of main group dimers

From the qualitative arguments we would not be able to say if the σ -state in the middle is below or above the π states. From the node counting, we would expect the σ -state to lie above the π states, because the latter have only one node plane, while the σ state has two. I believe that the reason is that a small perturbation such as an electric field perpendicular to the bond axis would deform the orbitals such that the two node planes would join and form one connected node plane.

The little diagram tells us already a lot about stability.

1. for alkali metal dimers such as Li_2 , Na_2 etc. we expect a reasonably strong bond. The bonding is analogous to that in the hydrogen molecule.
2. On the other hand we expect Be_2 , Mg_2 to be marginally stable, because there is one σ -bond and one σ^* -anti-bond, which largely cancel their effect. There will be some bonding though, because the σ -p orbitals mix into the lowest two states and thus stabilize them.
3. For the dimers B_2 , Al_2 , there will again be a net σ bond. Thus we expect its bonds to be clearly stronger than that of the dimers of the di-valent atoms.
4. Then we arrive at C_2 and Si_2 where the four lowest orbitals are occupied. Since we have two partially occupied degenerate orbitals, we need to be careful about spin-polarization. C_2 is a difficult molecule, because the ordering of π bonds and σ bond depends on the distance. When the σ bond is occupied, the system will have a net magnetic moment, because the two electrons can align their spins according to Hund's rule. When the σ orbital is unoccupied, the system will have a π double bond.
5. Now we come to the most stable ions such as N_2 . Dinitrogen actually forms a triple bond. It consists of the two degenerate bonding π orbitals one one net σ bond. Dinitrogen is so non-reactive that it is often used to package food to avoid oxidation. Even though the atmosphere consists of 70% of nitrogen molecules, we need to supply nitrogen compounds in the form of fertilizer, to allow the excessive plant growth required for agriculture. Only some bacteria are able to transform dinitrogen to a form that can be metabolized.
6. Now we come to the chalcogenides³ such as O_2 and S_2 . Oxygen has two electrons in the π^* orbitals. Thus its net bonding corresponds to a double bond. However, it is stabilized by Hund's rule. The two electrons in the π^* states are spin paired. Thus O_2 has a net magnetic moment and a triplet spin splitting. That is if we apply a magnetic field, we will see three absorption lines.
7. The halogen dimers are again only weakly bond. They have a net σ bond, but all the gain from π bonding is compensated by the π^* anti-bonds.
8. The Nobel gases do not bind, because all bonding orbitals are compensated with anti-bonding orbitals.

3.7 Bond types

- σ -bond. The wave function of a sigma bond is approximately axially symmetric. An example is the bond in the H_2 molecule.
- π -bond. A π bond has a node plane parallel to the bond axis. An example are two p orbitals which stand perpendicular to the bond axis. It is weaker than a σ bond because the orbitals

³chalcogenide is spelled with a hard "ch" such as in "chemistry". Chalcogenides are oxides, sulfides, selenides, tellurides, that is compounds of the oxygen group. Oxides alone are not named chalcogenides unless grouped together with one of the heavier elements.

do not point towards each other resulting in smaller matrix elements. An example is the planar molecule ethene (C_2H_2), where two p-orbitals on the carbon atom combine in a π bond in addition to the σ -bond

- **Double bond** is typically a π bond combined with a σ bond. The example is again ethene.
- A **triple bond** is two π -bonds combined with a single bond. An example is N_2 .
- **Three-center bond** involves three orbitals in a row. A simple example is the hypothetical linear H_3 molecule. It forms a fully bonding orbital, a non-bonding orbital, to which the center atom does not contribute, and a fully anti-bonding orbital. The three center bond plays a role for five-valent atoms such as P . Such atoms form trigonal bi-pyramids. There are three equatorial sp^2 orbitals and a three-center bond along the z-axis.
- The best example for an **aromatic bond** is benzene (germ.:Benzol nicht Benzin!). It has the formula unit C_6H_6 . The carbon form a six-fold ring. After we formed the sigma bonds there are six electrons available to form three double bonds. There are however not three double bonds and three single bonds but all the bond lengths are symmetric.

The wave function is best constructed from symmetry arguments

$$|\psi_n\rangle = \sum_j |\chi_j\rangle e^{-2\pi i \frac{nj}{6}} \sqrt{\frac{1}{6}}$$

where the χ_i are the p_z orbitals on the individual carbon atoms. The Hamilton matrix has the form $H_{i,i} = \bar{\epsilon}$ and $H_{i,i+1} = H_{i-1,i} = -t$.

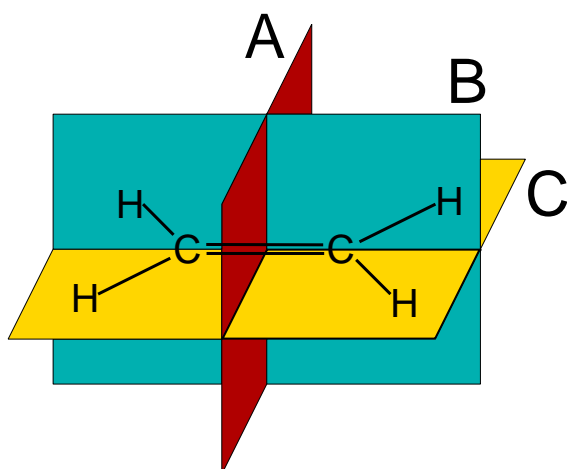
The energies are $\epsilon_n = \bar{\epsilon} + t(e^{2\pi i n/6} + e^{-2\pi i n/6}) = \epsilon_n = \bar{\epsilon} - 2t \cos 2\pi n/6$. Thus there is the fully symmetric ground state at $\bar{\epsilon} - 2t$. Then there are two degenerate occupied states at $\bar{\epsilon} - t$, two degenerate unoccupied states at $\bar{\epsilon} + t$ and a fully anti-bonding state at $\bar{\epsilon} + t$

3.8 Worked example: orbitals of the ethene

The molecule **ethene**, also called ethylene, has the formula unit C_2H_4 and forms a planar structure, where each carbon atom has two bonds to hydrogen and one to the other carbon atom with a bond angle of approximately 120° .

Select Basisset

First we decide which orbitals we wish to include in the basis. We use the relevant orbitals, which are the four hydrogen s-orbitals, and the s- and p-orbitals on carbon. That is we work with twelve basis functions.

Determine symmetry operations

We begin determining the symmetry operators of methane.

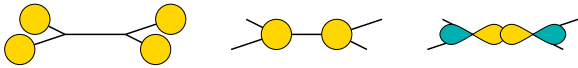
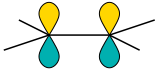

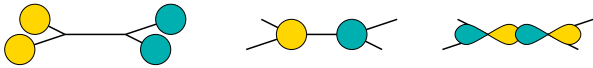
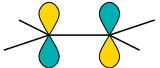

- A mirror plane in the molecular plane. (C)
- A mirror plane perpendicular to the C-C bond (A)
- a mirror plane containing the bond but perpendicular to the molecular plane (B)
- a two fold rotation about the bond axis

Determine symmetrized orbitals

- We start with the symmetry plane (A), perpendicular to the bond and determine the symmetric and antisymmetric orbitals.

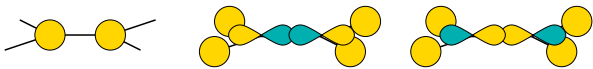
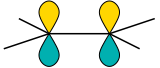

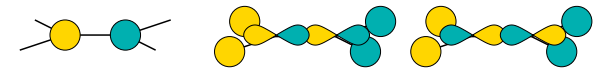
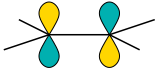
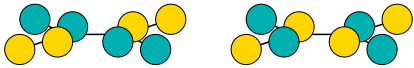
A+	
A-	

A+B+	
A+B-	
A-B+	
A-B-	

$A+B+C+$	
$A+B+C-$	
$A+B-C+$	
$A-B+C+$	
$A-B-C-$	
$A-B-C+$	

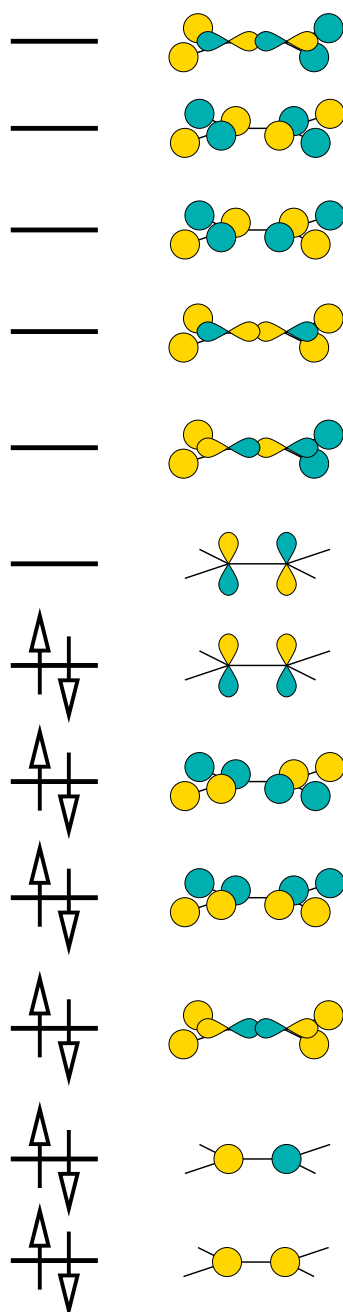
Form bond orbitals

We ended up with two 1×1 blocks, two 2×2 blocks and two 3×3 blocks of the Hamiltonian. Because the 3×3 blocks are difficult to handle, we form bonding and antibonding orbitals between the hydrogen orbitals and the carbon-p-orbitals, which are energetically in a similar position.

$A+B+C+$	
$A+B+C-$	
$A+B-C+$	
$A-B+C+$	
$A-B-C-$	
$A-B-C+$	

Now we can align the orbitals on an energy axis. Without a proper diagonalization this step can be nothing more than an educated guess. However it usually is sufficient to determine which orbitals are occupied and which are empty. Furthermore we can usually guess, which are the highest occupied and the lowest unoccupied orbitals, which is important for chemical considerations. We order the orbitals according to the bonding character. We place the s-orbitals on carbon lowest. Then we place

the bonding orbitals low in energy, and the fully antibonding up. If there is a competition between σ and π -bonds, the σ bonds dominate.



Difficult is the decision for the two states above the lowest unoccupied state, because there is a competition between CH-bonds with CC-bonds. We could as well have placed them below the π antibond. These orbitals can hybridize a little with the carbon s -orbitals, which would place them higher up on energy, concentrating their weight onto the anti-bonds.

3.9 Worked example: orbitals of the methane

The molecule **methane** has the formula unit CH_3 and forms a tetrahedron. Let us work out its eigenstates:

Select Basisset

First we decide which orbitals we wish to include in the basis. We use the relevant orbitals, which are the four hydrogen s-orbitals, one carbon s-orbital and the three carbon p-orbitals. That is we work with eight basis functions.

Determine symmetry operations

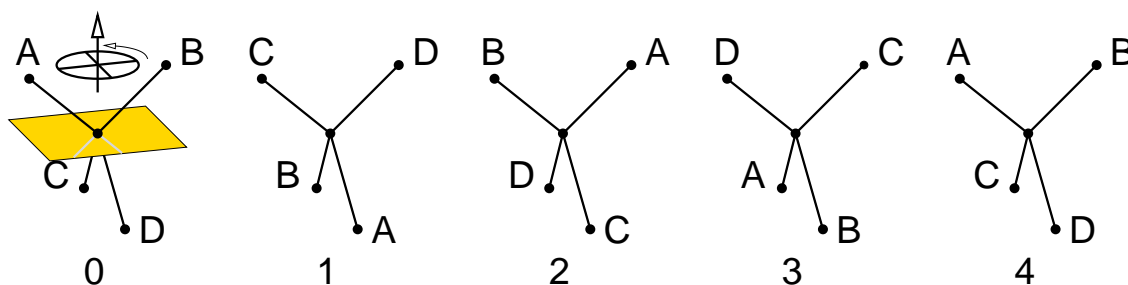
We begin determining the symmetry operators of methane.

- six mirror planes through a pair of hydrogen and the central carbon atom.
- four three fold axis along a C-H bond.
- six two-fold rotations about any axis through the central carbon and the mid-point between two hydrogen atoms.
- A rotation about a two-fold axis by 90° , followed by a mirror plane perpendicular to the axis passing through the central carbon atom.

Determine symmetrized orbitals

Now we need to select a number of symmetry operators which commute. Two transformations commute, if we transform an object in sequence by both transformations, and the result is identical irrespective of the object chosen. For example two reflections with perpendicular mirror planes commute. They do not commute if they have another angle.

Let us start with the rotation by 90° followed by a reflection. This operation brings an object into its original position after it has been applied four times.



This operation produces the identity after four-fold application. The eigenvalues are therefore $1, i, -1, -i$.

- Let us construct all orbitals for the eigenvalue 1. according to Eq. 3.10.
 - We start with one hydrogen orbital on the site A. We transform it once by the symmetry operation and multiply with the eigenvalue, namely 1, which results in a hydrogen orbital with the same sign on site D. We take this orbital, apply the symmetry operation again and obtain, after multiplication with 1, an orbital at site B. The third operation produces an orbital at site C. We add the four orbitals together, and obtain the orbital shown in Fig. 3.7.
 - We see immediately, that we obtain the same orbital, irrespective of which orbital we started out from.

- Now we proceed with the s -orbital on the carbon atom. This orbital falls on itself after each transformation. Since its copies are multiplied with 1, the orbital remains unchanged.
- Next we proceed to the p -orbitals. Because the p_z orbital changes its sign after each transformation, its copies add to zero. The p_x and p_y orbitals change their sign after every two operations and therefore also cancel out.

In total we obtain exactly two symmetrized orbital with eigenvalue 1 of the symmetry operation.

- We proceed to eigenvalue -1 .
 - We begin again with a hydrogen orbital. After each transformation we need to multiply the orbital with -1 . Thus the orbital enters with a positive sign on sites A and B and with negative sign on sites C and D. After adding up we obtain the symmetrized orbital shown in Fig. 3.7 in the box with eigenvalue -1 .
 - the carbon s orbital does not produce a symmetrized orbital in this class, because its copy add up to zero after multiplication with the factors 1 and -1 .
 - The p_z orbital is a symmetry orbital in this class, because the symmetry operation simply reverts its sign. After multiplication with the eigenvalue, namely -1 , we obtain the original orbital.
 - the p_x and p_y orbitals are rotated by 90° in each operation. That is, after two operations, they revert their sign. After two operations we need to multiply with the square of the eigenvalue. Thus the copies of the orbitals cancel each other, and do not contribute to this symmetry class.

Also in this class we obtain exactly two orbitals.

- Now we proceed to the complex valued eigenvalue i .
 - We start with an s orbital and obtain two real-valued orbitals with opposite sign on the upper two atoms, and two imaginary-valued orbitals with opposite sign on the lower two hydrogen atoms. Thus the symmetrized orbital is complex valued.
 - the s -orbital on carbon cancels out, because it falls on itself under the operation and $i + i^2 + i^3 + i^4 = i - 1 - i + 1 = 0$.
 - Also the p_z orbital cancels out, because it changes its sign and $i - i^2 + i^3 - i^4 = 0$.
 - the p_x and p_y orbitals are transformed into each other by the symmetry operation. From p_x we obtain a symmetrized orbital $\frac{1}{\sqrt{2}}(|p_x\rangle + i|p_y\rangle)$. The p_y orbital produces the same symmetrized orbital with an additional factor i . Note, that this orbital is an eigenstate to \hat{L}_z with eigenvalue $m = 1$.
- for the eigenvalue $-i$, we obtain the same symmetrized orbitals as for the eigenvalue i , only that the orbitals are complex conjugate.

Thus we have divided the 8×8 Hamiltonian in four 2×2 blocks.

Form bond and antibonding orbitals

Next we diagonalize the 2×2 blocks of the Hamiltonian expressed by symmetrized orbitals and thus obtain bonding and antibonding orbitals.

In order to align the orbitals on an energy axis we need to know the energies and hopping matrix elements. Because the carbon s -orbital lies energetically below the carbon p -orbital, we can conclude that the average value of the bonding and antibonding orbitals that contain the carbon s -orbital lies below that of the p -orbitals. Furthermore we recognize that the type and number of interactions for all bonding orbitals containing the carbon p -orbital is the same. Thus we conclude that they are degenerate. The same holds true for the corresponding antibonding orbitals. This leads us to the schematic assignment of the electron states of methane shown in Fig. 3.9.

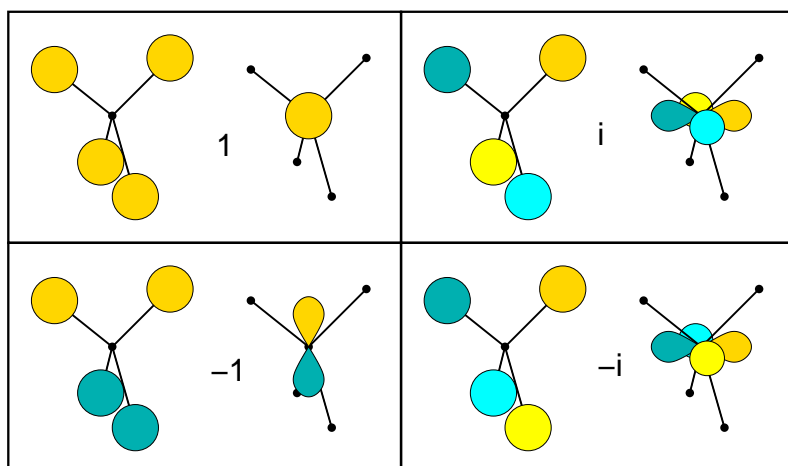


Fig. 3.7: Symmetrized orbitals of methane. The numbers refer to the eigenvalue of the symmetry operation, namely a fourfold rotation about a vertical axis combined with a mirror operation about the horizontal mid-plane. The golden and green lobes have values $+1$ and -1 , and the bright yellow and cyan lobes have values $+i$ and $-i$ respectively. .

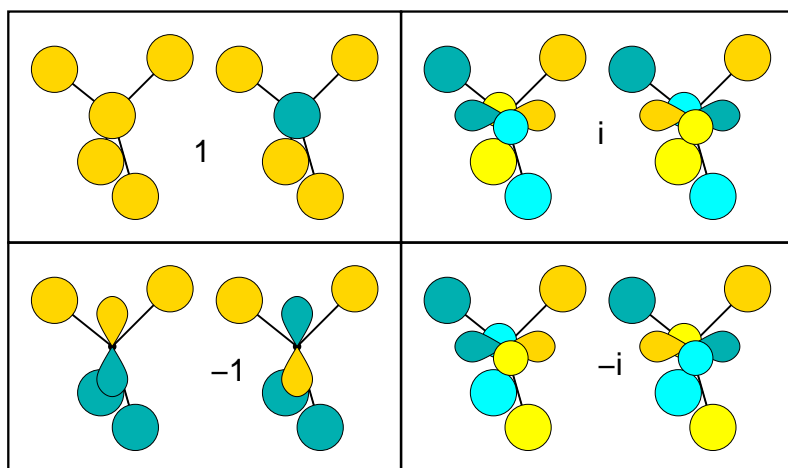
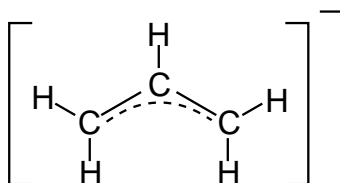


Fig. 3.8: Bonding and antibonding orbital, according to symmetry class. .

3.10 Worked example: orbitals of the allyl ion

let us work out the molecular orbitals of the allyl anion C_3H_5^- .



The allyl ion is a planar molecule.

- First we work out the symmetry operations of the molecule. The molecule has the following

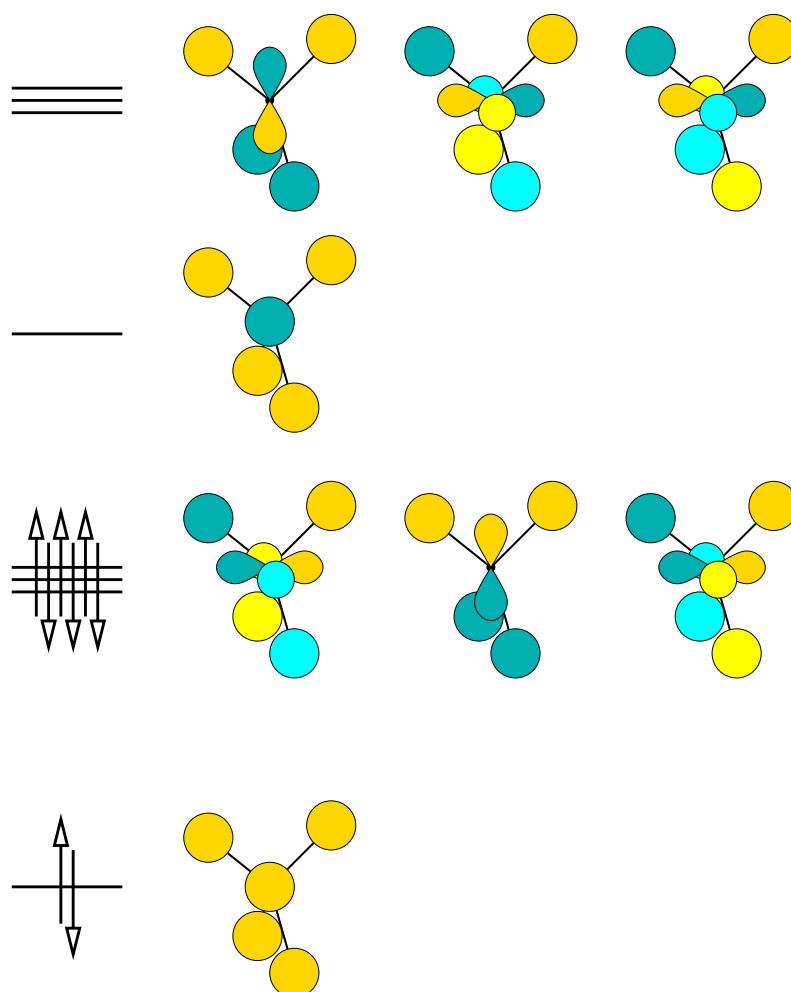


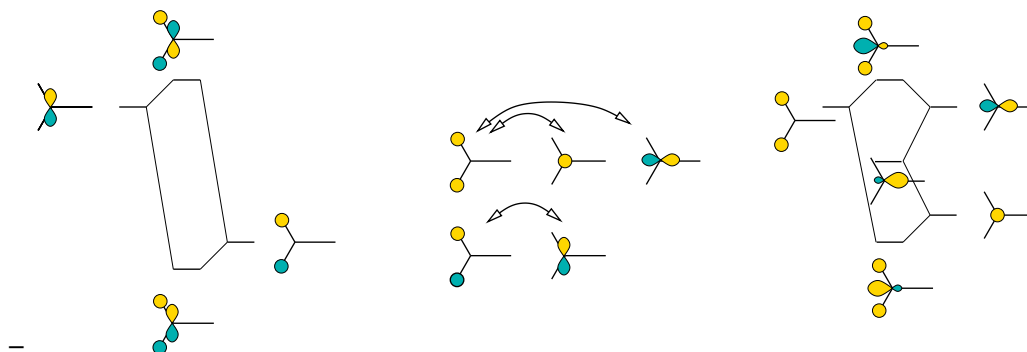
Fig. 3.9: Symmetry eigenstates and energy level ordering of methane. The blue and bright-yellow lobes correspond to the imaginary part of the wave function. The imaginary part can be avoided by a suitable superposition of the two wave functions that are complex conjugate of each other. While the resulting states are still eigenstates of the Hamilton operator, they are no more eigenstates of the symmetry operators. .

symmetry operations.

- a mirror plane in the plane of the molecule
 - a mirror plane perpendicular to the molecular plane, containing the central C-H bond.
 - a two-fold rotation about an axis through the central C-H bond.
- Now we work out the symmetrized orbitals. We start with every “atomic” orbital and construct the symmetrized orbital according to Eq. 3.10 by adding the orbitals obtained from the first by applying the symmetry operation repeatedly and multiplication with the eigenvalue of the symmetry operation to the corresponding power.

		H-s			C-s		C-p		
A	B								
+	+								
-	+								
+	-								
-	-								

- We check the number of symmetrized orbitals, which must be identical to the number of orbitals we started from: There have been 5 hydrogen s-orbitals, 3 carbon s-orbitals and 9 carbon p-orbitals, that is in total 17 orbitals. We also have 17 symmetrized orbitals.
- Since we ended up with sub blocks of the Hamiltonian of up to eight orbitals we need to go a step further. We use an approximate symmetry of the CH₂ end groups and determine symmetrized orbitals for these fragments. We are careful not to mix states from different symmetry classes of the entire molecule, in order to avoid destroying the block-diagonalization of the Hamiltonian reached so far.
 - We determine the symmetry groups of the end group.



- now we compose again the symmetrized orbitals with the locally symmetrized end groups

A	B										
+	+										
-	+										
+	-										
-	-										

- We notice that there are only few orbitals that still interact with each other, if we ignore the weak interactions of orbitals pointing away of each other. We diagonalize the last few 2 × 2 matrices and thus obtain an approximate idea of the eigenstates.

A B		
+	+	
-	+	
+	-	
-	-	

- We divide the orbitals into bonding and antibonding orbitals. This is not necessarily as straightforward as in this case. Then we count the number of valence electrons, which is 18, resulting in 9 filled orbitals. We fill up the bonding orbitals first, proceeding to the non-bonding orbitals. We find that the non-bonding π orbital is the highest occupied orbital.

A B		
+	+	
-	+	
+	-	
-	-	

The wave functions calculated from first principles are shown below in figure 3.10. We recognize good agreement for some of the wave functions and poor agreement for others. We have been able to identify the highest occupied orbital. We also recognize that the main character of the states is similar in our estimated orbitals and the ab-initio wave functions.

The main error is that states lying in a similar energy region are hybridized incorrectly: That is a superposition of those states from our estimate would allow us to construct the true eigenstates. The limitations of the above procedure are not untypical. Like in this case, however, they usually do not strongly affect stability considerations. The reason behind this is that a unitary transformation of completely filled or of completely empty states does not affect the energy. If the intermixing between filled and occupied orbitals would be equally undetermined, the results would not be reliable, and one should resort to ab-initio calculations.

3.11 Exercise: sketch orbitals

- sketch wave functions and energy level diagram for a water molecule. The water molecule H_2O has a bond angle of about 104° . The hydrogen orbitals are located slightly above the oxygen p orbitals.
- The cyclopentadienyl ion has the formula $[\text{C}_5\text{H}_5]^-$. It is a five-membered ring. Work out first the orbitals for one bead and use then the knowledge about eigenstates for ring systems.
- sketch the wave functions of ethene (ethylene) C_2H_4 .

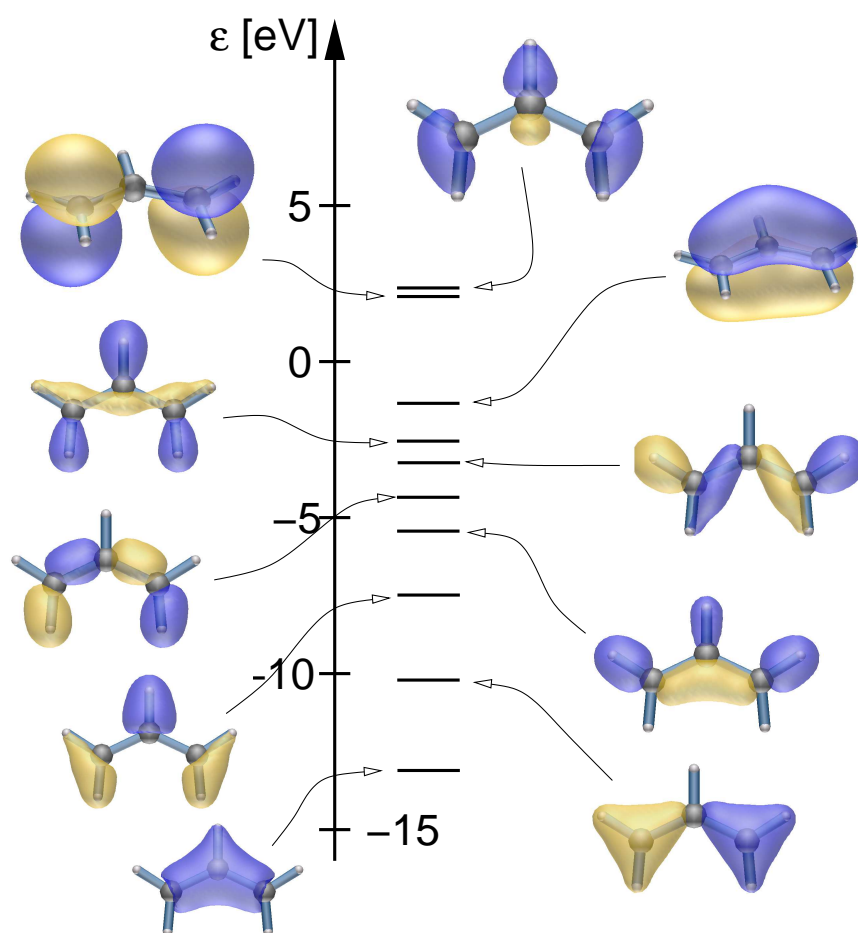


Fig. 3.10: PAW calculation of the one-particle orbitals of the allyl ion. The highest state shown is mostly localized in the vacuum.

Chapter 4

From bonds to bands

So far we have employed a local picture of bonding. In solid state physics another viewpoint became popular, based on the concept of reciprocal space and band structures.

In order to approach the concepts in a simple way we again choose a simple model system, namely the jellium model.

4.1 The Jellium model

For the electron gas the model system is the **free electron gas** or the **jellium model**. The jellium model consists of electrons and a spatially constant, positive charge background, which ensures that the overall system is neutral.

Because of translational symmetry, the potential is spatially constant. Thus the one-particle states are simply plane waves.

$$\phi_{\vec{k},\sigma}(\vec{r}, \sigma') = \frac{1}{\sqrt{\Omega}} e^{i\vec{k}\vec{r}} \delta_{\sigma,\sigma'} \quad (4.1)$$

We consider here states in a very large, but finite, volume Ω such as the universe. The states are normalized to one within this volume.

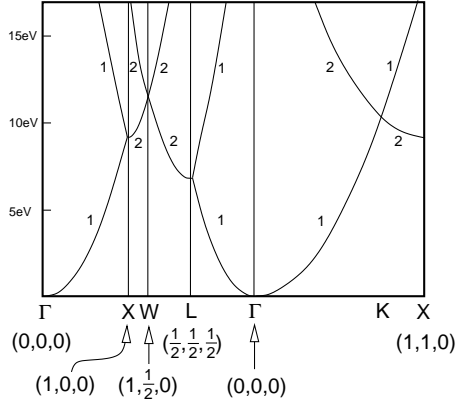
This is an unusual notation for an ideally infinite system. Using this notation we avoid having to distinguish discrete and continuous sections of the spectrum and different normalization conditions for localized and extended states. A disadvantage is that extended states have a nearly vanishing amplitude, and that the spacing in k-space is extremely small. For a finite volume, only discrete values for \vec{k} are allowed. We will later see that in the final expression the factors Ω from the normalization can be translated into a volume element in k-space, so that the sums can be converted into integrals.

The dispersion relation of free electrons forms a parabola

$$\epsilon_{\vec{k},\sigma} = V_0 + \frac{(\hbar k)^2}{2m_e}$$

where V_0 is the value of the potential.

The jellium model approximates real metals surprisingly well, even though the potential of the nuclei is far from being a constant. In a hand-waving manner we can say that the valence electrons are expelled from the nuclear region by the Pauli repulsion of the core electrons, so that they move around in a region with fairly constant potential. The true story is a little more subtle though... In Fig. 4.1 the band structure of free and non-interacting electron gas is shown in a unit cell corresponding to alumina and compared to the calculated band structure of alumina. We can see that the free electron gas already provides a fairly good description of some realistic systems.



CB-Figs/albsdos.eps

Fig. 4.1: Band structure of free, non-interacting electrons. The lattice is an fcc-cell with a lattice constant of 4.05 \AA corresponding to aluminum. The high symmetry points are given in units of $\frac{2\pi}{a_{lat}}$. The numbers indicate the degeneracy beyond spin-degeneracy. On the right-hand side, the band structure of aluminum is shown in comparison.

4.2 Density of States

4.2.1 Motivation

While the dispersion relation contains a wealth of information, that is very important for transport problems or the interaction of quasi-particles, for many purposes the k -dispersion is not relevant. In those cases the additional information of the k -dispersion obscures the truly important information.

Thermodynamic potentials such as the free energy can be written, for non-interacting, identical particles as a sum over energy levels.

$$\langle A \rangle_{\beta, \mu} = \sum_n f_{T, \mu}(\epsilon_n) \langle \psi_n | \hat{A} | \psi_n \rangle = \int d\epsilon f_{T, \mu}(\epsilon) \underbrace{\sum_n \delta(\epsilon - \epsilon_n) \langle \psi_n | \hat{A} | \psi_n \rangle}_{D_A(\epsilon)}$$

where

$$f_{T, \mu}(\epsilon) = \left(1 + e^{\frac{1}{k_B T}(\epsilon - \mu)} \right)^{-1}$$

is the Fermi distribution function.

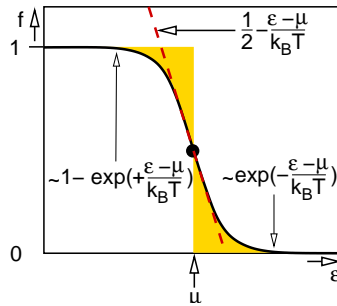


Fig. 4.2: Fermi distribution $f(\epsilon) = (1 + e^{\frac{1}{k_B T}(\epsilon - \mu)})^{-1}$.

The density of states separates “thermodynamic information” such as temperature and chemical potential from the “system information” which refers to the energies and matrix elements of individual states.

One can go one step further and separate out the observable A , if one introduces a local basiset $|\chi_\alpha\rangle$ and corresponding projector functions $\langle\pi_\alpha|$, that obey the bi-orthogonality condition $\langle\pi_\alpha|\chi_\beta\rangle = \delta_{\alpha,\beta}$. For an orthonormal basiset one may choose the projector functions equal to the basis-functions themselves. For non-orthonormal basisets, the projector functions carry another inverse overlap matrix. One can verify that

$$|\psi\rangle = \sum_{\alpha} |\chi_\alpha\rangle \langle\pi_\alpha|\psi\rangle \quad \text{if } \langle\pi_\alpha|\chi_\beta\rangle = \delta_{\alpha,\beta}$$

Insertion into the expression for the expectation value above yields

$$\begin{aligned} \langle A \rangle_{\beta,\mu} &= \int d\epsilon f_{T,\mu}(\epsilon) \sum_n \delta(\epsilon - \epsilon_n) \sum_{\alpha,\beta} \langle\psi_n|\pi_\alpha\rangle \langle\chi_\alpha|\hat{A}|\chi_\beta\rangle \langle\pi_\beta|\psi_n\rangle \\ &= \int d\epsilon \sum_{\alpha,\beta} f_{T,\mu}(\epsilon) \underbrace{\sum_n \langle\pi_\beta|\psi_n\rangle \delta(\epsilon - \epsilon_n) \langle\psi_n|\pi_\alpha\rangle}_{D_{\beta,\alpha}(\epsilon)} \langle\chi_\alpha|\hat{A}|\chi_\beta\rangle \end{aligned}$$

In this way we have managed a division of the expression into

- thermodynamic information, i.e the Fermi distribution function
- system-dependent information, the density of states

$$D_{\alpha,\beta}(\epsilon) \stackrel{\text{def}}{=} \sum_n \langle\pi_\beta|\psi_n\rangle \delta(\epsilon - \epsilon_n) \langle\psi_n|\pi_\alpha\rangle \quad (4.2)$$

and the

- observable information, namely the matrix element $\langle\chi_\alpha|\hat{A}|\chi_\beta\rangle$.

Most important is the **total density of states**, where the operator A is the unit operator.

$$D(\epsilon) = \sum_n \delta(\epsilon - \epsilon_n)$$

Often also **projected density of states** are used, where the density of states is projected onto a certain orbital

$$D_{\alpha,\alpha}(\epsilon) = \sum_n \delta(\epsilon - \epsilon_n) \langle\psi_n|\chi_\alpha\rangle \langle\chi_\alpha|\psi_n\rangle$$

In order to investigate bonding one also uses off-diagonal elements of the density of states matrix. There are several variants: Mulliken’s overlap populations and the Crystal orbital overlap contributions (COOP) of Hoffman and Hughbanks use the overlap matrix elements A a variant more directly related to the energetics are the and the **Crystal Orbital Hamilton Populations (COHP)**[10].

$$COHP_{\alpha,\beta}(\epsilon) = D_{\alpha,\beta}(\epsilon) \langle\chi_\beta|\hat{H}|\chi_\alpha\rangle$$

The energetic information contained in the density of states is important because it provides some insight into how robust a certain expectation value is against perturbations of the system.

4.2.2 Density of States for extended systems

For molecules, the total density of states is simply a series of Delta functions. For extended systems this is no more true, but the density of states becomes a continuous function.

The one-particle density of states can be obtained from the dispersion relation $\epsilon(p)$. Independent particles in a constant potential have a conserved momentum $\vec{p} = \hbar\vec{k}$. This implies that they can be described by plane waves

$$\Psi(\vec{r}) = \frac{1}{\sqrt{V}} e^{i\vec{k}\vec{r}}$$

Note that even electrons in a periodic potential, that is electrons in a crystal, have a conserved momentum. The wave function is not a plane wave, but a plane wave modulated by some periodic, p dependent function, as seen in the **Bloch theorem**. These dispersion relations are called **band structure** and can be calculated with first-principles calculations. Also lattice vibrations in a crystal can be classified by their wave vector, resulting in a phonon band structure.

If we consider a system with periodic boundary conditions in a box with side-lengths L_x, L_y, L_z , the states are quantized, so that $k_i L_i = 2\pi n_i$ where n_i is an arbitrary integer. Thus there are only states with $\vec{k} = (\frac{2\pi}{L_x} i, \frac{2\pi}{L_y} j, \frac{2\pi}{L_z} k)$, where i, j, k are arbitrary integers. The volume V of the box is $V = L_x L_y L_z$.

Thus the density of states is

$$D(\epsilon) = \sum_{i,j,k} \delta\left(\epsilon\left(\underbrace{\frac{2\pi\hbar}{L_x} i}_{p_x}, \underbrace{\frac{2\pi\hbar}{L_y} j}_{p_y}, \underbrace{\frac{2\pi\hbar}{L_z} k}_{p_z}\right) - \epsilon\right)$$

We can attribute to each state a volume in k -space, namely

$$\Delta V_k = \frac{2\pi}{L_x} \frac{2\pi}{L_y} \frac{2\pi}{L_z} = \frac{(2\pi)^3}{V} \quad (4.3)$$

Using the relation $\vec{p} = \hbar\vec{k}$ we can convert this volume into a volume element in momentum space, namely

$$\Delta V_p = \frac{(2\pi\hbar)^3}{V} \quad (4.4)$$

If the size of the box, that is L_x, L_y, L_z , is made very large, the volume element attributed to a single state in momentum space becomes very small. Thus we can replace the sum by an integral, where ΔV_p is represented by $d^3 p$.

$$\begin{aligned} D(\epsilon) &= \frac{V}{(2\pi\hbar)^3} \sum_{i,j,k} \underbrace{\frac{(2\pi\hbar)^3}{V}}_{\rightarrow d^3 p} \delta(\epsilon(\vec{p}_{i,j,k}) - \epsilon) \\ &\stackrel{L_i \rightarrow \infty}{=} \frac{V}{(2\pi\hbar)^3} \int d^3 p \delta(\epsilon(\vec{p}) - \epsilon) \end{aligned} \quad (4.5)$$

It is intuitively clear that the expression for the density of states is related to a surface integral over a surface of constant energy. This will be shown in the following.

In order to transform the expression for the density of states into a surface integral in momentum space, it is convenient to introduce the **number of states** $N(\epsilon)$.

The number of states is defined as the number of states that lie below the energy epsilon.

$$N(\epsilon) = \sum_{i,j,k} \theta(\epsilon - \epsilon(p_{i,j,k})) \stackrel{V \rightarrow \infty}{=} \frac{V}{(2\pi\hbar)^3} \int d^3 p \theta(\epsilon - \epsilon(\vec{p})) \quad (4.6)$$

where $\theta(x)$ is the Heaviside function $\theta(x)$, which vanishes for $x < 0$ and is equal to unity for $x > 0$. The Heaviside function is related to the δ -function via

$$\theta(x) = \int_{-\infty}^x dx' \delta(x') \quad \Leftrightarrow \quad \partial_x \theta(x) = \delta(x) \quad (4.7)$$

This allows us to relate the number of states to the density of states. Thus we obtain

$$\begin{aligned} \partial_\epsilon N(\epsilon) &\stackrel{\text{Eq. 4.6}}{=} \frac{V}{(2\pi\hbar)^3} \int d^3p \partial_\epsilon \theta(\epsilon - \epsilon(\vec{p})) \stackrel{\text{Eq. 4.7}}{=} \frac{V}{(2\pi\hbar)^3} \int d^3p \delta(\epsilon - \epsilon(\vec{p})) \\ &\stackrel{\text{Eq. 4.5}}{=} D(\epsilon) \end{aligned} \quad (4.8)$$

Here we show how the volume integral with the delta function can be converted into a surface integral.

$$D(\epsilon) \stackrel{\text{Eq. 4.8}}{=} \partial_\epsilon N(\epsilon) = \lim_{\Delta \rightarrow 0} \frac{V}{(2\pi\hbar)^3} \int d^3p \underbrace{\frac{\theta(\epsilon + \Delta - \epsilon(p)) - \theta(\epsilon - \epsilon(p))}{\Delta}}_{\rightarrow \delta(\epsilon - \epsilon(p))}$$

The integral over the difference of the two Heaviside function corresponds to the volume of a volume sheet, which is enclosed by the surfaces defined by $\epsilon(\vec{p}) = \epsilon$ and $\epsilon(\vec{p}) = \epsilon + \Delta$.

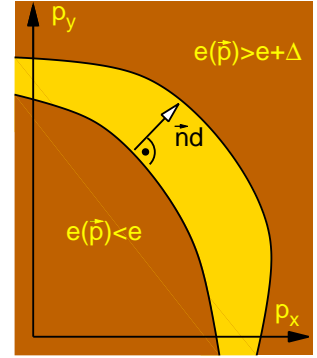
Let us calculate the distance of two points on the two surfaces. Let us pick one point \vec{p}_0 on the surface defined by $\epsilon(\vec{p}) = \epsilon$. The closest neighbor on the other surface \vec{p}_1 lies opposite to \vec{p}_0 , that is $\vec{p}_1 = \vec{p}_0 + \vec{n} \cdot d$, where d is the distance of the points and $\vec{n} = \frac{1}{|\vec{\nabla}_p \epsilon|} \vec{\nabla}_p \epsilon$ is the normal vector of the surface. \vec{p}_1 lies on the other surface and therefore fulfills

$$\begin{aligned} \epsilon(\vec{p}_1) &= \underbrace{\epsilon}_{\epsilon(\vec{p}_0)} + \Delta \\ \Rightarrow \epsilon(\vec{p}_0) + \Delta &= \epsilon(\vec{p}_0 + \vec{n} \cdot d) \stackrel{\text{Taylor}}{=} \epsilon(\vec{p}_0) + \vec{n} \cdot d \vec{\nabla}_p \epsilon + O(d^2) \\ \Rightarrow d &= \frac{\Delta}{\vec{n} \vec{\nabla}_p \epsilon} = \frac{\Delta}{\frac{\vec{\nabla}_p \epsilon}{|\vec{\nabla}_p \epsilon|} \vec{\nabla}_p \epsilon} = \frac{\Delta}{|\vec{\nabla}_p \epsilon|} \end{aligned}$$

Thus we obtain the thickness d of the sheet. Note that the thickness depends on the position on the sheet. The volume element of the sheet can then be written as $d^3p = dA \cdot d$

Thus we can write the volume as

$$D(\epsilon) = \frac{V}{(2\pi\hbar)^3} \oint d^2A_p \frac{1}{|\vec{\nabla}_p \epsilon|}$$



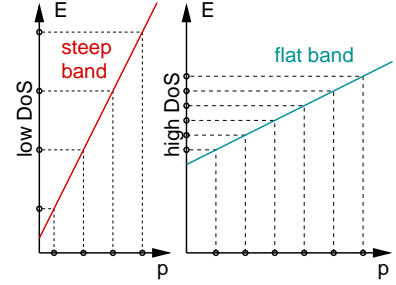
Thus we obtain the density of states from the dispersion relation as

ONE-PARTICLE DENSITY OF STATES PER VOLUME

$$g(\epsilon) \stackrel{\text{def}}{=} \frac{1}{V} D(\epsilon) = \int \frac{d^3 p}{(2\pi\hbar)^3} \delta(\epsilon - \epsilon(\vec{p})) = \frac{1}{(2\pi\hbar)^3} \oint d^2 A_p \frac{1}{|\vec{\nabla}_p \epsilon(p)|} \quad (4.9)$$

Note that $\vec{\nabla}_p \epsilon(p)$ is the velocity (group-velocity) of the particle. This follows from Hamilton's equation $\dot{x}_i = \frac{\partial H(\vec{p}, \vec{x})}{\partial p_i}$. It also follows from the expression of the group velocity of a wave packet $v_i = \frac{\partial \omega(\vec{k})}{\partial k_i} = \frac{\partial \epsilon(\vec{p})}{\partial p_i}$.

Thus the density of states is proportional to the area of a constant energy surface and inversely proportional to the mean velocity of the particles at the constant energy surface. Thus, flat bands, which correspond to slow particles have a large contribution to the density of states. Steep bands, which are related to fast particles, contribute little to the density of states at a given energy, but they contribute over a large energy range.



In the following we will calculate the density of states of two model systems the free particle with and without mass.

4.2.3 Free particle density of states with mass

The dispersion relation of a particle with mass is

$$\epsilon(p) = \frac{p^2}{2m}$$

The density of states is obtained exploiting the fact that $|\vec{p}|$ is constant on a surface of constant energy

$$\begin{aligned} D(\epsilon) &= \frac{V}{(2\pi\hbar)^3} \oint dA \frac{1}{|\nabla_p \epsilon|} = \frac{V}{(2\pi\hbar)^3} \underbrace{4\pi p^2}_{\int dA} \frac{1}{|\vec{p}|/m} \\ &\stackrel{|\vec{p}|=\sqrt{2m\epsilon}}{=} \frac{V}{(2\pi\hbar)^3} 4\pi (\sqrt{2m\epsilon})^2 \frac{1}{\sqrt{2m\epsilon}/m} \\ &= 2\pi V \left(\frac{\sqrt{2m}}{2\pi\hbar} \right)^3 \sqrt{\epsilon} \end{aligned} \quad (4.10)$$

One should remember that the density of states has a square-root behavior in three dimensions. Note however that two-dimensional particles such as a 2-dimensional electron gas has a radically different density of states. A one-dimensional particle, such as an electron in a one-dimensional conductor has a density of states proportional to $\frac{1}{\sqrt{\epsilon}}$, a particle moving in two dimensions has a density of states which is constant.

This model is important to describe the behavior of states at band edges. For example the electron states of a semiconductor at both sides of the Fermi level are the ones relevant for the electric and thermodynamic properties of a semiconductor. When we approximate the band about the minimum to second order, we obtain an approximate dispersion relation

$$\epsilon(p) = \epsilon_c + \frac{1}{2} (\vec{p} - \vec{p}^0) \mathbf{m}^{*-1} (\vec{p} - \vec{p}^0)$$

where ϵ_c is the conduction band minimum, \vec{p}^0 is the momentum of the minimum and \mathbf{m}^* is the effective mass tensor. \mathbf{m}^* is nothing but the inverse of the second derivatives of $\epsilon(\vec{p})$ at the band

edge. It is important to note that the effective mass can be a tensor. Furthermore there may be several degenerate minima, so that one obtained different types of conduction electrons.

Similarly we can expand the top of the valence band to quadratic order about the minimum. These are the hole bands. The mass is negative. Since it is a missing electron that conducts, the hole has also a negative charge. The hole is conceptually analogous to the antiparticle of the electron, the positron. It is quite common that concepts from elementary particle physics carry over into solid state physics. In the latter however the phenomena can be observed at much lower energies and put into practical use.

Interesting is also the behavior in lower dimensions

$$D^d(\epsilon) = \left(\frac{\sqrt{2mL}}{2\pi\hbar} \right)^d S_d \theta(\epsilon) \epsilon^{\frac{d}{2}-1} = \begin{cases} \frac{\sqrt{2mL}}{2\pi\hbar} 2\theta(\epsilon) \epsilon^{-\frac{1}{2}} & \text{for } d = 1 \\ \left(\frac{\sqrt{2mL}}{2\pi\hbar} \right)^2 2\pi\theta(\epsilon) \epsilon & \text{for } d = 2 \\ \left(\frac{\sqrt{2mL}}{2\pi\hbar} \right)^3 4\pi\theta(\epsilon) \epsilon^{\frac{1}{2}} & \text{for } d = 3 \end{cases} \quad (4.11)$$

where $S_d = 2d^{\frac{d}{2}}/\Gamma(\frac{1}{2}d)$, that is $S_1 = 2, S_2 = 2\pi, S_3 = 4\pi$, is the surface area of a unit sphere in d dimensions and $\Gamma(x)$ is the Gamma function (<http://mathworld.wolfram.com/Hypersphere.html>). $\theta(x)$ is the Heaviside step function which vanishes for negative arguments and equals unity for positive arguments.

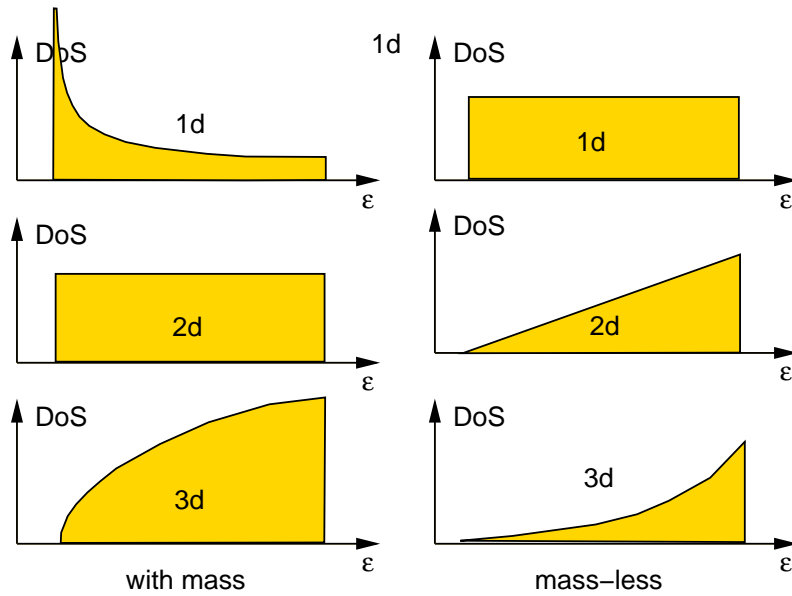


Fig. 4.3: Density of states for particles with and without mass, that is with linear and parabolic dispersion in one, two and three dimensions

4.2.4 Free particle density of states without mass

Mass-less particles are used to describe, for example, the acoustical branch of phonons (lattice vibrations). It can also be used to describe electrons in a metal: In thermodynamics only the electrons near the Fermi level are of relevance, so that the band structure $\epsilon(k)$ can be approximated in this region by a linear dispersion relation. Another example where the dispersion relation is linear is light, i.e. photons.

The dispersion relation of a particle without mass is

$$\epsilon(p) = c|\vec{p}|$$

where c is the speed of light, if we discuss photons, or the speed of sound if we discuss phonons, that is lattice vibrations. For metals c is called the Fermi velocity.

The density of states is obtained exploiting the fact that $|\vec{p}|$ is constant on a surface of constant energy

$$D^d(\epsilon) = \left(\frac{L}{2\pi\hbar c}\right)^d S_d \theta(\epsilon) \epsilon^{d-1} = \begin{cases} \frac{L}{2\pi\hbar c} 2\theta(\epsilon) & \text{for } d = 1 \\ \left(\frac{L}{2\pi\hbar c}\right)^2 2\pi\theta(\epsilon)\epsilon & \text{for } d = 2 \\ \left(\frac{L}{2\pi\hbar c}\right)^3 4\pi\theta(\epsilon)\epsilon^2 & \text{for } d = 3 \end{cases} \quad (4.12)$$

4.3 Real and reciprocal lattice

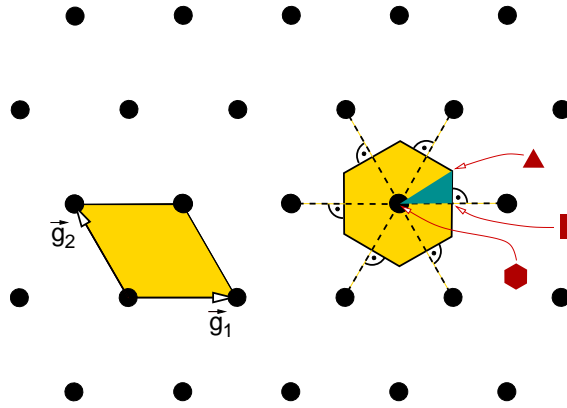


Fig. 4.4: Illustration of the Brillouin zone and high-symmetry points for a plane hexagonal lattice. On the left the unit cell of the reciprocal lattice is shown. On the right the Brillouin zone is shown, which consists of all points that are closer to one lattice point than to any other. In the Brillouin zone there is the irreducible zone, which contains all points that are symmetry inequivalent. The corners of the irreducible zone are high-symmetry points.

Most solids are crystals. This implies that the atoms are located on regular positions. The clearest evidence of this regular arrangement are the crystal faces of gem stones. This arrangement results in a symmetry, the lattice periodicity. Lattice translation symmetry is a discrete translational symmetry.

4.3.1 Real and reciprocal lattice: One-dimensional example

Let us consider a linear chain of hydrogen atoms as the most simple model of a one-dimensionally periodic crystal of hydrogen atoms shown in Fig. 4.5. It is a model system, which is not stable in reality. However it allows to develop the concepts.

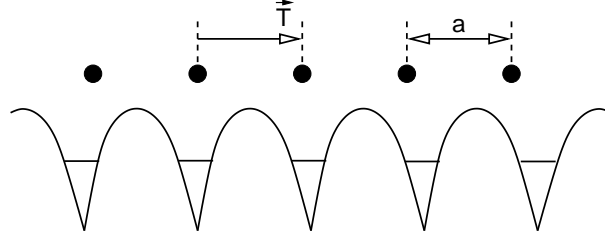


Fig. 4.5: Linear chain of hydrogen atoms. The lattice spacing is a . The balls represent the atoms. The graph sketched below represents the potential as function of position. The primitive lattice vector is \vec{T} which has the length a . The primitive reciprocal lattice vector has the length $2\pi/a$.

The periodicity of the chain implies that for every atom at position \vec{R}_0 there are also equivalent atoms at the positions $\vec{R}_n = \vec{R}_0 + n\vec{T}$, where n is any integer. \vec{T} is the **primitive lattice vector**. **General lattice vectors** are $\vec{t}_n = n\vec{T}$. The primitive lattice vector is the smallest possible lattice vector, that fully describes the lattice periodicity. Its length is called the **lattice constant** a .

Not only the atomic positions are regular, but also the potential is **periodic**, that is $v(\vec{r} + \vec{t}_n) = v(\vec{r})$. A periodic potential has a discrete Fourier transform

$$v(\vec{r}) = \sum_n e^{i\vec{G}_n \vec{r}} V_n$$

where the vectors $\vec{G}_n = n\vec{g}$ are the **general reciprocal lattice vectors**. The **primitive reciprocal lattice vector** is denoted by \vec{g} . The length of the primitive reciprocal lattice vector is inversely proportional to the real-space lattice constant a , that is $|\vec{g}| = \frac{2\pi}{a}$.

4.3.2 Real and reciprocal lattice in three dimensions

Let us now generalize the expressions to three a three-dimensional lattice. Fig. 4.3.2 demonstrates the concepts developed in the following. Corresponding to the three spatial directions there are now three primitive lattice vectors, which we denote by $\vec{T}_1, \vec{T}_2, \vec{T}_3$. Note that in two or three dimensions there is no unique choice of primitive lattice vectors. The three primitive lattice vectors span the **primitive unit cell**.

A general lattice vector $\vec{t}_{i,j,k}$ can be expressed by the **primitive lattice vectors** $\vec{T}_1, \vec{T}_2, \vec{T}_3$ as

$$\vec{t}_{i,j,k} = i\vec{T}_1 + j\vec{T}_2 + k\vec{T}_3 \hat{=} \underbrace{\begin{pmatrix} T_{x,1} & T_{x,2} & T_{x,3} \\ T_{y,1} & T_{y,2} & T_{y,3} \\ T_{z,1} & T_{z,2} & T_{z,3} \end{pmatrix}}_{\mathbf{T}} \begin{pmatrix} i \\ j \\ k \end{pmatrix}$$

where i, j, k are arbitrary integers.

It is often convenient to combine the lattice vectors into a 3×3 matrix \mathbf{T} as shown above. Often the atomic positions \vec{R}_n are provided in **relative positions** \vec{X} which are defined as

$$\vec{R}_n = \mathbf{T} \vec{X}_n \quad \Leftrightarrow \quad \vec{X}_n = \mathbf{T}^{-1} \vec{R}_n$$

A potential is called periodic with respect to these lattice translations, if $V(\vec{r} + \vec{t}_{i,j,k}) = V(\vec{r})$.

RECIPROCAL LATTICE

The reciprocal lattice is given by those values of the wave vector \vec{G} , for which the corresponding plane waves $e^{i\vec{G}\vec{r}}$ have the same periodicity as the real-space lattice.

The primitive reciprocal-lattice vectors \vec{g}_n for $n = 1, 2, 3$ are defined in three dimensions as

$$\vec{g}_n \vec{T}_m = 2\pi \delta_{n,m} \quad (4.13)$$

Thus, in three dimensions the reciprocal lattice vectors can be obtained as

$$\vec{g}_1 = 2\pi \frac{\vec{T}_2 \times \vec{T}_3}{\vec{T}_1 (\vec{T}_2 \times \vec{T}_3)} \quad , \quad \vec{g}_2 = 2\pi \frac{\vec{T}_3 \times \vec{T}_1}{\vec{T}_2 (\vec{T}_3 \times \vec{T}_1)} \quad , \quad \vec{g}_3 = 2\pi \frac{\vec{T}_1 \times \vec{T}_2}{\vec{T}_3 (\vec{T}_1 \times \vec{T}_2)}$$

It is easily shown that these expressions fulfill the defining equation Eq. 4.13 for the reciprocal lattice vectors. Note that the expressions for the second and third lattice vector are obtained from the first by cyclic commutation of the indices.

Because the vector product is perpendicular to the two vectors forming it, every reciprocal lattice vector is perpendicular to two real-space lattice vectors. This brings us to the physical meaning of the reciprocal lattice vectors: Two real space lattice vectors define a lattice plane. A plane can be defined either by two linearly independent vectors in the plane or alternatively by the plane normal. The reciprocal lattice vectors apparently define lattice planes, because they are plane normals.

Let us now consider the distance Δ_n of two neighboring lattice planes. It is obtained by projecting one vector pointing \vec{T}_n from one plane to the other onto a normalized plane normal $\vec{g}_n/|\vec{g}_n|$.

$$\begin{aligned} \Delta_n &= \vec{T}_n \frac{\vec{g}_n}{|\vec{g}_n|} \stackrel{\text{Eq. 4.13}}{=} \frac{2\pi}{|\vec{g}_n|} \\ \Rightarrow \quad |\vec{g}_n| &= \frac{2\pi}{\Delta_n} \end{aligned}$$

PHYSICAL MEANING OF RECIPROCAL LATTICE VECTORS

- The reciprocal lattice vectors are perpendicular to the lattice planes of the real-space lattice.
- The length of the *primitive* reciprocal lattice vectors is 2π divided by the distance of the lattice planes.

We can form a 3×3 matrix \mathbf{g} from the three primitive reciprocal lattice vectors.

$$\mathbf{g} \stackrel{\text{def}}{=} \begin{pmatrix} g_{x,1} & g_{x,2} & g_{x,3} \\ g_{y,1} & g_{y,2} & g_{y,3} \\ g_{z,1} & g_{z,2} & g_{z,3} \end{pmatrix}$$

The definition Eq. 4.13 of the reciprocal lattice vectors can be expressed in matrix form as

$$\mathbf{g}^\top \mathbf{T} \stackrel{\text{Eq. 4.13}}{=} 2\pi \mathbf{1} \quad (4.14)$$

Thus the matrix \mathbf{g} is obtained as

$$\mathbf{g} \stackrel{\text{Eq. 4.14}}{=} 2\pi (\mathbf{T}^{-1})^\top \quad (4.15)$$

The general reciprocal lattice vectors are

$$\vec{G}_{i,j,k} = i\vec{g}_1 + j\vec{g}_2 + k\vec{g}_3$$

The reciprocal lattice vectors play an important role in the Fourier transform of periodic functions. All plane waves that are periodic with the lattice vectors \vec{T}_n are characterized by a reciprocal lattice vector.

$$\begin{aligned} e^{i\vec{G}(\vec{r}+\vec{T}_n)} &= e^{i\vec{G}\vec{r}} \\ \Rightarrow \vec{G}(\vec{r} + \vec{T}_n) &= \vec{G}\vec{r} + 2\pi m_n \\ \Rightarrow \vec{G}\vec{T}_n &= 2\pi m_n \\ \Rightarrow \vec{G}\mathbf{T} &= 2\pi\vec{m} \\ \Rightarrow \vec{G} &= 2\pi\vec{m}\mathbf{T}^{-1} = 2\pi(\mathbf{T}^{-1})^\top \vec{m} \end{aligned}$$

where m_n are integers. The allowed values for \vec{G} are exactly those of the reciprocal lattice. This was the motivation for the definition Eq. 4.14.

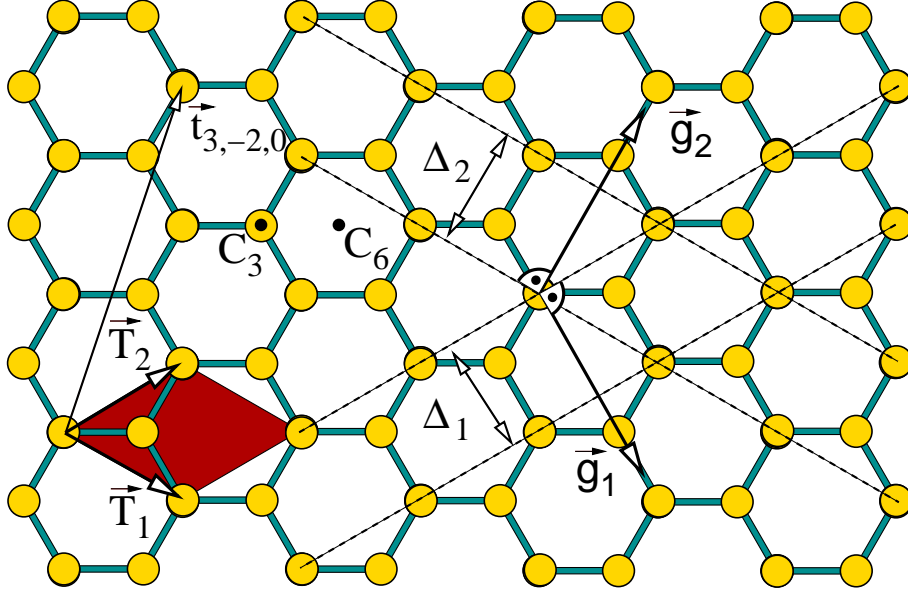


Fig. 4.6: Translational and rotational symmetry of a single graphite sheet and demonstration of reciprocal lattice vectors. Graphite is a layered material, which consists of sheets as the one shown. The yellow balls indicate the carbon atoms and the blue sticks represent the bonds. In graphite these two-dimensional sheets are stacked on top of each other, where every second sheet is shifted such that an atom falls vertically below the point indicated by C_6 . Here we only consider the symmetry of a single sheet. The elementary unit cell is indicated by the red parallelogram, which is spanned by the elementary lattice vectors \vec{T}_1 and \vec{T}_2 . The third lattice vector points perpendicular to the sheet towards you. An example for a general lattice vector is $\vec{t}_{3,-2,0} = 3\vec{T}_1 - 2\vec{T}_2 + 0\vec{T}_3$. The lattice planes indicated by the dashed lines. The lattice planes are perpendicular to the sheet. The distance of the lattice planes are indicated by Δ_1 and Δ_2 . The elementary reciprocal lattice vectors are \vec{g}_1 and \vec{g}_2 . The third reciprocal lattice vector points perpendicular out of the plane towards you. Note that the reciprocal lattice vectors have the unit "inverse length". Thus their length is considered irrelevant in this real space figure. The axis through C_3 standing perpendicular to the plane is a three-fold rotation axis of the graphite crystal. The axis through C_6 perpendicular to the plane is a 6-fold rotation axis of the graphite sheet, but only a three-fold rotation axis of the graphite crystal. (Note that a rotation axis for the graphite crystal must be one for both sheets of the crystal). In addition there is a mirror plane lying in the plane. Furthermore there are several mirror planes perpendicular to the plane: One passing through every atom with one of the three bonds lying in the plane and one perpendicular each bond passing through the bond center.

4.4 Bloch Theorem

In order to make the description of an infinite crystal tractable, we exploit translational symmetry to block-diagonalize the Hamiltonian. The theoretical basis is Bloch's theorem.

BLOCH'S THEOREM

The eigenstates of the Hamiltonian with crystal symmetry $\hat{S}(\vec{t})$, i.e. $[\hat{H}, \hat{S}(\vec{t})]_- = 0$, can be written as a product

$$\psi_{\vec{k},n}(\vec{r}) = \vec{u}_{\vec{k},n}(\vec{r})e^{i\vec{k}\vec{r}} \quad (4.16)$$

of a periodic function $u_{\vec{k},n}(\vec{r})$ with a plane wave $e^{i\vec{k}\vec{r}}$. $\hat{S}(\vec{t})$ is a translation operator for the real space translation vector \vec{t} .

...or...

The Hamiltonian of a crystal is block diagonal for Bloch states, that is

$$\langle \psi_{\vec{k}} | \hat{H} | \psi_{\vec{k}'} \rangle = 0 \quad \text{for } \vec{k} \neq \vec{k}'$$

when

$$\psi_{\vec{k}}(\vec{r}) = \vec{u}_{\vec{k}}(\vec{r})e^{i\vec{k}\vec{r}} \quad \text{where } u_{\vec{k}}(\vec{r} + \vec{t}) = u_{\vec{k}}(\vec{r})$$

The underlying idea of Bloch's theorem is to Block-diagonalize the Hamiltonian by finding the eigenstates of the translation operators.

Let $\hat{S}(\vec{t})$ be the translation operator for a given lattice translation $\vec{t} = \vec{T}_1 i + \vec{T}_2 j + \vec{T}_3 k$.

$$\hat{S}(\vec{t}) = \int d^3r |\vec{r} + \vec{t}\rangle \langle \vec{r}| \quad (4.17)$$

Translation operator and canonical momentum

A general theorem is that any translation for an unbounded continuous variable can be expressed by the canonical momentum.

$$\hat{S}(\vec{t}) = e^{-\frac{i}{\hbar} \hat{p} \vec{t}} \quad (4.18)$$

This relation will be used for the Proof of Bloch's theorem. It is discussed to some extent in ΦSX: Quantum Physics. Let us anyway go quickly over the proof.

Proof of Eq. 4.18:

1. First we define a basis of momentum eigenstates¹

$$\begin{aligned} \hat{p}|\vec{p}\rangle &= |\vec{p}\rangle \vec{p} && \text{eigenvalue equation} \\ \langle \vec{p} | \vec{p}' \rangle &= (2\pi\hbar)^3 \delta(\vec{p} - \vec{p}') && \text{orthonormality} \\ \hat{1} &= \int \frac{d^3p}{(2\pi\hbar)^3} |\vec{p}\rangle \langle \vec{p}| && \text{completeness} \end{aligned}$$

The real space wave function of the momentum eigenstates are plane waves

$$\langle \vec{r} | \vec{p} \rangle = e^{\frac{i}{\hbar} \vec{p} \vec{r}} \quad \text{real space representation}$$

which provides a transformation between the momentum and position eigenstates.

2. Let us now work out a matrix element that we will need in the following:

$$\langle \vec{r} | e^{-\frac{i}{\hbar} \hat{p} \vec{t}} | \vec{p} \rangle = \underbrace{\langle \vec{r} | \vec{p} \rangle}_{e^{\frac{i}{\hbar} \vec{p} \vec{r}}} e^{-\frac{i}{\hbar} \vec{p} \vec{t}} = e^{\frac{i}{\hbar} \vec{p}(\vec{r} - \vec{t})} = \langle \vec{r} - \vec{t} | \vec{p} \rangle$$

¹There are various definitions for momentum eigenstates in the literature, that differ by their normalization.

3. Now we are ready to bring the operator defined by Eq. 4.18 into the form Eq. 4.17, which is the definition of the translation operator.

$$\begin{aligned}
 e^{-\frac{i}{\hbar} \hat{p} \vec{t}} &= \underbrace{\int d^3 r |\vec{r}\rangle \langle \vec{r}|}_{\hat{1}} e^{-\frac{i}{\hbar} \hat{p} \vec{t}} \underbrace{\int \frac{d^3 p}{(2\pi\hbar)^3} |\vec{p}\rangle \langle \vec{p}|}_{\hat{1}} \\
 &= \int d^3 r |\vec{r}\rangle \int \frac{d^3 p}{(2\pi\hbar)^3} \underbrace{\left(\langle \vec{r} | e^{-\frac{i}{\hbar} \hat{p} \vec{t}} | \vec{p} \rangle \right)}_{\langle \vec{r} - \vec{t} | \vec{p} \rangle} \langle \vec{p} | \\
 &= \int d^3 r |\vec{r}\rangle \langle \vec{r} - \vec{t} | \underbrace{\int \frac{d^3 p}{(2\pi\hbar)^3} |\vec{p}\rangle \langle \vec{p}|}_{\hat{1}} \\
 &= \int d^3 r |\vec{r} + \vec{t}\rangle \langle \vec{r} | \stackrel{\text{Eq. 4.17}}{=} \hat{S}(\vec{t}) \quad \text{q.e.d}
 \end{aligned}$$

Proof of Bloch's theorem

Let us assume that $|\psi\rangle$ is an eigenstate of the lattice translation, i.e.

$$\underbrace{\langle \vec{r} | \hat{S}(\vec{t}) | \psi \rangle}_{\psi(\vec{r} - \vec{t})} \stackrel{\text{Eq. 4.18}}{=} \underbrace{\langle \vec{r} | \psi \rangle}_{\psi(\vec{r})} \underbrace{e^{-\frac{i}{\hbar} \vec{p} \vec{t}}}_{e^{-i\vec{k} \vec{t}}}$$

Now we multiply this equation with $e^{-i\vec{k}(\vec{r} - \vec{t})}$

$$\psi(\vec{r} - \vec{t}) e^{-i\vec{k}(\vec{r} - \vec{t})} = \psi(\vec{r}) e^{-i\vec{k} \vec{r}}$$

which says that the function u defined as

$$u(\vec{r}) = \psi(\vec{r}) e^{-i\vec{k} \vec{r}}$$

is periodic. Thus the eigenstate of the lattice translation is a product of a periodic function $u(\vec{r})$ and a plane wave.

We have shown before that the eigenstates of a Hamiltonian can be expressed a superposition of eigenstates of its symmetry operator. Thus also the eigenstates of the Hamiltonian with lattice symmetry can be written in the form of a Bloch wave, and the wave vector is a quantum number for this system. This finishes the proof of Bloch's theorem.

4.5 Reduced zone scheme

Because the function $u_k(\vec{r})$ has only Fourier components at the reciprocal lattice vectors, it is periodic with the real space lattice symmetry.

This is the reason why band structures are not represented in an **extended zone scheme** but in a **reduced zone scheme**.

- in the extended zone scheme the band structure of free electrons would be a single parabola, and would extend to infinity in reciprocal space.
- in the **periodic zone scheme**, the free electron would consists of many parabola centered at the reciprocal lattice points. Thus, the reciprocal zone scheme is periodic with the periodicity of the reciprocal lattice.

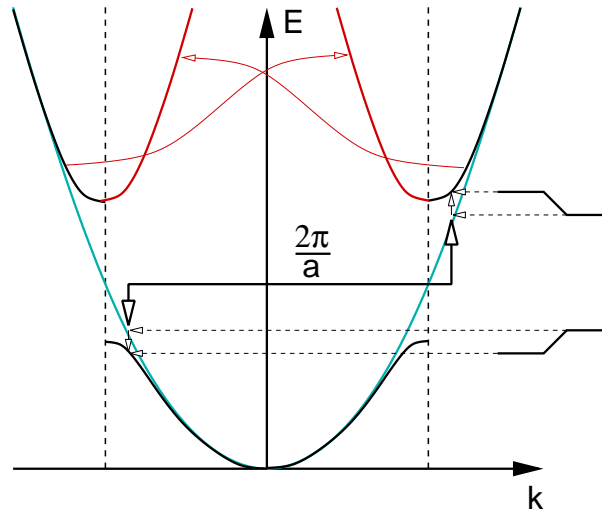


Fig. 4.7: Schematic demonstration how a periodic potential results in a coupling between states with the same wave vector in the reduced zone scheme

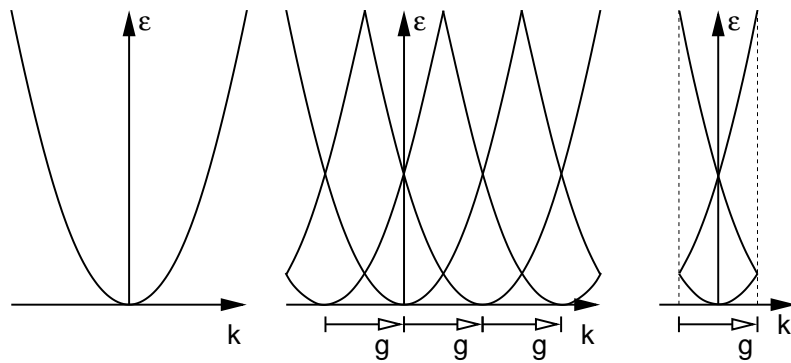


Fig. 4.8: Extended, periodic and reduced zone scheme for a one-dimensional free particle.

- in the reduced zone scheme, only the irreducible part of the periodic zone scheme is shown, that is one single repeat unit. The band structures shown in Fig. 4.1 are in a reduced zone scheme. There are several choices for the repeat units of the reciprocal lattice. One choice is simply the primitive unit cell of the reciprocal lattice. However, the shape of the unit cell does not have the point-group symmetry of the reciprocal lattice. Therefore one instead chooses the **Wigner Seitz cell**² of the reciprocal lattice, which is called the **Brillouin zone**.

In the reduced zone scheme, all wave vectors connected by a reciprocal lattice vector, fall on top of the same point in the Brillouin zone. Thus, a Hamiltonian that has lattice periodicity couples all points that lie at the same point in the Brillouin zone. This is demonstrated in Fig. 4.7.

From perturbation theory we know that the splitting of two interacting states is large when the two states are close or even degenerate. Thus the largest effect in the band structure occurs right at the boundary of the irreducible zone, where the degeneracy of the free electron gas is lifted by the periodic potential. Thus, local band gaps appear at the surface of the Brillouin zone. This band gap, however, is usually warped, so that there is no energy window, that completely lies in all local band gaps. In that case the material remains a metal.

²The Wigner Seitz cell of a lattice consists of all points that are closer to the origin than to any other lattice point. Thus, it is enclosed by planes perpendicular to the lattice vectors cutting the lattice vector in half.

4.6 Bands and orbitals

So far we have discussed the band structures as a variation of the dispersion relation of the free electron bands. However this point of view obscures the relation to chemical binding and the local picture of the wave functions.

The band structure can also be constructed starting from local orbitals. This is demonstrated here for the two-dimensional square lattice with atoms having s- and p-orbitals in the plane.

In order to simplify the work, we restrict ourselves to the high symmetry points Γ , X and M of the two-dimensional reciprocal unit cell.

The real space lattice vectors are

$$\vec{T}_1 = \begin{pmatrix} 1 \\ 0 \end{pmatrix} a \quad \text{and} \quad \vec{T}_2 = \begin{pmatrix} 0 \\ 1 \end{pmatrix} a$$

The corresponding reciprocal space lattice vectors are

$$\vec{g}_1 = \begin{pmatrix} 1 \\ 0 \end{pmatrix} \frac{2\pi}{a} \quad \text{and} \quad \vec{g}_2 = \begin{pmatrix} 0 \\ 1 \end{pmatrix} \frac{2\pi}{a}$$

The high-symmetry points are

$$k_\Gamma = 0 = \begin{pmatrix} 0 \\ 0 \end{pmatrix} \frac{2\pi}{a} \quad ; \quad k_X = \frac{1}{2}\vec{g}_1 = \begin{pmatrix} 1 \\ 0 \end{pmatrix} \frac{\pi}{a} \quad \text{and} \quad k_M = \frac{1}{2}(\vec{g}_1 + \vec{g}_2) = \begin{pmatrix} 1 \\ 1 \end{pmatrix} \frac{\pi}{a}$$

The first step is to construct Bloch waves out of the atomic orbitals, by multiplying them with $e^{i\vec{k}\vec{T}}$, where \vec{T} is the lattice translation of the atom relative to the original unit cell. This is illustrated in Fig. 4.9 on page 71.

- At the Γ , the phase factor for a lattice translation of the orbital is one. Thus we repeat the orbital from the central unit cell in all other unit cells.
- At the X point, the phase factor for a lattice translation along the first lattice vector is $e^{i\vec{k}_X\vec{T}_1} = e^{i\pi} = -1$ and the phase factor for the lattice translation along the second lattice vector \vec{T}_2 is $e^{i\vec{k}_X\vec{T}_2} = +1$. Thus if we go to the right the sign of the orbital alternates, while in the vertical direction the orbital remains the same.
- At the M point, the phase factor alternates in each lattice direction, resulting in a checkerboard pattern.

Next we need to set up the Hamilton matrix elements for each k-point, using the Slater-Koster parameters. For a back-on-the-envelope estimate the nearest neighbor matrix elements will be sufficient. The matrix elements are firstly ϵ_s and ϵ_p , the energies of the orbitals without any hybridization. Secondly we need the hopping matrix elements $t_{ss\sigma}$, $t_{pp\sigma}$, $t_{pp\pi}$. In principle we would also need $t_{sp\sigma}$, but that matrix element will not be needed in our example.

In our simple example, the Bloch states are already eigenstates of the Hamiltonian so that we only need to calculate their energy. We obtain

Γ	X	M
$\epsilon_p + t_{pp\sigma} - t_{pp\pi}$	$\epsilon_p + t_{pp\sigma} + t_{pp\pi}$	$\epsilon_p - t_{pp\sigma} + t_{pp\pi}$
$\epsilon_p + t_{pp\sigma} - t_{pp\pi}$	$\epsilon_p - t_{pp\sigma} - t_{pp\pi}$	$\epsilon_p - t_{pp\sigma} + t_{pp\pi}$
$\epsilon_s + 2t_{ss\sigma}$	ϵ_s	$\epsilon_s + 2t_{ss\sigma}$

If there is a band structure available, we can estimate the Hamilton matrix elements from that. Otherwise we just make an educated guess.

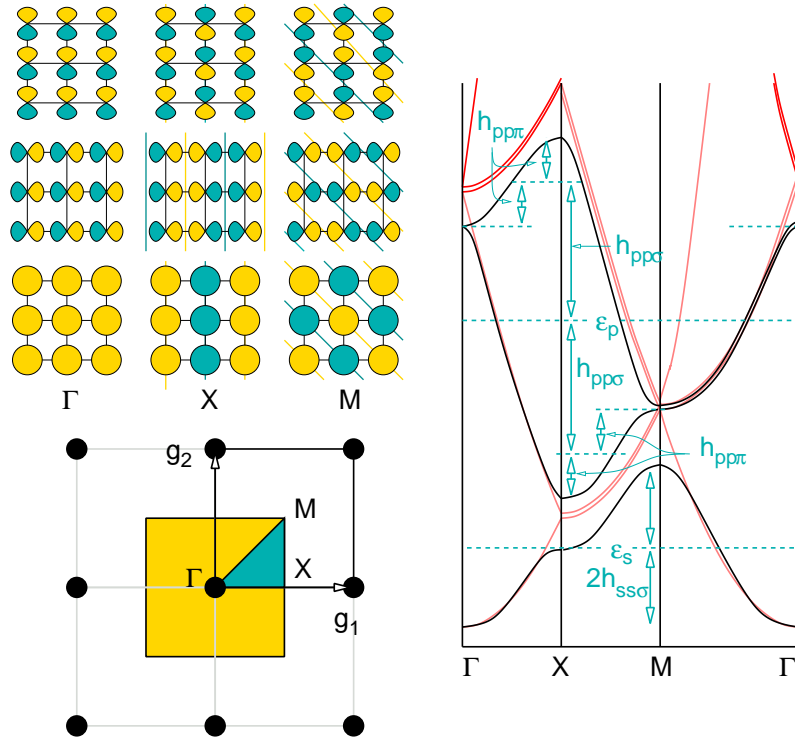


Fig. 4.9: Illustration of a band structure in real and reciprocal space for a planar square lattice. Bottom left: The reciprocal lattice is spanned by the reciprocal lattice vectors \vec{g}_1 and \vec{g}_2 . The yellow square is the corresponding Brillouin zone. The green inset is the Brillouin zone, whose corners are the high symmetry points Γ , X and M . On the top left the corresponding basis functions made from one s-orbital and two p-orbitals in a Bloch-basis are shown. These states are also eigenstates of the Hamiltonian, because the coupling vanishes due to point group symmetry at the high-symmetry points. On the top right a schematic band structure is shown and compared to a free-electron band (red).

4.7 Calculating band structures in the tight-binding model

Now we wish to calculate the band structure. Let us begin with a tight-binding basisset with the usual assumption that the tight-binding orbitals shall be orthogonal. The tight-binding orbitals shall be represented by kets $|\vec{r}, \alpha\rangle$, where \vec{r} denotes a discrete lattice-translation vector and α denotes the type of the orbital such as an s , p_x , p_y , p_z , ... orbital on a specific site in the unit cell.

A Bloch wave can be represented as

$$\begin{aligned}
 |\Psi_{\vec{k},n}\rangle &= \sum_{\vec{r},\alpha} |\vec{r},\alpha\rangle \langle \vec{r},\alpha | \Psi_{\vec{k},n}\rangle \\
 &\stackrel{\text{Eq. 4.16}}{=} \sum_{\vec{r},\alpha} |\vec{r},\alpha\rangle \langle \vec{r},\alpha | \int d^3r |\vec{r}\rangle e^{i\vec{k}\vec{r}} \langle \vec{r} | u_{\vec{k},n}\rangle \\
 &= \sum_{\vec{r},\alpha} |\vec{r},\alpha\rangle e^{i\vec{k}\vec{r}} \langle \vec{r},\alpha | \int d^3r |\vec{r}\rangle e^{i\vec{k}(\vec{r}-\vec{r})} \langle \vec{r} | u_{\vec{k},n}\rangle \\
 &\stackrel{u(\vec{r})=u(\vec{r}-\vec{r})}{=} \sum_{\vec{r},\alpha} |\vec{r},\alpha\rangle e^{i\vec{k}\vec{r}} \langle \vec{r},\alpha | \int d^3r |\vec{r}\rangle e^{i\vec{k}(\vec{r}-\vec{r})} \langle \vec{r}-\vec{r} | u_{\vec{k},n}\rangle \\
 &\stackrel{\vec{r}\rightarrow\vec{r}+\vec{r}}{=} \sum_{\vec{r},\alpha} |\vec{r},\alpha\rangle e^{i\vec{k}\vec{r}} \int d^3r \underbrace{\langle \vec{r},\alpha | \vec{r}+\vec{r} \rangle}_{\langle \vec{0},\alpha | \vec{r} \rangle} e^{i\vec{k}\vec{r}} \underbrace{\langle \vec{r} | u_{\vec{k},n}\rangle}_{\langle \vec{r} | \Psi_{\vec{k},n}\rangle} \\
 &= \sum_{\vec{r},\alpha} |\vec{r},\alpha\rangle e^{i\vec{k}\vec{r}} \langle \vec{0},\alpha | \Psi_{\vec{k},n}\rangle \tag{4.19}
 \end{aligned}$$

This shows us how we can represent the entire wave function with a vector $c_\alpha = \langle \vec{0},\alpha | \Psi_{\vec{k},n}\rangle$, which has the dimension of the number of orbitals in the elementary unit cell.

Our next goal is to find an equation for this vector. We will use the matrix elements of the Hamilton operator in the basis of tight-binding orbitals

The Hamilton operator in the basis of tight-binding orbitals is

$$\langle \vec{r},\alpha | \hat{H} | \vec{r}',\beta \rangle = h_{\vec{r},\alpha,\vec{r}',\beta}$$

Now let us work use the Schrödinger equation

$$\begin{aligned}
 \hat{H} |\Psi_{\vec{k},n}\rangle &= |\Psi_{\vec{k},n}\rangle \epsilon_{k,n} \\
 \stackrel{\text{Eq. 4.19}}{\Rightarrow} \sum_{\vec{r},\alpha} \hat{H} |\vec{r},\alpha\rangle e^{i\vec{k}\vec{r}} \langle \vec{0},\alpha | \Psi_{\vec{k},n}\rangle &= \sum_{\vec{r},\alpha} |\vec{r},\alpha\rangle e^{i\vec{k}\vec{r}} \langle \vec{0},\alpha | \Psi_{\vec{k},n}\rangle \epsilon_{k,n} \\
 \stackrel{\langle \vec{0},\beta |}{\Rightarrow} \sum_{\vec{r},\alpha} \underbrace{\langle \vec{0},\beta | \hat{H} | \vec{r},\alpha \rangle}_{h_{\vec{0},\beta,\vec{r},\alpha}} e^{i\vec{k}\vec{r}} \langle \vec{0},\alpha | \Psi_{\vec{k},n}\rangle &= \sum_{\vec{r},\alpha} \underbrace{\langle \vec{0},\beta | \vec{r},\alpha \rangle}_{\delta_{\vec{0},\vec{r}} \delta_{\alpha,\beta}} e^{i\vec{k}\vec{r}} \langle \vec{0},\alpha | \Psi_{\vec{k},n}\rangle \epsilon_{k,n} \\
 \Rightarrow \underbrace{\left[\sum_{\vec{r},\alpha} h_{\vec{0},\beta,\vec{r},\alpha} e^{i\vec{k}\vec{r}} \right]}_{h_{\alpha,\beta}(\vec{k})} \langle \vec{0},\alpha | \Psi_{\vec{k},n}\rangle &= \langle \vec{0},\beta | \Psi_{\vec{k},n}\rangle \epsilon_{k,n}
 \end{aligned}$$

Thus we obtained a k -dependent eigenvalue equation in matrix form with a finite and usually small dimension. This problem can be broken down into smaller subproblems, if we exploit the symmetry arguments that we used earlier for the molecules. Symmetry can be used especially at the high-symmetry points and lines in reciprocal space, where the band structure is usually represented.

Worked example

Let us consider the example of a linear chain of s -orbitals. The infinite Hamiltonian has the form

$$\mathbf{h} = \begin{pmatrix} \epsilon_s & h_{ss\sigma} & 0 & \dots \\ h_{ss\sigma} & \epsilon_s & h_{ss\sigma} & 0 & \dots \\ 0 & h_{ss\sigma} & \epsilon_s & h_{ss\sigma} & 0 & \dots \\ \dots & 0 & h_{ss\sigma} & \epsilon_s & h_{ss\sigma} & 0 & \dots \\ \vdots & & 0 & h_{ss\sigma} & \epsilon_s & h_{ss\sigma} & 0 \end{pmatrix}$$

The Hamilton matrix elements can also be written as

$$h_{i,1,j,1} = \sum_i \epsilon_s \delta_{i,j} + h_{ss\sigma} (\delta_{i,j+1} + \delta_{i,j-1})$$

Thus the k-dependent Hamiltonian yields

$$\epsilon(k) = \epsilon_s + 2h_{ss\sigma} \cos(k)$$

Note that $h_{ss\sigma}$ is negative, because it is approximately equal to the overlap matrix element multiplied with the potential in the bond-center. The potential is negative.

Chapter 5

From atoms to solids

In this chapter I want to describe how one can construct an approximate density of states for materials. The density of states in turn already provides insight into many of the electronic properties of a material. A rough density of states can already be constructed without the knowledge of the atomic structure of a material. Much of it depends only on the composition.

5.1 The Atom

5.1.1 The generalized hydrogen atom

When we think of an atom the first thought is the generalized hydrogen atom. A generalized hydrogen atom is an atom with **non-interacting electrons**, which may have any atomic number Z . The Schrödinger equation of the generalized hydrogen atom can be solved analytically.

The energy levels of a generalized hydrogen atom are

$$\epsilon_{n,\ell,m,s} = -\frac{m_e e^4}{(4\pi\epsilon_0 \hbar)^2} \frac{Z^2}{2n^2}$$

The states are characterized by the quantum numbers

- the principal quantum number n
- the angular momentum quantum number $\ell \in \{0, \dots, n-1\}$. The main angular momenta are also indicated by the letters s, p, d, f for $\ell = 0, 1, 2, 3$.
- the magnetic quantum number $m \in \{-\ell, \dots, \ell\}$
- the spin quantum number $s \in \{\uparrow, \downarrow\}$.

Many of these quantum numbers are degenerate.

- The degeneracy of different angular momentum quantum numbers ℓ is a consequence of the Z/r potential, which has a dynamical symmetry that conserves the so-called **Laplace-Runge-Lenz vector**¹. This degeneracy is lifted as soon as the potential obtains a shape different from the $1/r$ shape.
- The degeneracy of the magnetic quantum number is a consequence of the spherical symmetry of the atom.

¹See ΦSX: Quantum mechanics, Appendix “ ℓ degeneracy of the hydrogen atom”.

- The degeneracy of the spin eigenvalues is there simply because it does not enter the Hamiltonian.

The generalized hydrogen atom has the following multiplets

n	degeneracy	valence configuration
1	2	2s
2	8	2s+6p
3	18	2s+6p+10d
4	32	2s+6p+10d+14f
5	50	2s+6p+10d+14f+18g
6	72	2s+6p+10d+14f+18g+22h
7	88	2s+6p+10d+14f+18g+22h+16i

5.1.2 Lifting the ℓ -degeneracy: Aufbau principle

The generalized hydrogen atom assumes that the electrons do not interact with each other. If we consider the Coulomb repulsion between the electrons, each electron effectively sees not only the nucleus, but the entire core including the inner electrons.

As a result, the outer electrons experience a potential of the form

$$v_{eff}(r) = \frac{-Z_{eff}e^2}{4\pi\epsilon_0 r}$$

where the effective atomic number $Z_{eff} = Z - N_{core}$ is given by the charge of the nucleus and those of the inner electrons, the core electrons.

Quite a few observations can be rationalized by the simple model, that the Coulomb potential of the nucleus is screened by the inner electrons.

- **Screening of the nuclear Coulomb attraction:** The bare Coulomb potential is too attractive and would place the valence electrons at much too low energy. If the atomic number is reduced to the effective atomic number, the valence electrons of all atoms are placed in a similar energy region. This explains why atoms in the same group behave similar, and why the period they belong to is secondary.
- **Lifting the ℓ degeneracy:** The observation is that
 - for a given atom, the s -electrons always lie below the p -electrons with the same principal quantum number and that
 - the $3d$ -electrons become occupied only in the 4-th period instead of the 3rd period and
 - that the $4d$ -electrons become occupied only in the 6-th period instead of the 4th period

This effect can be traced to the contraction of the core orbitals.

The “accidental” ℓ degeneracy of the generalized hydrogen atom can be described as a balance between zentrifugal force and core repulsion, that both act against the nuclear Coulomb attraction.

- The zentrifugal force puts a penalty onto states with larger angular momentum. A higher angular momentum implies a stronger zentrifugal force, that pushes electrons away from then nucleus.²

²The concept of zentrifugal force can be seen in the radial Schrödinger equation for the radial $R(r)$ part of the

- **Core repulsion**, on the other hand, puts a penalty to states with lower angular momentum. Core repulsion only acts between electrons with the same angular momentum³. Because there are more core shells with lower angular momentum, the core repulsion acts stronger on the low-angular momentum states.

In the real atom the subtle balance between zentrifugal force and core repulsion is broken, because the inner electrons are more contracted so that the core repulsion is weakened. The reduced core repulsion stabilizes⁴ the states with lower angular momentum.

The core electrons are contracted because there are less inner electron-shells screening the nuclear attraction of the core shells than of the valence electrons.

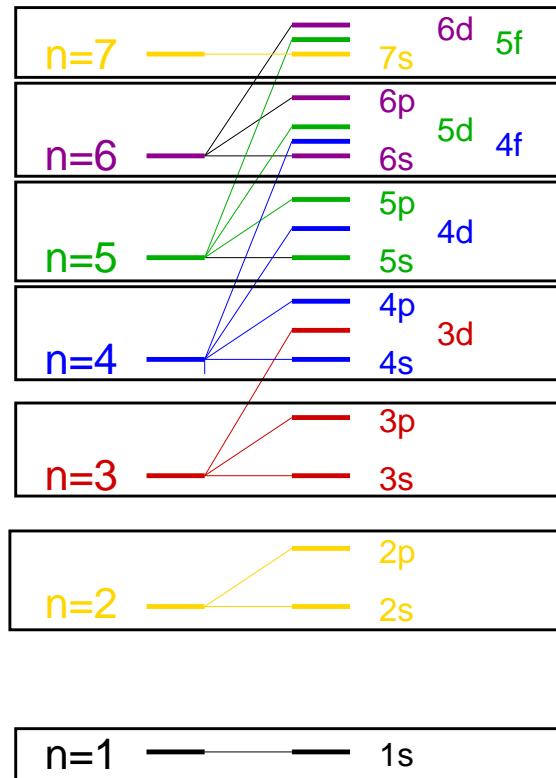


Fig. 5.1: Aufbau principle. Shown is a hypothetical energy diagram constructed such that the occupation from bottom up directly leads to the periodic table. (I have drawn the figure such that it suggests an upward shift of shells with higher angular momentum. This may be misleading as we trace the origin to a stabilization of shells with lower angular momentum.)

wave function $\Psi(\vec{r}) = R(|\vec{r}|)Y_{\ell,m}(\vec{r})$

$$\left(-\frac{\hbar^2}{2m} \partial_r^2 + \underbrace{\frac{\hbar^2}{2m} \frac{\ell(\ell+1)}{r^2}}_{v_{zf}(r)} - \frac{Ze^2}{2m_0 r} - \epsilon_n \right) rR(r) = 0$$

The radial part experiences an additional ℓ -dependent potential that pushes the electrons away from the nucleus.

³Core repulsion is due to the condition that wave functions are orthogonal. This condition in turn is a consequence of the Pauli principle. Because states with different angular momentum are orthogonal by their angular motion, there is no additional effect from core orthogonalization. Core repulsion is a variant of Pauli repulsion.

⁴shifts the energy levels down in energy

Radial extent is determined by principal quantum number

The radial extent of the orbitals is, surprisingly, rather similar for orbitals with the same principal quantum number n . A consequence is that the 4s and 4p orbitals in a transition metal behave almost like free electrons, while the 3d-orbitals are core-like and interact only weakly with neighboring atoms.

This explains that the d-electrons of transition metal elements form weak bonds that can be broken easily. This makes them ideal for catalytic behavior. A catalyst must form a bond with the transition state of a reaction, thus lowering the reaction barrier, but this bond must also be able to break again, so that the catalyst can return into its original form. The f-electrons behave like true core electrons, with the exception that the f-shell is only partially filled.

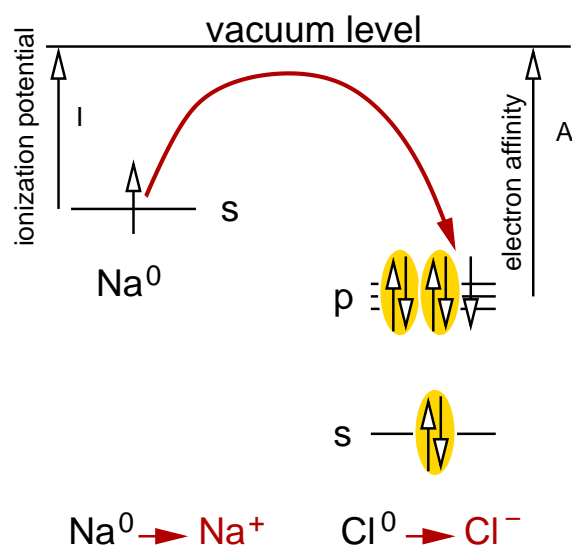
The crossing of 3d and 4s orbitals for increasing atomic number is evident from the periodic table. However, in compounds it is much less evident. In a compound, transition metals normally lose their s-electrons. Because the s-electrons are located far from the nucleus, they experience the Pauli repulsion from the electrons of any neighboring atoms. This shifts their electron levels up, so that the s-electrons are transferred into the d-shell. We could say that the Pauli repulsion by the core electrons is compensated by that of the neighboring atoms.

Even when the metals are in their elemental form, these metals can be considered cations immersed into a free electron gas formed by the s-electrons.

5.2 From atoms to ions

5.2.1 Ionization potential and electron affinity

Even before atoms are brought together, they may already exchange electrons. This is the onset for the formation of an ionic bond. My experience is that this should be the first step to rationalize chemical bonding in compounds made from different atoms.



The energy to move an electron to the **vacuum level** is the **ionization potential**. The energy to move an electron from the vacuum level to an atom is called the **electron affinity**.

Thus the energy gained by transferring electrons is the difference between the ionization potential and the electron affinity.

$$\Delta E_1 = A - I$$

Once the ions are formed, they attract each other electrically, and additional energy

$$\Delta E_2 = \frac{Q_1 Q_2}{4\pi\epsilon_0 |\vec{R}_1 - \vec{R}_2|}$$

is gained by bringing them closer together.

The third effect playing a role is the onsite Coulomb repulsion of the electrons. Adding a second electron to an atom is more difficult than adding the first, because the two additional electrons repel each other. Therefore, the electron gain for transferring electrons becomes weaker with each electron already transferred.

The direction of the charge transfer can be read from the **electronegativities**. Mulliken's electronegativity[11] is proportional to the mean value of electron affinity and ionization potential. Electrons are transferred from the electropositive (less electronegative) atoms to the more electronegative atoms. Therefore the first step that we consider when bringing atoms into a material, is to transfer electrons, so that the electropositive atoms give electrons to electronegative atoms. Electropositive atoms are predominantly to the left of the periodic table and electronegative atoms are on the right.

The limit for the electron transfer is reached when an electron shell is completely full or empty.

5.2.2 Oxidation states and electron count

In my experience, the best way to rationalize the electronic structure of a solid material is to use the fully ionic model as starting point.

This electron transfer is not always unique. If it is not obvious how the electrons are transferred, one can consider both choices or select one of them. If it is not obvious how to choose, it is also not important.

Let us do some examples. Use the periodic table to identify the number and type of available valence electrons.

- $\text{NaCl} \rightarrow \text{Na}^+ \text{Cl}^-$
- $\text{MgO} \rightarrow \text{Mg}^{2+} \text{O}^{2-}$
- $\text{SiO}_2 \rightarrow \text{Si}^{4+} \text{O}_2^{2-}$
- $\text{SrTiO}_3 \rightarrow \text{Sr}^{2+} \text{Ti}^{4+} \text{O}_3^{2-}$
- $\text{LaAlO}_3 \rightarrow \text{La}^{3+} \text{Al}^{3+} \text{O}_3^{2-}$
- $\text{CaMnO}_3 \rightarrow \text{Ca}^{2+} \text{Mn}^{4+} \text{O}_3^{2-}$. The Mn atom keeps three some of its seven d-electrons. The number of d-electrons left on Mn is determined by the number of electrons that can be passed to the oxygen atoms
- $\text{CO}_2 \rightarrow \text{C}^{4+} \text{O}_2^{2-}$
- $\text{GaAs} \rightarrow \text{Ga}^{3+} \text{As}^{3-}$. GaAs is a *III – V* compound. It belongs to the same structural class as silicon, but instead of four-valent electrons its consists of atoms with three and with five valence electrons.

Interesting is the case at surfaces or interfaces. Take as an example the interface between SrTiO_3 and LaAlO_3 . SrTiO_3 is a perovskite which consists of alternating planes of TiO_2 and SrO . LaAlO_3 has the same structure wit planes of AlO_2 and LaO . A the interface a 2-dimensional electron gas is formed because the charges at the interface cannot becompensated.

Another case is the polar (111) surface of an oxide such as Al_2O_3 . The oxide has alternating layers of Al and O. At the oxygen terminated surface there is a net charge. This charge has to enter

the Al-states, which is unfavorable. In humid air, it can also react with water so that the oxygen atoms are converted into hydroxyl groups having less net charge.

A common misconception is that the ionic construction reflects the real charge distribution. There are various definitions of the charge of an atom. Here we use the concept of an oxidation state. What we use here are the oxidation states. The oxidation state is an extremely valuable tool to predict the position of band gaps and of the stability of a material.

The **oxidation state** is a hypothetical charge that an atom would have if all bonds would be fully ionic. (See IUPAC definition on p. 80)

The oxidation state is based on the convention that an electron is fully attributed to the more electron acceptor. In reality, however, this orbital is a superposition of orbitals of electron donor and electron acceptor. Therefore some of the charge distribution remains at the electron donor. This explains the seeming contradiction between charge distribution and formal charges.

Even for an ionic compound, the charge density does not deviate much from that of overlapping atomic charge densities. The formation of an ionic bond does not lead to a large rearrangement of the charge distribution because of the following: The electrons of an electropositive atom are loosely bound and therefore located at large distance from the nucleus. In a compound, the nearest neighbors are located at the same distance, so that little charge rearrangement is required to transfer an electron.

OXIDATION STATE

"A measure of the degree of oxidation of an atom in a substance. It is defined as the charge an atom might be imagined to have when electrons are counted according to an agreed-upon set of rules:

1. the oxidation state of a free element (uncombined element) is zero;
2. for a simple (monatomic) ion, the oxidation state is equal to the net charge on the ion;
3. hydrogen has an oxidation state of 1 and oxygen has an oxidation state of -2 when they are present in most compounds. (Exceptions to this are that hydrogen has an oxidation state of -1 in hydrides of active metals, e.g. LiH, and oxygen has an oxidation state of -1 in peroxides, e.g. H₂O₂;
4. the algebraic sum of oxidation states of all atoms in a neutral molecule must be zero, while in ions the algebraic sum of the oxidation states of the constituent atoms must be equal to the charge on the ion. For example, the oxidation states of sulfur in H₂S, S₈ (elementary sulfur), SO₂, SO₃, and H₂SO₄ are, respectively: -2, 0, +4, +6 and +6. The higher the oxidation state of a given atom, the greater is its degree of oxidation; the lower the oxidation state, the greater is its degree of reduction."

Source IUPAC. Compendium of Chemical Terminology, 2nd ed. (the "Gold Book"). Compiled by A. D. McNaught and A. Wilkinson. Blackwell Scientific Publications, Oxford (1997). XML on-line corrected version: <http://goldbook.iupac.org> (2006-) created by M. Nic, J. Jirat, B. Kosata; updates compiled by A. Jenkins. ISBN 0-9678550-9-8. doi:10.1351/goldbook.

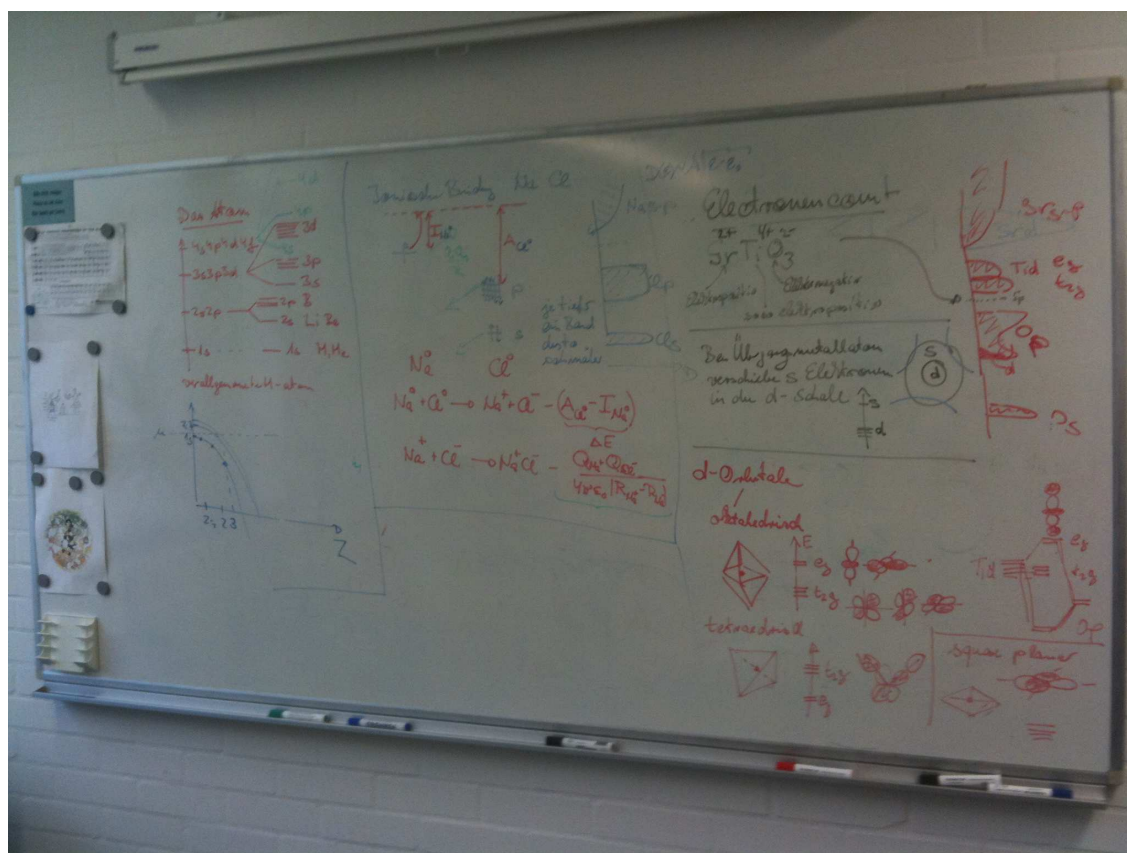
5.2.3 Transition metals

Transition metals are again special. They contain two different types of electrons: weakly bound s electrons and core-like d-electrons. When a compound is formed, one should first transfer the s-electrons to the d-electron shell. While s- and d-electrons in an atom are nearly degenerate, the Pauli Repulsion by a neighboring atom shifts the weakly bound s-electrons up in energy, while leaving the d-electrons untouched. Thus in a compound the near degeneracy is lifted and of little relevance any more.

One can also view the s-electrons as extremely electropositive and the d-electrons as much less

electropositive.

- electron transfer
- electron count
- upshift of s-versus-d electrons (s-electrons are electropositive) Model of transition metal as positive ion cores in a sea of electrons
- tiefe Baender sind schmaeler (lokalisierte zustände); 3d-bänder sind so lokalisiert wie 3sp bänder etc.
- crystal field splitting (octahedral, tetrahedral)



5.3 Prototypical density of states

- simple metals (Na, Al)
- transition metals
- covalent compounds (Si)
- simple oxides or ionic compounds
- transition metal oxides

5.4 Canonical band structures

Andersen recognized that also in band structures one can recognize characteristic patterns. This lead to the **Canonical Band theory**[12, 13, 14]

The canonical band theory allows one to construct approximate band structures from basic patterns, namely the bands of individual orbitals. First one investigates a band of orbitals with a pure angular momentum character in a given structure. Only then one investigates the interaction of the bands among each other.

The canonical bands for s, p and d-orbitals are shown in Fig. ???. These canonical bands need to be scaled with the band width, and shifted in energy so that their center agrees with the true energy level.

In the second step one considers the hybridization between the bands. The main effect is that bands usually avoid crossing each other. That is, each crossing, except for those dictated by symmetry, are converted into avoided crossings.

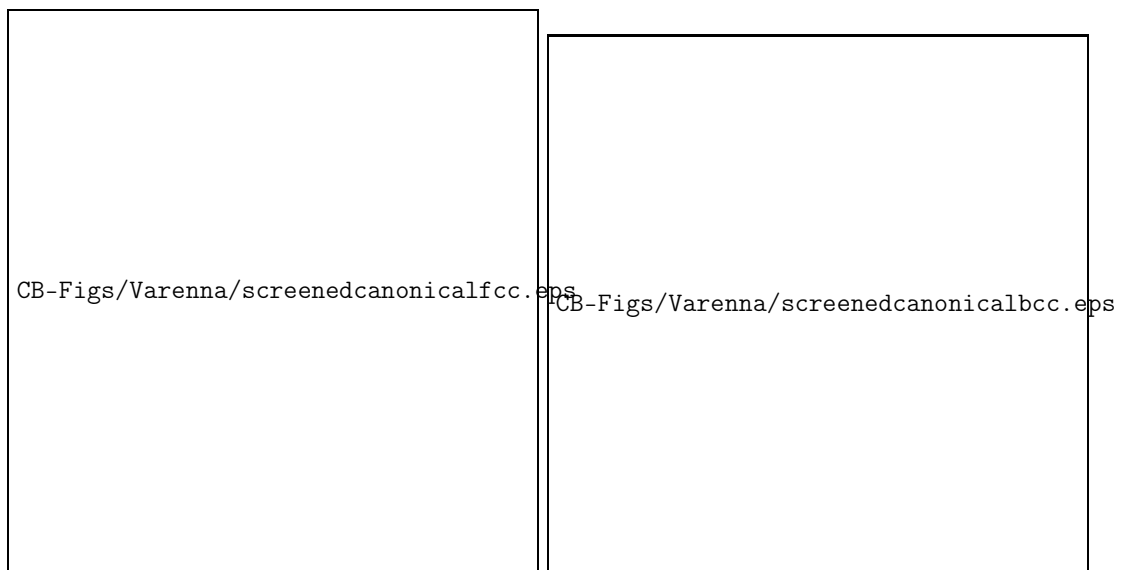
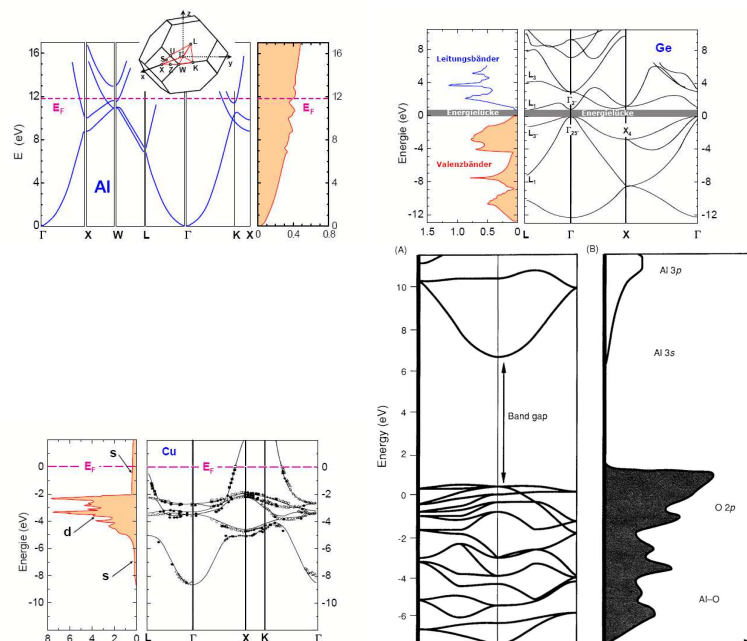


Fig. 5.2: Canonical bands for the fcc (left) and the bcc (right) structures. the canonical bands for s-, p-, and d orbitals are shown from bottom to top. (From O.K. Andersen et al. Varennna notes)

CB-Figs/Varenna/dosbccfcchcp.eps

CB-Figs/Varenna/deltaebccfcchcp.eps

Fertig: 14. Jun., 07 14. Doppelstunde

Fig. 5.3: Band structure of alumina (Al₂O₃), lower right, from R.H. French[?].

5.5 Van Hove Singularities

This section is not done

Van Hove singularities[15] are the non-analytical points of the density of states function. Because their shape is rather characteristic, we may use it to extract physical information.

5.5.1 Dimensionality

At first we look for rather global features, that allow to extract information of the intrinsic dimensionality of the problem. Questions may be of a material contains structures, where the electrons are confined in effectively one-dimensional structures.

- zero d. delta functions
- band edge, linear dispersion, 1d,2d,3d. (compare graphite <http://arxiv.org/pdf/cond-mat/0408326v1.pdf> http://prola.aps.org/pdf/PR/v71/i9/p622_1, graphene DOS, phonon dos)
- band edge, parabolic dispersion, 1d,2d,3d
- saddle point 2d and relation to 1d- band edges
- saddle points 3d, relation to (1d?) and 2d band edges
- refer to DOS when discussing Peierls distortion.
- relate to Landau Levels (effective reduction of dimensionality??)

Chapter 6

The Standard model of solid-state physics

from P.E. Blöchl, Φ SX: The electronic structure of matter Solid state physics has, in contrast to elementary particle physics, the big advantage that the fundamental particles and their interactions are completely known. The particles are electrons and nuclei¹ and their interaction is described by electromagnetism. Gravitation is such a weak force at small distances that it is completely dominated by the electromagnetic interaction. The strong force, which is active inside the nucleus, has such a short range that it does not affect the relative motion of electrons and nuclei.

Some argue that solid-state physics is not at the very frontier of research, because its particles and interactions are fully known. However, a second look shows the contrary: While the constituents are simple, the complexity develops via the interaction of many of these simple particles. The simple constituents act together to form an entire zoo of phenomena of fascinating complexity.

The dynamics is described by the Schrödinger equation:

$$i\hbar\partial_t|\Phi\rangle = \hat{H}|\Phi\rangle \quad (6.1)$$

where the wave function depends on the coordinates of all electrons and nuclei in the system. In addition it depends on the spin degrees of freedom of the electrons. Thus a wave function for N electrons and M nuclei has the form

$$\Phi_{\sigma_1, \dots, \sigma_N}(\vec{r}_1, \dots, \vec{r}_N, \vec{R}_1, \dots, \vec{R}_M)$$

where we denote the electronic coordinates by a lower-case \vec{r} and the nuclear positions by an uppercase \vec{R} . The symbols σ_j are the spin indices, which may assume values $\sigma_j \in \{-\frac{1}{2}, +\frac{1}{2}\}$. We will often use the notation $\sigma_j \in \{\downarrow, \uparrow\}$. The spin quantum number in z-direction is $s_z = \hbar\sigma$.

Often we will also combine position and spin index of the electrons in the form $\vec{x} = (\sigma, \vec{r})$, so that

$$\Phi(\vec{x}_1, \dots, \vec{x}_N, \vec{R}_1, \dots, \vec{R}_M) \stackrel{\text{def}}{=} \Phi_{\sigma_1, \dots, \sigma_N}(\vec{r}_1, \dots, \vec{r}_N, \vec{R}_1, \dots, \vec{R}_M)$$

For the integrations and summations we use the short-hand notation

$$\int d^4x \stackrel{\text{def}}{=} \sum_{\sigma \in \{\uparrow, \downarrow\}} \int d^3r \quad (6.2)$$

¹The cautious reader may object that the nuclei are objects that are far from being fully understood. However, the only properties that are relevant for us are their charge, their mass, and their size.

Most important is the antisymmetry of the wave function with respect to interchange of two electrons, which is the cause for the **Pauli principle**

PAULI-PRINCIPLE

$$\Phi(\dots, \vec{x}_i, \dots, \vec{x}_j, \dots, \vec{R}_1, \dots, \vec{R}_M) = -\Phi(\dots, \vec{x}_j, \dots, \vec{x}_i, \dots, \vec{R}_1, \dots, \vec{R}_M) \quad (6.3)$$

An electronic many-particle wave function for Fermions is antisymmetric under particle exchange. As a consequence, no two electrons with the same spin can occupy same point in space or the same one-particle orbital.

The Standard Model

Now we arrive at the most important equation, which will be the basis of all that will be said in this book. This equation specifies the many-particle Hamiltonian of our standard model of solid-state physics.

HAMILTONIAN OF THE STANDARD MODEL

The Hamiltonian for a many particle system, such as a molecule or a solid, is

$$\begin{aligned} \hat{H} = & \underbrace{\sum_{j=1}^M \frac{-\hbar^2}{2M_j} \vec{\nabla}_{\vec{R}_j}^2}_{E_{kin,nuc}} + \underbrace{\sum_{i=1}^N \frac{-\hbar^2}{2m_e} \vec{\nabla}_{\vec{r}_i}^2}_{E_{kin,e}} \\ & + \underbrace{\frac{1}{2} \sum_{i \neq j}^M \frac{e^2 Z_i Z_j}{4\pi\epsilon_0 |\vec{R}_i - \vec{R}_j|}}_{E_{C,nuc-nuc}} - \underbrace{\sum_{i=1}^N \sum_{j=1}^M \frac{e^2 Z_j}{4\pi\epsilon_0 |\vec{r}_i - \vec{R}_j|}}_{E_{C,e-nuc}} \\ & + \underbrace{\frac{1}{2} \sum_{i \neq j}^N \frac{e^2}{4\pi\epsilon_0 |\vec{r}_i - \vec{r}_j|}}_{E_{C,e-e}} \end{aligned} \quad (6.4)$$

The electrons are characterized by their charge $q = -e$, their mass m_e and their position \vec{r}_j . The nuclei are characterized by their masses M_j , their atomic numbers Z_j and their positions \vec{R}_j . The first term, denoted by $E_{kin,nuc}$, describes the kinetic energy of the nuclei. The second term, denoted by $E_{kin,e}$, describes the kinetic energy of the electrons. The third term, denoted by $E_{C,nuc-nuc}$, describes the electrostatic repulsion between the nuclei. The fourth term, denoted by $E_{C,e-nuc}$, describes the electrostatic attraction between electrons and nuclei. The last term, denoted by $E_{C,e-e}$, describes the electrostatic repulsion between the electrons.

Deficiencies of the standard model

No model is perfect. Therefore let me discuss here, what I consider its main deficiencies. The following effects are missing:

- **Relativistic effects** are important for the heavier elements, because the deep Coulomb potential of the nuclei results in relativistic velocities for the electrons near the nucleus. Relativistic effects are important for magnetic effects such as the **magnetic anisotropy**.
- **Magnetic fields** have only a small effect on solids. The dominant magnetic properties of

materials do not originate from magnetic interactions, but result from exchange effects of the spin-distribution. Important are, however, **stray fields**, which tend to force the magnetization at a surface to be in-plane. Magnetic effects are also important to simulate the results of NMR or Mössbauer experiments, which are sensitive to the magnetic interaction of nuclei and electrons.

- **Size, shape and spin of the nuclei** play a role in certain nuclear experiments which measure isomer shifts, electric-field gradients and magnetic hyperfine parameters.
- **Photons.** The use of electrostatics is justified, because the electrons and nuclei are moving sufficiently slow that the electrostatic field responds instantaneously. Excitations by photons can be treated explicitly.

These effects are not necessarily ignored, but can be incorporated into the standard model, when required.

Dimensional Bottleneck

It is immediately clear that the standard model, as simple as it can be stated, is impossible to solve as such. To make this argument clear let us estimate the amount of storage needed to store the wave function of a simple molecule such as N_2 . Each coordinate may be discretized into 100 grid points. For 2 nuclei and 14 electrons we need $100^{(3 \cdot 16)}$ grid points. In addition, we need to consider the 2^{14} sets of spin indices. Thus we need to store about $2^{14} \cdot 100^{3 \cdot 16} \approx 10^{100}$ numbers. One typical hard disk can hold about 100 GByte = 10^{14} Byte, which corresponds to 10^{13} complex numbers. A complex number occupies 16 byte. This implies that we would need 10^{87} hard discs to store a single wave function. A hard-disc occupies a volume of $5 \text{ cm} \times 5 \text{ cm} \times 0.5 \text{ cm} = 1.25 \times 10^{-5} \text{ m}^3$. The volume occupied by the hard discs with our wave function would be 10^{82} m^3 corresponding to a sphere with a radius of 10^{27} m or 10^{11} light years! I hope that this convinced you that there is a problem...

The problem described here is called the **dimensional bottle-neck**.

In order to make progress we need to simplify the problem. Thus we have to make approximations and we will develop simpler models that can be understood in detail. This is what solid state physics is about.

In the following we will perform a set of common approximations, and will describe their limitations.

Chapter 7

Spin orbitals

Before we continue, let me point out a special property of our one-particle wave functions.

When I first learned about spins and magnetic moments I was puzzled by the special role, which was attributed to the z-coordinate. I learned that an electron can have a spin pointing parallel or antiparallel to the z-axis. The direction of the z-axis however is arbitrary. It seemed as if the physics changed, when I turned my head.

Indeed there is nothing special about the z-coordinate. Here, we show that the more general formulation describes electrons by two-component spinors. With this formulation we can form wave functions that have a spin in an arbitrary direction. This restores the rotational symmetry that appears to be broken in a simple-minded formulation.

We use here **two-component spinor wave functions**, which are also called **spin-orbitals**

$$\phi(\vec{x}) = \phi(\vec{r}, \sigma) = \langle \vec{r}, \sigma | \phi \rangle$$

Spin-orbitals actually consists of two complex wave functions, one for the spin-down $\phi(\vec{r}, \downarrow)$ and one for the spin up contribution $\phi(\vec{r}, \uparrow)$. One can write the spin orbitals also as two-component spinor

$$\begin{pmatrix} \phi(\vec{r}, \uparrow) \\ \phi(\vec{r}, \downarrow) \end{pmatrix} \stackrel{\text{def}}{=} \begin{pmatrix} \langle \vec{r}, \uparrow | \phi \rangle \\ \langle \vec{r}, \downarrow | \phi \rangle \end{pmatrix}$$

PHYSICAL MEANING OF A SPIN-WAVE FUNCTION

The square of a component of a spin wavefunction is the probability density $P_\sigma(\vec{r})$ for finding a particle with the specified spin orientation at a specific position \vec{r} .

This rule is completely analogous to the rule that the absolute square of a scalar wave function is the probability density $P(\vec{r}) = \psi^*(\vec{r})\psi(\vec{r})$ of finding a particle at a given position \vec{r} .

Note, however, that the wave function contains much more information than that just mentioned. Just as a regular wave function also contains the information about the momentum distribution or the probability distribution of any other observable, the spin-wave function contains in addition also the full information on the spin orientation.¹

¹This does not imply that it contains the information on all three vector components. Because the spin-components do not commute, the value of two spin components cannot be precise simultaneously. However we obtain the probability for the orientation of the spin along any axis.

Relation to spin eigenstates

This notation is a little puzzling at first, because one usually works with spin-eigenfunctions, for which one of the components vanishes. The spin is defined as

$$\hat{S} = \frac{\hbar}{2} \hat{\sigma} \quad (7.1)$$

where the three components of the vector $\hat{\sigma}$ are

$$\hat{\sigma}_i = \int d^3r \sum_{\sigma, \sigma'=1}^2 |\vec{r}, \sigma\rangle \sigma_{i, \sigma, \sigma'} \langle \vec{r}, \sigma|$$

Somewhat confusing are the different indices for the different vector spaces: The index i can have the values x, y, z and refers to the components of the vector $\vec{\sigma}$. Each component of the vector $\vec{\sigma}$ is a scalar operator. The indices σ, σ' are indices in the two-dimensional spinor space. That is, σ_i is a (2×2) matrix for each value of i . These (2×2) matrices are the **Pauli matrices**²

$$\sigma_x = \begin{pmatrix} 0 & 1 \\ 1 & 0 \end{pmatrix}, \quad \sigma_y = \begin{pmatrix} 0 & -i \\ i & 0 \end{pmatrix}, \quad \sigma_z = \begin{pmatrix} 1 & 0 \\ 0 & -1 \end{pmatrix} \quad (7.2)$$

As a worked example let us determine the expectation value of the operator \hat{S}_x for a one-particle state $|\phi\rangle$

$$\begin{aligned} \langle \phi | \hat{S}_x | \phi \rangle &= \langle \phi | \left[\frac{\hbar}{2} \int d^3r \sum_{\sigma, \sigma'=1}^2 |\vec{r}, \sigma\rangle \sigma_{x, \sigma, \sigma'} \langle \vec{r}, \sigma| \right] | \phi \rangle \\ &= \frac{\hbar}{2} \int d^3r \left[\sum_{\sigma, \sigma'=1}^2 \langle \phi | \vec{r}, \sigma \rangle \sigma_{x, \sigma, \sigma'} \langle \vec{r}, \sigma | \phi \rangle \right] \\ &= \frac{\hbar}{2} \int d^3r \left[\begin{pmatrix} \langle \phi | \vec{r}, \uparrow \rangle \\ \langle \phi | \vec{r}, \downarrow \rangle \end{pmatrix} \begin{pmatrix} 0 & 1 \\ 1 & 0 \end{pmatrix} \begin{pmatrix} \langle \vec{r}, \uparrow | \phi \rangle \\ \langle \vec{r}, \downarrow | \phi \rangle \end{pmatrix} \right] \\ &= \frac{\hbar}{2} \int d^3r [\langle \phi | \vec{r}, \uparrow \rangle \langle \vec{r}, \downarrow | \phi \rangle + \langle \phi | \vec{r}, \downarrow \rangle \langle \vec{r}, \uparrow | \phi \rangle] \\ &= \frac{\hbar}{2} \int d^3r [\phi^*(\vec{r}, \uparrow) \phi(\vec{r}, \downarrow) + \phi^*(\vec{r}, \downarrow) \phi(\vec{r}, \uparrow)] \end{aligned}$$

We obtain the spin density, that is the probability that we find a particle at position \vec{r} multiplied with the average spin expectation value in x-direction of that particle.

For a spin orbital that is an eigenstate of S_z , one of the spinor components vanishes.

$$\begin{aligned} \hat{S}_z |\phi_\uparrow\rangle &= |\phi_\uparrow\rangle \left(+\frac{\hbar}{2} \right) \quad \Rightarrow \quad \begin{pmatrix} \langle \vec{r}, \uparrow | \phi_\uparrow \rangle \\ \langle \vec{r}, \downarrow | \phi_\uparrow \rangle \end{pmatrix} = \begin{pmatrix} \phi_\uparrow(\vec{r}, \uparrow) \\ 0 \end{pmatrix} \\ \hat{S}_z |\phi_\downarrow\rangle &= |\phi_\downarrow\rangle \left(-\frac{\hbar}{2} \right) \quad \Rightarrow \quad \begin{pmatrix} \langle \vec{r}, \uparrow | \phi_\downarrow \rangle \\ \langle \vec{r}, \downarrow | \phi_\downarrow \rangle \end{pmatrix} = \begin{pmatrix} 0 \\ \phi_\downarrow(\vec{r}, \downarrow) \end{pmatrix} \end{aligned}$$

Note that the indices \uparrow, \downarrow indicate the quantum number, while the pointers to the spinor components are treated as argument, so that they can be distinguished from the quantum numbers. The quantum number indicates that the orbital is an eigenstate to some symmetry operator.

²The matrices are made of the matrix elements $\langle \sigma | \hat{\sigma}_i | \sigma' \rangle$ of the operator $\hat{\sigma}$. σ and σ' can assume the two values \uparrow, \downarrow .

The spin-orbitals have the advantage that they allow to describe orbitals, for which the spin does not point along the z-axis, but it can also point, for example, to the right or in any other direction. For a spin orbital the spin direction can actually vary in space. Such an orbital is called non-collinear, because the spins are not aligned.

Problem with conventional notation

In the literature, one usually uses another notation, namely

$$\phi_\sigma(\vec{r}) \stackrel{\text{def}}{=} \phi(\vec{r}, \sigma)$$

Here, it is difficult to distinguish the role of σ as a coordinate and as quantum number. One usually uses one-particle orbitals with only one spin component, for which σ is a quantum number. In our notation this would be, – for a spin-up particle –,

$$\phi_\uparrow(\vec{r}, \sigma) = \langle \vec{r}, \sigma | \phi_\uparrow \rangle \hat{=} \begin{pmatrix} \langle \vec{r}, \uparrow | \phi_\uparrow \rangle \\ 0 \end{pmatrix}$$

The orbital still has two components, but one of them, namely $\phi_\uparrow(\vec{r}, \downarrow)$ vanishes. With the common notation, it is difficult to write down expressions that do not break the rotational symmetry for the spin direction.

Magnetization

So-far we used the spin operator to determine the expectation value of the spin. Now we would like to obtain the spin density or the magnetization respectively. In order to describe the principles, let us work out the charge density as a trivial example:

We know the projector $\hat{P}(\vec{r})$ onto a certain point in space \vec{r} , which is

$$\hat{P}(\vec{r}) \stackrel{\text{def}}{=} \sum_{\sigma} |\vec{r}, \sigma\rangle \langle \vec{r}, \sigma| = |\vec{r}, \downarrow\rangle \langle \vec{r}, \downarrow| + |\vec{r}, \uparrow\rangle \langle \vec{r}, \uparrow|$$

We obtain the charge density as expectation value of $\hat{P}(\vec{r})$, multiplied with the electron charge $q_e = -e$.

$$\begin{aligned} \rho(\vec{r}) &= \langle \phi | [q \hat{P}(\vec{r})] | \phi \rangle = q \langle \phi | \left[\sum_{\sigma} |\vec{r}, \sigma\rangle \langle \vec{r}, \sigma| \right] | \phi \rangle \\ &= q \sum_{\sigma} \langle \phi | \vec{r}, \sigma \rangle \langle \vec{r}, \sigma | \phi \rangle \\ &= q \left(\langle \phi | \vec{r}, \downarrow \rangle \langle \vec{r}, \downarrow | \phi \rangle + \langle \phi | \vec{r}, \uparrow \rangle \langle \vec{r}, \uparrow | \phi \rangle \right) \end{aligned}$$

Hence, the charge density is, up to the factor q , the sum of the spin-up and spin-down densities. After this introduction, we can analogously determine the magnetization.

The magnetization operator is obtained as product of the factor³ $\frac{q}{m}$, the spin operator and the

³The classical ratio of magnetic moment and angular momentum is $\frac{q}{2m}$, which however assumes a constant ratio the mass- and charge distribution in space. While the “distribution” of electrons leads to such a constant ratio, the properties of a single electron may differ in a classical picture. In a quantum mechanical description the electron is point-like with a certain gyromagnetic ratio, that follows directly from the relativistic Dirac equation.

projection operator onto a point in space.

$$\begin{aligned}
 \hat{m}_i(\vec{r}) &\stackrel{\text{def}}{=} \frac{q}{m} \hat{P}(\vec{r}) \hat{S}_i = \frac{q\hbar}{2m} \hat{P}(\vec{r}) \hat{\sigma}_i \\
 &= \frac{q\hbar}{2m} \underbrace{\left[\sum_{\sigma} |\vec{r}, \sigma\rangle \langle \vec{r}, \sigma| \right]}_{\hat{P}(\vec{r})} \underbrace{\left[\int d^3r' \sum_{\sigma', \sigma''} |\vec{r}', \sigma'\rangle \sigma_{i, \sigma', \sigma''} \langle \vec{r}', \sigma''| \right]}_{\hat{\sigma}_i} \\
 &= \frac{q\hbar}{2m} \sum_{\sigma} \int d^3r' \sum_{\sigma', \sigma''} |\vec{r}, \sigma\rangle \underbrace{\langle \vec{r}, \sigma | \vec{r}', \sigma' \rangle}_{\delta(\vec{r}-\vec{r}')\delta_{\sigma, \sigma'}} \sigma_{i, \sigma', \sigma''} \langle \vec{r}', \sigma''| \\
 &= \frac{q\hbar}{2m} \sum_{\sigma, \sigma''} |\vec{r}, \sigma\rangle \sigma_{i, \sigma, \sigma''} \langle \vec{r}, \sigma''|
 \end{aligned}$$

The factor $\mu_B \stackrel{\text{def}}{=} \frac{e\hbar}{2m_e}$ is the **Bohr magneton**, which is approximately equal to the magnetic moment of an electron. Spin and magnetic moment of the electron point in opposite directions due to the negative charge of the electron.

MAGNETIZATION OPERATOR

$$\hat{\vec{m}}(\vec{r}) = \frac{q\hbar}{2m} \sum_{\sigma, \sigma'} |\vec{r}, \sigma\rangle \vec{\sigma}_{\sigma, \sigma'} \langle \vec{r}, \sigma'| \quad (7.3)$$

with the Pauli matrices $\vec{\sigma}$ defined in Eq. 7.2.

More explicitly we obtain

$$\begin{aligned}
 \rho(r) &= q \begin{pmatrix} \langle \phi | \vec{r}, \uparrow \rangle \\ \langle \phi | \vec{r}, \downarrow \rangle \end{pmatrix} \begin{pmatrix} 1 & 0 \\ 0 & 1 \end{pmatrix} \begin{pmatrix} \langle \vec{r}, \uparrow | \phi \rangle \\ \langle \vec{r}, \downarrow | \phi \rangle \end{pmatrix} \\
 &= q [\phi^*(\vec{r}, \uparrow) \phi(\vec{r}, \uparrow) + \phi^*(\vec{r}, \downarrow) \phi(\vec{r}, \downarrow)] \\
 m_x(r) &= \frac{q\hbar}{2m} \begin{pmatrix} \langle \phi | \vec{r}, \uparrow \rangle \\ \langle \phi | \vec{r}, \downarrow \rangle \end{pmatrix} \begin{pmatrix} 0 & 1 \\ 1 & 0 \end{pmatrix} \begin{pmatrix} \langle \vec{r}, \uparrow | \phi \rangle \\ \langle \vec{r}, \downarrow | \phi \rangle \end{pmatrix} \\
 &= \frac{q\hbar}{2m_e} [\phi^*(\vec{r}, \uparrow) \phi(\vec{r}, \downarrow) + \phi^*(\vec{r}, \downarrow) \phi(\vec{r}, \uparrow)] \\
 m_y(r) &= \frac{q\hbar}{2m} \begin{pmatrix} \langle \phi | \vec{r}, \uparrow \rangle \\ \langle \phi | \vec{r}, \downarrow \rangle \end{pmatrix} \begin{pmatrix} 0 & -i \\ i & 0 \end{pmatrix} \begin{pmatrix} \langle \vec{r}, \uparrow | \phi \rangle \\ \langle \vec{r}, \downarrow | \phi \rangle \end{pmatrix} \\
 &= -i \frac{q\hbar}{2m} [\phi^*(\vec{r}, \uparrow) \phi(\vec{r}, \downarrow) - \phi^*(\vec{r}, \downarrow) \phi(\vec{r}, \uparrow)] \\
 m_z(r) &= \frac{q\hbar}{2m} \begin{pmatrix} \langle \phi | \vec{r}, \uparrow \rangle \\ \langle \phi | \vec{r}, \downarrow \rangle \end{pmatrix} \begin{pmatrix} 1 & 0 \\ 0 & -1 \end{pmatrix} \begin{pmatrix} \langle \vec{r}, \uparrow | \phi \rangle \\ \langle \vec{r}, \downarrow | \phi \rangle \end{pmatrix} \\
 &= \frac{q\hbar}{2m} [\phi^*(\vec{r}, \uparrow) \phi(\vec{r}, \uparrow) - \phi^*(\vec{r}, \downarrow) \phi(\vec{r}, \downarrow)]
 \end{aligned}$$

The two-component spinor descriptions follows from the **Pauli equation**. The Pauli equation is the non-relativistic limit of the **Dirac equation**, the relativistic one-particle equation for electrons. In the Dirac equation each particle has four components. Two components describe spin-up and spin-down electrons, and the two other components describe spin-up and spin-down positrons. The **positron**[16] is the anti-particle of the electron. In the non-relativistic limit, the electronic and positronic components become independent of each other, so that the electrons can be described by a two-component spinor wave function.

A Slater determinant of N spin-orbitals corresponds to 2^N Slater determinants of one-component one-particle orbitals, according to the N spin indices.

Chapter 8

Many-Particle wave functions

8.1 Mathematical Preparation: The Levi-Civita Symbol or the fully antisymmetric tensor

In the following we will represent wave functions by determinants. In order to work with determinants the Levi-Civita symbol, which is also called the fully antisymmetric tensor, has been introduced. Here, we define the fully antisymmetric tensor and derive some formulas, which will be needed later.

Definition

The **Levi-Civita symbol**¹, also called the **fully antisymmetric tensor** is a **rank**² N Tensor defined by the following properties

- For ascending indices the Levi-Civita symbol has the value one:

$$\epsilon_{1,2,3,\dots,N} = 1$$

- The Levi-Civita symbol changes sign with any pairwise permutation of its indices
- The Levi-Civita symbol vanishes whenever at least two indices are pairwise identical

Relation to determinants

The determinant of a $N \times N$ matrix \mathbf{A} is defined by the Levi-Civita symbol $\epsilon_{i,j,k,l,\dots}$ as

$$\det[\mathbf{A}] = \sum_{i,j,k,\dots} \epsilon_{i,j,k,\dots} A_{1,i} A_{2,j} A_{3,k} \dots$$

Vector product (not needed)

A common and useful application of the Levi-Civita Symbol is to express the vector product in three dimensions by its components.

$$\vec{a} = \vec{b} \times \vec{c} \quad \Leftrightarrow \quad a_i = \sum_{j,k} \epsilon_{i,j,k} b_j c_k$$

¹Tullio Levi-Civita (1873-1941): Italian mathematician. Invented the covariant derivative. Made tensor-algebra popular, which was used in Einstein's theory of general relativity.

²The rank is the number of indices that define a tensor element. Note, that there is another more limited definition of the word rank.

Laplace expansion theorem (not needed)

Let D be the determinant of an $N \times N$ matrix \mathbf{A} , and let $D_{N-1}^{i,j}$ be the determinant of the matrix obtained from \mathbf{A} by deleting the i -th line and the j -th column. Then

$$D = \sum_{j=1}^N (-1)^{i+j} A_{i,j} D_{N-1}^{i,j}$$

The Laplace expansion theorem can be applied twice, leading to

$$D = \sum_{i=1}^N \sum_{k=1}^N (-1)^{i+j+k+l} A_{i,j} A_{k,l} D_{N-2}^{i,k,j,l}$$

where $D^{i,k,j,l}$ is the determinant of the matrix \mathbf{A} with the i -th and k -th line, and the j -th and l -th column deleted.

8.2 Symmetry and quantum mechanics

In the following, we will be concerned with the symmetry of the Hamilton operator under permutation of particles. Therefore, I will revisit the main **symmetry** arguments discussed in ΦSX :Quantum Physics. This is a series of arguments may be worthwhile to keep in mind.

A symmetry of an object is a transformation, that leaves the appearance of the object unchanged. For example a square is symmetric under four-fold rotation. A physical system, which is identified by a Hamiltonian, is symmetric under a transformation, if every solution of the equation of motion, the Schrödinger equation, is transformed onto another solution of the same equations.

1. Definition of a **transformation operator**. An operator \hat{S} can be called a transformation, if it conserves the norm for any state, that is if

$$\forall |\psi\rangle \quad \langle \psi | \psi \rangle \stackrel{|\phi\rangle = \hat{S}|\psi\rangle}{=} \langle \phi | \phi \rangle \quad (8.1)$$

2. A transformation operator \hat{S} is unitary, that is

$$\hat{S}^\dagger \hat{S} = 1 \quad (8.2)$$

Proof:

$$\forall |\psi\rangle \quad \langle \psi | \hat{S}^\dagger \hat{S} | \psi \rangle \stackrel{\text{Eq. 8.1}}{=} \langle \psi | \psi \rangle \quad \Rightarrow \quad \hat{S}^\dagger \hat{S} = 1$$

3. Definition of a **symmetry**: A system is called symmetric under the transformation \hat{S} , if, for any solution of the Schrödinger equation describing that system, also $\hat{S}|\Psi\rangle$ is a solution of the same Schrödinger equation. That is, if

$$\left(i\hbar \partial_t |\Psi\rangle = \hat{H} |\Psi\rangle \right) \stackrel{|\Phi\rangle \stackrel{\text{def}}{=} \hat{S}|\Psi\rangle}{\Rightarrow} \left(i\hbar \partial_t |\Phi\rangle = \hat{H} |\Phi\rangle \right) \quad (8.3)$$

4. The commutator of the Hamilton operator with its symmetry operator vanishes, that is $[\hat{H}, \hat{S}]_- = 0$:

Proof:

$$\begin{aligned}
 i\hbar\partial_t|\Phi\rangle &= \hat{H}|\Phi\rangle \\
 |\Phi\rangle &\stackrel{\text{def}}{=} \hat{S}|\Psi\rangle \Rightarrow i\hbar\partial_t\hat{S}|\Psi\rangle = \hat{H}\hat{S}|\Psi\rangle \\
 \partial_t\hat{S} &\stackrel{=0}{=} \hat{S}(i\hbar\partial_t|\Psi\rangle) = \hat{H}\hat{S}|\Psi\rangle \\
 i\hbar\partial_t|\Psi\rangle &\stackrel{= \hat{H}|\Psi\rangle}{=} \hat{S}\hat{H}|\Psi\rangle = \hat{H}\hat{S}|\Psi\rangle \\
 \underbrace{(\hat{H}\hat{S} - \hat{S}\hat{H})}_{[\hat{H}, \hat{S}]_-} |\Psi\rangle &= 0
 \end{aligned}$$

Because this equation holds for any solution of the Schrödinger equation, it holds for any wave function, because any function can be written as superposition of solutions of the Schrödinger equation. (The latter form a complete set of functions.) Therefore

SYMMETRY AND COMMUTATOR

The commutator between the Hamilton operator \hat{H} with its (time-independent^a) symmetry operators \hat{S} vanishes.

$$[\hat{H}, \hat{S}]_- = 0$$

Thus, one usually identifies a symmetry by working out the commutator with the Hamiltonian.

^aFor time-dependent symmetry operators, the more general rule is $[\hat{H}, \hat{S}]_- = i\hbar\partial_t\hat{S}$. An example for a time-dependent symmetry is that between two relatively moving frames of inertia.

5. The matrix elements of the Hamilton operator between two eigenstates of the symmetry operator with different eigenvalues vanish. That is

$$(\hat{S}|\Psi_s\rangle = |\Psi_s\rangle s \quad \wedge \quad \hat{S}|\Psi_{s'}\rangle = |\Psi_{s'}\rangle s' \quad \wedge \quad s \neq s') \Rightarrow \langle\Psi_s|\hat{H}|\Psi_{s'}\rangle = 0$$

Proof: In the following we will need an expression for $\langle\Psi_s|\hat{S}$, which we will work out first:

- We start by showing that the absolute value of an eigenvalue of a unitary operator is equal to one, that is $s = e^{i\phi}$ where ϕ is real. With an eigenstate $|\psi_s\rangle$ of \hat{S} we obtain

$$s^* \langle\psi_s|\psi_s\rangle s \stackrel{\hat{S}|\psi_s\rangle = |\psi_s\rangle s}{=} \langle\hat{S}\psi_s|\hat{S}\psi_s\rangle = \langle\psi_s|\underbrace{\hat{S}^\dagger\hat{S}}_{=1}|\psi_s\rangle = \langle\psi_s|\psi_s\rangle \Rightarrow |s| = 1 \quad (8.4)$$

- Next, we show that the eigenvalues of the Hermitian conjugate operator \hat{S}^\dagger of a unitary operator \hat{S} are the complex conjugates of the eigenvalues of \hat{S} .

$$\begin{aligned}
 &\Rightarrow |\psi_s\rangle \stackrel{\text{Eq. 8.2}}{=} \underbrace{\hat{S}^\dagger\hat{S}}_{=1}|\psi_s\rangle \stackrel{\hat{S}|\psi_s\rangle = |\psi_s\rangle s}{=} \hat{S}^\dagger|\psi_s\rangle s \\
 &\Rightarrow \hat{S}^\dagger|\psi_s\rangle s \stackrel{\text{Eq. 8.4}}{=} |\psi_s\rangle \underbrace{s^*}_{=1} \\
 &\Rightarrow \hat{S}^\dagger|\psi_s\rangle = |\psi_s\rangle s^* \\
 &\Rightarrow \langle\psi_s|\hat{S} = s\langle\psi_s|
 \end{aligned}$$

- With this, we are ready to show that the matrix elements of the Hamilton operator between two eigenstates of the symmetry operator with different eigenvalues vanish.

$$\begin{aligned}
 0 \quad & \begin{array}{l} [\hat{H}, \hat{S}]_- = 0 \\ \hat{S}|\Psi_s\rangle = |\Psi_s\rangle s, \text{etc.} \\ s \neq s' \Rightarrow \end{array} & \langle \Psi_s | [\hat{H}, \hat{S}]_- | \Psi_{s'} \rangle = \langle \Psi_s | \hat{H} \hat{S} | \Psi_{s'} \rangle - \langle \Psi_s | \hat{S} \hat{H} | \Psi_{s'} \rangle \\
 & \langle \Psi_s | \hat{H} | \Psi_{s'} \rangle s' - s \langle \Psi_s | \hat{H} | \Psi_{s'} \rangle = \langle \Psi_s | \hat{H} | \Psi_{s'} \rangle (s' - s) \\
 & \Rightarrow \langle \Psi_s | \hat{H} | \Psi_{s'} \rangle = 0
 \end{aligned}$$

q.e.d

Thus we have shown that the Hamilton operator is block diagonal in a representation of eigenstates of its symmetry operators. The eigenstates of the Hamilton operator can be obtained for each block individually. For us it is more important that a wave function that starts out as an eigenstate of a symmetry operator to a given eigenvalue, will always remain an eigenvalue to the same eigenvalue. In other words the eigenvalue of the symmetry operator is a conserved quantity. (Note however, that the eigenvalue of a symmetry operator usually has complex eigenvalues.)

The eigenvalues of the symmetry operators are related to the **quantum numbers**.

8.3 Slater determinants

Identical particles

Electrons with identical spin are indistinguishable. This says that there is no conceivable experiment that discriminates between two electrons, except for their spin. Thus, there is a symmetry with respect to exchange of two particles, and the Hamiltonian for indistinguishable particles commutes with the permutation operator of two particles.

The **two-particle permutation operator** is defined as

$$\hat{P}_{ij}^{(2)} \Psi(\dots, \vec{x}_i, \dots, \vec{x}_j, \dots) = \Psi(\dots, \vec{x}_j, \dots, \vec{x}_i, \dots)$$

The eigenstates of the Hamiltonian are eigenstates of the permutation operator. Because $\left(\hat{P}_{ij}^{(2)}\right)^2 = \hat{1}$, the permutation operator has the two eigenvalues, namely +1 and -1. Thus, the wave functions are fully symmetric or fully antisymmetric with respect to the permutation of two particle coordinates. Particles with a symmetric wave function are called **Bosons** and particle with antisymmetric wave function are called **Fermions**. Bosons are particles with integer spin such as photons, mesons, gluons, gravitons, etc, which are usually related to an interaction, while Fermions are particles with half-integer spin such as electrons, protons, neutrons, quarks, etc.

Unlike other symmetries, this symmetry is not a property of a specific Hamiltonian, but it is a property of the particles themselves. If the particles are indistinguishable, there is no conceivable Hamiltonian, that is not symmetric under permutation of two of these particles. If we could construct only one Hamiltonian that is not symmetric, we could design an experiment, just by realizing this Hamiltonian, that distinguishes two of such particles

The electron exchange is illustrated in Fig. 8.1. Except for the color, which distinguishes the two electrons, left and right situations are identical. Note, that for the particle exchange both spatial and spin-indices have to be exchanged simultaneously. Since the electrons are indistinguishable, no distinguishing property like the color indicated can exist.

Fermions, such as electrons, have an antisymmetric wave function, that is

$$\hat{P}_{ij}^{(2)} |\Psi\rangle = -|\Psi\rangle$$

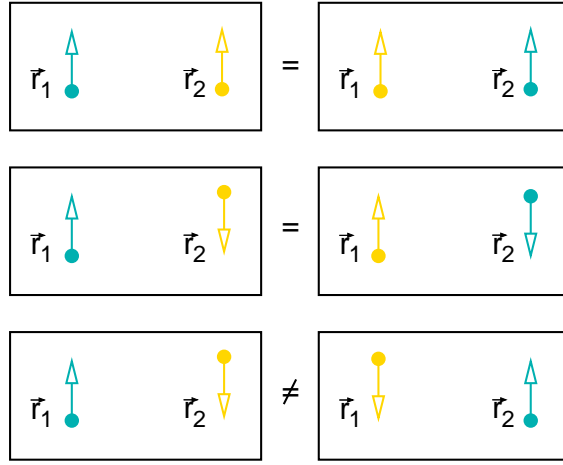


Fig. 8.1: Demonstration of the particle exchange. For the two figures at the top, left and right situations are identical except for a color of the particles. For identical particles there is no property such as the color that allows one to distinguish them. Thus $\Psi(\vec{x}_1, \vec{x}_2) = -\Psi(\vec{x}_2, \vec{x}_1)$ or $\Psi(\vec{r}_1, \sigma_1, \vec{r}_2, \sigma_2) = -\Psi(\vec{r}_2, \sigma_2, \vec{r}_1, \sigma_1)$. In the bottom figure, the particle positions are exchanged but not their spin. Thus the two configurations are not identical. In this case we may also view electrons with up and down spin as distinguishable particles, because they have different spin.

Permutation operator

The most simple way to construct a many-particle wave function, is to take the product of **one-particle wave functions**, such as

$$\Phi(\vec{x}_1, \vec{x}_2, \dots) = \phi_a(\vec{x}_1)\phi_b(\vec{x}_1) \dots$$

However, such a product wave function is not yet antisymmetric with respect to permutation. Therefore we need to antisymmetrize it. We use the N-particle permutation operator $\hat{P}_{i_1, \dots, i_N}$ that is defined as follows

N-PARTICLE PERMUTATION OPERATOR

$$\hat{P}_{i_1, \dots, i_N} := \int d^4x_1 \dots \int d^4x_N |\vec{x}_{i_1}, \dots, \vec{x}_{i_N}\rangle \langle \vec{x}_1, \dots, \vec{x}_N| \quad (8.5)$$

The permutation operator reorders the coordinates so that the first particle is placed onto the position of the particle i_1 and so on. This implies that the coordinates of the i_1 -th particle are placed on the first position, which is the one of the first particle

In order to make the function of the operator more transparent, let us rewrite it as an operator of real-space functions. Consider a state $|\vec{y}_1, \dots, \vec{y}_N\rangle$, which describes a particle distribution where the first particle is at position \vec{y}_1 , the second at \vec{y}_2 and so on. Application of the permutation operator $\hat{P}_{i_1, \dots, i_N}$ yields

$$\begin{aligned} \hat{P}_{i_1, \dots, i_N} |\vec{y}_1, \dots, \vec{y}_N\rangle &\stackrel{\text{Eq. 8.5}}{=} \int d^4x_1 \dots \int d^4x_N |\vec{x}_{i_1}, \dots, \vec{x}_{i_N}\rangle \underbrace{\langle \vec{x}_1, \dots, \vec{x}_N | \vec{y}_1, \dots, \vec{y}_N \rangle}_{\delta(\vec{x}_1 - \vec{y}_2) \dots \delta(\vec{x}_N - \vec{y}_N)} \\ &= |\vec{y}_{i_1}, \dots, \vec{y}_{i_N}\rangle \end{aligned}$$

In the new state the first particle (first vector in the state) is at \vec{y}_{i_1} , that is at the position where the particle i_1 has been before the permutation.

In the following it will be more convenient to work with the adjoint permutation operator.

$$\hat{P}_{i_1, \dots, i_N}^\dagger \stackrel{\text{Eq. 8.5}}{=} \int d^4 x_1 \dots \int d^4 x_N |\vec{x}_1, \dots, \vec{x}_N\rangle \langle \vec{x}_{i_1}, \dots, \vec{x}_{i_N}| \quad (8.6)$$

Because the permutation operator is unitary, its adjoint is at the same time its inverse. The application of the adjoint permutation operator on an arbitrary wave function yields

$$\begin{aligned} \hat{P}_{i_1, \dots, i_N}^\dagger \Psi(\vec{y}_1, \dots, \vec{y}_N) &= \langle \vec{y}_1, \dots, \vec{y}_N | \hat{P}_{i_1, \dots, i_N}^\dagger | \Psi \rangle \\ &\stackrel{\text{Eq. 8.6}}{=} \int d^4 x_1 \dots \int d^4 x_N \underbrace{\langle \vec{y}_1, \dots, \vec{y}_N | \vec{x}_1, \dots, \vec{x}_N \rangle}_{\delta(\vec{y}_1 - \vec{x}_{i_1}) \dots \delta(\vec{y}_N - \vec{x}_{i_N})} \underbrace{\langle \vec{x}_{i_1}, \dots, \vec{x}_{i_N} | \Psi \rangle}_{\Psi(\vec{x}_1, \dots, \vec{x}_N)} \\ &= \Psi(\vec{y}_{i_1}, \dots, \vec{y}_{i_N}) \end{aligned}$$

Antisymmetrize wave functions

The exchange operator P_{i_1, \dots, i_N} applied to a fermionic wave function has the eigenvalue -1 if the sequence i_1, \dots, i_N is obtained by an odd number of permutations from regular order $1, 2, 3, \dots, N$, and it has the eigenvalue $+1$ for an even number of permutations. These values are those of the fully antisymmetric tensor or the Levy-Civita symbol.

EIGENVALUES OF THE PERMUTATION OPERATOR

A many-fermion state is an eigenstate of the permutation operators

$$P_{i_1, \dots, i_N} |\Psi^F\rangle = |\Psi^F\rangle \epsilon_{i_1, \dots, i_N} \quad (8.7)$$

with eigenvalues given by the fully antisymmetric tensor defined in section 8.1.

A many-boson state can be defined similarly, but the eigenvalues are $+1$ for any permutation of the particle coordinates.

$$P_{i_1, \dots, i_N} |\Psi^B\rangle = |\Psi^B\rangle \epsilon_{i_1, \dots, i_N}^2 \quad (8.8)$$

We can symmetrize a wave function $|\chi\rangle$ with respect to a symmetry operation \hat{S} to obtain an eigenstate $|\psi_\alpha\rangle$ of the symmetry eigenvalue $s_\alpha = e^{i\frac{2\pi}{N}\alpha}$

$$|\psi_\alpha\rangle = \sum_{n=0}^N \hat{S}^n |\chi\rangle s_\alpha^{-n} = \sum_{n=0}^N (\hat{S}^\dagger)^n |\chi\rangle s_\alpha^{+n} \quad (8.9)$$

With Eq. 8.9 we can construct a Fermionic state from a product state. A product state is in general neither symmetric nor antisymmetric with respect to permutations.

In this case we do not only have a single symmetry operation with a given multiplicity, but a set of non-commuting operations that form a symmetry group. The equation with a single operator can be looked upon as the sum of all members in the symmetry group with the corresponding eigenvalues, that are given by the eigenvalues of the generator of the group. We can generalize this concept by summing over all members of the group formed by all particle permutations with the corresponding eigenvalues.

$$|\Phi^F\rangle = \sum_{i_1, \dots, i_N=1}^N \hat{P}_{i_1, \dots, i_N}^\dagger |\chi\rangle \epsilon_{i_1, \dots, i_N} \quad (8.10)$$

Slater determinants

The most simple many-particle wave function is a product state $|\phi_1, \dots, \phi_N\rangle$, which can be written as

$$\langle \vec{x}_1, \dots, \vec{x}_N | \phi_1, \dots, \phi_N \rangle = \langle \vec{x}_1 | \phi_1 \rangle \cdots \langle \vec{x}_N | \phi_N \rangle = \phi_1(\vec{x}_1) \cdots \phi_N(\vec{x}_N) \quad (8.11)$$

A product state is not yet antisymmetric with respect to particle exchange, but with Eq. 8.9 it can be antisymmetrized. Using the N -particle permutation operator $\hat{P}_{i_1, \dots, i_N}$ and the fully antisymmetric tensor $\epsilon_{i_1, \dots, i_N}$ we can antisymmetrize a product wave function.

$$|\Phi^F\rangle \stackrel{\text{Eq. 8.12}}{=} \frac{1}{\sqrt{N!}} \sum_{i_1, \dots, i_N=1}^N \hat{P}_{i_1, \dots, i_N}^\dagger |\phi_1, \phi_2, \dots, \phi_N\rangle \epsilon_{i_1, \dots, i_N} \quad (8.12)$$

The pre-factor $\frac{1}{\sqrt{N!}}$ is the required normalization for an orthonormal set of one-particle wave functions: there are $N!$ distinct permutations of the N orbitals. Product states that differ by a permutation are orthonormal, if the one-particle states are orthonormal.

The corresponding wave function is

$$\begin{aligned} \Phi^F(\vec{x}_1, \vec{x}_2, \dots, \vec{x}_N) &= \frac{1}{\sqrt{N!}} \sum_{i_1, \dots, i_N} \epsilon_{i_1, \dots, i_N} \hat{P}_{i_1, \dots, i_N}^\dagger \phi_1(\vec{x}_1) \cdots \phi_N(\vec{x}_N) \\ &= \frac{1}{\sqrt{N!}} \sum_{i_1, \dots, i_N} \epsilon_{i_1, \dots, i_N} \phi_1(\vec{x}_{i_1}) \cdots \phi_N(\vec{x}_{i_N}) \end{aligned} \quad (8.13)$$

When one exploits the connection between Levi-Civita Symbol and the determinant discussed in section 8.1, the wave function Eq. 8.13 can also be written as a **Slater determinant**[17, 18]³

$$\Psi^F(\vec{x}_1, \dots, \vec{x}_N) = \frac{1}{\sqrt{N!}} \det \begin{vmatrix} \phi_1(\vec{x}_1) & \phi_1(\vec{x}_2) & \dots & \phi_1(\vec{x}_N) \\ \phi_2(\vec{x}_1) & \phi_2(\vec{x}_2) & \dots & \phi_2(\vec{x}_N) \\ \vdots & \vdots & \ddots & \vdots \\ \phi_N(\vec{x}_1) & \phi_N(\vec{x}_2) & \dots & \phi_N(\vec{x}_N) \end{vmatrix} \quad (8.14)$$

where $\epsilon_{i,j,k,\dots}$ is the fully antisymmetric tensor defined in Sec. 8.1. The Slater determinant exploits the property of the determinant, that it changes its sign under permutation of two columns of a matrix. In the Slater determinant the exchange of two columns corresponds to the exchange of two particle coordinates.

An antisymmetric wave function can be constructed even from a non-orthogonal set of one-particle orbitals by forming the corresponding determinant. However, unless the one-particle orbitals are orthonormal, the evaluation of matrix elements between Slater determinants is a nearly hopeless undertaking. Therefore, Slater determinants are usually built from an orthonormal set of one-particle orbitals.

As an example, the two-particle Slater determinant $|S_{a,b}\rangle$ of two one-particle states $\phi_a(\vec{x})$ and $\phi_b(\vec{x})$ is

$$S_{a,b}(\vec{x}_1, \vec{x}_2) = \langle \vec{x}_1 \vec{x}_2 | S_{a,b} \rangle = \frac{1}{\sqrt{2}} \left(\phi_a(\vec{x}_1) \phi_b(\vec{x}_2) - \phi_b(\vec{x}_1) \phi_a(\vec{x}_2) \right)$$

³According to a remark on Wikipedia, Heisenberg and Dirac proposed already in 1926 to write the antisymmetric wave function in a form of a determinant.

Bose wave functions

Analogous to the Slater determinant we can represent symmetrized product wave functions as a **permanent**. The permanent of a matrix $[A]$ can be written as

$$\text{perm}[A] = \sum_{i_1, \dots, i_N} \epsilon_{i_1, \dots, i_N}^2 A_{1, i_1} A_{2, i_2} \cdots A_{N, i_N}$$

We see from Eq. 8.8 that the permanent plays for bosons the same role as the determinant for Fermions.

A Bose wave function obtained by symmetrization of a product wave function has the form

$$\Psi^B(\vec{x}_1, \dots, \vec{x}_N) = \frac{1}{\sqrt{N!}} \sum_{i_1, \dots, i_N} \epsilon_{i_1, \dots, i_N}^2 \phi_1(\vec{x}_1) \cdots \phi_N(\vec{x}_N)$$

If the one-particle states are orthonormal, also the resulting "Permanent-wave functions" built from the same one-particle basis set are orthonormal.

General many-fermion wave function

It is important to realize that not every antisymmetric wave function can be represented as a Slater determinant. Slater determinants are derived from product wave functions and thus have a rather restricted form.

However, the Slater determinants that can be constructed from a complete, orthonormal set of one-particle wave functions $\{|\phi_1\rangle, |\phi_2\rangle, \dots\}$ form a complete orthonormal basis for antisymmetric many-particle states. (without proof)⁴

A general N-particle state can be constructed as follows: Let us consider a complete and orthonormal one-particle basis set $|\phi_1\rangle, |\phi_2\rangle, \dots$. A subset of N such basis functions, namely $|\phi_{i_1}\rangle, |\phi_{i_2}\rangle, \dots, |\phi_{i_N}\rangle$ defines a particular Slater determinant $|S_{i_1, i_2, \dots, i_N}\rangle$. A general antisymmetric N-particle state $|\Psi\rangle$ can be written as a sum over all Slater determinants

$$|\Psi\rangle = \sum_{i_1, i_2, \dots, i_N=1; i_j \neq i_k}^{\infty} |S_{i_1, i_2, \dots, i_N}\rangle c_{i_1, i_2, \dots}$$

where the $c_{i_1, i_2, \dots}$ are the (complex) expansion coefficients.

Number representation

We have learned that a Slater determinant is defined by a subset of N states from a given one-particle basis. Thus we can form a vector with one-component for each one-particle orbital. If we set the components equal to one for the orbitals in the set and equal to zero for all orbitals not in the set, we arrive at the number representation for Slater determinants

$$|S_{i_1, \dots, i_N}\rangle = |0, 0, \underbrace{1}_{\text{pos } i_1}, 0, 0, 0, \underbrace{1}_{\text{pos } i_2}, \underbrace{1}_{\text{pos } i_3}, 0, \dots\rangle$$

This allows to write a general fermionic state in the form

$$|\Psi\rangle = \sum_{\sigma_1=0}^1 \sum_{\sigma_2=0}^1 \cdots \sum_{\sigma_\infty=0}^1 |\sigma_1, \sigma_2, \dots, \sigma_\infty\rangle c_{\sigma_1, \sigma_2, \dots, \sigma_\infty} = \sum_{\vec{\sigma}} |\vec{\sigma}\rangle c_{\vec{\sigma}}$$

⁴Note that the one-particle states need not be orthonormal to fulfill the completeness condition. The requirement of orthonormal wave functions is necessary to obtain a orthonormal basis for the N-particle states and to make the evaluation of matrix elements feasible.

Chapter 9

The Hartree-Fock approximation

The **Hartree-Fock method**[17, 19, 20] is an electronic structure method that is the work-horse of quantum chemistry. Today it plays an important role as a starting point of more accurate and involved methods. The Hartree Fock method had a predecessor, the **Hartree method**[21, 22], which, however, does not play an important role in practice.

The basic idea of the Hartree-Fock method is to restrict the wave functions to single Slater determinants[17]. For this Slater determinant, the energy is determined as expectation value of the true many-particle Hamiltonian. That is, the Hartree Fock approximation takes the complete electron-electron interaction into account. Furthermore the one-particle orbitals are optimized to yield the lowest energy.

One can easily show that the Hartree-Fock energy always provides an upper bound for the energy. The Hamilton operator is, up to a constant, positive definite and the ground state is the state with the lowest energy. As we restricted our wave function to single Slater determinants, the wave function is, normally, not the ground state and therefore higher in energy than the ground-state energy.

9.1 One-electron and two-particle operators

The Born-Oppenheimer Hamiltonian Eq. 12.4 for an N-electron system has the form

$$E = E_{NN} + \langle \Psi | \sum_{i=1}^N \hat{h}_i + \frac{1}{2} \sum_{i \neq j} \hat{W}_{ij} | \Psi \rangle$$

Where

$$E_{NN}(\vec{R}_1, \dots, \vec{R}_N) \stackrel{\text{def}}{=} \frac{1}{2} \sum_{i \neq j}^M \frac{e^2 Z_i Z_j}{4\pi\epsilon_0 |\vec{R}_i - \vec{R}_j|} \quad (9.1)$$

is the electrostatic repulsion between the nuclei, and the operators acting on the electrons can be divided into one-particle terms \hat{h}_i and two-particle terms \hat{W}_{ij} .

The one-particle terms describe the kinetic and potential energy of the electrons in an external potential $v_{\text{ext}}(\vec{r})$

$$\hat{h}_i = \int d^4 x_1 \dots \int d^4 x_N |\vec{x}_1, \dots, \vec{x}_N\rangle \left[\frac{-\hbar^2}{2m_e} \vec{\nabla}_{\vec{r}_i}^2 + v_{\text{ext}}(\vec{r}_i) \right] \langle \vec{x}_1, \dots, \vec{x}_N | \quad (9.2)$$

The external potential describes the electrostatic attraction between electrons and nuclei.

$$v_{\text{ext}}(\vec{r}; \vec{R}_1, \dots, \vec{R}_M) = - \sum_{j=1}^M \frac{e^2 Z_j}{4\pi\epsilon_0 |\vec{r} - \vec{R}_j|} \quad (9.3)$$

The two-particle operator describes the interaction between the electrons

$$\hat{W}_{ij} = \int d^4x_1 \cdots \int d^4x_N |\vec{x}_1, \dots, \vec{x}_N\rangle \frac{e^2}{4\pi\epsilon_0 |\vec{r}_i - \vec{r}_j|} \langle \vec{x}_1, \dots, \vec{x}_N| \quad (9.4)$$

The indices on \hat{h}_i and \hat{W}_{ij} determine, onto which electron coordinates the operator acts.

The **one-particle operators** act on the coordinates of one particle at a time. The kinetic energy and the external potential are examples for one-particle operators, because they can be determined for each particle individually and then be summed up. The interaction energy Eq. 9.4 on the other hand depends on the coordinates of two particles simultaneously and is therefore a true **two-particle operator**. It is the two-particle term that is the cause for the dazzling complexity of many-particle physics.

Let us consider a general operator in real space

$$\begin{aligned} \hat{A} &= \underbrace{\int d^4x_1 \cdots \int d^4x_N |\vec{x}_1, \dots, \vec{x}_N\rangle \langle \vec{x}_1, \dots, \vec{x}_N|}_{\hat{1}} \cdot \underbrace{\hat{A} \int d^4x'_1 \cdots \int d^4x'_N |\vec{x}'_1, \dots, \vec{x}'_N\rangle \langle \vec{x}'_1, \dots, \vec{x}'_N|}_{\hat{1}} \\ &= \int d^4x_1 \cdots \int d^4x_N \int d^4x'_1 \cdots \int d^4x'_N |\vec{x}_1, \dots, \vec{x}_N\rangle \cdot \langle \vec{x}_1, \dots, \vec{x}_N | \hat{A} | \vec{x}'_1, \dots, \vec{x}'_N \rangle \langle \vec{x}'_1, \dots, \vec{x}'_N | \end{aligned}$$

A general matrix element has therefore $2N$ arguments.

- If the matrix element of an operator has the special form

$$\langle \vec{x}_1, \dots, \vec{x}_N | \hat{A} | \vec{x}'_1, \dots, \vec{x}'_N \rangle = \sum_{i=1}^N A(\vec{x}_i, \vec{x}'_i) \prod_{j \neq i} \delta(\vec{x}_j - \vec{x}'_j)$$

we call the operator a **one-particle operator**.

- If furthermore the function $A(\vec{x}, \vec{x}')$ has the special form that it is diagonal in the primed and unprimed arguments, i.e.

$$A(\vec{x}, \vec{x}') = a(\vec{x}) \delta(\vec{x} - \vec{x}')$$

we call the one-particle operator **local**.

- If the matrix element of an operator has the special form

$$\langle \vec{x}_1, \dots, \vec{x}_N | \hat{A} | \vec{x}'_1, \dots, \vec{x}'_N \rangle = \frac{1}{2} \sum_{i,j=1}^N A(\vec{x}_i, \vec{x}_j, \vec{x}'_i, \vec{x}'_j) \prod_{k \neq \{i,j\}} \delta(\vec{x}_k - \vec{x}'_k)$$

we call the operator a **two-particle operator**.

- If furthermore the function $A(\vec{x}_1, \vec{x}_2, \vec{x}'_1, \vec{x}'_2)$ has the special form that it is diagonal in the primed and unprimed arguments, i.e.

$$A(\vec{x}_1, \vec{x}_2, \vec{x}'_1, \vec{x}'_2) = a(\vec{x}_1, \vec{x}_2) \delta(\vec{x}_1 - \vec{x}'_1) \delta(\vec{x}_2 - \vec{x}'_2)$$

we call the two-particle operator **local**.

9.2 Expectation values of Slater determinants

Let us now work out the expectation values for the one-particle and two particle operators for a Slater determinant.

9.2.1 Expectation value of a one-particle operator

Here, we will work out the expectation value of a one-particle operator for a Slater determinant. An example for such a one-particle operator is the non-interacting part of the Hamiltonian.

Explicit example for the two-particle wave function

The two-particle Slater determinant of two one-particle orbitals $|\phi_a\rangle$ and $|\phi_b\rangle$ has the form

$$\underbrace{\langle \vec{r}_1 \vec{r}_2 | \Psi \rangle}_{\Psi(\vec{r}_1, \vec{r}_2)} = \frac{1}{\sqrt{2}} \underbrace{\left[\langle \vec{r}_1 | \phi_a \rangle \langle \vec{r}_2 | \phi_b \rangle - \langle \vec{r}_1 | \phi_b \rangle \langle \vec{r}_2 | \phi_a \rangle \right]}_{\phi_a(\vec{r}_1)\phi_b(\vec{r}_2) - \phi_b(\vec{r}_1)\phi_a(\vec{r}_2)} \quad (9.5)$$

To avoid unnecessary complication we drop the spin-coordinates, that is we consider spin-less fermions.

As an specific example for a one-particle operator, we consider the particle-density operator $\hat{n}(\vec{r})$ defined as

$$\hat{n}(\vec{r}) = \int d^3 r_1 \int d^3 r_2 |\vec{r}_1, \vec{r}_2\rangle \left[\delta(\vec{r} - \vec{r}_1) + \delta(\vec{r} - \vec{r}_2) \right] \langle \vec{r}_1, \vec{r}_2 |$$

The electron density is

$$\begin{aligned} n(\vec{r}) &= \langle \Psi | \hat{n}(\vec{r}) | \Psi \rangle \\ &= \int d^3 r_1 \int d^3 r_2 \Psi^*(\vec{r}_1, \vec{r}_2) \left[\delta(\vec{r} - \vec{r}_1) + \delta(\vec{r} - \vec{r}_2) \right] \Psi(\vec{r}_1, \vec{r}_2) \\ &\stackrel{\Psi(\vec{r}_1, \vec{r}_2) = -\Psi(\vec{r}_2, \vec{r}_1)}{=} \int d^3 r_1 \int d^3 r_2 \Psi^*(\vec{r}_1, \vec{r}_2) \delta(\vec{r} - \vec{r}_1) \Psi(\vec{r}_1, \vec{r}_2) \\ &\quad + \int d^3 r_1 \int d^3 r_2 \Psi^*(\vec{r}_2, \vec{r}_1) \delta(\vec{r} - \vec{r}_2) \Psi(\vec{r}_2, \vec{r}_1) \\ &\stackrel{\vec{r}_1 \leftrightarrow \vec{r}_2}{=} 2 \int d^3 r_1 \int d^3 r_2 \Psi^*(\vec{r}_1, \vec{r}_2) \delta(\vec{r} - \vec{r}_1) \Psi(\vec{r}_1, \vec{r}_2) \\ &\stackrel{\text{Eq. 9.5}}{=} 2 \int d^3 r_1 \int d^3 r_2 \frac{1}{\sqrt{2}} \left[\phi_a(\vec{r}_1) \phi_b(\vec{r}_2) - \phi_a(\vec{r}_2) \phi_b(\vec{r}_1) \right]^* \\ &\quad \cdot \delta(\vec{r} - \vec{r}_1) \frac{1}{\sqrt{2}} \left[\phi_a(\vec{r}_1) \phi_b(\vec{r}_2) - \phi_a(\vec{r}_2) \phi_b(\vec{r}_1) \right] \\ &= \int d^3 r_1 \int d^3 r_2 \phi_a^*(\vec{r}_1) \phi_b^*(\vec{r}_2) \delta(\vec{r} - \vec{r}_1) \phi_a(\vec{r}_1) \phi_b(\vec{r}_2) \\ &\quad - \int d^3 r_1 \int d^3 r_2 \phi_a^*(\vec{r}_1) \phi_b^*(\vec{r}_2) \delta(\vec{r} - \vec{r}_1) \phi_a(\vec{r}_2) \phi_b(\vec{r}_1) \\ &\quad - \int d^3 r_1 \int d^3 r_2 \phi_a^*(\vec{r}_2) \phi_b^*(\vec{r}_1) \delta(\vec{r} - \vec{r}_1) \phi_a(\vec{r}_1) \phi_b(\vec{r}_2) \\ &\quad + \int d^3 r_1 \int d^3 r_2 \phi_a^*(\vec{r}_2) \phi_b^*(\vec{r}_1) \delta(\vec{r} - \vec{r}_1) \phi_a(\vec{r}_2) \phi_b(\vec{r}_1) \\ &= \underbrace{\langle \phi_a | \vec{r} \rangle \langle \vec{r} | \phi_a \rangle}_{=1} \underbrace{\langle \phi_b | \phi_b \rangle}_{=0} - \underbrace{\langle \phi_a | \vec{r} \rangle \langle \vec{r} | \phi_b \rangle}_{=0} \underbrace{\langle \phi_b | \phi_a \rangle}_{=0} \\ &\quad - \underbrace{\langle \phi_b | \vec{r} \rangle \langle \vec{r} | \phi_a \rangle}_{=0} \underbrace{\langle \phi_a | \phi_b \rangle}_{=0} + \underbrace{\langle \phi_b | \vec{r} \rangle \langle \vec{r} | \phi_b \rangle}_{=1} \underbrace{\langle \phi_a | \phi_a \rangle}_{=1} \\ &= \phi_a^*(\vec{r}) \phi_a(\vec{r}) + \phi_b^*(\vec{r}) \phi_b(\vec{r}) \end{aligned}$$

Let us mention a few observations:

- The number of terms is drastically reduced just because we have used an orthonormal set of one-particle wave functions. This is the sole reason of using orthonormal basissets in many-particle physics.
- The sum over particles is turned into a sum over orbitals. This is true for a Slater determinant, but not for a general many particle states.
- The antisymmetry of the wave function ensures that the same expectation value is obtained if we work out a property of the first or the second electron.

General derivation

Now we will determine the same result in its full generality: First, we evaluate only the matrix element of the one-particle operator \hat{h}_1 , that acts only on the coordinates of only one particle, namely the first. This result is then generalized for the other particles and the summed up to obtain the expectation value of the non-interacting part of the Hamiltonian..

To be concise, we write here the detailed expressions for the matrix elements of the one-particle Hamilton operator, we have in mind

$$\begin{aligned} \langle \phi | \hat{h} | \phi \rangle &= \int d^4x \int d^4x' \langle \phi | \vec{x} \rangle \underbrace{\left(-\frac{\hbar^2}{2m_e} \vec{\nabla}^2 + v(\vec{r}) \right)}_{\langle \vec{x} | \hat{h} | \vec{x}' \rangle} \langle \vec{x}' | \phi \rangle \\ &= \sum_{\sigma} \int d^3r \phi^*(\vec{r}, \sigma) \left[\frac{-\hbar^2}{2m_e} \vec{\nabla}^2 + v_{\text{ext}}(\vec{r}) \right] \phi(\vec{r}, \sigma) \end{aligned} \quad (9.6)$$

The one-particle Hamiltonian \hat{h}_j acting on the j -th particle in a many particle wave function Ψ yields the expectation value

$$\langle \Psi | \hat{h}_j | \Psi \rangle = \int d^4x_1 \dots \int d^4x_N \Psi^*(\vec{x}_1, \dots, \vec{x}_N) \left(\frac{-\hbar^2}{2m_e} \vec{\nabla}_j^2 + v_{\text{ext}}(\vec{r}_j) \right) \Psi(\vec{x}_1, \dots, \vec{x}_N)$$

so that the matrix element for two product wave functions is

$$\langle \phi_1, \dots, \phi_N | \hat{h}_j | \psi_1, \dots, \psi_N \rangle = \langle \phi_1 | \psi_1 \rangle \dots \langle \phi_j | \hat{h}_j | \psi_j \rangle \dots \langle \phi_N | \psi_N \rangle \quad (9.7)$$

The Slater determinant, given in Eq. 8.14, has the form

$$\langle \vec{x}_1, \dots, \vec{x}_N | \Psi \rangle = \frac{1}{\sqrt{N!}} \sum_{i_1, \dots, i_N=1}^N \epsilon_{i_1, \dots, i_N} \langle \vec{x}_1 | \phi_{i_1} \rangle \dots \langle \vec{x}_N | \phi_{i_N} \rangle \quad (9.8)$$

Thus, the matrix element of a one-particle operator Eq. 9.2 acting only on the first electron

coordinate is

$$\begin{aligned}
 \langle \Psi | \sum_{i=1}^N \hat{h}_i | \Psi \rangle &= N \langle \Psi | \hat{h}_1 | \Psi \rangle \\
 &\stackrel{\text{Eq. 9.8}}{=} N \cdot \frac{1}{N!} \sum_{i_1, i_2, \dots, i_N} \sum_{j_1, j_2, \dots, j_N} \epsilon_{i_1, i_2, \dots, i_N} \langle \phi_{i_1} \dots \phi_{i_N} | \hat{h}_1 | \phi_{j_1} \dots \phi_{j_N} \rangle \epsilon_{j_1, j_2, \dots, j_N} \\
 &\stackrel{\text{Eq. 9.7}}{=} N \frac{1}{N!} \sum_{i_1, i_2, \dots, i_N} \sum_{j_1, j_2, \dots, j_N} \epsilon_{i_1, i_2, \dots, i_N} \epsilon_{j_1, j_2, \dots, j_N} \underbrace{\langle \phi_{i_1} | \hat{h}_1 | \phi_{j_1} \rangle}_{\delta_{i_1 j_1}} \underbrace{\langle \phi_{i_2} | \phi_{j_2} \rangle}_{\delta_{i_2 j_2}} \dots \underbrace{\langle \phi_{i_N} | \phi_{j_N} \rangle}_{\delta_{i_N j_N}} \\
 &= N \frac{1}{N!} \sum_{i_1, j_1=1}^N \langle \phi_{i_1} | \hat{h}_1 | \phi_{j_1} \rangle \underbrace{\sum_{i_2, \dots, i_N} \epsilon_{i_1, i_2, \dots, i_N} \epsilon_{j_1, i_2, \dots, i_N}}_{\delta_{i_1 j_1} (N-1)!} \\
 &= \sum_{j=1}^N \langle \phi_j | \hat{h}_1 | \phi_j \rangle
 \end{aligned}$$

In the last step we exploited, that the sum over j_1 only contributes when $j_1 = i_1$. There is only one orbital left if all the orbitals but the first are determined. Thus, the first orbital must be the same for both Levi-Civita Symbols.

Thus, we obtain the expectation value of the one-particle Hamiltonian for a Slater determinant $|\Psi\rangle$ as

EXPECTATION VALUE OF A ONE-PARTICLE OPERATOR WITH A SLATER-DETERMINANT

$$\langle \Psi | \sum_{i=1}^N \hat{h}_i | \Psi \rangle = \sum_{i=1}^N \langle \phi_i | \hat{h} | \phi_i \rangle \quad (9.9)$$

Here, $|\Psi\rangle$ is a N-particle Slater-determinant built from the one-particle orbitals $|\phi_i\rangle$, and $\sum_{i=1}^N \hat{h}_i$ is a one-particle operator.

Expectation values of common one-particle operators with Slater determinants

Analogously, the expectation value of any one-particle operator with a Slater determinant can be represented by a sum over one-particle orbitals. Thus, we obtain the expression for the density

$$n(\vec{r}) = \langle \Psi | \sum_{i=1}^N \sum_{\sigma} \left(|\vec{r}, \sigma\rangle \langle \vec{r}, \sigma| \right)_i | \Psi \rangle = \sum_{i=1}^N \sum_{\sigma} \phi_i^*(\vec{r}, \sigma) \phi_i(\vec{r}, \sigma) \quad (9.10)$$

where

$$\left(|\vec{r}\rangle \langle \vec{r}| \right)_i \stackrel{\text{def}}{=} \int d^4 x_1 \dots \int d^4 x_N |\vec{x}_1, \dots, \vec{x}_N\rangle \delta(\vec{r} - \vec{r}_i) \langle \vec{x}_1, \dots, \vec{x}_N|$$

The expectation value of the kinetic energy for a Slater determinant has the form

$$E_{kin} = \langle \Psi | \sum_{i=1}^N \frac{\hat{p}_i^2}{2m_e} | \Psi \rangle = \sum_{i=1}^N \sum_{\sigma} \int d^3 r \phi_i^*(\vec{r}, \sigma) \frac{-\hbar^2}{2m_e} \nabla^2 \phi_i(\vec{r}, \sigma) \quad (9.11)$$

9.2.2 Expectation value of a two-particle operator

Let us now turn to the two-particle term. We introduce the symbol

$$W(\vec{r}, \vec{r}') = \frac{e^2}{4\pi\epsilon_0|\vec{r} - \vec{r}'|}$$

The interaction is independent of the spin index. Furthermore it is local in the two coordinates.¹

We start out as for the expectation value of a one-particle operator and consider only the interaction between the first two electrons. That is the operator acts only on the first two sets of particle coordinates.

$$\begin{aligned} E_W &= \langle \Psi | \frac{1}{2} \sum_{i \neq j}^N \hat{W}_{ij} | \Psi \rangle = \frac{N(N-1)}{2} \langle \Psi | \hat{W}_{1,2} | \Psi \rangle \\ &= \frac{N(N-1)}{2} \frac{1}{N!} \sum_{i_1, i_2, \dots, i_N} \sum_{j_1, j_2, \dots, j_N} \epsilon_{i_1, i_2, \dots, i_N} \epsilon_{j_1, j_2, \dots, j_N} \langle \phi_{i_1} \dots \phi_{i_N} | \hat{W}_{12} | \phi_{j_1} \dots \phi_{j_N} \rangle \\ &= \frac{1}{2 \cdot (N-2)!} \sum_{i_1, i_2, \dots, i_N} \sum_{j_1, j_2, \dots, j_N} \epsilon_{i_1, i_2, \dots, i_N} \epsilon_{j_1, j_2, \dots, j_N} \langle \phi_{i_1} \phi_{i_2} | \hat{W}_{12} | \phi_{j_1} \phi_{j_2} \rangle \underbrace{\langle \phi_{i_3} | \phi_{j_3} \rangle}_{\delta_{i_3 j_3}} \dots \underbrace{\langle \phi_{i_N} | \phi_{j_N} \rangle}_{\delta_{i_N j_N}} \\ &= \frac{1}{2 \cdot (N-2)!} \sum_{i_1, i_2, j_1, j_2} \langle \phi_{i_1} \phi_{i_2} | \hat{W}_{12} | \phi_{j_1} \phi_{j_2} \rangle \underbrace{\sum_{i_3, \dots, i_N} \epsilon_{i_1, i_2, i_3, \dots, i_N} \epsilon_{j_1, j_2, i_3, \dots, i_N}}_{(N-2)! \epsilon_{i_1, i_2} \epsilon_{j_1, j_2} \text{ for } i_1, i_2 \in \{j_1, j_2\}} \\ &= \frac{1}{2} \sum_{i_1, i_2} \sum_{j_1, j_2 \in \{i_1, i_2\}} \langle \phi_{i_1} \phi_{i_2} | \hat{W}_{12} | \phi_{j_1} \phi_{j_2} \rangle \underbrace{\epsilon_{i_1, i_2} \epsilon_{j_1, j_2}}_{\delta_{i_1 j_1} \delta_{i_2 j_2} - \delta_{i_1 j_2} \delta_{i_2 j_1}} \\ &= \frac{1}{2} \sum_{i_1, i_2} \left(\langle \phi_{i_1} \phi_{i_2} | \hat{W}_{12} | \phi_{i_1} \phi_{i_2} \rangle - \langle \phi_{i_1} \phi_{i_2} | \hat{W}_{12} | \phi_{i_2} \phi_{i_1} \rangle \right) \end{aligned}$$

Note, that we exploited in the last step that the two interaction terms cancel when the indices i_1 and i_2 are identical. Therefore they need not be excluded from the sum. The latter formula is more convenient to discuss the physical implications, while the former is commonly used in the quantum chemical literature.

We recognize the result of the indistinguishability of the electrons: The interaction between any two electrons is identical to any other pair. Since there are $\frac{N(N-1)}{2}$ ordered pairs and thus $N(N-1)$ unordered pairs, the pre factor $\frac{1}{N(N-1)}$ drops out, and we obtain

$$\langle \Psi | \frac{1}{2} \sum_{i \neq j}^N \hat{W}_{ij} | \Psi \rangle = \frac{1}{2} \sum_{i,j=1}^N \left[\langle \phi_i \phi_j | \hat{W} | \phi_i \phi_j \rangle - \langle \phi_i \phi_j | \hat{W} | \phi_j \phi_i \rangle \right] \quad (9.12)$$

¹A general two particle operator has the form

$$\begin{aligned} \hat{W}_{1,2} &= \int dx_1 \dots \int dx_N \int dx'_1 \dots \int dx'_N |\vec{x}_1, \dots, \vec{x}_N\rangle \langle \vec{x}_1, \dots, \vec{x}_N | \hat{W}_{1,2} | \vec{x}'_1, \dots, \vec{x}'_N\rangle \langle \vec{x}'_1, \dots, \vec{x}'_N | \\ &= \int dx_1 \dots \int dx_N \int dx'_1 \int dx'_2 |\vec{x}_1, \dots, \vec{x}_N\rangle \langle \vec{x}_1, \dots, \vec{x}_N | \hat{W}_{1,2} | \vec{x}'_1, \vec{x}'_2, \vec{x}_3, \dots, \vec{x}_N\rangle \langle \vec{x}'_1, \vec{x}'_2, \vec{x}_3, \dots, \vec{x}_N | \\ &= \int dx_1 \dots \int dx_N \int dx'_1 \int dx'_2 |\vec{x}_1, \dots, \vec{x}_N\rangle \langle \vec{x}_1, \vec{x}_2 | \hat{W}_{1,2} | \vec{x}'_1, \vec{x}'_2\rangle \langle \vec{x}'_1, \vec{x}'_2, \vec{x}_3, \dots, \vec{x}_N | \end{aligned}$$

Thus, a general two particle operator is nonlocal in the two particle coordinates and therefore depends on four arguments.

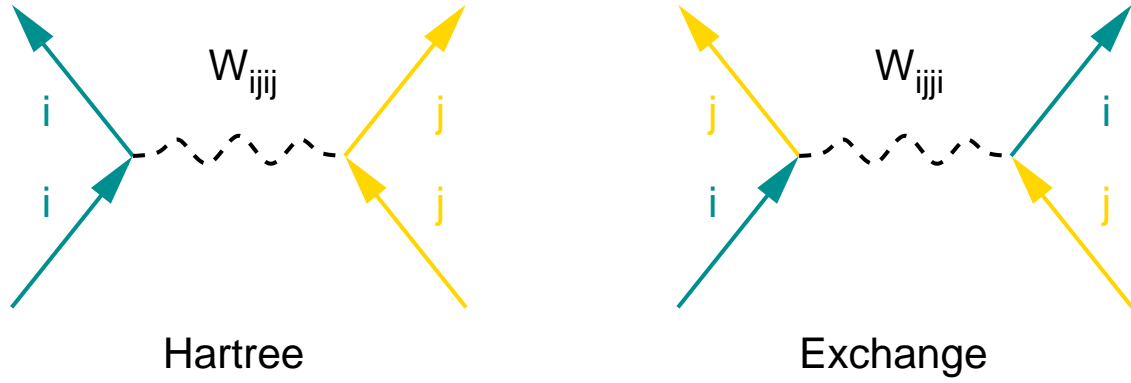


Fig. 9.1: The left diagram describes that two particles are scattered by the Coulomb interaction. The right diagram describes the same process, but the two electrons are exchanged. The second process is possible, because the two electrons are indistinguishable so that we cannot detect if the two electrons are still the same or not.

To be concise, we write here the detailed expressions for the matrix elements used in the above equation Eq. 9.12

$$\langle \phi_a \phi_b | \hat{W} | \phi_c \phi_d \rangle = \sum_{\sigma, \sigma'} \int d^3r \int d^3r' \phi_a^*(\vec{r}, \sigma) \phi_b^*(\vec{r}', \sigma') \frac{e^2}{4\pi\epsilon_0 |\vec{r} - \vec{r}'|} \phi_c(\vec{r}, \sigma) \phi_d(\vec{r}', \sigma') \quad (9.13)$$

Homework: Work out the expectation value of the Coulomb interaction between two electrons for a two-electron Slater determinant. Consider once a Slater determinant from non-orthonormal one-particle orbitals and once for orthonormal one-particle orbitals. Investigate the role of the spin indices.

9.3 Hartree energy

The surprising fact of Eq. 9.12 is the appearance of two terms. Therefore let us try to give some physical meaning to the two contributions.

The first interaction term in Eq. 9.12 is the so-called **Hartree energy**. The Hartree energy turns out to be the classical electrostatic interaction of the electron density.

$$\begin{aligned} E_H &= \frac{1}{2} \sum_{i,j} \sum_{\sigma, \sigma'} \int d^3r \int d^3r' \phi_i^*(\vec{r}, \sigma) \phi_j^*(\vec{r}', \sigma') \frac{e^2}{4\pi\epsilon_0 |\vec{r} - \vec{r}'|} \phi_i(\vec{r}, \sigma) \phi_j(\vec{r}', \sigma') \\ &= \frac{1}{2} \int d^3r \int d^3r' \underbrace{\left[\sum_{i, \sigma} \phi_i^*(\vec{r}, \sigma) \phi_i(\vec{r}, \sigma) \right]}_{n(\vec{r})} \frac{e^2}{4\pi\epsilon_0 |\vec{r} - \vec{r}'|} \underbrace{\left[\sum_{j, \sigma'} \phi_j^*(\vec{r}', \sigma') \phi_j(\vec{r}', \sigma') \right]}_{n(\vec{r}')} \end{aligned} \quad (9.14)$$

The equation can be simplified using the definition of the charge density $\rho(\vec{r})$, or the electron density $n(\vec{r})$, as

$$\rho(\vec{r}) = -en(\vec{r}) = -e \underbrace{\sum_{i=1}^N \sum_{\sigma} \phi_i^*(\vec{r}, \sigma) \phi_i(\vec{r}, \sigma)}_{n(\vec{r})}$$

Thus, we obtain the final expression for the Hartree energy

HARTREE ENERGY

$$E_H = \frac{1}{2} \int d^3r \int d^3r' \frac{\rho(\vec{r})\rho(\vec{r}')}{4\pi\epsilon_0|\vec{r}-\vec{r}'|} \quad (9.15)$$

9.4 Exchange energy

Exchange energy

The Hartree energy is clearly not the correct electrostatic energy, as it describes the interaction of N electrons with N electrons. However, each electron can only interact with $N - 1$ electrons. Thus, the Hartree term also includes, incorrectly, the interaction of each electron with itself.

This so-called **self interaction** is subtracted by the so-called **exchange energy**, the second interaction term in Eq. 9.12

$$E_X = -\frac{1}{2} \sum_{i,j} \sum_{\sigma,\sigma'} \int d^3r \int d^3r' \phi_i^*(\vec{r},\sigma) \phi_j^*(\vec{r}',\sigma') \frac{e^2}{4\pi\epsilon_0|\vec{r}-\vec{r}'|} \phi_j(\vec{r},\sigma) \phi_i(\vec{r}',\sigma') \quad (9.16)$$

The exchange term consists of the electrostatic interaction of densities

$$n_{ij}(\vec{r}) \stackrel{\text{def}}{=} \sum_{\sigma} \phi_i(\vec{r},\sigma) \phi_j^*(\vec{r},\sigma)$$

The exchange energy can be written as

$$E_X = -\frac{1}{2} \sum_{i,j} \frac{e^2 n_{ij}(\vec{r}) n_{ji}(\vec{r}')}{4\pi\epsilon_0|\vec{r}-\vec{r}'|}$$

while the Hartree term has the form

$$E_H = \frac{1}{2} \sum_{i,j} \frac{e^2 n_{ii}(\vec{r}) n_{jj}(\vec{r}')}{4\pi\epsilon_0|\vec{r}-\vec{r}'|}$$

Self interaction

All pair densities with different indices integrate to zero and the one with identical indices integrate to one, that is

$$\int d^3r n_{ij}(\vec{r}) = \langle \phi_j | \phi_i \rangle = \delta_{ij}$$

Thus, if we can expect that the dominant contribution results from the diagonal terms. This so-called **self-interaction energy**

$$\begin{aligned} E_{SI} &= +\frac{1}{2} \sum_i \sum_{\sigma,\sigma'} \int d^3r \int d^3r' \phi_i^*(\vec{r},\sigma) \phi_i^*(\vec{r}',\sigma') \frac{e^2}{4\pi\epsilon_0|\vec{r}-\vec{r}'|} \phi_i(\vec{r},\sigma) \phi_i(\vec{r}',\sigma') \\ &= -\frac{1}{2} \sum_i \int d^3r \int d^3r' \frac{e^2 n_{ii}(\vec{r}) n_{ii}(\vec{r}')}{4\pi\epsilon_0|\vec{r}-\vec{r}'|} \end{aligned}$$

describes the electrostatic interaction of each electron with itself, that has been included in the Hartree correction. There is a well-known electronic structure method, based on density functional theory, which uses the same trick to get rid of artificial self-interaction terms.[23]. This theory subtracts the self energy from the Hartree term and thus includes the so-called self-interaction correction $E_{SIC} = -E_{SI}$.

Exchange and spin alignment

Only electron pairs with identical spin contribute the exchange energy. This can be shown when one considers one-particle spin-orbitals with defined spin along the z-axis. That is, each one-particle spin-orbital has only one spin component, the other being zero.

- If the two orbitals have the same spin, for example pointing into the $+\vec{e}_z$ direction, they can be written as

$$\phi_i(\vec{x}) = \begin{pmatrix} \phi_i(\vec{r}, \uparrow) \\ 0 \end{pmatrix} \quad \text{and} \quad \phi_j(\vec{x}) = \begin{pmatrix} \phi_j(\vec{r}, \uparrow) \\ 0 \end{pmatrix}$$

The resulting exchange-energy would be formed from the densities

$$\sum_{\sigma} \phi_i(\vec{r}, \sigma) \phi_j^*(\vec{r}, \sigma) = \phi_i(\vec{r}, \uparrow) \phi_j^*(\vec{r}, \uparrow)$$

so that its contribution has the form

$$\begin{aligned} \Delta E_X &= -\frac{1}{2} \sum_{\sigma} \int d^3r \int d^3r' \frac{e^2 \phi_i^*(\vec{r}, \sigma) \phi_j(\vec{r}, \sigma) \phi_j^*(\vec{r}', \sigma) \phi_i(\vec{r}', \sigma)}{4\pi\epsilon_0 |\vec{r} - \vec{r}'|} \\ &= -\frac{1}{2} \sum_{\sigma} \int d^3r \int d^3r' \frac{e^2 \phi_i^*(\vec{r}, \uparrow) \phi_j(\vec{r}, \uparrow) \phi_j^*(\vec{r}', \uparrow) \phi_i(\vec{r}', \uparrow)}{4\pi\epsilon_0 |\vec{r} - \vec{r}'|} \end{aligned}$$

- If the two orbitals have the opposite spin, they can be written as

$$\phi_i(\vec{x}) = \begin{pmatrix} \phi_{i,\uparrow}(\vec{r}) \\ 0 \end{pmatrix} \quad \text{and} \quad \phi_j(\vec{x}) = \begin{pmatrix} 0 \\ \phi_{j,\downarrow}(\vec{r}) \end{pmatrix}$$

The contribution to the exchange energy vanishes, because

$$\sum_{\sigma} \phi_i(\vec{r}, \sigma) \phi_j(\vec{r}, \sigma) = \phi_i(\vec{r}, \uparrow) \cdot 0 + 0 \cdot \phi_j(\vec{r}, \downarrow) = 0$$

HUND'S RULE AND FERROMAGNETISM

Exchange acts only between electrons pairs with the same spin. Because exchange counteracts the Coulomb repulsion due to its changed sign, it favors if many electrons have the same spin.

A result is **Hund's 1st rule**: *For a given electron configuration, the term with maximum multiplicity has the lowest energy. The multiplicity is equal to $2S+1$, where S is the total spin angular momentum for all electrons. The term with lowest energy is also the term with maximum S .*

The same effect is responsible for the tendency of some solids to become **ferromagnetic**. Due to the finite band width of metals, spin-alignment leads to some loss of kinetic energy. The balance of kinetic energy and exchange determines whether ferromagnetism wins.

9.5 Hartree-Fock equations

The Hartree Fock energy is an upper bound

The Hartree-Fock method yields an estimate E_{HF} for the ground state energy E_{GS} as

$$\begin{aligned} E_{GS} \leq E_{HF} = \min_{[\phi_i(\vec{x})]} & \left[E_{NN} + \sum_{i=1}^N \langle \phi_i | \hat{h} | \phi_i \rangle \right. \\ & + \frac{1}{2} \sum_{i,j=1}^N \left[\langle \phi_i \phi_j | \hat{W} | \phi_i \phi_j \rangle - \langle \phi_i \phi_j | \hat{W} | \phi_j \phi_i \rangle \right] \\ & \left. - \sum_{i,j} \Lambda_{i,j} [\langle \phi_i | \phi_j \rangle - \delta_{i,j}] \right] \end{aligned}$$

The last term ensures the orthonormality of the one-particle orbitals using the method of Lagrange multipliers. The matrix elements are defined in Eq. 9.6 and Eq. 9.13. The energy E_{NN} describes the Coulomb repulsion of the nuclei as defined in Eq. 9.1.

The minimum condition yields the **Hartree-Fock equations**.

Hartree-Fock equations

Wirtinger derivatives

The derivation is almost analogous to the derivation of the Euler-Lagrange equations. Special is that here we work with fields, the one-particle wave functions, and that the variational parameters are complex. It is advantageous to use the **Wirtinger derivatives**, which are described briefly in ΦSX: Klassische Mechanik.

The essence of Wirtinger derivatives is that we can write the identity

$$df(\text{Re}[c], \text{Im}[c]) = \frac{df}{d\text{Re}[c]} d\text{Re}[c] + \frac{df}{d\text{Im}[c]} d\text{Im}[c] = \frac{df}{dc} dc + \frac{df}{dc^*} dc^* = df(c, c^*)$$

for the first variation of f . Thus, we can form the variations of a function of complex arguments, as if the variable and its complex conjugate were completely independent variables.

For the functional derivatives we use

$$\begin{aligned} \frac{d\Psi_n^*(\vec{r}, \sigma)}{d\Psi_k^*(\vec{r}_0, \sigma_0)} &= \delta(\vec{r} - \vec{r}_0) \delta_{\sigma, \sigma_0} \delta_{n,k} \\ \frac{d\Psi_n(\vec{r}, \sigma)}{d\Psi_k^*(\vec{r}_0, \sigma_0)} &= 0 \end{aligned}$$

$$\begin{aligned} & \left[\frac{-\hbar^2}{2m_e} \vec{\nabla}^2 + \sum_{j=1}^M \frac{-e^2 Z}{4\pi\epsilon_0 |\vec{r} - \vec{R}_j|} + \int d^3 r' \frac{e^2 n(\vec{r}')}{4\pi\epsilon_0 |\vec{r} - \vec{r}'|} \right] \phi_i(\vec{r}, \sigma) \\ & - \sum_{j=1}^N \sum_{\sigma'} \int d^3 r' \frac{e^2 \phi_j^*(\vec{r}', \sigma') \phi_i(\vec{r}', \sigma')}{4\pi\epsilon_0 |\vec{r} - \vec{r}'|} \phi_j(\vec{r}, \sigma) - \sum_{j=1}^N \phi_j(\vec{r}, \sigma) \Lambda_{j,i} = 0 \end{aligned}$$

Note that this is not a simple Schrödinger equation, because it mixes all orbitals.

However, we can rewrite the equations to obtain a true Hamiltonian, which acts on all wave

functions in the same way:

$$\begin{aligned} & \left[\frac{-\hbar^2}{2m_e} \nabla^2 + \sum_{j=1}^M \frac{-e^2 Z}{4\pi\epsilon_0 |\vec{r} - \vec{R}_j|} + \int d^3 r' \frac{e^2 n(\vec{r}')}{4\pi\epsilon_0 |\vec{r} - \vec{r}'|} \right] \phi_i(\vec{r}, \sigma) \\ & - \sum_{\sigma'} \int d^3 r' \underbrace{\left[\sum_{j=1}^N \frac{e^2 \phi_j^*(\vec{r}, \sigma) \phi_j(\vec{r}', \sigma')}{4\pi\epsilon_0 |\vec{r} - \vec{r}'|} \right]}_{-V_{X,\sigma,\sigma'}(\vec{r}, \vec{r}') = -\langle \vec{x} | V_X | \vec{x}' \rangle} \phi_i(\vec{r}', \sigma') - \sum_j \phi_j(\vec{r}, \sigma) \Lambda_{j,i} = 0 \end{aligned} \quad (9.17)$$

This form actually shows that the one-particle orbitals can be superimposed so that the matrix Λ becomes diagonal. It can be shown that the system of equations is invariant under a unitary transformation of the one-particle orbitals. Thus, one can use the matrix that diagonalizes Λ , to bring the equations into a diagonal form. Hence we can write the Hartree-Fock equations as true eigenvalue equations.

Non-local potential

However the price to pay is that we have to deal with a truly non-local potential in the exchange term. What is a **non-local potential**? Consider an arbitrary operator \hat{A}

$$\begin{aligned} \langle \psi | \hat{A} | \phi \rangle &= \langle \psi | \underbrace{\left[\int d^3 r |\vec{r}\rangle \langle \vec{r}| \right]}_{\hat{1}} \hat{A} \underbrace{\left[\int d^3 r' |\vec{r}'\rangle \langle \vec{r}'| \right]}_{\hat{1}} | \phi \rangle \\ &= \int d^3 r \int d^3 r' \underbrace{\langle \psi | \vec{r} \rangle}_{\psi^*(\vec{r})} \underbrace{\langle \vec{r} | \hat{A} | \vec{r}' \rangle}_{A(\vec{r}, \vec{r}')} \underbrace{\langle \vec{r}' | \phi \rangle}_{\phi(\vec{r}')} \\ &= \int d^3 r \int d^3 r' \psi^*(\vec{r}) A(\vec{r}, \vec{r}') \phi(\vec{r}') \end{aligned}$$

Thus, a general one-particle operator has always two sets of coordinates in its real space representation. We call them non-local because they act on two positions at the same time. It is a special property of most potentials, that they are local. For a **local operator** or **local potential** \hat{V} the real space matrix elements are diagonal in real space, that is

$$V(\vec{r}, \vec{r}') \stackrel{\text{def}}{=} \langle \vec{r} | \hat{V} | \vec{r}' \rangle = V(\vec{r}) \delta(\vec{r} - \vec{r}')$$

so that its matrix elements can be represented by a single real space integral.

Self-consistency cycle

The Hartree-Fock equations are **self-consistent equations**. This means that the Hamiltonian depends itself on the wave functions. Thus, the problem has to be solved iteratively.

- We start out with trial wave functions to determine the Hamiltonian.
- Then we obtain new wave functions from the eigenvalue problem
- New and old wave functions are mixed, which is often necessary to obtain convergence of the cycle.

If the new and old wave functions or the new and old Hamiltonian are identical, the wave functions are consistent with the Hamiltonian and the Hartree Fock equations are solved.

In the quantum chemical literature the term self-consistent equations is used synonymous with Hartree-Fock equations. This is misleading because there are many other schemes that also require a self-consistent cycle.

Fock operator

We can now write the Hamilton operator of the Hartree Fock equation, namely the so-called **Fock operator**

FOCK OPERATOR

$$\begin{aligned}\hat{H} = & \sum_{\sigma} \int d^3 r |\vec{r}, \sigma\rangle \left(\frac{-\hbar^2}{2m_e} \vec{\nabla}^2 - \sum_{j=1}^M \frac{Z_j e^2}{4\pi\epsilon_0 |\vec{r} - \vec{R}_j|} + \int d^3 r' \frac{n(\vec{r}') e^2}{4\pi\epsilon_0 |\vec{r} - \vec{r}'|} \right) \langle \vec{r}, \sigma| \\ & - \sum_{\sigma, \sigma'} \int d^3 r \int d^3 r' |\vec{r}, \sigma\rangle \frac{e^2 \phi_{j,\sigma}^*(\vec{r}) \phi_{j,\sigma'}(\vec{r}')}{4\pi\epsilon_0 |\vec{r} - \vec{r}'|} \langle \vec{r}', \sigma'| \\ & + \left[\hat{1} - \sum_{j=1}^n |\phi_j\rangle \langle \phi_j| \right] \hat{C} \left[\hat{1} - \sum_{j=1}^n |\phi_j\rangle \langle \phi_j| \right]\end{aligned}$$

The operator \hat{C} in the last term is completely arbitrary. Because of the projection operator on both sides, it only acts on the “unoccupied” one-particle wave functions. Because this Hamilton operator is never applied to the unoccupied states, it is also irrelevant. We included this term here to show that the Hartree-Fock operator contains a lot of arbitrariness and that furthermore the action of the operator on the unoccupied states is arbitrary.

Note that the Hartree Fock total energy is not identical to the sum of one-particle energies as it is the case for non-interacting particles.

9.6 Hartree-Fock of the free-electron gas

Let us now study the free-electron gas in the Hartree Fock approximation. Our goal is to determine the changes of the dispersion relation, when the electron-electron interaction is switched on.

First we determine non-local potential as defined in Eq. 9.17.

$$V_x(\vec{x}, \vec{x}') \stackrel{\text{Eq. 9.17}}{=} - \left[\sum_j \frac{e^2 \phi_j^*(\vec{x}) \phi_j(\vec{x}')}{4\pi\epsilon_0 |\vec{r} - \vec{r}'|} \right] \quad (9.18)$$

$$\stackrel{\text{Eq. D.3}}{=} \frac{e^2 \delta_{\sigma, \sigma'}}{4\pi\epsilon_0 s} \frac{1}{(2\pi)^3} \frac{4\pi}{3} k_F^3 \left[3 \frac{(k_F s) \cos(k_F s) - \sin(k_F s)}{(k_F s)^3} \right] \quad (9.19)$$

where $s = |\vec{r} - \vec{r}'|$ and k_F is the Fermi momentum.

Now we need to evaluate the expectation values of this potential in order to obtain the energy shifts:

$$\begin{aligned}d\epsilon_{\vec{k}, \sigma} &= \frac{1}{\Omega} \int d^3 r \int d^3 r' V_x(|\vec{r} - \vec{r}'|, \sigma, \sigma') e^{i\vec{k}(\vec{r} - \vec{r}')} \\ &= -\frac{e^2}{4\pi\epsilon_0} \frac{2k_F}{\pi} \left[\frac{1}{2} + \frac{1 - a^2}{4a} \ln \left| \frac{1 + a}{1 - a} \right| \right]\end{aligned}$$

Here, $a = |\vec{k}|/k_F$. The function in parenthesis is shown in Fig. 9.3

We find, as shown in Fig. 9.4, that the occupied band width is larger in Hartree-Fock than for the non-interacting free electrons. However, the experimental band width of real free-electron-like

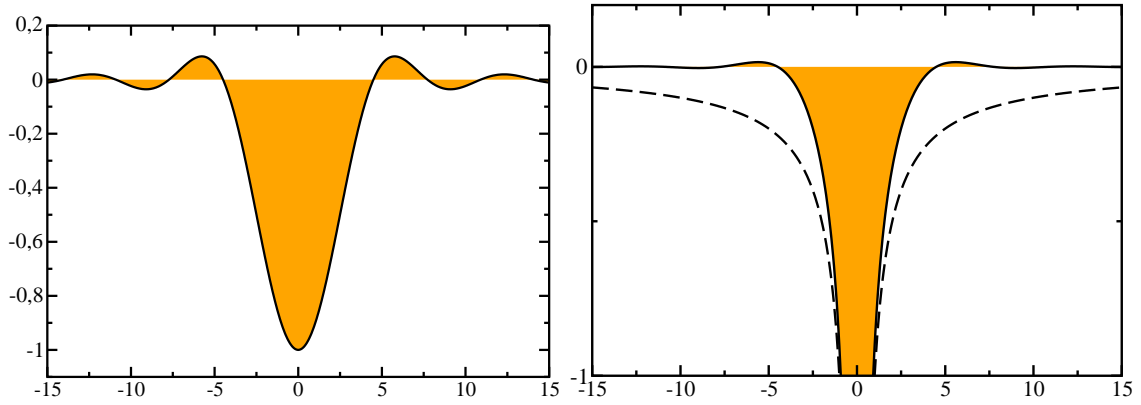


Fig. 9.2: The shape of the non-local exchange potential (right) for a free electron gas as calculated in the Hartree Fock method. The dashed line corresponds to a Coulomb interaction. The function $3 \frac{x \cos(x) - \sin(x)}{x^3}$ is shown on the left-hand side.

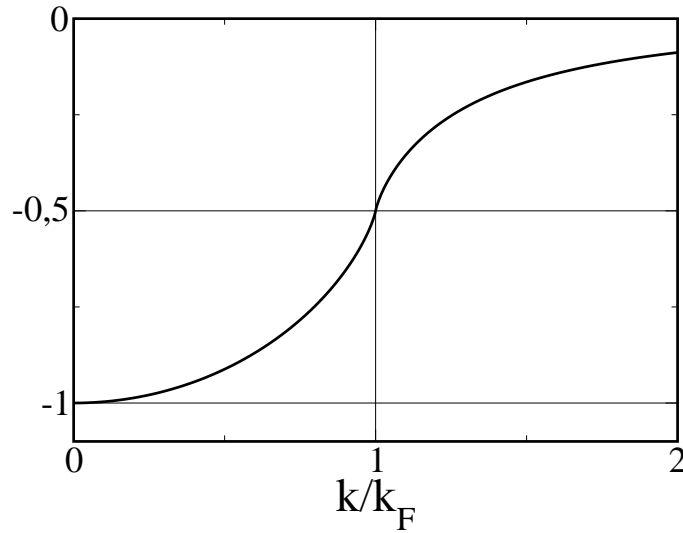


Fig. 9.3: The function $f(a) = -\left(\frac{1}{2} + \frac{1-a^2}{4a} \ln \left| \frac{1+a}{1-a} \right| \right)$ as function of $a = k/k_F$. Note that the slope for $k = k_F$ is infinite. For $k \gg k_F$ the function approaches zero.

materials is smaller. For potassium the band width of the free electron gas is 2 eV. The Hartree-Fock result is 5.3 eV, while the band width of real potassium is in the range 1.5-1.6 eV.[?]

A second problem[?] of the Hartree-Fock theory is that the density of states at the Fermi level vanishes. This is again in contradiction with experiment, which is described pretty well with $\sqrt{\epsilon}$ -behavior of the density of states. The experimental result is closer to the free electron gas. The discrepancy is related to the fact that the electron can not respond to the potential describing the interaction. Note that the wave functions are still plane waves.²

²This argument as such is not conclusive. The band structure is obtained for a fixed potential. The potential depends explicitly on the number of electrons. In an experiment the Fermi-level is measured for example by extracting an electron, which changes the electron number and therefore the interaction potential of Hartree Fock.

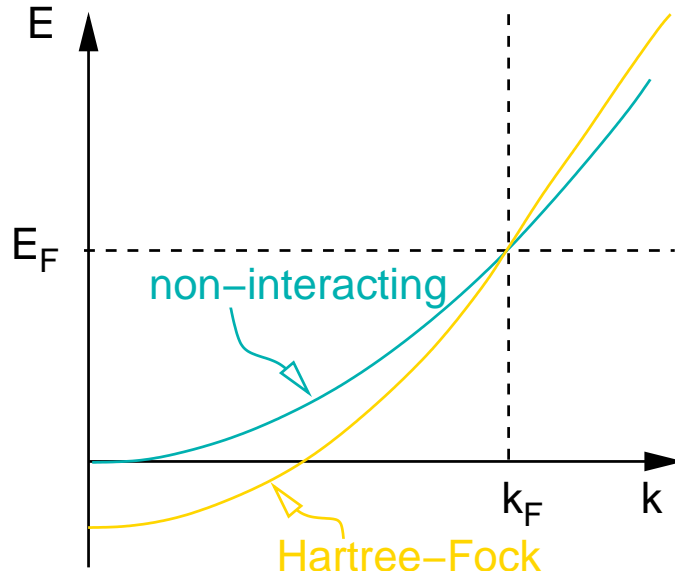


Fig. 9.4: Dispersion relation of the free electron gas as calculated with Hartree Fock and without interactions. The two dispersion relations are shifted so that their Fermi-level agrees.

9.7 Beyond the Hartree Fock Theory: Correlations

The result obtained by the Hartree Fock approximation always lies above the correct result. The energy difference is called electron correlation. The term was coined by Per-Olov Löwdin. [P.-O. Löwdin, "Correlation Problem in Many-Electron quantum mechanics", Adv. Chem. Phys. 2, 207 (1959)]

In this article I will point out a number of failures of Hartree Fock theory, in order to introduce into the terminology of correlations.

9.7.1 Left-right and in-out correlation

The notation of left-right correlation and in-out correlation has been termed by Kolos and Roothaan[24], who performed accurate calculations for the hydrogen molecule.

Left-right correlation describes that the two electrons in one bond are most likely on the opposite sides of the bond. This principle is violated by a Slater determinant build from bonding orbitals.

Let us consider a hydrogen molecule. We start from a one-particle basis $|L, \uparrow\rangle, |L, \downarrow\rangle, |R, \uparrow\rangle, |R, \downarrow\rangle$, where L refers to the left atom and R refers to the right atom. First we transform the basis onto bonding and antibonding orbitals.

$$|B, \uparrow\rangle \stackrel{\text{def}}{=} \frac{1}{\sqrt{2}}(|L, \uparrow\rangle + |R, \uparrow\rangle) \quad (9.20)$$

$$|B, \downarrow\rangle \stackrel{\text{def}}{=} \frac{1}{\sqrt{2}}(|L, \downarrow\rangle + |R, \downarrow\rangle) \quad (9.21)$$

$$|A, \uparrow\rangle \stackrel{\text{def}}{=} \frac{1}{\sqrt{2}}(|L, \uparrow\rangle - |R, \uparrow\rangle) \quad (9.22)$$

$$|A, \downarrow\rangle \stackrel{\text{def}}{=} \frac{1}{\sqrt{2}}(|L, \downarrow\rangle - |R, \downarrow\rangle) \quad (9.23)$$

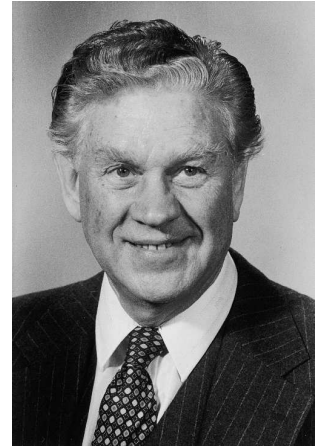


Fig. 9.5: Per-Olov Löwdin, Swedish physicist and theoretical chemist 1916-2000. Courtesy of the American Philosophical Society. (9.20)

Now we form a Slater determinant from the two bonding orbitals

$$\begin{aligned}
 \Psi_g(\vec{r}_1, \sigma_1, \vec{r}_2, \sigma_2) &= \frac{1}{\sqrt{2}} \left(\langle \vec{r}_1, \sigma_1 | B, \uparrow \rangle \langle \vec{r}_2, \sigma_2 | B, \downarrow \rangle - \langle \vec{r}_1, \sigma_1 | B, \downarrow \rangle \langle \vec{r}_2, \sigma_2 | B, \uparrow \rangle \right) \\
 &= \frac{1}{2} \left\{ \langle \vec{r}_1, \sigma_1 | (|L, \uparrow\rangle + |R, \uparrow\rangle) \langle \vec{r}_2, \sigma_2 | (|L, \downarrow\rangle + |R, \downarrow\rangle) \right. \\
 &\quad \left. - \langle \vec{r}_1, \sigma_1 | (|L, \downarrow\rangle + |R, \downarrow\rangle) \langle \vec{r}_2, \sigma_2 | (|L, \uparrow\rangle + |R, \uparrow\rangle) \right\} \\
 &= \frac{1}{2} \left\{ \left(\langle \vec{r}_1, \sigma_1 | L, \uparrow \rangle \langle \vec{r}_1, \sigma_1 | R, \uparrow \rangle \right) \left(\langle \vec{r}_2, \sigma_2 | L, \downarrow \rangle + \langle \vec{r}_2, \sigma_2 | R, \downarrow \rangle \right) \right. \\
 &\quad \left. - \left(\langle \vec{r}_1, \sigma_1 | L, \downarrow \rangle \langle \vec{r}_1, \sigma_1 | R, \downarrow \rangle \right) \left(\langle \vec{r}_2, \sigma_2 | L, \uparrow \rangle + \langle \vec{r}_2, \sigma_2 | R, \uparrow \rangle \right) \right\} \\
 &= \frac{1}{2} \left\{ \left(\langle \vec{r}_1, \sigma_1 | L, \uparrow \rangle \langle \vec{r}_2, \sigma_2 | L, \downarrow \rangle - \langle \vec{r}_1, \sigma_1 | L, \downarrow \rangle \langle \vec{r}_2, \sigma_2 | L, \uparrow \rangle \right) \right. \\
 &\quad + \left(\langle \vec{r}_1, \sigma_1 | L, \uparrow \rangle \langle \vec{r}_2, \sigma_2 | R, \downarrow \rangle - \langle \vec{r}_1, \sigma_1 | R, \downarrow \rangle \langle \vec{r}_2, \sigma_2 | L, \uparrow \rangle \right) \\
 &\quad + \left(\langle \vec{r}_1, \sigma_1 | R, \uparrow \rangle \langle \vec{r}_2, \sigma_2 | L, \downarrow \rangle - \langle \vec{r}_1, \sigma_1 | L, \downarrow \rangle \langle \vec{r}_2, \sigma_2 | R, \uparrow \rangle \right) \\
 &\quad \left. + \left(\langle \vec{r}_1, \sigma_1 | R, \uparrow \rangle \langle \vec{r}_2, \sigma_2 | R, \downarrow \rangle - \langle \vec{r}_1, \sigma_1 | R, \downarrow \rangle \langle \vec{r}_2, \sigma_2 | R, \uparrow \rangle \right) \right\} \\
 &= \frac{1}{\sqrt{2}} [(\uparrow\downarrow, 0) + (\downarrow, \uparrow) + (\uparrow, \downarrow) + (0, \uparrow\downarrow)]
 \end{aligned}$$

Thus, the Slater determinant of the bonding orbitals contains determinants where both electrons are either both localized to the right or with both electrons localized on the left side. These ionized configuration lie high in energy of the bond is long. This is the explanation that the Hartree Fock theory in this form results in a too large dissociation energy.

In order to obtain the correct limit, namely $\frac{1}{\sqrt{2}}(\uparrow, \downarrow) + (\downarrow, \uparrow)$ we need to mix in the Slater determinant with the antibonding orbitals.

$$\Psi_u(\vec{r}_1, \sigma_1, \vec{r}_2, \sigma_2) = \frac{1}{\sqrt{2}} [(\uparrow\downarrow, 0) - (\downarrow, \uparrow) - (\uparrow, \downarrow) + (0, \uparrow\downarrow)]$$

9.7.2 In-out correlation

- “in-out” correlation
- left-right correlation
- angular correlation
- radial correlation
- dynamic
- nondynamic
- near-degeneracy
- long-range
- shortrange

9.7.3 Spin contamination

9.7.4 Dynamic and static correlation

In quantum chemistry the definition of dynamic and static correlation is opposite to that used by physicists. In Quantum chemistry, static correlation is the effect of very few Slater determinants that

contribute to the ground state with approximately equal weight. That static correlation is present if the dominant Slater determinant has a weight less than about 95% of the complete wave function.

Dynamic correlation on the other hand are the small contribution of many Slater determinants, lowering the energy. Dynamic correlation is important to describe the cusp condition: The Coulomb hole has a cusp in the density at the site of the observer electron. Because all one-particle orbitals are smooth, many Slater-determinants are required to build up this cusp as superposition of smooth wave functions.

Chapter 10

Density functional theory

from P.E. Blöchl, Ab-initio Simulations with the CP-PAW code: A tutorial

10.1 Introduction

On the nanoscale, materials around us have a surprisingly simple structure: The standard model of solid state physics and chemistry only knows of two types of particles, namely the nuclei making up the periodic table and the electrons. Only one kind of interaction between them needs to be considered, namely the electrostatic interaction. Even magnetic forces are important only in rare occasions. All other fundamental particles and interactions are irrelevant for chemistry.

The behavior of these particles can be described by the Schrödinger equation (or better the relativistic Dirac equation), which is easily written down. However, the attempt to solve this equation for any system of interest fails miserably due to what Walter Kohn termed the exponential wall [25].

To obtain an impression of the powers of the exponential wall, imagine the wave function of a N_2 molecule, having two nuclei and fourteen electrons. For N particles, the Schrödinger equation is a partial differential equation in $3N$ dimensions. Let us express the wave function on a grid with about 100 points along each spatial direction and let us consider two spin states for each electron. Such a wave function is represented by $2^{14}100^{3 \times 16} \approx 10^{100}$ complex numbers. A data server for this amount of data, made of current tera-byte hard disks, would occupy a volume with a diameter of 10^{10} light years!

Treating the nuclei as classical particles turned out to be a good approximation, but the quantum nature of the electrons cannot be ignored. A great simplification is to describe electrons as non-interacting quasi particles. Instead of one wave function in $3N$ dimensions, one only needs to describe N wave functions in three dimensions each, a dramatic simplification from 10^{100} to 10^7 numbers.

While the independent-particle model is very intuitive, and while it forms the basis of most text books on solid-state physics, materials physics, and chemistry, the Coulomb interaction between electrons is clearly not negligible.

Here, density-functional theory [26, 27] comes to our rescue: it provides a rigorous mapping from interacting electrons onto a system of non-interacting electrons. Unfortunately, the exact mapping is utterly complicated, and this is where all the complexity goes. Luckily, there are simple approximations that are both, intuitive and surprisingly accurate. Furthermore, with the help of clever algorithms, density-functional calculations can be performed on current computers for large systems with several hundred atoms in a unit cell or a molecule. The microscopic insight gained from density functional calculations is a major source of progress in solid state physics, chemistry, material science, and biology.

In the first part of this article, I will try to familiarize the novice reader with the basics of density-functional theory, provide some guidance into common approximations and give an idea of the type

of problems that can be studied with density functional theory.

Beyond this article, I recommend the insightful review articles on density functional theory by Jones and Gunnarsson [28], Baerends [29], von Barth [30], Perdew [31], Yang [32], and their collaborators.

Solving the one-particle Schrödinger equation, which results from density-functional theory, for real materials is a considerable challenge. Several avenues have been developed to their solution. This is the field of electronic structure methods, which will be discussed in the second part of this article. This part is taken from earlier versions by Clemens Först, Johannes Kästner and myself [33, 34].

10.2 Basics of density-functional theory

The dynamics of the electron wave function is governed by the Schrödinger equation $i\hbar\partial_t|\Psi\rangle = \hat{H}|\Psi\rangle$ with the N -particle Hamiltonian \hat{H} .

$$\hat{H} = \sum_{j=1}^N \left(\frac{-\hbar^2}{2m_e} \nabla_j^2 + v_{\text{ext}}(\vec{r}_j) \right) + \frac{1}{2} \sum_{i \neq j}^N \frac{e^2}{4\pi\epsilon_0 |\vec{r}_i - \vec{r}_j|}. \quad (10.1)$$

With m_e we denote the electron mass, with ϵ_0 the vacuum permittivity, e is the elementary charge and \hbar is the Planck quantum divided by 2π . The Coulomb potentials of the nuclei have been combined into an external potential $v_{\text{ext}}(\vec{r})$.

All N -electron wave functions $\Psi(\vec{x}_1, \dots, \vec{x}_N)$ obey the Pauli principle, that is they change their sign, when two of its particle coordinates are exchanged.

We use a notation that combines the position vector $\vec{r} \in \mathbb{R}^3$ of an electron with its discrete spin coordinate $\sigma \in \{\uparrow, \downarrow\}$ into a single vector $\vec{x} := (\vec{r}, \sigma)$. Similarly, we use the notation of a four-dimensional integral $\int d^4x := \sum_{\sigma} \int d^3r$ for the sum over spin indices and the integral over the position. With the generalized symbol $\delta(\vec{x} - \vec{x}') := \delta_{\sigma, \sigma'} \delta(\vec{r} - \vec{r}')$ we denote the product of Kronecker delta of the spin coordinates and Dirac's delta function for the positions. While, at first sight, it seems awkward to combine continuous and discrete numbers, this notation is less error prone than the notation that treats the spin coordinates as indices, where they can be confused with quantum numbers. During the first reading, the novice can ignore the complexity of the spin coordinates, treating \vec{x} like a coordinate. During careful study, he will nevertheless have the complete and concise expressions.

One-particle reduced density matrix and two-particle density

In order to obtain the ground state energy $E = \langle \Psi | \hat{H} | \Psi \rangle$ we need to perform 2^N integrations in $3N$ dimensions each, i.e.

$$E = \int d^4x_1 \cdots \int d^4x_N \Psi^*(\vec{x}_1, \dots, \vec{x}_N) \hat{H} \Psi(\vec{x}_1, \dots, \vec{x}_N). \quad (10.2)$$

However, only two different types of integrals occur in the expression for the energy, so that most of these integrations can be performed beforehand leading to two quantities of physical significance.

- One of these quantities is the one-particle reduced density matrix $\rho^{(1)}(\vec{x}, \vec{x}')$, which allows one to evaluate all expectation values of one-particle operators such as the kinetic energy and the external potential,

$$\rho^{(1)}(\vec{x}, \vec{x}') := N \int d^4x_2 \cdots \int d^4x_N \Psi(\vec{x}, \vec{x}_2, \dots, \vec{x}_N) \Psi^*(\vec{x}', \vec{x}_2, \dots, \vec{x}_N). \quad (10.3)$$

- The other one is the two-particle density $n^{(2)}(\vec{r}, \vec{r}')$, which allows to determine the interaction between the electrons,

$$n^{(2)}(\vec{r}, \vec{r}') := N(N-1) \sum_{\sigma, \sigma'} \int d^4x_3 \cdots \int d^4x_N |\Psi(\vec{x}, \vec{x}', \vec{x}_3, \dots, \vec{x}_N)|^2. \quad (10.4)$$

If it is confusing that there are two different quantities depending on two particle coordinates, note that the one-particle reduced density matrix $\rho^{(1)}$ depends on two \vec{x} -arguments of the same particle, while the two-particle density $n^{(2)}$ depends on the positions of two different particles.

With these quantities the total energy is

$$E = \int d^4x' \int d^4x \delta(\vec{x}' - \vec{x}) \left(\frac{-\hbar^2}{2m_e} \vec{\nabla}^2 + v_{\text{ext}}(\vec{r}) \right) \rho^{(1)}(\vec{x}, \vec{x}') + \frac{1}{2} \int d^3r \int d^3r' \frac{e^2 n^{(2)}(\vec{r}, \vec{r}')}{4\pi\epsilon_0 |\vec{r} - \vec{r}'|}, \quad (10.5)$$

where the gradient of the kinetic energy operates on the first argument \vec{r} of the density matrix.

One-particle reduced density matrix and natural orbitals

In order to make oneself familiar with the one-particle reduced density matrix, it is convenient to diagonalize it. The eigenstates $\varphi_n(\vec{r})$ are called natural orbitals [35] and the eigenvalues \bar{f}_n are their occupations. The index n labeling the natural orbitals may stand for a set of quantum numbers.

The density matrix can be written in the form

$$\rho^{(1)}(\vec{x}, \vec{x}') = \sum_n \bar{f}_n \varphi_n(\vec{x}) \varphi_n^*(\vec{x}'). \quad (10.6)$$

The natural orbitals are orthonormal one-particle orbitals, i.e.

$$\int d^4x \varphi_m^*(\vec{x}) \varphi_n(\vec{x}) = \delta_{m,n}. \quad (10.7)$$

Due to the Pauli principle, occupations are non-negative and never larger than one [36]. The natural orbitals already point the way to the world of effectively non-interacting electrons.

The one-particle density matrix provides us with the electron density

$$n^{(1)}(\vec{r}) = \sum_{\sigma} \rho^{(1)}(\vec{x}, \vec{x}) = \sum_{\sigma} \sum_n \bar{f}_n \varphi_n^*(\vec{x}) \varphi_n(\vec{x}). \quad (10.8)$$

With the natural orbitals, the total energy Eq. 10.5 obtains the form

$$E = \sum_n \bar{f}_n \int d^4x \varphi_n^*(\vec{x}) \frac{-\hbar^2}{2m} \vec{\nabla}^2 \varphi_n(\vec{x}) + \int d^3r v_{\text{ext}}(\vec{r}) n^{(1)}(\vec{r}) + \frac{1}{2} \int d^3r \int d^3r' \frac{e^2 n^{(2)}(\vec{r}, \vec{r}')}{4\pi\epsilon_0 |\vec{r} - \vec{r}'|}. \quad (10.9)$$

Two-particle density and exchange-correlation hole

The physical meaning of the two-particle density $n^{(2)}(\vec{r}, \vec{r}')$ is the following: For particles that are completely uncorrelated, meaning that they do not even experience the Pauli principle, the two particle density would be¹ the product of one-particle densities, i.e. $n^{(2)}(\vec{r}, \vec{r}') = n^{(1)}(\vec{r}) n^{(1)}(\vec{r}')$. If one particle is at position \vec{r}_0 , the density of the remaining $N - 1$ particles is the conditional density

$$\frac{n^{(2)}(\vec{r}_0, \vec{r})}{n^{(1)}(\vec{r}_0)}. \quad (10.10)$$

The conditional density is the electron density as function of \vec{r} seen by one of the electrons at \vec{r}_0 . This observer electron obviously only sees the remaining $N - 1$ electrons.

¹This is correct only up to a term that vanishes in the limit of infinite particle number.

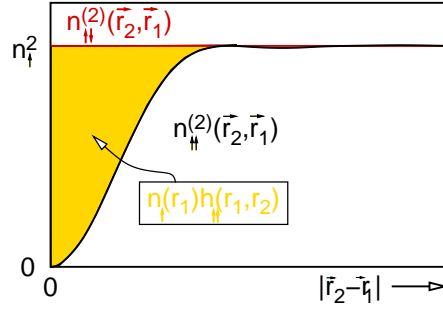


Fig. 10.1: Two-particle density of the non-interacting electron gas for like-spin and opposite spin. Also shown is the relation to the exchange hole $h(\vec{r}_1, \vec{r}_2)$

It is convenient to express the two-particle density by the hole function $h(\vec{r}_0, \vec{r})$, i.e.

$$n^{(2)}(\vec{r}_0, \vec{r}) = n^{(1)}(\vec{r}_0) \left[n^{(1)}(\vec{r}) + h(\vec{r}_0, \vec{r}) \right]. \quad (10.11)$$

This equation defines the hole function as

$$h(\vec{r}_0, \vec{r}) = \frac{n^{(2)}(\vec{r}_0, \vec{r})}{n^{(1)}(\vec{r}_0)} - n^{(1)}(\vec{r}). \quad (10.12)$$

One electron at position \vec{r}_0 does not “see” the total electron density $n^{(1)}(\vec{r})$ with N electrons, but only the density of the $N - 1$ other electrons, because it does not see itself. The hole function $h(\vec{r}_0, \vec{r})$ is simply the difference of the total electron density and the electron density seen by the observer electron at \vec{r}_0 .

The division of the two-particle density in Eq. 10.11 suggests that we split the electron-electron interaction into the so-called **Hartree energy**

$$E_H \stackrel{\text{def}}{=} \frac{1}{2} \int d^3r \int d^3r' \frac{e^2 n^{(1)}(\vec{r}) n^{(1)}(\vec{r}')}{4\pi\epsilon_0 |\vec{r} - \vec{r}'|} \quad (10.13)$$

and the **potential energy of exchange and correlation**

$$U_{xc} \stackrel{\text{def}}{=} \int d^3r n^{(1)}(\vec{r}) \frac{1}{2} \int d^3r' \frac{e^2 h(\vec{r}, \vec{r}')}{4\pi\epsilon_0 |\vec{r} - \vec{r}'|}. \quad (10.14)$$

Keep in mind that U_{xc} is *not* the exchange correlation energy. The difference between U_{xc} and the exchange-correlation energy E_{xc} is a kinetic energy correction that will be discussed later in Eq. 10.21.

The hole function has a physical meaning: An electron sees the total density minus the electrons accounted for by the hole. Thus, each electron not only experiences the electrostatic potential of the total electron density $n^{(1)}(\vec{r})$, but also the attractive potential of its own exchange correlation hole $h(\vec{r}_0, \vec{r})$.

A few facts for this hole density are apparent:

1. Because each electron of a N -electron system sees $N - 1$ other electrons, the hole function integrates to exactly minus one electron

$$\int d^3r h(\vec{r}_0, \vec{r}) = -1 \quad (10.15)$$

irrespective of the position \vec{r}_0 of the observing electron.

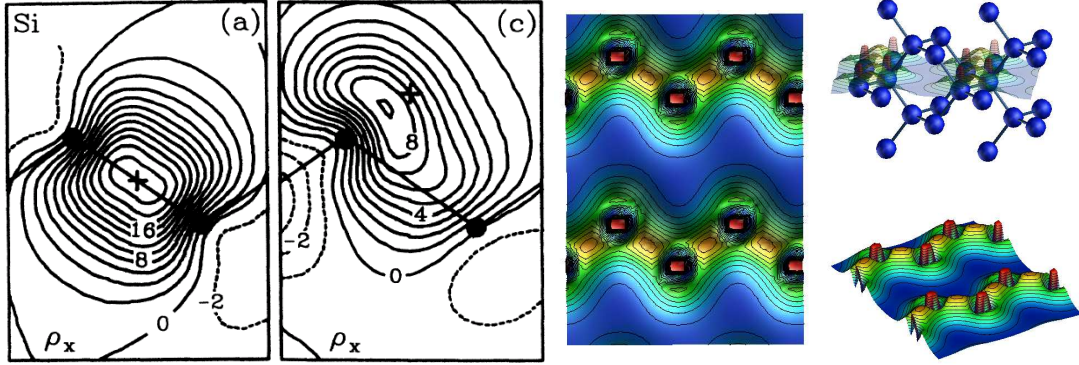


Fig. 10.2: Exchange hole in silicon from [37]. The cross indicates the position of the observer electron. The black spheres and the lines indicate the atomic positions and bonds in the (110) plane.

2. The density of the remaining $N - 1$ electrons can not be larger than the total electron density. This implies

$$h(\vec{r}_0, \vec{r}) \geq -n^{(1)}(\vec{r}) . \quad (10.16)$$

3. Due to the Pauli principle, no other electron with the same spin as the observer electron can be at the position \vec{r}_0 . Thus the on-top hole $h(\vec{r}_0, \vec{r}_0)$ obeys the limits [38]

$$-\frac{1}{2}n^{(1)}(\vec{r}_0) \geq h(\vec{r}_0, \vec{r}_0) \geq -n^{(1)}(\vec{r}_0) . \quad (10.17)$$

4. Assuming locality, the hole function vanishes at large distances from the observer electron at \vec{r}_0 , i.e.

$$h(\vec{r}_0, \vec{r}) \rightarrow 0 \quad \text{for} \quad |\vec{r} - \vec{r}_0| \rightarrow \infty . \quad (10.18)$$

With locality I mean that the density does not depend on the position or the presence of an observer electron, if the latter is very far away.

A selfmade functional

It is fairly simple to make our own density functional²: For a given density, we choose a simple shape for the hole function, such as a spherical box. Then we scale the value and the radius such that the hole function integrates to -1 , and that its value is opposite equal to the spin density at its center. The electrostatic potential of this hole density at its center is the exchange-correlation energy for the observer electron. Our model has an exchange correlation energy³ of

$$U_{xc}[n^{(1)}] \approx -\frac{1}{2} \int d^3r n^{(1)}(\vec{r}) \left(\frac{3}{4} \frac{e^2}{4\pi\epsilon_0} \sqrt{\frac{2\pi}{3}} \left(n^{(1)}(\vec{r}) \right)^{\frac{1}{3}} \right) \sim \int d^3r \left(n^{(1)}(\vec{r}) \right)^{\frac{4}{3}} . \quad (10.19)$$

The derivation is an elementary exercise and is given in the appendix. The resulting energy per electron ϵ_{xc} is given on the right-hand side of Fig. 10.3 indicated as “model” and compared with the

²A functional $F[y]$ maps a function $y(x)$ to a number F . It is a generalization of the function $F(\vec{y})$ of a vector \vec{y} , where the vector index of \vec{y} is turned into a continuous argument x .

³For this model we do not distinguish between the energy of exchange and correlation and its potential energy contribution

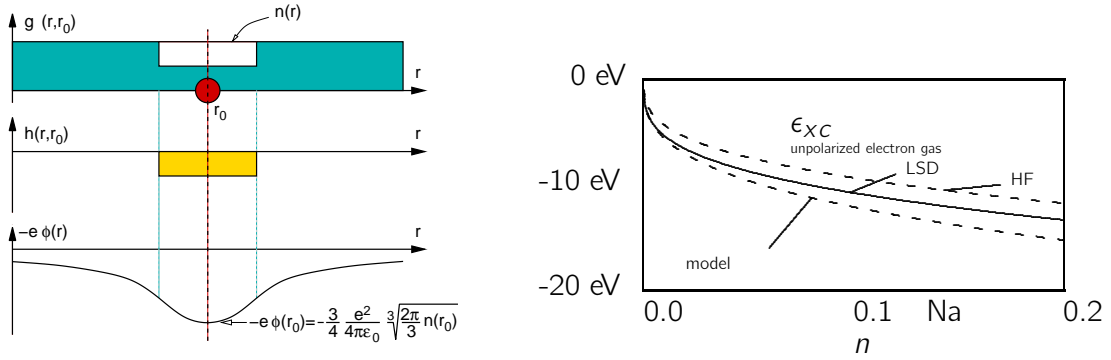


Fig. 10.3: Left: Scheme to demonstrate the construction of the exchange correlation energy from a simple model. Right: exchange correlation energy per electron ϵ_{xc} as function of electron density from our model, Hartree-Fock approximation and the exact result. The symbol “Na” indicates the density of Sodium.

exact result indicated as “LSD”⁴ and the Hartree-Fock result indicated as “HF” for a homogeneous electron gas.

The agreement with the correct result, which is surprisingly good for such a crude model, provides an idea of how robust the density-functional theory is with respect to approximations. While this model has been stripped to the bones, it demonstrates the way physical insight enters the construction of density functionals. Modern density functionals are far more sophisticated and exploit much more information [39], but the basic method of construction is similar.

Kinetic energy

While the expression for the kinetic energy in Eq. 10.9 seems familiar, there is a catch to it. In order to know the natural orbitals and the occupations we need access to the many-particle wave function or at least to its reduced density matrix.

A good approximation for the kinetic energy of the interacting electrons is the kinetic energy functional $T_s[n^{(1)}]$ of the ground state of non-interacting electrons with the same density as the true system. It is defined by

$$\begin{aligned}
 T_s[n^{(1)}] = \min_{\{f_n \in [0,1], |\psi_n\rangle\}} & \left\{ \sum_n f_n \int d^4x \psi_n^*(\vec{x}) \frac{-\hbar^2 \nabla^2}{2m} \psi_n(\vec{x}) \right. \\
 & + \int d^3r v_{eff}(\vec{r}) \left(\left[\sum_n f_n \sum_\sigma \psi_n^*(\vec{x}) \psi_n(\vec{x}) \right] - n^{(1)}(\vec{r}) \right) \\
 & \left. - \sum_{n,m} \Lambda_{m,n} \left(\langle \psi_n | \psi_m \rangle - \delta_{n,m} \right) \right\}. \quad (10.20)
 \end{aligned}$$

Note that $f_n \neq \bar{f}_n$ and that the so-called Kohn-Sham orbitals $\psi_n(\vec{x})$ differ⁵ from the natural orbitals $\varphi_n(\vec{x})$. Natural orbitals and Kohn-Sham wave functions are fairly similar, while the occupations f_n of Kohn-Sham orbitals differ considerably from those \bar{f}_m of the natural orbitals. The effective potential $v_{eff}(\vec{r})$ is the Lagrange multiplier for the density constraint. $\Lambda_{m,n}$ is the Lagrange multiplier for the orthonormality. Diagonalization of $\mathbf{\Lambda}$ yields a diagonal matrix with the one-particle energies on the diagonal.

⁴LSD stands for “local spin-density” and denotes the local spin-density approximation (LSDA). Modern implementations do not only use the total density as fundamental variable, but also the spin density.

⁵To be precise, Kohn-Sham orbitals are the natural orbitals for non-interacting electrons of a given density. They are however different from the natural orbitals of interacting electrons at the same density.

This kinetic energy $T_s[n^{(1)}]$ is a unique functional of the density, which is the first sign that we are approaching a density-functional theory. Also it is the introduction of this kinetic energy, where we made for the first time a reference to a ground state. Density functional theory as described here is inherently a ground-state theory.

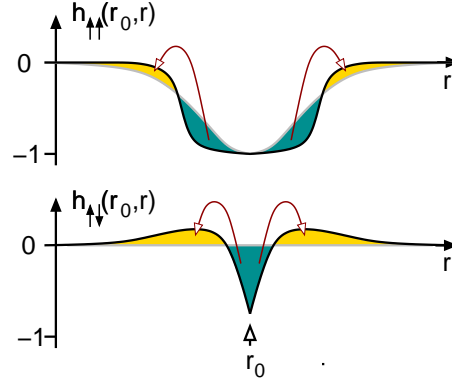


Fig. 10.4: Illustration of the correlation hole. The exchange hole, present without interaction, is deformed by the Coulomb reaction. Because this deformation must respect the charge sum rule, this deformation makes the hole more compact. The dominant effect is on the opposite-spin direction, because the like-spin electrons are already at a distance by the exchange hole.

Why does the true kinetic energy of the interacting system differ from that of the non-interacting energy? Consider the hole function of a non-interacting electron gas. When inserted into Eq. 10.14 for U_{xc} the potential energy of exchange and correlation, we obtain a contribution to the total energy that is called exchange energy. The interaction leads to a second energy contribution that is called correlation energy. Namely, when the interaction is switched on, the wave function is deformed in such a way that the Coulomb repulsion between the electrons is reduced. This makes the hole function more compact. However, there is a price to pay when the wave functions adjust to reduce the Coulomb repulsion between the electrons, namely an increase of the kinetic energy: Pushing electrons away from the neighborhood of the reference electrons requires work to be performed against the kinetic pressure of the electron gas, which raises the kinetic energy. Thus, the system has to find a compromise between minimizing the electrostatic repulsion of the electrons and increasing its kinetic energy. As a result, the correlation energy has a potential-energy contribution and a kinetic-energy contribution.

This tradeoff can be observed in Fig. 10.3. The correct exchange correlation energy is close to our model at low densities, while it becomes closer to the Hartree-Fock result at high densities. This is consistent with the fact that the electron gas can easily be deformed at low densities, while the deformation becomes increasingly costly at high densities due to the larger pressure of the electron gas.

The difference between T_s and the true kinetic energy is combined with the potential energy of exchange and correlation U_{xc} from Eq. 10.14 into the exchange correlation energy E_{xc} , i.e.

$$E_{xc} = U_{xc} + \sum_n \bar{f}_n \int d^4x \varphi_n^*(\vec{x}) \frac{-\hbar^2}{2m} \vec{\nabla}^2 \varphi_n(\vec{x}) - T_s[n^{(1)}]. \quad (10.21)$$

Note, that the $\phi_n(\vec{x})$ and the \bar{f}_n are natural orbitals and occupations of the interacting electron gas, and that they differ from the Kohn-Sham orbitals $\psi_n(\vec{x})$ and occupations f_n .

Total energy

The total energy obtains the form

$$\begin{aligned}
 E = & \min_{|\Phi\rangle, \{|\psi_n\rangle, f_n \in [0,1]\}} \left\{ \sum_n f_n \int d^4x \psi_n^*(\vec{x}) \frac{-\hbar^2}{2m} \vec{\nabla}^2 \psi_n(\vec{x}) \right. \\
 & + \int d^3r v_{eff}(\vec{r}) \left(\left[\sum_n f_n \sum_\sigma \psi_n^*(\vec{x}) \psi_n(\vec{x}) \right] - n^{(1)}(\vec{r}) \right) + \int d^3r v_{ext}(\vec{r}) n^{(1)}(\vec{r}) \\
 & \left. + \frac{1}{2} \int d^3r \int d^3r' \frac{e^2 n^{(1)}(\vec{r}) n^{(1)}(\vec{r}')}{4\pi\epsilon_0 |\vec{r} - \vec{r}'|} + E_{xc} - \sum_{n,m} \Lambda_{m,n} \left(\langle \psi_n | \psi_m \rangle - \delta_{n,m} \right) \right\}. \quad (10.22)
 \end{aligned}$$

This equation shall be read as follows: For a given many-particle wave function $|\Phi\rangle$ we extract the density $n^{(1)}(\vec{r})$ and the corresponding Kohn-Sham orbitals $|\psi_n(\vec{x})$ and occupations f_n . Kohn-Sham orbitals $|\psi_n\rangle$ and occupations f_n are obtained by an independent minimization of the kinetic energy for the density $n^{(1)}(\vec{r})$. Only E_{xc} needs yet to be calculated directly from the many-particle wave function. This is done for all many-particle wave functions until the minimum of the total energy has been found.

Because we still need the full many particle wave function to determine the expression above, Eq. 10.22 is not yet a functional of the density.

If, however, we were able to express the exchange-correlation energy E_{xc} as a functional of the density alone, there would be no need for the many-particle wave function at all and the terrors of the exponential wall would be banned. We could minimize Eq. 10.22 with respect to the density, Kohn-Sham orbitals and their occupations.

Let us, for the time being, simply assume that $E_{xc}[n^{(1)}]$ is a functional of the electron density and explore the consequences of this assumption. Later, I will show that this assumption is actually valid.

The minimization in Eq. 10.22 with respect to the one-particle wave functions yields the Kohn-Sham equations

$$\left[\frac{-\hbar^2}{2m_e} \vec{\nabla}^2 + v_{eff}(\vec{r}) - \epsilon_n \right] \psi_n(\vec{x}) = 0 \quad \text{with} \quad \int d^4x \psi_m(\vec{x}) \psi_n(\vec{x}) = \delta_{m,n}. \quad (10.23)$$

The Kohn-Sham energies ϵ_n are the diagonal elements of the Lagrange multiplier Λ , when the latter is forced to be diagonal.

The requirement that the derivative of the total energy Eq. 10.22 with respect to the density vanishes, yields an expression for the effective potential

$$v_{eff}(\vec{r}) = v_{ext}(\vec{r}) + \int d^3r' \frac{e^2 n^{(1)}(\vec{r}')}{4\pi\epsilon_0 |\vec{r} - \vec{r}'|} + \frac{\delta E_{xc}[n^{(1)}]}{\delta n^{(1)}(\vec{r})}. \quad (10.24)$$

Both equations, together with the density constraint

$$n^{(1)}(\vec{r}) = \sum_n f_n \sum_\sigma \psi_n^*(\vec{x}) \psi_n(\vec{x}), \quad (10.25)$$

form a set of coupled equations, that determine the electron density and the total energy. This set of coupled equations, Eqs. 10.23, 10.24, and 10.25, is what is solved in the so-called self-consistency loop. Once the set of self-consistent equations has been solved, we obtain the electron density and we can evaluate the total energy.

In practice, one often makes the assumption that the non-interacting electrons in the effective potential closely resemble the true interacting electrons, and extracts a wealth of other physical properties from the Kohn-Sham wave functions $|\psi_n\rangle$ and the Kohn-Sham energies ϵ_n . However, there is little theoretical backing for this approach and, if it fails, one should not blame density functional theory!

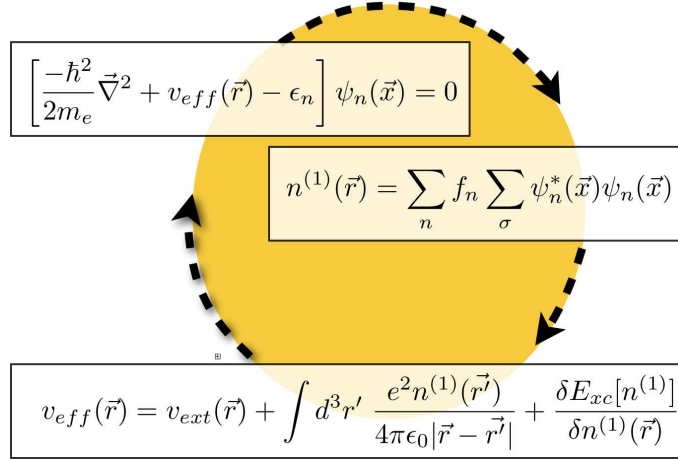


Fig. 10.5: Self-consistency cycle.

Is there a density functional?

The argument leading to the self-consistent equations, Eqs. 10.23, 10.24, and 10.25, relied entirely on the hope that exchange correlation functional can be expressed as a functional of the electron density. In fact, this can easily be shown, if we restrict us to ground state densities. The proof goes back to the seminal paper by Levy [40, 41].

Imagine that one could construct all fermionic many-particle wave functions. For each of these wave functions, we can determine in a unique way the electron density

$$n^{(1)}(\vec{r}) = N \sum_{\sigma} \int d^3x_2 \dots \int d^3x_N |\Psi(\vec{x}, \vec{x}_2, \dots, \vec{x}_N)|^2. \quad (10.26)$$

Having the electron densities, we sort the wave functions according to their density. For each density, I get a mug $M[n^{(1)}]$ that holds all wave functions with that density, that is written on the label of the mug.

Now we turn to each mug $M[n^{(1)}]$ in sequence and determine for each the wave function with the lowest energy. Because the external potential energy is the same for all wave functions with the same density, we need to consider only the kinetic energy operator \hat{T} and the operator \hat{W} of the electron-electron interaction, and we do not need to consider the external potential.

$$F^{\hat{W}}[n^{(1)}] = \min_{|\Psi\rangle \in M[n^{(1)}]} \langle \Psi | \hat{T} + \hat{W} | \Psi \rangle \quad (10.27)$$

$F^{\hat{W}}[n^{(1)}]$ is the universal density functional. It is universal in the sense that it is an intrinsic property of the electron gas and absolutely independent of the external potential.

Next, we repeat the same construction as that for a universal density functional, but now we leave out the interaction \hat{W} and consider only the kinetic energy \hat{T} .

$$F^0[n^{(1)}] = \min_{|\Psi\rangle \in M[n^{(1)}]} \langle \Psi | \hat{T} | \Psi \rangle \quad (10.28)$$

The resulting functional $F^0[n^{(1)}]$ is nothing but the kinetic energy of non-interacting electrons $T_s[n^{(1)}]$.

Now we can write down the total energy as functional of the density

$$E[n^{(1)}] = F^{\hat{W}}[n^{(1)}] + \int d^3r v_{\text{ext}}(\vec{r}) n^{(1)}(\vec{r}) \quad (10.29)$$

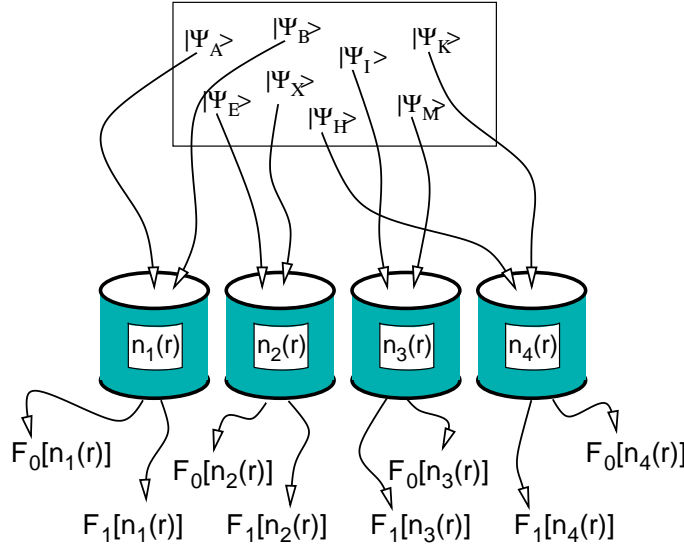


Fig. 10.6: Illustration for Levy's proof that there exists a density functional.

When we compare Eq. 10.29 with Eq. 10.22, we obtain an expression for the exchange correlation energy.

$$E_{xc}[n^{(1)}] = F^{\hat{W}}[n^{(1)}(\vec{r})] - F^0[n^{(1)}(\vec{r})] - \frac{1}{2} \int d^3r \int d^3r' \frac{e^2 n^{(1)}(\vec{r}) n^{(1)}(\vec{r}')}{4\pi\epsilon_0 |\vec{r} - \vec{r}'|} \quad (10.30)$$

This completes the proof that the exchange correlation energy is a functional of the electron density. The latter was the assumption for the derivation of the set of self-consistent equations, Eqs. 10.23, 10.24, and 10.25 for the Kohn-Sham wave functions $\psi_n(\vec{x})$.

With this, I finish the description of the theoretical basis of density-functional theory. We have seen that the total energy can rigorously be expressed as a functional of the density or, in practice, as a functional of a set of one-particle wave functions, the Kohn-Sham wave functions and their occupations. Density functional theory per se is not an approximation and, in contrast to common belief, it is not a mean-field approximation. Nevertheless, we need to introduce approximations to make density functional theory work. This is because the exchange correlation energy $E_{xc}[n^{(1)}]$ is not completely known. These approximations will be discussed in the next section.

10.3 Adiabatic connection

At this point I want to demonstrate a theorem that is central to the thinking within density functional theory. It allows to express the difference between the kinetic energy of the interacting and the non-interacting wave function by the exchange correlation hole for various strengths of the electron-electron interaction.

Let us proceed as in Levy's proof, but now we use a Hamiltonian with a scaled interaction

$$\hat{H}(\lambda) = \hat{T} + \lambda \hat{W}$$

The extreme values, $\lambda = 0$ and $\lambda = 1$ describe the non-interacting and the interacting electron gas, respectively.

For each value of λ we determine

$$F^{\lambda \hat{W}} = \min_{|\Psi\rangle \in M[n^{(1)}]} \langle \Psi | \hat{T} + \lambda \hat{W} | \Psi \rangle = \langle \bar{\Psi}_\lambda[n^{(1)}] | \hat{T} + \lambda \hat{W} | \bar{\Psi}_\lambda[n^{(1)}] \rangle$$

Note, that the wave function $|\bar{\Psi}_\lambda[n^{(1)}]\rangle$ of the minimum depends on λ .

The fully interacting functional can be obtained as an integral over the derivative

$$F^{\hat{W}}[n^{(1)}] = F^0[n^{(1)}] + \int_0^1 d\lambda \frac{\partial F^{\lambda\hat{W}}[n^{(1)}]}{\partial \lambda}$$

Using the minimum condition the derivative of the functional with respect to λ can be expressed entirely by the interaction energy.

In order to make the minimum condition explicit, we include the density and the normalization constraint in the constrained search. Thus the functional is written as

$$F^{\lambda\hat{W}}[n^{(1)}] = \min_{|\Psi\rangle} \langle \Psi | \hat{T} + \lambda \hat{W} | \Psi \rangle + \int d^3r v_{eff,\lambda}(\vec{r}) \left(\langle \Psi | \hat{n}(\vec{r}) | \Psi \rangle - n^{(1)}(\vec{r}) \right) - E \left(\langle \Psi | \Psi \rangle - 1 \right)$$

The minimum condition is

$$\left[\hat{T} + \lambda \hat{W} + \int d^3r v_{eff,\lambda}(\vec{r}) \hat{n}(\vec{r}) - E_\lambda \right] |\bar{\Psi}_\lambda\rangle = 0$$

Now we can perform the derivative of

$$F^{\lambda\hat{W}}[n^{(1)}] = \langle \bar{\Psi}_\lambda | \hat{T} + \lambda \hat{W} | \bar{\Psi}_\lambda \rangle + \int d^3r v_{eff,\lambda}(\vec{r}) \left(\langle \bar{\Psi}_\lambda | \hat{n}(\vec{r}) | \bar{\Psi}_\lambda \rangle - n^{(1)}(\vec{r}) \right) - E_\lambda \left(\langle \bar{\Psi}_\lambda | \bar{\Psi}_\lambda \rangle - 1 \right)$$

as

$$\begin{aligned} \frac{d}{d\lambda} F^{\lambda\hat{W}}[n^{(1)}] &= \left\langle \frac{d\bar{\Psi}_\lambda}{d\lambda} \left| \underbrace{\left(\hat{T} + \lambda \hat{W} + \int d^3r v_{eff,\lambda}(\vec{r}) \hat{n}(\vec{r}) - E_\lambda \right)}_{=0} \right| \bar{\Psi}_\lambda \right\rangle \\ &= \left\langle \bar{\Psi}_\lambda \left| \underbrace{\left(\hat{T} + \lambda \hat{W} + \int d^3r v_{eff,\lambda}(\vec{r}) \hat{n}(\vec{r}) - E_\lambda \right)}_{=0} \right| \frac{d\bar{\Psi}_\lambda}{d\lambda} \right\rangle \\ &= \langle \bar{\Psi}_\lambda | \hat{W} | \bar{\Psi}_\lambda \rangle + \int d^3r \frac{dv_{eff,\lambda}}{d\lambda}(\vec{r}) \underbrace{\left(\langle \bar{\Psi}_\lambda | \hat{n}(\vec{r}) | \bar{\Psi}_\lambda \rangle - n^{(1)}(\vec{r}) \right)}_{=0} - \frac{dE_\lambda}{d\lambda} \underbrace{\left(\langle \bar{\Psi}_\lambda | \bar{\Psi}_\lambda \rangle - 1 \right)}_{=0} \\ &= \langle \bar{\Psi}_\lambda | \hat{W} | \bar{\Psi}_\lambda \rangle \end{aligned}$$

Thus we can express the functional as

$$\begin{aligned} F^{\hat{W}}[n^{(1)}] &= T_s[n^{(1)}] + \int_0^1 d\lambda \langle \bar{\Psi}_\lambda | \hat{W} | \bar{\Psi}_\lambda \rangle \\ &= T_s[n^{(1)}] + \frac{1}{2} \int d^3r \int d^3r' \frac{e^2 n^{(1)}(\vec{r}) n^{(1)}(\vec{r}')}{4\pi\epsilon_0 |\vec{r} - \vec{r}'|} + \int d^3r n^{(1)}(\vec{r}) \int d^3r' \frac{e^2 \langle h_\lambda(\vec{r}, \vec{r}') \rangle}{4\pi\epsilon_0 |\vec{r} - \vec{r}'|} \end{aligned}$$

where

$$h_{av}(\vec{r}, \vec{r}') = \int_0^1 d\lambda h_\lambda(\vec{r}, \vec{r}')$$

10.4 Jacob's ladder of density functionals

The development of density functionals is driven by mathematical analysis of the exact exchange correlation hole [39, 31], physical insight and numerical benchmark calculations on real systems. The functionals evolved in steps from one functional form to another, with several parameterizations at each level. Perdew pictured this development by Jacob's ladder leading up to heaven [42, 31]. In his analogy the different rungs of the ladder represent the different levels of density functionals leading to the unreachable, ultimately correct functional.

JACOB'S LADDER OF DENSITY FUNCTIONALS

The different stairs of Jacobs Ladder of density functionals are

1. LDA (local density approximation): the exchange correlation hole is taken from the free electron gas. These functionals exhibit strong overbinding. While the van-der Waals bond is not considered in these functionals, the overbinding mimicked van-der-Waals bonding, albeit for the wrong reason.
2. GGA (generalized gradient approximation): These functionals not only use the electron density but also its gradient to estimate the asymmetry of the exchange-correlation hole with respect to the reference electrons. As a result surfaces are energetically favored compared to LDA and the overbinding is strongly reduced.
3. meta-GGA: in addition to the gradient also the kinetic energy density is used as a parameter. The kinetic energy is a measure for the flexibility of the electron gas.
4. Hybrid functionals: Hybrid functional include a fraction of exact exchange. This functionals improve the description of left-right correlations.
5. Exact: An exact density functional can be obtained using the constrained search formalism using many-particle techniques.

10.5 X_α method

Even before the invention of density functional theory per se, the so-called X_α method has been introduced. Today, the X_α method has mostly historical value. The X_α method uses the expression for the exchange of a homogeneous electron gas instead of the exchange-correlation energy. However, the exchange energy has been scaled with a parameter, namely X_α , that has been adjusted to Hartree Fock calculations. The results are shown in Fig. 10.7.

The rationale behind the X_α -method is a dimensional argument. Choose a given shape for the exchange correlation hole, but scale it according to the density and the electron sum rule. Then the exchange correlation energy per electron always scales like $n^{\frac{1}{3}}$. Each shape corresponds to a pre-factor.

Consider a given shape described by a function $f(\vec{r})$ with

$$\begin{aligned} f(\vec{0}) &= 1 \\ \int d^3r f(\vec{r}) &= 1 \end{aligned}$$

Now, we express the hole function by the function f by scaling its magnitude at the origin such that the amplitude of the hole cancels the electron density. Secondly, we stretch the function in space so that the sum rule, which says that the hole must integrate to -1 , is fulfilled. These conditions yield

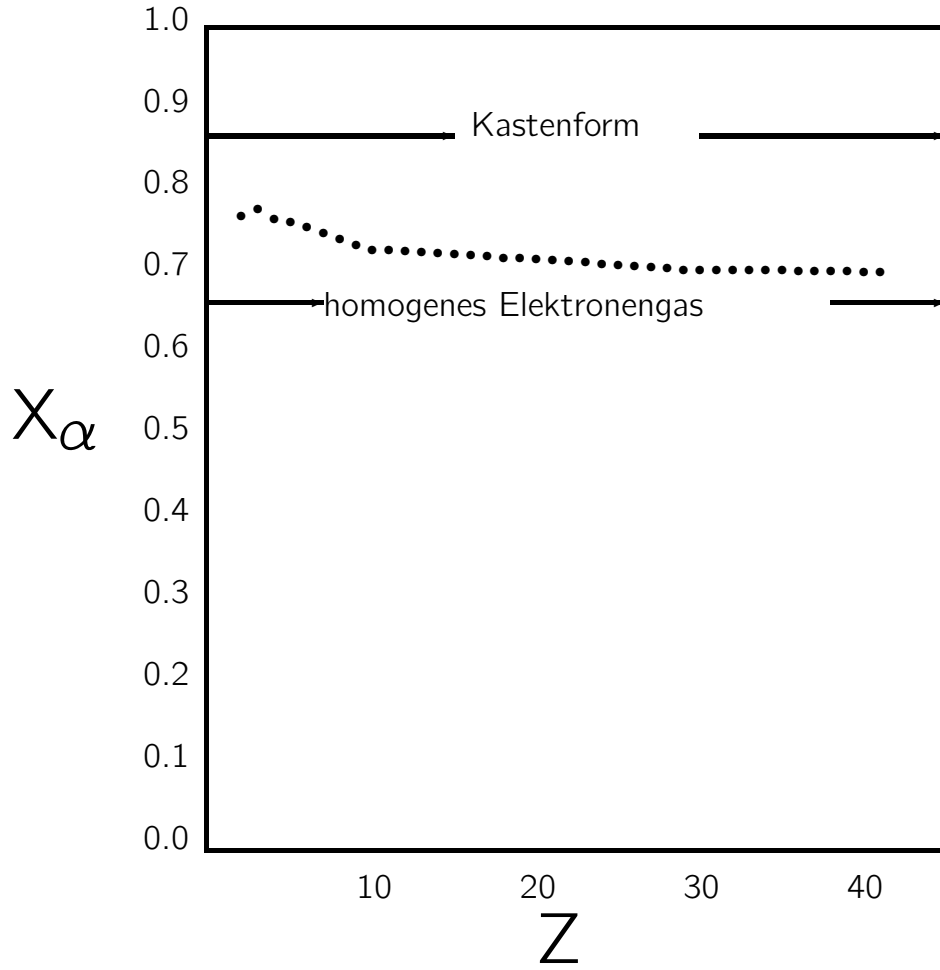


Fig. 10.7: X_α value obtained by comparison of the atomic energy with exact Hartree-Fock calculations as function of atomic number of the atom.[7, 43]

the model for the exchange correlation hole.

$$h(\vec{r}_0, \vec{r}) = -n(\vec{r}_0)f\left(\frac{|\vec{r} - \vec{r}_0|}{n(\vec{r}_0)^{\frac{1}{3}}}\right)$$

The corresponding exchange correlation energy per electron is

$$\epsilon_{xc}(\vec{r}) = -\frac{1}{2} \int d^3r' \frac{e^2}{4\pi\epsilon_0|\vec{r} - \vec{r}'|} f\left(\frac{|\vec{r} - \vec{r}'|}{n(\vec{r})^{\frac{1}{3}}}\right)$$

If we introduce a variable transform

$$\vec{y} = \frac{\vec{r} - \vec{r}'}{n(\vec{r})^{\frac{1}{3}}}$$

we obtain

$$\epsilon_{xc}(\vec{r}) = -\frac{n(\vec{r})^{\frac{1}{3}}}{2} \int d^3y' \frac{e^2}{4\pi\epsilon_0|\vec{y}'|} f(\vec{y}') = -C n^{\frac{1}{3}}$$

where C is a constant that is entirely defined by the shape function $f(\vec{r})$.

In general, the X_α method yields larger band gaps than density functional theory. The latter severely underestimates band gaps. This is in accord with the tendency of Hartree Fock to overestimate band gaps. In contrast to Hartree Fock, however, the X_α method is superior for the description of metals because it does not lead to a vanishing density of states at the Fermi level.

LDA, the big surprise

The first density functionals used in practice were based on the local-density approximation (LDA). The hole function for an electron at position \vec{r} has been approximated by the one of a homogeneous electron gas with the same density as $n^{(1)}(\vec{r})$. The exchange correlation energy for the homogeneous electron gas has been obtained by quantum Monte Carlo calculations [44] and analytic calculations [45]. The local density approximation has been generalized early to local spin-density approximation (LSD) [46].

Truly surprising was how well the theory worked for real systems. Atomic distances could be determined within a few percent of the bond length and energy differences in solids were surprisingly good.

This was unexpected, because the density in real materials is far from homogeneous. Gunnarsson and Lundquist [47] explained this finding with sumrules that are obeyed by the local density approximation: Firstly, the exchange correlation energy depends only on the spherical average of the exchange correlation hole. Of the radial hole density only the first moment contributes, while the second moment is fixed by the sum-rule that the electron density of the hole integrates to -1 . Thus we can use

$$\int d^3r \frac{e^2 h(\vec{r}_0, \vec{r})}{4\pi\epsilon_0 |\vec{r} - \vec{r}_0|} = -\frac{e^2}{4\pi\epsilon_0} \frac{\int_0^\infty dr r \langle h(\vec{r}_0, \vec{r}) \rangle_{|\vec{r}-\vec{r}_0|=r}}{\int_0^\infty dr r^2 \langle h(\vec{r}_0, \vec{r}) \rangle_{|\vec{r}-\vec{r}_0|=r}} \quad (10.31)$$

where the angular brackets imply the angular average of $\vec{r} - \vec{r}_0$. This dependence on the hole density is rather insensitive to small changes of the hole density. Even for an atom, the *spherically averaged* exchange hole closely resembles that of the homogeneous electron gas [28], as demonstrated in Fig. 10.8.

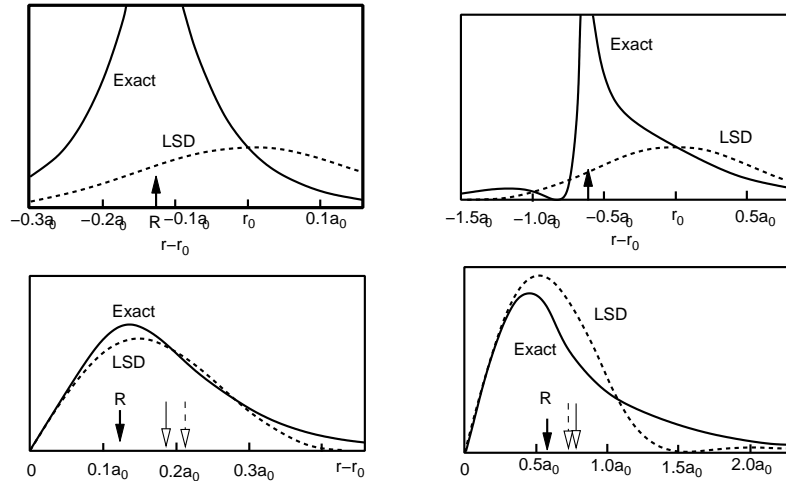


Fig. 10.8: Exchange hole of the nitrogen atom for an electron close to the nucleus (left) and further from the nucleus (right). As seen in the top figures, the true hole is centered at the nucleus, and the exchange hole of the free electron gas is centered on the electron. Despite the differences the integrands for the exchange energy, i.e. the spherical average multiplied by $\frac{1}{2} \cdot 4\pi r^2 \cdot \frac{e^2}{4\pi\epsilon_0 r}$, shown at the bottom, closely resembles each other. Redrawn from [28].

The main deficiency of the LDA was the strong overbinding with bond energies in error by about one electron volt. On the one hand, this rendered LDA useless for most applications in chemistry. On the other hand, the problem was hardly visible in solid state physics where bonds are rarely broken, but rearranged so that errors cancelled.

GGA, entering chemistry

Being concerned about the large density variations in real materials, one tried to include the first terms of a Taylor expansion in the density gradients. These attempts failed miserably. The culprit has been a violation of the basic sum rules as pointed out by Perdew [48]. The cure was a cutoff for the gradient contributions at high gradients, which lead to the class of generalized gradient approximations (GGA) [49].

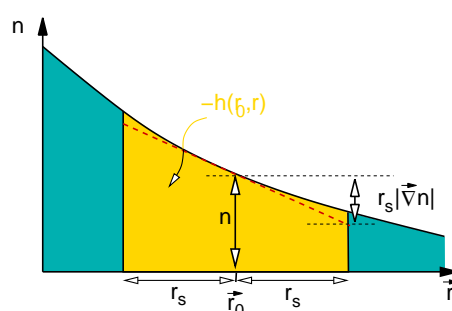


Fig. 10.9: Definition of the reduced gradient. The density gradient is made dimension-less by multiplication with the Seitz radius r_s representing the average size of the exchange correlation hole and by division by the density. The Seitz radius is defined by $\frac{4\pi}{3}r_s^3n = 1$, where n is the electron density. If the reduced gradient exceeds one the center of the exchange correlation hole moves away from the electron to avoid negative two-particle densities.

Becke [50] provides an intuitive description for the workings of GGA's, which I will sketch here in a simplified manner: Becke uses an ansatz $E_{xc} = \int d^3r A(n(\vec{r}))F(x(\vec{r}))$ for the exchange-correlation energy where $n(\vec{r})$ is the local density and $x = |\vec{\nabla}n|/n^{4/3}$ is a dimensionless reduced gradient. Do not confuse this symbol with the combined position-and-spin coordinate \vec{x} . The function A is simply the LDA expression and $F(x)$ is the so-called enhancement factor. The large-gradient limit of $F(x)$ is obtained from a simple physical argument:

Somewhat surprisingly, the reduced gradient is largest not near the nucleus but in the exponentially decaying charge-density tails as shown in Fig. 10.10. For an electron that is far from an atom, the hole is on the atom, because a hole can only be dug where electrons are. Thus the Coulomb interaction energy of the electron with its hole is $-\frac{e^2}{4\pi\epsilon_0 r}$, where r is the distance of the reference electron from the atom. As shown in appendix 10.7.2, the enhancement factor can now be obtained by enforcing this behavior for exponentially decaying densities.

As a result, the exchange and correlation energy per electron in the tail region of the electron density falls off with the inverse distance in GGA, while it has a much faster, exponential decay in the LDA. Thus, the tail region is stabilized by GGA. This contribution acts like a negative "surface energy".

When a bond between two atoms is broken, the surface is increased. In GGA this bond-breaking process is more favorable than in LDA, and, hence, the bond is weakened. Thus the GGA cures the overbinding error of the LDA.

These gradient corrections greatly improved the bond energies and made density functional theory useful also for chemists. The most widely distributed GGA functional is the Perdew-Burke-Ernzerhof (PBE) functional [51].

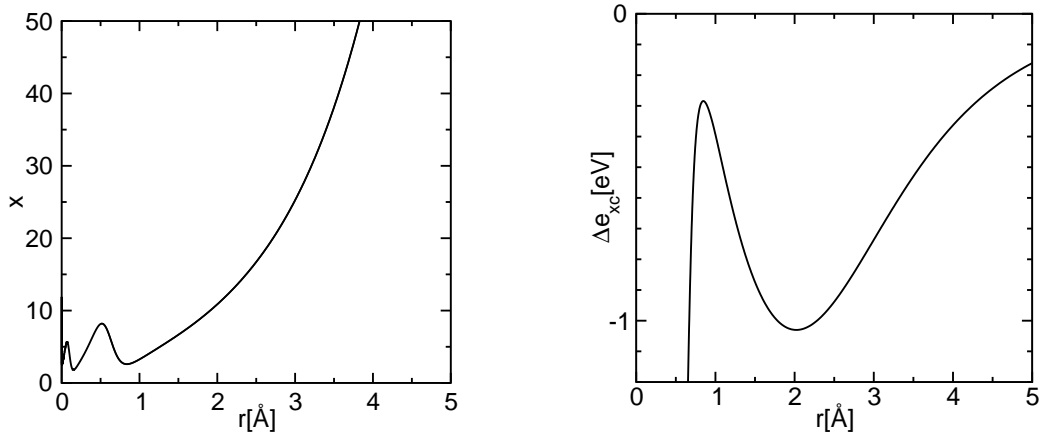


Fig. 10.10: Left figure: reduced density gradient $x = |\vec{\nabla}n|/n^{4/3}$ of a silicon atom as function of distance from the nucleus demonstrating that the largest reduced gradients occur in the exponential tails. Right figure: additional contribution from the gradient correction (PBE versus PW91 LDA) of the exchange correlation energy per electron. The figure demonstrates that the gradient correction stabilizes the tails of the wave function. The covalent radius of silicon is at 1.11 Å.

Meta GGA's

The next level of density functionals are the so-called meta GGA's [52, 53, 54] that include not only the gradient of the density, but also the second derivatives of the density. These functionals can be reformulated so that the additional parameter is the kinetic-energy density instead of the second density derivatives. Perdew recommends his TPSS functional [55].

Hybrid functionals

Another generation of functionals are hybrid functionals [56, 57], which replace some of the exchange energy by the exact exchange

$$E_X^{HF} = -\frac{1}{2} \sum_{m,n} \bar{f}_m \bar{f}_n \int d^4x \int d^4x' \frac{e^2 \psi_m^*(\vec{x}) \psi_n(\vec{x}) \psi_n^*(\vec{x}') \psi_m(\vec{x}')}{4\pi\epsilon_0 |\vec{r} - \vec{r}'|} \quad (10.32)$$

where \bar{f}_n and the $\psi_n(\vec{x})$ are the Kohn-Sham occupations and wave functions, respectively.

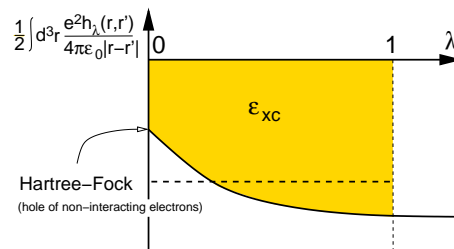


Fig. 10.11: Demonstration of the guiding idea of behind hybrid functionals, namely adiabatic connection. The exchange correlation energy can be written as an integral of the potential energy of exchange of interaction over the integration strength. This integrand may be approximated by an weighted average of the

The motivation for this approach goes back to the adiabatic connection formula [58, 59, 47]

$$E_{xc}[n(\vec{r})] = \int_0^1 d\lambda U_{xc}^{\lambda\hat{W}}[n(\vec{r})] = \int d^3r n(\vec{r}) \int_0^1 d\lambda \frac{1}{2} \int d^3r' \frac{h_\lambda(\vec{r}, \vec{r}')}{4\pi\epsilon_0|\vec{r} - \vec{r}'|} \quad (10.33)$$

which expresses the exchange correlation energy as an integral of the potential energy of exchange and correlation over the interaction strength λ . Here the interaction in the Hamiltonian is scaled by a factor λ , leading to a λ -dependent universal functional $F^{\lambda\hat{W}}[n^{(1)}]$. The interaction energy can be expressed by

$$\begin{aligned} F^{\hat{W}}[n] &= F^0[n] + \int_0^1 d\lambda \frac{d}{d\lambda} F^{\lambda\hat{W}}[n] \\ &= T_s[n] + \frac{1}{2} \int d^3r \int d^3r' \frac{e^2 n(\vec{r}) n(\vec{r}')}{4\pi\epsilon_0|\vec{r} - \vec{r}'|} + \int_0^1 d\lambda U_{xc}^{\lambda\hat{W}}[n] \end{aligned} \quad (10.34)$$

which leads via Eq. 10.30 to Eq. 10.33. Using perturbation theory, the derivative of $F^{\lambda\hat{W}}[n]$ simplifies to the expectation value $\langle \Psi(\lambda) | \hat{W} | \Psi(\lambda) \rangle$ of the interaction, which is the potential energy of exchange and correlation evaluated for a many-particle wave function obtained for the specified given interaction strength.

The underlying idea of the hybrid functionals is to interpolate the integrand between the end points. In the non-interacting limit, i.e. for $\lambda = 0$ the integrand $U_{xc}^{\lambda\hat{W}}$ is exactly given by the exact exchange energy of Eq. 10.32. For the full interaction, on the other hand, the LDA or GGA functionals are considered correctly. Thus a linear interpolation would yield

$$E_{xc} = \frac{1}{2} \left(U_{xc}^0 + U_{xc}^{\hat{W}} \right) = \frac{1}{2} \left(E_X^{HF} + U_{xc}^{\hat{W}} \right) = E_{xc}^{GGA} + \frac{1}{2} \left(E_X^{HF} - E_X^{GGA} \right). \quad (10.35)$$

Depending on whether the λ -dependence is a straight line or whether it is convex, the weight factor may be equal or smaller than $\frac{1}{2}$. Perdew [60] has given arguments that a factor $\frac{1}{4}$ would actually be better than a factor $\frac{1}{2}$.

Hybrid functionals perform substantially better than GGA functionals regarding binding energies, band gaps and reaction energies. However, they are flawed for the description of solids. The reason is that the exact exchange hole in a solid is very extended. These long-range tails are screened away quickly when the interaction is turned on, because they are cancelled by the correlation. Effectively, we should use a smaller mixing factor for the long range part of the exchange hole. This can be taken into account, by cutting off the long-range part of the interaction for the calculation of the Hartree-Fock exchange [61]. This approach improves the results for band gaps while reducing the computational effort [62].

The effective cancellation of the long-ranged contribution of exchange with a similar contribution from correlation, which is also considered properly already in the LDA, is one of the explanation for the superiority of the LDA over the Hartree-Fock approximation.

The most widely used hybrid functional is the B3LYP functional [63], which is, however, obtained from a parameter fit to a database of simple molecules. The functional PBE0 [64, 65] is born out of the famous PBE GGA functional and is a widely distributed parameter-free functional.

LDA+U and local hybrid functionals

Starting from a completely different context, Anisimov et. al. [66] introduced the so-called LDA+U method, which, as described below, has some similarities to the hybrid functionals above.

The main goal was to arrive at a proper description of transition metal oxides, which tend to be Mott insulators, while GGA calculations predict them often to be metals. The remedy was to add a correlation term⁶ [67] borrowed from the Hubbard model and to correct the resulting double counting

⁶The expression given here looks unusually simple. This is due to the notation of spin orbitals, which takes care of the spin indices.

of the interactions by E_{dc} .

$$E = E^{GGA} + \frac{1}{2} \sum_R \sum_{\alpha, \beta, \gamma, \delta \in \mathcal{C}_R} U_{\alpha, \beta, \gamma, \delta} \left(\rho_{\gamma, \alpha} \rho_{\delta, \beta} - \rho_{\delta, \alpha} \rho_{\gamma, \beta} \right) - E_{dc} \quad (10.36)$$

$$U_{\alpha, \beta, \gamma, \delta} = \int d^4x \int d^4x' \frac{e^2 \chi_\alpha^*(\vec{x}) \chi_\beta^*(\vec{x}') \chi_\gamma(\vec{x}) \chi_\delta(\vec{x}')}{4\pi\epsilon_0 |\vec{r} - \vec{r}'|} \quad (10.37)$$

$$\rho_{\alpha, \beta} = \langle \pi_\alpha | \psi_n \rangle f_n \langle \psi_n | \pi_\beta \rangle, \quad (10.38)$$

where $|\chi_\alpha\rangle$ are atomic tight-binding orbitals and $|\pi_\alpha\rangle$ are their projector functions.⁷ The additional energy is a Hartree-Fock exchange energy, that only considers the exchange for specified sets of local orbitals. The exchange term does only consider a subset of orbitals \mathcal{C}_R for each atom R and it ignores the contribution involving orbitals centered on different atoms.

Novak et al. [68] made the connection to the hybrid functionals explicit and restricted the exact exchange contribution of a hybrid functional to only a shell of orbitals. While in the LDA+U method the bare Coulomb matrix elements are reduced by a screening factor, in the hybrid functionals it is the mixing factor that effectively plays the same role. Both LDA+U and the local hybrid method have in common that they radically remove the contribution of off-site matrix elements of the interaction. Tran et al. [69] applied this method to transition metal oxides and found results that are similar to those of the full implementation of hybrid functionals.

Van der Waals interactions

One of the major difficulties for density functionals is the description of van der Waals forces, because it is due to the quantum mechanical synchronization of charge fluctuations on distinct molecules. I refer the reader to the work made in the group of Lundqvist [70, 71, 72].

10.6 Benchmarks, successes and failures

The development of density functionals has profited enormously from careful benchmark studies. The precondition is a data set of test cases for which reliable and accurate experimental data exist. The most famous data sets are the G1 and G2 databases [73, 74, 75, 76] that have been set up to benchmark quantum-chemistry codes. Becke [77, 78, 57, 79, 80] set a trend by using these large sets of test cases for systematic studies of density functionals. In order to separate out the accuracy of the density functionals, it is vital to perform these calculations on extremely accurate numerical methods. Becke used basis-set free calculations that were limited to small molecules while being extremely accurate. Paier et al. [81, 82, 83, 62] have later performed careful comparisons of two methods, Gaussian and the projector augmented-wave method, to single out the error of the electronic structure method.

Overall, the available density functionals predict molecular structures very well. Bond distances agree with the experiment often within one percent. Bond angles come out within a few degrees.

The quality of total energies depends strongly on the level of functionals used. On the LDA level bonds are overestimated in the 1 eV range, on the GGA level these errors are reduced to about 0.3 eV, and hybrid functionals reduce the error by another factor of 2. The ultimate goal is to reach chemical accuracy, which is about 0.05 eV. Such an accuracy allows to predict reaction rates at room temperature within a factor of 10.

Band gaps are predicted to be too small with LDA and GGA. The so-called band gap problem has been one of the major issues during the development of density functionals. Hybrid functionals clearly

⁷Projector functions obey the biorthogonality condition $\langle \chi_\alpha | \pi_\beta \rangle = \delta_{\alpha, \beta}$. Within the sub-Hilbert space of the tight-binding orbitals, i.e. for wave functions of the form $|\psi\rangle = \sum_\alpha |\chi_\alpha\rangle c_\alpha$, the projector functions decompose the wave function into tight binding orbitals, i.e. $|\psi\rangle = \sum_\alpha |\chi_\alpha\rangle \langle \pi_\alpha | \psi \rangle$. A similar projection is used extensively in the projector augmented-wave method described later.

improve the situation. A problem is the description of materials with strong electron correlations. For LDA and GGA many insulating transition metal oxides are described as metals. This changes again for the hybrid functionals, which turns them into antiferromagnetic insulators, which is a dramatic improvement.

10.7 Appendix to chapter DFT

10.7.1 Model exchange-correlation energy

We consider a model with a constant density and a hole function that describes a situation, where all electrons of the same spin are repelled completely from a sphere centered at the reference electron

The hole function has the form

$$h(\vec{r}, \vec{r}_0) = \begin{cases} -\frac{1}{2}n(\vec{r}_0) & \text{for } |\vec{r} - \vec{r}_0| < r_h \\ 0 & \text{otherwise} \end{cases}$$

where $n(\vec{r})$ is the electron density and the hole radius $r_h = \sqrt[3]{\frac{2}{4\pi n}}$ is the radius of the sphere, which is determined such that the exchange correlation hole integrates to -1 , i.e. $\frac{4\pi}{3}r_h^3(\frac{1}{2}n) = 1$.

The potential of a homogeneously charged sphere with radius r_h and one positive charge is

$$v(r) = \frac{e^2}{4\pi\epsilon_0} \begin{cases} -\frac{3}{2r_h} + \frac{1}{2r_h} \left(\frac{r}{r_h}\right)^2 & \text{for } r \leq r_h \\ -\frac{1}{r} & \text{for } r > r_h \end{cases}$$

where $r = |\vec{r} - \vec{r}_0|$.

With Eq. 10.14 we obtain for the potential contribution of the exchange correlation energy

$$U_{xc} = - \int d^3r n(\vec{r})v(r=0) = - \int d^3r \frac{e^2}{4\pi\epsilon_0} \frac{3}{4} \sqrt{\frac{2\pi}{3}} \cdot n^{\frac{4}{3}}$$

10.7.2 Large-gradient limit of the enhancement factor

An exponentially decaying density

$$n(r) = \exp(-\lambda r) \quad (10.39)$$

has a reduced gradient

$$x := \frac{|\vec{\nabla} n|}{n^{\frac{4}{3}}} = \lambda \exp(+\frac{1}{3}\lambda r) \quad (10.40)$$

We make the following ansatz for the exchange correlation energy per electron

$$\epsilon_{xc}(n, x) = -C n^{\frac{1}{3}} F(x) \quad (10.41)$$

where only the local exchange has been used and C is a constant.

Enforcing the long-distance limit of the exchange correlation energy per electron for exponentially decaying densities

$$\epsilon_{xc}((n(r), x(r))) = -\frac{1}{2} \frac{e^2}{4\pi\epsilon_0 r} \quad (10.42)$$

yields

$$F(x) = \frac{e^2}{4\pi\epsilon_0 r(x) 2C n^{\frac{1}{3}}(r(x))} \quad (10.43)$$

Using Eqs. 10.39 and 10.40, we express the radius and the density by the reduced gradient, i.e.

$$r(x) = -\frac{3}{\lambda} \left(\ln[\lambda] - \ln[x] \right) \quad (10.44)$$

$$n(x) = n(r(x)) = \lambda^3 x^{-3}, \quad (10.45)$$

and obtain

$$\begin{aligned} F(x) &= \frac{e^2}{4\pi\epsilon_0 \left[-\frac{3}{\lambda} \left(\ln[\lambda] - \ln[x] \right) \right] \left[2C\lambda x^{-1} \right]} = \left(\frac{e^2}{4\pi\epsilon_0 \cdot 6C} \right) \frac{x^2}{x \ln(\lambda) - x \ln(x)} \\ &\xrightarrow{x \rightarrow \infty} - \left(\frac{e^2}{4\pi\epsilon_0 \cdot 6C} \right) \frac{x^2}{x \ln(x)} \end{aligned} \quad (10.46)$$

Now we need to ensure that $F(0) = 1$, so that the gradient correction vanishes for the homogeneous electron gas, and that $F(x) = F(-x)$ to enforce spin reversal symmetry. There are several possible interpolations for these requirements, but the simplest is

$$F(x) = 1 - \frac{\beta x^2}{1 + \frac{4\pi\epsilon_0}{e^2} \cdot 6C\beta x \cdot \operatorname{asinh}(x)} \quad (10.47)$$

This is the enhancement factor for exchange used by Becke in his B88 functional [50].

Chapter 11

Electronic structure methods and the PAW method

This section is related to earlier versions [33, 34] written together with J. Kästner and C. Först.

11.1 Introduction

The main goal of electronic structure methods is to solve the Schrödinger equation for the electrons in a molecule or solid, to evaluate the resulting total energies, forces, response functions and other quantities of interest. In this chapter we describe the basic ideas behind the main electronic structure methods such as the pseudopotential and the augmented wave methods and provide selected pointers to contributions that are relevant for a beginner. We give particular emphasis to the Projector Augmented Wave (PAW) method developed by one of us, an electronic structure method for ab-initio molecular dynamics with full wavefunctions. We feel that it allows best to show the common conceptional basis of the most widespread electronic structure methods in materials science.

The methods described below require as input only the charge and mass of the nuclei, the number of electrons and an initial atomic geometry. They predict binding energies accurate within a few tenths of an electron volt and bond-lengths in the 1-2 percent range. Currently, systems with few hundred atoms per unit cell can be handled. The dynamics of atoms can be studied up to tens of pico-seconds. Quantities related to energetics, the atomic structure and to the ground-state electronic structure can be extracted.

In order to lay a common ground and to define some of the symbols, let us briefly touch upon the density functional theory [26, 27]. It maps a description for interacting electrons, a nearly intractable problem, onto one of non-interacting electrons in an effective potential. Within density functional theory, the total energy is written as

$$E[\{\psi_n(\vec{r})\}, \{\vec{R}_R\}] = \sum_n f_n \langle \psi_n | \frac{\hat{p}^2}{2m_e} | \psi_n \rangle + \frac{1}{2} \int d^3r \int d^3r' \frac{e^2 (n(\vec{r}) + Z(\vec{r})) (n(\vec{r}') + Z(\vec{r}'))}{4\pi\epsilon_0 |\vec{r} - \vec{r}'|} + E_{xc}[n], \quad (11.1)$$

where $Z(\vec{r}) = -\sum_R Z_R \delta(\vec{r} - \vec{R}_R)$ is the nuclear charge density expressed in electron charges. Z_R is the atomic number of a nucleus at position \vec{R}_R .

The electronic ground state is determined by minimizing the total energy functional $E[\Psi_n]$ of Eq. 11.1 at a fixed ionic geometry. The one-particle wave functions have to be orthogonal. This constraint is implemented with the method of Lagrange multipliers. We obtain the ground-state

wave functions from the extremum condition for

$$Y[\{|\psi_n\rangle\}, \mathbf{\Lambda}] = E[\{|\psi_n\rangle\}] - \sum_{n,m} [\langle\psi_n|\psi_m\rangle - \delta_{n,m}] \Lambda_{m,n} \quad (11.2)$$

with respect to the wavefunctions and the Lagrange multipliers $\Lambda_{m,n}$. The extremum condition for the wavefunctions has the form

$$\hat{H}|\psi_n\rangle f_n = \sum_m |\psi_m\rangle \Lambda_{m,n} , \quad (11.3)$$

where $\hat{H} = \frac{1}{2m_e} \hat{p}^2 + \hat{v}_{\text{eff}}$ is the effective one-particle Hamilton operator.

The corresponding effective potential depends itself on the electron density via

$$v_{\text{eff}}(\vec{r}) = \int d^3r' \frac{e^2 (n(\vec{r}') + Z(\vec{r}'))}{4\pi\epsilon_0 |\vec{r} - \vec{r}'|} + \mu_{xc}(\vec{r}) , \quad (11.4)$$

where $\mu_{xc}(\vec{r}) = \frac{\delta E_{xc}[n(\vec{r})]}{\delta n(\vec{r})}$ is the functional derivative of the exchange and correlation functional.

After a unitary transformation that diagonalizes the matrix of Lagrange multipliers $\mathbf{\Lambda}$, we obtain the Kohn-Sham equations

$$\hat{H}|\psi_n\rangle = |\psi_n\rangle \epsilon_n . \quad (11.5)$$

The one-particle energies ϵ_n are the eigenvalues of the matrix with the elements $\Lambda_{n,m}(f_n + f_m)/(2f_n f_m)$ [84].

The one-electron Schrödinger equations, namely the Kohn-Sham equations given in Eq. 10.23, still pose substantial numerical difficulties: (1) in the atomic region near the nucleus, the kinetic energy of the electrons is large, resulting in rapid oscillations of the wavefunction that require fine grids for an accurate numerical representation. On the other hand, the large kinetic energy makes the Schrödinger equation stiff, so that a change of the chemical environment has little effect on the shape of the wavefunction. Therefore, the wavefunction in the atomic region can be represented well already by a small basis set. (2) In the bonding region between the atoms the situation is opposite. The kinetic energy is small and the wavefunction is smooth. However, the wavefunction is flexible and responds strongly to the environment. This requires large and nearly complete basis sets.

Combining these different requirements is non-trivial and various strategies have been developed.

- The atomic point of view has been most appealing to quantum chemists. Basis functions are chosen that resemble atomic orbitals. This choice exploits that the wavefunction in the atomic region can be described by a few basis functions, while the chemical bond is described by the overlapping tails of these atomic orbitals. Most techniques in this class are a compromise of, on the one hand, a well adapted basis set, where the basis functions are difficult to handle, and, on the other hand, numerically convenient basis functions such as Gaussians, where the inadequacies are compensated by larger basis sets.
- Pseudopotentials regard an atom as a perturbation of the free electron gas. The most natural basis functions for the free electron gas are plane waves. Plane-wave basis sets are in principle complete and suitable for sufficiently smooth wavefunctions. The disadvantage of the comparably large basis sets required is offset by their extreme numerical simplicity. Finite plane-wave expansions are, however, absolutely inadequate to describe the strong oscillations of the wavefunctions near the nucleus. In the pseudopotential approach the Pauli repulsion by the core electrons is therefore described by an effective potential that expels the valence electrons from the core region. The resulting wavefunctions are smooth and can be represented well by plane waves. The price to pay is that all information on the charge density and wavefunctions near the nucleus is lost.

- Augmented-wave methods compose their basis functions from atom-like wavefunctions in the atomic regions and a set of functions, called envelope functions, appropriate for the bonding in between. Space is divided accordingly into atom-centered spheres, defining the atomic regions, and an interstitial region in between. The partial solutions of the different regions are matched with value and derivative at the interface between atomic and interstitial regions.

The projector augmented-wave method is an extension of augmented wave methods and the pseudopotential approach, which combines their traditions into a unified electronic structure method.

After describing the underlying ideas of the various approaches, let us briefly review the history of augmented wave methods and the pseudopotential approach. We do not discuss the atomic-orbital based methods, because our focus is the PAW method and its ancestors.

11.2 Augmented wave methods

The augmented wave methods have been introduced in 1937 by Slater [85]. His method was called augmented plane-wave (APW) method. Later Korringa [86], Kohn and Rostoker [87] modified the idea, which lead to the so-called KKR method. The basic idea behind the augmented wave methods has been to consider the electronic structure as a scattered-electron problem: Consider an electron beam, represented by a plane wave, traveling through a solid. It undergoes multiple scattering at the atoms. If, for some energy, the outgoing scattered waves interfere destructively, so that the electrons can not escape, a bound state has been determined. This approach can be translated into a basis-set method with energy- and potential-dependent basis functions. In order to make the scattered wave problem tractable, a model potential had to be chosen: The so-called muffin-tin potential approximates the true potential by a potential that is spherically symmetric in the atomic regions, and constant in between.

Augmented-wave methods reached adulthood in the 1970s: O. K. Andersen [13] showed that the energy dependent basis set of Slater's APW method can be mapped onto one with energy independent basis functions by linearizing the partial waves for the atomic regions with respect to their energy. In the original APW approach, one had to determine the zeros of the determinant of an energy dependent matrix, a nearly intractable numerical problem for complex systems. With the new energy independent basis functions, however, the problem is reduced to the much simpler generalized eigenvalue problem, which can be solved using efficient numerical techniques. Furthermore, the introduction of well defined basis sets paved the way for full-potential calculations [88]. In that case, the muffin-tin approximation is used solely to define the basis set $|\chi_i\rangle$, while the matrix elements $\langle\chi_i|H|\chi_j\rangle$ of the Hamiltonian are evaluated with the full potential.

In the augmented wave methods one constructs the basis set for the atomic region by solving the radial Schrödinger equation for the spherically averaged effective potential

$$\left[\frac{-\hbar^2}{2m_e} \vec{\nabla}^2 + v_{eff}(\vec{r}) - \epsilon \right] \phi_{\ell,m}(\epsilon, \vec{r}) = 0 \quad (11.6)$$

as function of the energy. Note that a partial wave $\phi_{\ell,m}(\epsilon, \vec{r})$ is an angular-momentum eigenstate and can be expressed as a product of a radial function and a spherical harmonic. The energy-dependent partial wave is expanded in a Taylor expansion about some reference energy $\epsilon_{\nu,\ell}$

$$\phi_{\ell,m}(\epsilon, \vec{r}) = \phi_{\nu,\ell,m}(\vec{r}) + (\epsilon - \epsilon_{\nu,\ell}) \dot{\phi}_{\nu,\ell,m}(\vec{r}) + O((\epsilon - \epsilon_{\nu,\ell})^2), \quad (11.7)$$

where $\phi_{\nu,\ell,m}(\vec{r}) = \phi_{\ell,m}(\epsilon_{\nu,\ell}, \vec{r})$. The energy derivative of the partial wave $\dot{\phi}_{\nu,\ell,m}(\vec{r}) = \left. \frac{\partial \phi_{\ell,m}(\epsilon, \vec{r})}{\partial \epsilon} \right|_{\epsilon_{\nu,\ell}}$ is obtained from the energy derivative of the Schrödinger equation

$$\left[\frac{-\hbar^2}{2m_e} \vec{\nabla}^2 + v_{eff}(\vec{r}) - \epsilon_{\nu,\ell} \right] \dot{\phi}_{\nu,\ell,m}(\vec{r}) = \phi_{\nu,\ell,m}(\vec{r}). \quad (11.8)$$

Next, one starts from a regular basis set, such as plane waves, Gaussians or Hankel functions. These basis functions are called envelope functions $|\tilde{\chi}_i\rangle$. Within the atomic region they are replaced by the partial waves and their energy derivatives, such that the resulting wavefunction $\chi_i(\vec{r})$ is continuous and differentiable. The augmented envelope function has the form

$$\chi_i(\vec{r}) = \tilde{\chi}_i(\vec{r}) - \sum_R \theta_R(\vec{r}) \tilde{\chi}_i(\vec{r}) + \sum_{R,\ell,m} \theta_R(\vec{r}) [\phi_{\nu,R,\ell,m}(\vec{r}) a_{R,\ell,m,i} + \dot{\phi}_{\nu,R,\ell,m}(\vec{r}) b_{R,\ell,m,i}] . \quad (11.9)$$

$\theta_R(\vec{r})$ is a step function that is unity within the augmentation sphere centered at \vec{R}_R and zero elsewhere. The augmentation sphere is atom-centered and has a radius about equal to the covalent radius. This radius is called the muffin-tin radius, if the spheres of neighboring atoms touch. These basis functions describe only the valence states; the core states are localized within the augmentation sphere and are obtained directly by a radial integration of the Schrödinger equation within the augmentation sphere.

The coefficients $a_{R,\ell,m,i}$ and $b_{R,\ell,m,i}$ are obtained for each $|\tilde{\chi}_i\rangle$ as follows: The envelope function is decomposed around each atomic site into spherical harmonics multiplied by radial functions

$$\tilde{\chi}_i(\vec{r}) = \sum_{\ell,m} u_{R,\ell,m,i}(|\vec{r} - \vec{R}_R|) Y_{\ell,m}(\vec{r} - \vec{R}_R) . \quad (11.10)$$

Analytical expansions for plane waves, Hankel functions or Gaussians exist. The radial parts of the partial waves $\phi_{\nu,R,\ell,m}$ and $\dot{\phi}_{\nu,R,\ell,m}$ are matched with value and derivative to $u_{R,\ell,m,i}(|\vec{r}|)$, which yields the expansion coefficients $a_{R,\ell,m,i}$ and $b_{R,\ell,m,i}$.

If the envelope functions are plane waves, the resulting method is called the linear augmented plane-wave (LAPW) method. If the envelope functions are Hankel functions, the method is called linear muffin-tin orbital (LMTO) method.

A good review of the LAPW method [13] has been given by Singh [89]. Let us now briefly mention the major developments of the LAPW method: Soler [90] introduced the idea of additive augmentation: While augmented plane waves are discontinuous at the surface of the augmentation sphere if the expansion in spherical harmonics in Eq. 11.9 is truncated, Soler replaced the second term in Eq. 11.9 by an expansion of the plane wave with the same angular momentum truncation as in the third term. This dramatically improved the convergence of the angular momentum expansion. Singh [91] introduced so-called local orbitals, which are non-zero only within a muffin-tin sphere, where they are superpositions of ϕ and $\dot{\phi}$ functions from different expansion energies. Local orbitals substantially increase the energy transferability. Sjöstedt [92] relaxed the condition that the basis functions are differentiable at the sphere radius. In addition she introduced local orbitals, which are confined inside the sphere, and that also have a kink at the sphere boundary. Due to the large energy cost of kinks, they will cancel, once the total energy is minimized. The increased variational degree of freedom in the basis leads to a dramatically improved plane-wave convergence [93].

The second variant of the linear methods is the LMTO method [13]. A good introduction into the LMTO method is the book by Skriver [94]. The LMTO method uses Hankel functions as envelope functions. The atomic spheres approximation (ASA) provides a particularly simple and efficient approach to the electronic structure of very large systems. In the ASA the augmentation spheres are blown up so that the sum of their volumes is equal to the total volume. Then, the first two terms in Eq. 11.9 are ignored. The main deficiency of the LMTO-ASA method is the limitation to structures that can be converted into a closed packed arrangement of atomic and empty spheres. Furthermore, energy differences due to structural distortions are often qualitatively incorrect. Full potential versions of the LMTO method, that avoid these deficiencies of the ASA have been developed. The construction of tight binding orbitals as superposition of muffin-tin orbitals [95] showed the underlying principles of the empirical tight-binding method and prepared the ground for electronic structure methods that scale linearly instead of with the third power of the number of atoms. The third generation LMTO [96] allows to construct true minimal basis sets, which require only one orbital per electron pair for insulators. In addition, they can be made arbitrarily accurate in the valence band region, so that a matrix diagonalization becomes unnecessary. The

first steps towards a full-potential implementation, that promises a good accuracy, while maintaining the simplicity of the LMTO-ASA method, are currently under way. Through the minimal basis-set construction the LMTO method offers unrivaled tools for the analysis of the electronic structure and has been extensively used in hybrid methods combining density functional theory with model Hamiltonians for materials with strong electron correlations [97].

11.3 Pseudopotentials

Pseudopotentials have been introduced to (1) avoid describing the core electrons explicitly and (2) to avoid the rapid oscillations of the wavefunction near the nucleus, which normally require either complicated or large basis sets.

The pseudopotential approach can be traced back to 1940 when C. Herring invented the orthogonalized plane-wave method [98]. Later, Phillips [99] and Antončik [100] replaced the orthogonality condition by an effective potential, which mimics the Pauli repulsion by the core electrons and thus compensates the electrostatic attraction by the nucleus. In practice, the potential was modified, for example, by cutting off the singular potential of the nucleus at a certain value. This was done with a few parameters that have been adjusted to reproduce the measured electronic band structure of the corresponding solid.

Hamann, Schlüter and Chiang [101] showed in 1979 how pseudopotentials can be constructed in such a way that their scattering properties are identical to that of an atom to first order in energy. These first-principles pseudopotentials relieved the calculations from the restrictions of empirical parameters. Highly accurate calculations have become possible especially for semiconductors and simple metals. An alternative approach towards first-principles pseudopotentials by Zunger and Cohen [102] even preceded the one mentioned above.

The idea behind the pseudopotential construction

In order to construct a first-principles pseudopotential, one starts out with an all-electron density-functional calculation for a spherical atom. Such calculations can be performed efficiently on radial grids. They yield the atomic potential and wavefunctions $\phi_{\ell,m}(\vec{r})$. Due to the spherical symmetry, the radial parts of the wavefunctions for different magnetic quantum numbers m are identical.

For the valence wavefunctions one constructs pseudo wavefunctions $|\tilde{\phi}_{\ell,m}\rangle$. There are numerous ways [103, 104, 105, 106] to construct those pseudo wavefunctions: Pseudo wave functions are identical to the true wave functions outside the augmentation region, which is called core region in the context of the pseudopotential approach. Inside the augmentation region the pseudo wavefunction should be nodeless and have the same norm as the true wavefunctions, that is $\langle \tilde{\phi}_{\ell,m} | \tilde{\phi}_{\ell,m} \rangle = \langle \phi_{\ell,m} | \phi_{\ell,m} \rangle$ (compare Figure 11.1).

From the pseudo wavefunction, a potential $u_{\ell}(\vec{r})$ can be reconstructed by inverting the respective Schrödinger equation, i.e.

$$\left[-\frac{\hbar^2}{2m_e} \vec{\nabla}^2 + u_{\ell}(\vec{r}) - \epsilon_{\ell,m} \right] \tilde{\phi}_{\ell,m}(\vec{r}) = 0 \Rightarrow u_{\ell}(\vec{r}) = \epsilon + \frac{1}{\tilde{\phi}_{\ell,m}(\vec{r})} \cdot \frac{\hbar^2}{2m_e} \vec{\nabla}^2 \tilde{\phi}_{\ell,m}(\vec{r}) .$$

This potential $u_{\ell}(\vec{r})$ (compare Figure 11.1), which is also spherically symmetric, differs from one main angular momentum ℓ to the other. Note, that this *inversion of the Schrödinger equation* works only if the wave functions are nodeless.

Next we define an effective pseudo Hamiltonian

$$\hat{H}_{\ell} = -\frac{\hbar^2}{2m_e} \vec{\nabla}^2 + v_{\ell}^{ps}(\vec{r}) + \int d^3r' \frac{e^2 (\tilde{n}(\vec{r}') + \tilde{Z}(\vec{r}'))}{4\pi\epsilon_0 |\vec{r} - \vec{r}'|} + \mu_{xc}([n(\vec{r})], \vec{r}) , \quad (11.11)$$

where $\mu_{xc}(\vec{r}) = \delta E_{xc}[n] / \delta n(\vec{r})$ is the functional derivative of the exchange and correlation energy with respect to the electron density. Then, we determine the pseudopotentials v_{ℓ}^{ps} such that the

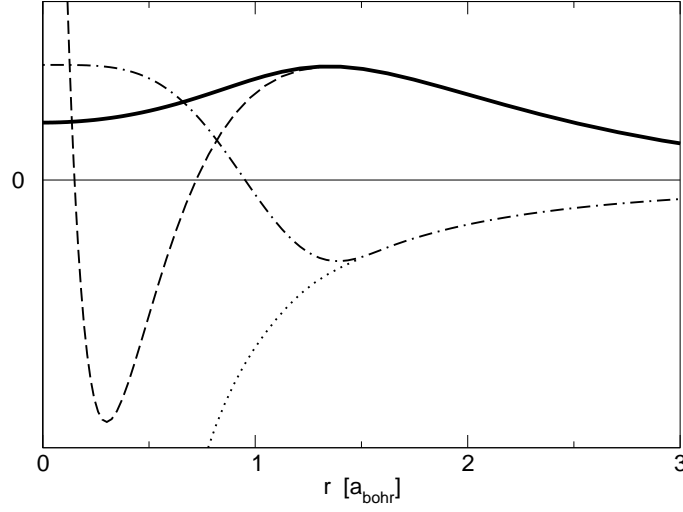


Fig. 11.1: Illustration of the pseudopotential concept at the example of the 3s wavefunction of Si. The solid line shows the radial part of the pseudo wavefunction $\tilde{\phi}_{\ell,m}$. The dashed line corresponds to the all-electron wavefunction $\phi_{\ell,m}$, which exhibits strong oscillations at small radii. The angular momentum dependent pseudopotential u_ℓ (dash-dotted line) deviates from the all-electron potential v_{eff} (dotted line) inside the augmentation region. The data are generated by the fhi98PP code [107].

pseudo Hamiltonian produces the pseudo wavefunctions, that is

$$v_\ell^{ps}(\vec{r}) = u_\ell(\vec{r}) - \int d^3r' \frac{e^2 (\tilde{n}(\vec{r}') + \tilde{Z}(\vec{r}'))}{4\pi\epsilon_0 |\vec{r} - \vec{r}'|} - \mu_{xc}([\tilde{n}(\vec{r})], \vec{r}) . \quad (11.12)$$

This process is called “unscreening”.

$\tilde{Z}(\vec{r})$ mimics the charge density of the nucleus and the core electrons. It is usually an atom-centered, spherical Gaussian that is normalized to the charge of nucleus and core electrons of that atom. In the pseudopotential approach, $\tilde{Z}_R(\vec{r})$ does not change with the potential. The pseudo density $\tilde{n}(\vec{r}) = \sum_n f_n \tilde{\psi}_n^*(\vec{r}) \tilde{\psi}_n(\vec{r})$ is constructed from the pseudo wavefunctions.

In this way, we obtain a different potential for each angular momentum channel. In order to apply these potentials to a given wavefunction, the wavefunction must first be decomposed into angular momenta. Then each component is applied to the pseudopotential v_ℓ^{ps} for the corresponding angular momentum.

The pseudopotential defined in this way can be expressed in a semi-local form¹

$$v^{ps}(\vec{r}, \vec{r}') = \bar{v}(\vec{r}) \delta(\vec{r} - \vec{r}') + \sum_{\ell,m} \left[Y_{\ell,m}(\vec{r}) [v_\ell^{ps}(\vec{r}) - \bar{v}(\vec{r})] \frac{\delta(|\vec{r}| - |\vec{r}'|)}{|\vec{r}|^2} Y_{\ell,m}^*(\vec{r}') \right] . \quad (11.13)$$

The local potential $\bar{v}(\vec{r})$ only acts on those angular momentum components that are not already considered explicitly in the non-local, angular-momentum dependent pseudopotentials v_ℓ^{ps} . Typically it is chosen to cancel the most expensive nonlocal terms, the one corresponding to the highest physically relevant angular momentum.

The pseudopotential $v^{ps}(\vec{r}, \vec{r}')$ is non-local as it depends on two position arguments, \vec{r} and \vec{r}' . The expectation values are evaluated as a double integral

$$\langle \tilde{\psi} | \hat{v}_{ps} | \tilde{\psi} \rangle = \int d^3r \int d^3r' \tilde{\psi}^*(\vec{r}) v^{ps}(\vec{r}, \vec{r}') \tilde{\psi}(\vec{r}') \quad (11.14)$$

¹A semi-local potential is local in the radial coordinate, but non-local in the angular coordinates.

The semi-local form of the pseudopotential given in Eq. 11.13 is computationally expensive. Therefore, in practice one uses a separable form of the pseudopotential [108, 109, 110]

$$\hat{v}^{ps} \approx \sum_{i,j} \hat{v}^{ps} |\tilde{\phi}_i\rangle [\langle \tilde{\phi}_j | \hat{v}^{ps} | \tilde{\phi}_i \rangle]_{i,j}^{-1} \langle \tilde{\phi}_j | \hat{v}^{ps} . \quad (11.15)$$

Thus, the projection onto spherical harmonics used in the semi-local form of Eq. 11.13 is replaced by a projection onto angular momentum dependent functions $\hat{v}^{ps} |\tilde{\phi}_i\rangle$.

The indices i and j are composite indices containing the atomic-site index R , the angular momentum quantum numbers ℓ, m and an additional index α . The index α distinguishes partial waves with otherwise identical indices R, ℓ, m when more than one partial wave per site and angular momentum is allowed. The partial waves may be constructed as eigenstates of the hamiltonian with the pseudopotential \hat{v}_ℓ^{ps} for a set of energies.

One can show that the identity of Eq. 11.15 holds by applying a wavefunction $|\tilde{\psi}\rangle = \sum_i |\tilde{\phi}_i\rangle c_i$ to both sides. If the set of pseudo partial waves $|\tilde{\phi}_i\rangle$ in Eq. 11.15 is complete, the identity is exact. The advantage of the separable form is that $\langle \tilde{\phi} | \hat{v}^{ps}$ is treated as one function, so that expectation values are reduced to combinations of simple scalar products $\langle \tilde{\phi}_i | \hat{v}^{ps} | \tilde{\psi} \rangle$.

The total energy of the pseudopotential method can be written in the form

$$E = \sum_n f_n \langle \tilde{\psi}_n | \frac{\hat{p}^2}{2m_e} | \tilde{\psi}_n \rangle + E_{self} + \sum_n f_n \langle \tilde{\psi}_n | \hat{v}_{ps} | \tilde{\psi}_n \rangle + \frac{1}{2} \int d^3r \int d^3r' \frac{e^2 (\tilde{n}(\vec{r}) + \tilde{Z}(\vec{r})) (\tilde{n}(\vec{r}') + \tilde{Z}(\vec{r}'))}{4\pi\epsilon_0 |\vec{r} - \vec{r}'|} + E_{xc}[\tilde{n}(\vec{r})] . \quad (11.16)$$

The constant E_{self} is adjusted such that the total energy of the atom is the same for an all-electron calculation and the pseudopotential calculation.

For the atom, from which it has been constructed, this construction guarantees that the pseudopotential method produces the correct one-particle energies for the valence states and that the wave functions have the desired shape.

While pseudopotentials have proven to be accurate for a large variety of systems, there is no strict guarantee that they produce the same results as an all-electron calculation, if they are used in a molecule or solid. The error sources can be divided into two classes:

- Energy transferability problems: Even for the potential of the reference atom, the scattering properties are accurate only in given energy window.
- Charge transferability problems: In a molecule or crystal, the potential differs from that of the isolated atom. The pseudopotential, however, is strictly valid only for the isolated atom.

The plane-wave basis set for the pseudo wavefunctions is defined by the shortest wave length $\lambda = 2\pi/|\vec{G}|$, where \vec{G} is the wave vector, via the so-called plane-wave cutoff $E_{PW} = \frac{\hbar^2 G_{max}^2}{2m_e}$ with $G_{max} = \max\{|\vec{G}|\}$. It is often specified in Rydberg ($1 \text{ Ry} = \frac{1}{2} \text{ H} \approx 13.6 \text{ eV}$). The plane-wave cutoff is the highest kinetic energy of all basis functions. The basis-set convergence can systematically be controlled by increasing the plane-wave cutoff.

The charge transferability is substantially improved by including a nonlinear core correction [111] into the exchange-correlation term of Eq. 11.16. Hamann [?] showed how to construct pseudopotentials also from unbound wavefunctions. Vanderbilt [?, ?] generalized the pseudopotential method to non-normconserving pseudopotentials, so-called ultra-soft pseudopotentials, which dramatically improves the basis-set convergence. The formulation of ultra-soft pseudopotentials has already many similarities with the projector augmented-wave method. Truncated separable pseudopotentials suffer sometimes from so-called ghost states. These are unphysical core-like states, which render the pseudopotential useless. These problems have been discussed by Gonze [112]. Quantities such as

hyperfine parameters that depend on the full wavefunctions near the nucleus, can be extracted approximately [113]. Good reviews of the pseudopotential methodology have been written by Payne *et al.* [?] and Singh [89].

In 1985 R. Car and M. Parrinello published the ab-initio molecular dynamics method [114]. Simulations of the atomic motion have become possible on the basis of state-of-the-art electronic structure methods. Besides making dynamical phenomena and finite temperature effects accessible to electronic structure calculations, the ab-initio molecular dynamics method also introduced a radically new way of thinking into electronic structure methods. Diagonalization of a Hamilton matrix has been replaced by classical equations of motion for the wavefunction coefficients. If one applies friction, the system is quenched to the ground state. Without friction truly dynamical simulations of the atomic structure are performed. By using thermostats [115, 116, 117, 118], simulations at constant temperature can be performed. The Car-Parrinello method treats electronic wavefunctions and atomic positions on an equal footing.

11.4 Projector augmented-wave method

The Car-Parrinello method had been implemented first for the pseudopotential approach. There seemed to be insurmountable barriers against combining the new technique with augmented wave methods. The main problem was related to the potential dependent basis set used in augmented wave methods: the Car-Parrinello method requires a well defined and unique total energy functional of atomic positions and basis set coefficients. Furthermore the analytic evaluation of the first partial derivatives of the total energy with respect to wave functions, $\frac{\partial E}{\partial \langle \psi_n |} = \hat{H}|\psi_n\rangle f_n$, and atomic positions, the forces $\vec{F}_j = -\vec{\nabla}_j E$, must be possible. Therefore, it was one of the main goals of the PAW method to introduce energy and potential independent basis sets, which were as accurate as the previously used augmented basis sets. Other requirements have been: (1) The method should at least match the efficiency of the pseudopotential approach for Car-Parrinello simulations. (2) It should become an exact theory when converged and (3) its convergence should be easily controlled. We believe that these criteria have been met, which explains why the use of the PAW method has become increasingly widespread today.

Transformation theory

At the root of the PAW method lies a transformation that maps the true wavefunctions with their complete nodal structure onto auxiliary wavefunctions that are numerically convenient. We aim for smooth auxiliary wavefunctions, which have a rapidly convergent plane-wave expansion. With such a transformation we can expand the auxiliary wave functions into a convenient basis set such as plane waves, and evaluate all physical properties after reconstructing the related physical (true) wavefunctions.

Let us denote the physical one-particle wavefunctions as $|\psi_n\rangle$ and the auxiliary wavefunctions as $|\tilde{\psi}_n\rangle$. Note that the tilde refers to the representation of smooth auxiliary wavefunctions and n is the label for a one-particle state and contains a band index, a k -point and a spin index. The transformation from the auxiliary to the physical wave functions is denoted by $\hat{\mathcal{T}}$, i.e.

$$|\psi_n\rangle = \hat{\mathcal{T}}|\tilde{\psi}_n\rangle. \quad (11.17)$$

Now we express the constrained density functional F of Eq. 11.2 in terms of our auxiliary wavefunctions

$$F[\{\hat{\mathcal{T}}|\tilde{\psi}_n\rangle\}, \{\Lambda_{m,n}\}] = E[\{\hat{\mathcal{T}}|\tilde{\psi}_n\rangle\}] - \sum_{n,m} [\langle \tilde{\psi}_n | \hat{\mathcal{T}}^\dagger \hat{\mathcal{T}} | \tilde{\psi}_m \rangle - \delta_{n,m}] \Lambda_{m,n}. \quad (11.18)$$

The variational principle with respect to the auxiliary wavefunctions yields

$$\hat{\mathcal{T}}^\dagger \hat{H} \hat{\mathcal{T}} |\tilde{\psi}_n\rangle = \hat{\mathcal{T}}^\dagger \hat{\mathcal{T}} |\tilde{\psi}_n\rangle \epsilon_n. \quad (11.19)$$

Again, we obtain a Schrödinger-like equation (see derivation of Eq. 11.5), but now the Hamilton operator has a different form, $\hat{H} = \hat{T}^\dagger \hat{H} \hat{T}$, an overlap operator $\hat{O} = \hat{T}^\dagger \hat{T}$ occurs, and the resulting auxiliary wavefunctions are smooth.

When we evaluate physical quantities, we need to evaluate expectation values of an operator \hat{A} , which can be expressed in terms of either the true or the auxiliary wavefunctions, i.e.

$$\langle \hat{A} \rangle = \sum_n f_n \langle \psi_n | \hat{A} | \psi_n \rangle = \sum_n f_n \langle \tilde{\psi}_n | \hat{T}^\dagger \hat{A} \hat{T} | \tilde{\psi}_n \rangle. \quad (11.20)$$

In the representation of auxiliary wavefunctions we need to use transformed operators $\hat{\tilde{A}} = \hat{T}^\dagger \hat{A} \hat{T}$. As it is, this equation only holds for the valence electrons. The core electrons are treated differently, as will be shown below.

The transformation takes us conceptionally from the world of pseudopotentials to that of augmented wave methods, which deal with the full wavefunctions. We will see that our auxiliary wavefunctions, which are simply the plane-wave parts of the full wavefunctions, translate into the wavefunctions of the pseudopotential approach. In the PAW method the auxiliary wavefunctions are used to construct the true wavefunctions and the total energy functional is evaluated from the latter. Thus it provides the missing link between augmented wave methods and the pseudopotential method, which can be derived as a well-defined approximation of the PAW method.

In the original paper [84], the auxiliary wavefunctions were termed pseudo wavefunctions and the true wavefunctions were termed all-electron wavefunctions, in order to make the connection more evident. We avoid this notation here, because it resulted in confusion in cases, where the correspondence is not clear-cut.

Transformation operator

So far we have described how we can determine the auxiliary wave functions of the ground state and how to obtain physical information from them. What is missing is a definition of the transformation operator \hat{T} .

The operator \hat{T} has to modify the smooth auxiliary wave function in each atomic region, so that the resulting wavefunction has the correct nodal structure. Therefore, it makes sense to write the transformation as identity plus a sum of atomic contributions \hat{S}_R

$$\hat{T} = \hat{1} + \sum_R \hat{S}_R. \quad (11.21)$$

For every atom, \hat{S}_R adds the difference between the true and the auxiliary wavefunction.

The local terms \hat{S}_R are defined in terms of solutions $|\phi_i\rangle$ of the Schrödinger equation for the isolated atoms. This set of partial waves $|\phi_i\rangle$ will serve as a basis set so that, near the nucleus, all relevant valence wavefunctions can be expressed as superposition of the partial waves with yet unknown coefficients as

$$\psi(\vec{r}) = \sum_{i \in R} \phi_i(\vec{r}) c_i \quad \text{for } |\vec{r} - \vec{R}_R| < r_{c,R}. \quad (11.22)$$

With $i \in R$ we indicate those partial waves that belong to site R .

Since the core wavefunctions do not spread out into the neighboring atoms, we will treat them differently. Currently we use the frozen-core approximation, which imports the density and the energy of the core electrons from the corresponding isolated atoms. The transformation \hat{T} shall produce only wavefunctions orthogonal to the core electrons, while the core electrons are treated separately. Therefore, the set of atomic partial waves $|\phi_i\rangle$ includes only valence states that are orthogonal to the core wavefunctions of the atom.

For each of the partial waves we choose an auxiliary partial wave $|\tilde{\phi}_i\rangle$. The identity

$$\begin{aligned} |\phi_i\rangle &= (\hat{1} + \hat{S}_R) |\tilde{\phi}_i\rangle \quad \text{for } i \in R \\ \hat{S}_R |\tilde{\phi}_i\rangle &= |\phi_i\rangle - |\tilde{\phi}_i\rangle \end{aligned} \quad (11.23)$$

defines the local contribution $\hat{\mathcal{S}}_R$ to the transformation operator. Since $\hat{1} + \hat{\mathcal{S}}_R$ should change the wavefunction only locally, we require that the partial waves $|\phi_i\rangle$ and their auxiliary counter parts $|\tilde{\phi}_i\rangle$ are pairwise identical beyond a certain radius $r_{c,R}$.

$$\phi_i(\vec{r}) = \tilde{\phi}_i(\vec{r}) \quad \text{for } i \in R \quad \text{and} \quad |\vec{r} - \vec{R}_R| > r_{c,R} \quad (11.24)$$

Note that the partial waves are not necessarily bound states and are therefore not normalizable unless we truncate them beyond a certain radius $r_{c,R}$. The PAW method is formulated such that the final results do not depend on the location where the partial waves are truncated, as long as this is not done too close to the nucleus and identical for auxiliary and all-electron partial waves.

In order to be able to apply the transformation operator to an arbitrary auxiliary wavefunction, we need to be able to expand the auxiliary wavefunction locally into the auxiliary partial waves

$$\tilde{\psi}(\vec{r}) = \sum_{i \in R} \tilde{\phi}_i(\vec{r}) c_i = \sum_{i \in R} \tilde{\phi}_i(\vec{r}) \langle \tilde{\rho}_i | \tilde{\psi} \rangle \quad \text{for } |\vec{r} - \vec{R}_R| < r_{c,R}, \quad (11.25)$$

which defines the projector functions $|\tilde{\rho}_i\rangle$. The projector functions probe the local character of the auxiliary wave function in the atomic region. Examples of projector functions are shown in Figure 11.2. From Eq. 11.25 we can derive $\sum_{i \in R} |\tilde{\phi}_i\rangle \langle \tilde{\rho}_i| = 1$, which is valid within $r_{c,R}$. It can be shown by insertion, that the identity Eq. 11.25 holds for any auxiliary wavefunction $|\tilde{\psi}\rangle$ that can be expanded locally into auxiliary partial waves $|\tilde{\phi}_i\rangle$, if

$$\langle \tilde{\rho}_i | \tilde{\phi}_j \rangle = \delta_{ij} \quad \text{for } i, j \in R. \quad (11.26)$$

Note that neither the projector functions nor the partial waves need to be mutually orthogonal. The projector functions are fully determined with the above conditions and a closure relation that is related to the unscreening of the pseudopotentials (see Eq. 90 in [84]).

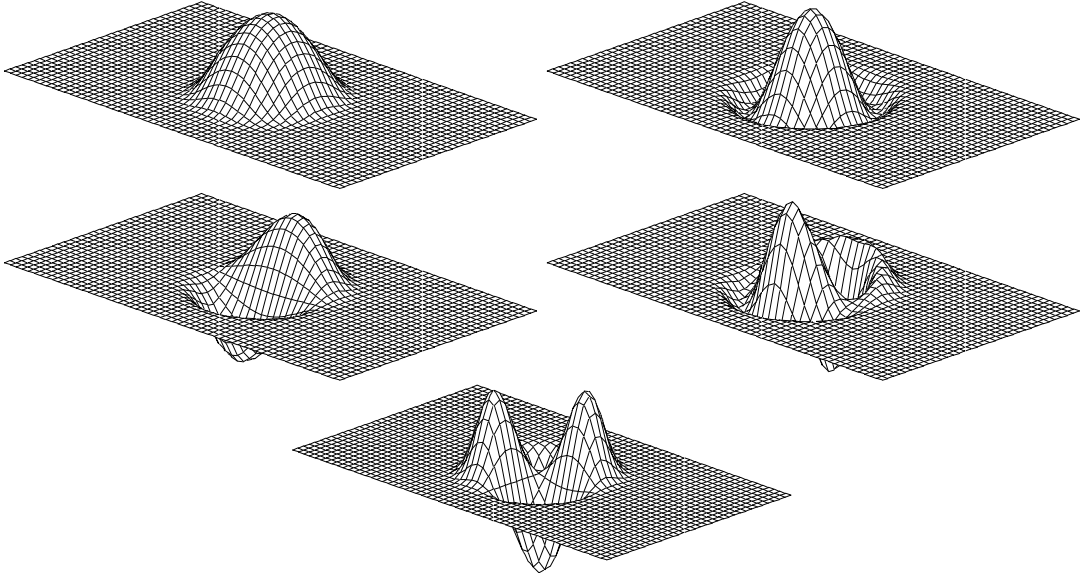


Fig. 11.2: Projector functions of the chlorine atom. Top: two s-type projector functions, middle: p-type, bottom: d-type.

By combining Eq. 11.23 and Eq. 11.25, we can apply $\hat{\mathcal{S}}_R$ to any auxiliary wavefunction.

$$\hat{\mathcal{S}}_R |\tilde{\psi}\rangle = \sum_{i \in R} \hat{\mathcal{S}}_R |\tilde{\phi}_i\rangle \langle \tilde{\rho}_i | \tilde{\psi} \rangle = \sum_{i \in R} (|\phi_i\rangle - |\tilde{\phi}_i\rangle) \langle \tilde{\rho}_i | \tilde{\psi} \rangle. \quad (11.27)$$

Hence, the transformation operator is

$$\hat{\mathcal{T}} = \hat{1} + \sum_i (|\phi_i\rangle - |\tilde{\phi}_i\rangle) \langle \tilde{\rho}_i |, \quad (11.28)$$

where the sum runs over all partial waves of all atoms. The true wave function can be expressed as

$$|\psi\rangle = |\tilde{\psi}\rangle + \sum_i \left(|\phi_i\rangle - |\tilde{\phi}_i\rangle \right) \langle \tilde{\rho}_i | \tilde{\psi} \rangle = |\tilde{\psi}\rangle + \sum_R \left(|\psi_R^1\rangle - |\tilde{\psi}_R^1\rangle \right) \quad (11.29)$$

with

$$|\psi_R^1\rangle = \sum_{i \in R} |\phi_i\rangle \langle \tilde{\rho}_i | \tilde{\psi} \rangle \quad (11.30)$$

$$|\tilde{\psi}_R^1\rangle = \sum_{i \in R} |\tilde{\phi}_i\rangle \langle \tilde{\rho}_i | \tilde{\psi} \rangle. \quad (11.31)$$

In Fig. 11.3 the decomposition of Eq. 11.29 is shown for the example of the bonding p- σ state of the Cl_2 molecule.

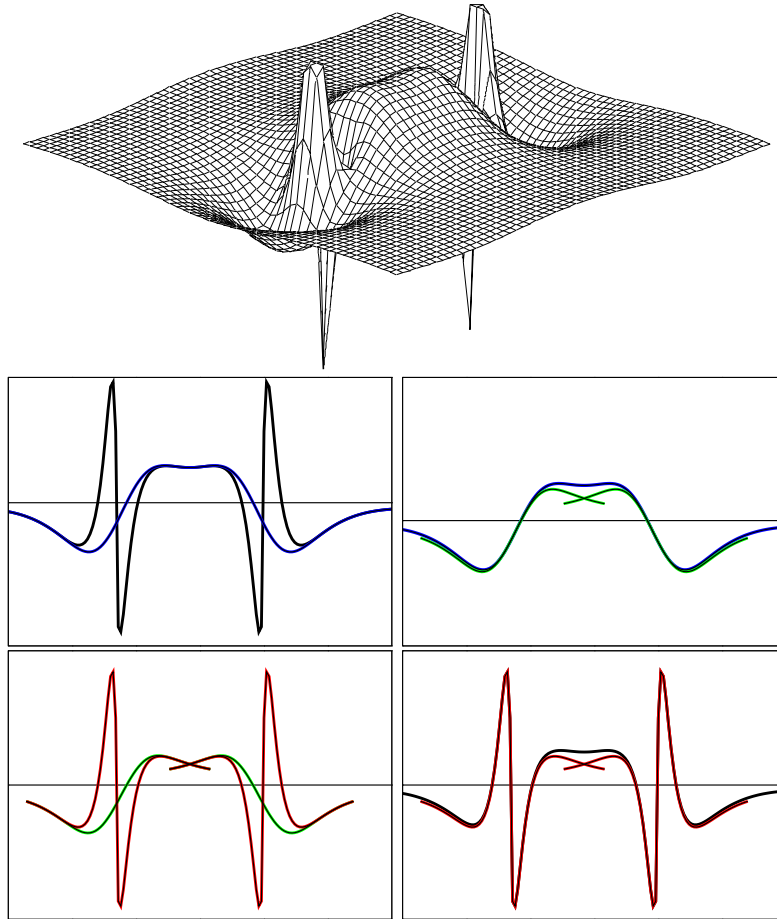


Fig. 11.3: Bonding p- σ orbital of the Cl_2 molecule and its decomposition into auxiliary wavefunction and the two one-center expansions. Top-left: True and auxiliary wave function; top-right: auxiliary wavefunction and its partial wave expansion; bottom-left: the two partial wave expansions; bottom-right: true wavefunction and its partial wave expansion.

To understand the expression Eq. 11.29 for the true wave function, let us concentrate on different regions in space. (1) Far from the atoms, the partial waves are, according to Eq. 11.24, pairwise identical so that the auxiliary wavefunction is identical to the true wave function, that is $\psi(\vec{r}) = \tilde{\psi}(\vec{r})$. (2) Close to an atom R , however, the auxiliary wavefunction is, according to Eq. 11.25, identical to

its one-center expansion, that is $\tilde{\psi}(\vec{r}) = \tilde{\psi}_R^1(\vec{r})$. Hence the true wavefunction $\psi(\vec{r})$ is identical to $\psi_R^1(\vec{r})$, which is built up from partial waves that contain the proper nodal structure.

In practice, the partial wave expansions are truncated. Therefore, the identity of Eq. 11.25 does not hold strictly. As a result, the plane waves also contribute to the true wavefunction inside the atomic region. This has the advantage that the missing terms in a truncated partial wave expansion are partly accounted for by plane waves. This explains the rapid convergence of the partial wave expansions. This idea is related to the additive augmentation of the LAPW method of Soler [90].

Frequently, the question comes up, whether the transformation Eq. 11.28 of the auxiliary wavefunctions indeed provides the true wavefunction. The transformation should be considered merely as a change of representation analogous to a coordinate transform. If the total energy functional is transformed consistently, its minimum will yield auxiliary wavefunctions that produce the correct wave functions $|\psi\rangle$.

Expectation values

Expectation values can be obtained either from the reconstructed true wavefunctions or directly from the auxiliary wave functions

$$\begin{aligned}\langle \hat{A} \rangle &= \sum_n f_n \langle \psi_n | \hat{A} | \psi_n \rangle + \sum_{n=1}^{N_c} \langle \phi_n^c | \hat{A} | \phi_n^c \rangle \\ &= \sum_n f_n \langle \tilde{\psi}_n | \hat{T}^\dagger \hat{A} \hat{T} | \tilde{\psi}_n \rangle + \sum_{n=1}^{N_c} \langle \phi_n^c | \hat{A} | \phi_n^c \rangle,\end{aligned}\quad (11.32)$$

where f_n are the occupations of the valence states and N_c is the number of core states. The first sum runs over the valence states, and second over the core states $|\phi_n^c\rangle$.

Now we can decompose the matrix element for a wavefunction ψ into its individual contributions according to Eq. 11.29.

$$\begin{aligned}\langle \psi | \hat{A} | \psi \rangle &= \langle \tilde{\psi} + \sum_R (\psi_R^1 - \tilde{\psi}_R^1) | \hat{A} | \tilde{\psi} + \sum_{R'} (\psi_{R'}^1 - \tilde{\psi}_{R'}^1) \rangle \\ &= \underbrace{\langle \tilde{\psi} | \hat{A} | \tilde{\psi} \rangle + \sum_R \left(\langle \psi_R^1 | \hat{A} | \psi_R^1 \rangle - \langle \tilde{\psi}_R^1 | \hat{A} | \tilde{\psi}_R^1 \rangle \right)}_{\text{part 1}} \\ &\quad + \underbrace{\sum_R \left(\langle \psi_R^1 - \tilde{\psi}_R^1 | \hat{A} | \tilde{\psi} - \tilde{\psi}_R^1 \rangle + \langle \tilde{\psi} - \tilde{\psi}_R^1 | \hat{A} | \psi_R^1 - \tilde{\psi}_R^1 \rangle \right)}_{\text{part 2}} \\ &\quad + \underbrace{\sum_{R \neq R'} \langle \psi_R^1 - \tilde{\psi}_R^1 | \hat{A} | \psi_{R'}^1 - \tilde{\psi}_{R'}^1 \rangle}_{\text{part 3}}\end{aligned}\quad (11.33)$$

Only the first part of Eq. 11.33 is evaluated explicitly, while the second and third parts of Eq. 11.33 are neglected, because they vanish for sufficiently local operators as long as the partial wave expansion is converged: The function $\psi_R^1 - \tilde{\psi}_R^1$ vanishes per construction beyond its augmentation region, because the partial waves are pairwise identical beyond that region. The function $\tilde{\psi} - \tilde{\psi}_R^1$ vanishes inside its augmentation region, if the partial wave expansion is sufficiently converged. In no region of space are both functions $\psi_R^1 - \tilde{\psi}_R^1$ and $\tilde{\psi} - \tilde{\psi}_R^1$ simultaneously nonzero. Similarly the functions $\psi_R^1 - \tilde{\psi}_R^1$ from different sites are never non-zero in the same region in space. Hence, the second and third parts of Eq. 11.33 vanish for operators such as the kinetic energy $\frac{\hbar^2}{2m_e} \vec{\nabla}^2$ and the real space projection operator $|r\rangle\langle r|$, which produces the electron density. For truly nonlocal operators the parts 2 and 3 of Eq. 11.33 would have to be considered explicitly.

The expression, Eq. 11.32, for the expectation value can therefore be written with the help of Eq. 11.33 as

$$\begin{aligned}
\langle \hat{A} \rangle &= \sum_n f_n \left(\langle \tilde{\psi}_n | \hat{A} | \tilde{\psi}_n \rangle + \langle \psi_n^1 | \hat{A} | \psi_n^1 \rangle - \langle \tilde{\psi}_n^1 | \hat{A} | \tilde{\psi}_n^1 \rangle \right) + \sum_{n=1}^{N_c} \langle \phi_n^c | \hat{A} | \phi_n^c \rangle \\
&= \sum_n f_n \langle \tilde{\psi}_n | \hat{A} | \tilde{\psi}_n \rangle + \sum_{n=1}^{N_c} \langle \tilde{\phi}_n^c | \hat{A} | \tilde{\phi}_n^c \rangle \\
&\quad + \sum_R \left(\sum_{i,j \in R} D_{ij} \langle \phi_j | \hat{A} | \phi_i \rangle + \sum_{n \in R}^{N_{c,R}} \langle \phi_n^c | \hat{A} | \phi_n^c \rangle \right) \\
&\quad - \sum_R \left(\sum_{i,j \in R} D_{ij} \langle \tilde{\phi}_j | \hat{A} | \tilde{\phi}_i \rangle + \sum_{n \in R}^{N_{c,R}} \langle \tilde{\phi}_n^c | \hat{A} | \tilde{\phi}_n^c \rangle \right), \tag{11.34}
\end{aligned}$$

where \mathbf{D} is the one-center density matrix defined as

$$D_{ij} = \sum_n f_n \langle \tilde{\psi}_n | \tilde{\rho}_j \rangle \langle \tilde{\rho}_i | \tilde{\psi}_n \rangle = \sum_n \langle \tilde{\rho}_i | \tilde{\psi}_n \rangle f_n \langle \tilde{\psi}_n | \tilde{\rho}_j \rangle. \tag{11.35}$$

The auxiliary core states, $|\tilde{\phi}_n^c\rangle$ allow us to incorporate the tails of the core wavefunction into the plane-wave part, and therefore assure that the integrations of partial wave contributions cancel exactly beyond r_c . They are identical to the true core states in the tails, but are a smooth continuation inside the atomic sphere. It is not required that the auxiliary wave functions are normalized.

Following this scheme, the electron density is given by

$$n(\vec{r}) = \tilde{n}(\vec{r}) + \sum_R \left(n_R^1(\vec{r}) - \tilde{n}_R^1(\vec{r}) \right) \tag{11.36}$$

$$\begin{aligned}
\tilde{n}(\vec{r}) &= \sum_n f_n \tilde{\psi}_n^*(\vec{r}) \tilde{\psi}_n(\vec{r}) + \tilde{n}_c(\vec{r}) \\
n_R^1(\vec{r}) &= \sum_{i,j \in R} D_{ij} \phi_j^*(\vec{r}) \phi_i(\vec{r}) + n_{c,R}(\vec{r}) \\
\tilde{n}_R^1(\vec{r}) &= \sum_{i,j \in R} D_{ij} \tilde{\phi}_j^*(\vec{r}) \tilde{\phi}_i(\vec{r}) + \tilde{n}_{c,R}(\vec{r}), \tag{11.37}
\end{aligned}$$

where $n_{c,R}$ is the core density of the corresponding atom and $\tilde{n}_{c,R}$ is the auxiliary core density, which is identical to $n_{c,R}$ outside the atomic region, but smooth inside.

Before we continue, let us discuss a special point: The matrix elements of a general operator with the auxiliary wavefunctions may be slowly converging with the plane-wave expansion, because the operator \hat{A} may not be well behaved. An example of such an operator is the singular electrostatic potential of a nucleus. This problem can be alleviated by adding an “intelligent zero”: If an operator \hat{B} is purely localized within an atomic region, we can use the identity between the auxiliary wavefunction and its own partial wave expansion

$$0 = \langle \tilde{\psi}_n | \hat{B} | \tilde{\psi}_n \rangle - \langle \tilde{\psi}_n^1 | \hat{B} | \tilde{\psi}_n^1 \rangle. \tag{11.38}$$

Now we choose an operator \hat{B} so that it cancels the problematic behavior of the operator \hat{A} , but is localized in a single atomic region. By adding \hat{B} to the plane-wave part and the matrix elements with its one-center expansions, the plane-wave convergence can be improved without affecting the converged result. A term of this type, namely \hat{v} will be introduced in the next section to cancel the Coulomb singularity of the potential at the nucleus.

Total energy

Like wavefunctions and expectation values, also the total energy can be divided into three parts.

$$E[\{\tilde{\psi}_n\}, \{R_R\}] = \tilde{E} + \sum_R (E_R^1 - \tilde{E}_R^1) \quad (11.39)$$

The plane-wave part \tilde{E} involves only smooth functions and is evaluated on equi-spaced grids in real and reciprocal space. This part is computationally most demanding, and is similar to the expressions in the pseudopotential approach.

$$\begin{aligned} \tilde{E} = & \sum_n \langle \tilde{\psi}_n | \frac{\hat{p}^2}{2m_e} | \tilde{\psi}_n \rangle + \frac{1}{2} \int d^3r \int d^3r' \frac{e^2 (\tilde{n}(\vec{r}) + \tilde{Z}(\vec{r})) (\tilde{n}(\vec{r}') + \tilde{Z}(\vec{r}'))}{4\pi\epsilon_0 |\vec{r} - \vec{r}'|} \\ & + \int d^3r \bar{v}(\vec{r}) \tilde{n}(\vec{r}) + E_{xc}[\tilde{n}] \end{aligned} \quad (11.40)$$

$\tilde{Z}(\mathbf{r})$ is an angular-momentum dependent core-like density that will be described in detail below. The remaining parts can be evaluated on radial grids in a spherical-harmonics expansion. The nodal structure of the wavefunctions can be properly described on a logarithmic radial grid that becomes very fine near the nucleus,

$$\begin{aligned} E_R^1 = & \sum_{i,j \in R} D_{ij} \langle \phi_j | \frac{\hat{p}^2}{2m_e} | \phi_i \rangle + \sum_{n \in R} \langle \phi_n^\zeta | \frac{\hat{p}^2}{2m_e} | \phi_n^\zeta \rangle \\ & + \frac{1}{2} \int d^3r \int d^3r' \frac{e^2 (n^1(\vec{r}) + Z(\vec{r})) (n^1(\vec{r}') + Z(\vec{r}'))}{|\vec{r} - \vec{r}'|} + E_{xc}[n^1] \end{aligned} \quad (11.41)$$

$$\begin{aligned} \tilde{E}_R^1 = & \sum_{i,j \in R} D_{ij} \langle \tilde{\phi}_j | \frac{\hat{p}^2}{2m_e} | \tilde{\phi}_i \rangle + \frac{1}{2} \int d^3r \int d^3r' \frac{e^2 (\tilde{n}^1(\vec{r}) + \tilde{Z}(\vec{r})) (\tilde{n}^1(\vec{r}') + \tilde{Z}(\vec{r}'))}{4\pi\epsilon_0 |\vec{r} - \vec{r}'|} \\ & + \int d^3r \bar{v}(\vec{r}) \tilde{n}^1(\vec{r}) + E_{xc}[\tilde{n}^1]. \end{aligned} \quad (11.42)$$

The compensation charge density $\tilde{Z}(\vec{r}) = \sum_R \tilde{Z}_R(\vec{r})$ is given as a sum of angular momentum dependent Gauss functions, which have an analytical plane-wave expansion. A similar term occurs also in the pseudopotential approach. In contrast to the norm-conserving pseudopotential approach, however, the compensation charge of an atom \tilde{Z}_R is non-spherical and constantly adapts instantaneously to the environment. It is constructed such that

$$n_R^1(\vec{r}) + Z_R(\vec{r}) - \tilde{n}_R^1(\vec{r}) - \tilde{Z}_R(\vec{r}) \quad (11.43)$$

has vanishing electrostatic multipole moments for each atomic site. With this choice, the electrostatic potentials of the augmentation densities vanish outside their spheres. This is the reason why there is no electrostatic interaction of the one-center parts between different sites.

The compensation charge density as given here is still localized within the atomic regions. A technique similar to an Ewald summation, however, allows it to be replaced by a very extended charge density. Thus we can achieve, that the plane-wave convergence of the total energy is not affected by the auxiliary density.

The potential $\bar{v} = \sum_R \bar{v}_R$, which occurs in Eqs. 11.40 and 11.42 enters the total energy in the form of “intelligent zeros” described in Eq. 11.38

$$0 = \sum_n f_n (\langle \tilde{\psi}_n | \bar{v}_R | \tilde{\psi}_n \rangle - \langle \tilde{\psi}_n^1 | \bar{v}_R | \tilde{\psi}_n^1 \rangle) = \sum_n f_n \langle \tilde{\psi}_n | \bar{v}_R | \tilde{\psi}_n \rangle - \sum_{i,j \in R} D_{ij} \langle \tilde{\phi}_i | \bar{v}_R | \tilde{\phi}_j \rangle. \quad (11.44)$$

The main reason for introducing this potential is to cancel the Coulomb singularity of the potential in the plane-wave part. The potential \bar{v} allows us to influence the plane-wave convergence beneficially, without changing the converged result. \bar{v} must be localized within the augmentation region, where Eq. 11.25 holds.

Approximations

Once the total energy functional provided in the previous section has been defined, everything else follows: Forces are partial derivatives with respect to atomic positions. The potential is the derivative of the non-kinetic energy contributions to the total energy with respect to the density, and the auxiliary Hamiltonian follows from derivatives $\tilde{H}|\tilde{\psi}_n\rangle$ with respect to auxiliary wave functions. The fictitious Lagrangian approach of Car and Parrinello [114] does not allow any freedom in the way these derivatives are obtained. Anything else than analytic derivatives will violate energy conservation in a dynamical simulation. Since the expressions are straightforward, even though rather involved, we will not discuss them here.

All approximations are incorporated already in the total energy functional of the PAW method. What are those approximations?

- Firstly we use the frozen-core approximation. In principle this approximation can be overcome.
- The plane-wave expansion for the auxiliary wavefunctions must be complete. The plane-wave expansion is controlled easily by increasing the plane-wave cutoff defined as $E_{PW} = \frac{1}{2}\hbar^2 G_{max}^2$. Typically we use a plane-wave cutoff of 30 Ry.
- The partial wave expansions must be converged. Typically we use one or two partial waves per angular momentum (ℓ, m) and site. It should be noted that the partial wave expansion is not variational, because it changes the total energy functional and not the basis set for the auxiliary wavefunctions.

We do not discuss here numerical approximations such as the choice of the radial grid, since those are easily controlled.

Relation to pseudopotentials

We mentioned earlier that the pseudopotential approach can be derived as a well defined approximation from the PAW method: The augmentation part of the total energy $\Delta E = E^1 - \tilde{E}^1$ for one atom is a functional of the one-center density matrix \mathbf{D} defined in Eq. 11.35. The pseudopotential approach can be recovered if we truncate a Taylor expansion of ΔE about the atomic density matrix after the linear term. The term linear in \mathbf{D} is the energy related to the nonlocal pseudopotential.

$$\begin{aligned}\Delta E(\mathbf{D}) &= \Delta E(\mathbf{D}^{at}) + \sum_{i,j} \left. \frac{\partial \Delta E}{\partial D_{ij}} \right|_{\mathbf{D}^{at}} (D_{ij} - D_{ij}^{at}) + O(\mathbf{D} - \mathbf{D}^{at})^2 \\ &= E_{self} + \sum_n f_n \langle \tilde{\psi}_n | \hat{V}^{ps} | \tilde{\psi}_n \rangle - \int d^3r \bar{v}(\vec{r}) \tilde{n}(\vec{r}) + O(\mathbf{D} - \mathbf{D})^2,\end{aligned}\quad (11.45)$$

which can directly be compared with the total energy expression Eq. 11.16 of the pseudopotential method. The local potential $\bar{v}(\vec{r})$ of the pseudopotential approach is identical to the corresponding potential of the projector augmented-wave method. The remaining contributions in the PAW total energy, namely \tilde{E} , differ from the corresponding terms in Eq. 11.16 only in two features: our auxiliary density also contains an auxiliary core density, reflecting the nonlinear core correction of the pseudopotential approach, and the compensation density $\tilde{Z}(\vec{r})$ is non-spherical and depends on the wave function. Thus we can look at the PAW method also as a pseudopotential method with a pseudopotential that adapts instantaneously to the electronic environment. In the PAW method, the explicit nonlinear dependence of the total energy on the one-center density matrix is properly taken into account.

What are the main advantages of the PAW method compared with the pseudopotential approach?

Firstly all errors can be systematically controlled, so that there are no transferability errors. As shown by Watson [?] and Kresse [119], most pseudopotentials fail for high spin atoms such as Cr. While it is probably true that pseudopotentials can be constructed that cope even with this situation, a

failure can not be known beforehand, so that some empiricism remains in practice: A pseudopotential constructed from an isolated atom is not guaranteed to be accurate for a molecule. In contrast, the converged results of the PAW method do not depend on a reference system such as an isolated atom, because PAW uses the full density and potential.

Like other all-electron methods, the PAW method provides access to the full charge and spin density, which is relevant, for example, for hyperfine parameters. Hyperfine parameters are sensitive probes of the electron density near the nucleus. In many situations they are the only information available that allows us to deduce atomic structure and chemical environment of an atom from experiment.

The plane-wave convergence is more rapid than in norm-conserving pseudopotentials and should in principle be equivalent to that of ultra-soft pseudopotentials [?]. Compared to the ultra-soft pseudopotentials, however, the PAW method has the advantage that the total energy expression is less complex and can therefore be expected to be more efficient.

The construction of pseudopotentials requires us to determine a number of parameters. As they influence the results, their choice is critical. Also the PAW methods provides some flexibility in the choice of auxiliary partial waves. However, this choice does not influence the converged results.

Recent developments

Since the first implementation of the PAW method in the CP-PAW code [84], a number of groups have adopted the PAW method. The second implementation, called PWPAPW, was done by the group of Holzwarth[?, 120, 121, 122]. Several codes, previously using pseudopotentials have extended their code to PAW. Among them are the VASP code with the PAW implementation of Kresse and Joubert[119]. The PAW implementation of the ABINIT code[123] has been done by Torrent et al.[124]. An independent PAW code has been developed by Valiev and Weare [?]. This implementation has entered the NWChem code [125, 126]. The PAW method has also been implemented by W. Kromen [127] into the EStCoMPP code of Blügel and Schröder. Other implementations are in the Quantum Espresso code [128]² and Socorro³. A real-space-grid based version of the PAW method is the code GPAW developed by Mortensen et al. [129].

Another branch of methods uses the reconstruction of the PAW method, without taking into account the full wavefunctions in the energy minimization. Following chemists' notation, this approach could be termed "post-pseudopotential PAW". This development began with the evaluation for hyperfine parameters from a pseudopotential calculation using the PAW reconstruction operator [113] and is now used in the pseudopotential approach to calculate properties that require the correct wavefunctions such as hyperfine parameters.

The implementation of the PAW method by Kresse and Joubert [119] has been particularly useful as they had an implementation of PAW in the same code as the ultra-soft pseudopotentials, so that they could critically compare the two approaches. Their conclusion is that both methods compare well in most cases, but they found that magnetic energies are seriously – by a factor two – in error in the pseudopotential approach, while the results of the PAW method were in line with other all-electron calculations using the linear augmented plane-wave method. As an aside, Kresse and Joubert claim incorrectly that their implementation is superior as it includes a term that is analogous to the non-linear core correction of pseudopotentials [111]: this term, however, is already included in the original version in the form of the pseudized core density. Recently, a careful comparison[130] has shown that the original formulation[84] is more reliable.

Several extensions of the PAW have been done in the recent years: For applications in chemistry truly isolated systems are often of great interest. As any plane-wave based method introduces periodic images, the electrostatic interaction between these images can cause serious errors. The problem has been solved by mapping the charge density onto a point charge model, so that the electrostatic interaction could be subtracted out in a self-consistent manner [131]. In order to include the influence

²Quantum Espresso is maintained by Stefano Gironcoli and Lorenzo Paulatto

³<http://dft.sandia.gov/socorro>. Socorro is maintained by Alan Wright and Normand Modine

of the environment, the latter was simulated by simpler force fields using the quantum-mechanics molecular-mechanics (QM-MM) approach [132].

In order to overcome the limitations of the density functional theory several extensions have been performed. Bengone [133] implemented the LDA+U approach into our CP-PAW code. Soon after this, Arnaud [?] accomplished the implementation of the GW approximation into our CP-PAW code. The VASP-version of PAW [?] and our CP-PAW code have now been extended to include a non-collinear description of the magnetic moments. In a non-collinear description, the Schrödinger equation is replaced by the Pauli equation with two-component spinor wavefunctions.

The PAW method has proven useful to evaluate electric field gradients [134] and magnetic hyperfine parameters with high accuracy [6]. Invaluable will be the prediction of NMR chemical shifts using the GIPAW method of Pickard and Mauri [135], which is based on their earlier work [136]. While the GIPAW is implemented in a post-pseudopotential manner, the extension to a self-consistent PAW calculation should be straightforward. An post-pseudopotential approach has also been used to evaluate core level spectra [?] and momentum matrix elements [?].

Chapter 12

Born-Oppenheimer approximation and Classical Limit

The **Born-Oppenheimer approximation**[137, 138] simplifies the many-particle problem considerably by separating the electronic and nuclear coordinates. This method is similar, but not identical to the method of separation of variables.

We refer here to the formalism as described in appendix VIII of the Book of Born and Huang[138]. The method apparently goes back to an article by M. Born from 1951[?]

12.1 Separation of electronic and nuclear degrees of freedom

Our ultimate goal is to determine the wave function $\Phi(\vec{x}_1, \dots, \vec{x}_N, \vec{R}_1, \dots, \vec{R}_M, t)$, which describes the electronic degrees of freedom $\vec{x}_1, \dots, \vec{x}_N$ and the atomic positions $\vec{R}_1, \dots, \vec{R}_M$. from the time-dependent Schrödinger equation Eq. 6.1

$$i\hbar\partial_t|\Phi(t)\rangle \stackrel{\text{Eq. 6.1}}{=} \hat{H}|\Phi(t)\rangle \quad (12.1)$$

where the Hamiltonian is the one given in Eq. 6.4.

In the Born-Oppenheimer approximation, one first determines the electronic eigenstates for a fixed set of atomic positions. This solution forms the starting point for the description of the dynamics of the nuclei.

We will formulate an ansatz for the time-dependent many-particle wave functions. For this ansatz we need the **Born-Oppenheimer wave functions**, which are the electronic wave function for a frozen set of nuclear positions.

Born-Oppenheimer wave functions and Born-Oppenheimer surfaces

Firstly, we construct the Born-Oppenheimer Hamiltonian \hat{H}^{BO} by removing all terms that depend on the momenta of the nuclei from the many-particle Hamiltonian given in Eq. 6.4.

$$\begin{aligned} \hat{H}^{BO}(\vec{R}_1, \dots, \vec{R}_M) = & \underbrace{\sum_{i=1}^N \frac{-\hbar^2}{2m_e} \nabla_{\vec{r}_i}^2}_{E_{kin,e}} + \underbrace{\frac{1}{2} \sum_{i \neq j}^M \frac{e^2 Z_i Z_j}{4\pi\epsilon_0 |\vec{R}_i - \vec{R}_j|}}_{E_{C,nuc-nuc}} - \underbrace{\sum_{i=1}^N \sum_{j=1}^M \frac{e^2 Z_j}{4\pi\epsilon_0 |\vec{r}_i - \vec{R}_j|}}_{E_{C,e-nuc}} \\ & + \underbrace{\frac{1}{2} \sum_{i \neq j}^N \frac{e^2}{4\pi\epsilon_0 |\vec{r}_i - \vec{r}_j|}}_{E_{C,e-e}} \end{aligned} \quad (12.2)$$

The Born-Oppenheimer Hamiltonian acts in the Hilbert space of electronic wave functions, and depends parametrically on the nuclear positions. In other words, the Born-Oppenheimer Hamiltonian does not contain any gradients acting on the nuclear positions.

In order to simplify the equations, I combine all the electronic coordinates and spin indices into a vector $\vec{x} = (\vec{x}_1, \dots, \vec{x}_N)$ and the nuclear positions into a $3M$ dimensional vector $\vec{R} = (\vec{R}_1, \dots, \vec{R}_M)$. Thus, the many-particle wave function acting on electrons and nuclei will be written as $\Phi(\vec{x}, \vec{R}, t) = \langle \vec{x}, \vec{R} | \Phi(t) \rangle$.

In addition, I introduce another notation, where the wave function is a function of atomic position, but a state $|\Phi(\vec{R}, t)\rangle$ acting in the Hilbert space of electronic states. that is $\Phi(\vec{x}, \vec{R}, t) = \langle \vec{x} | \Phi(\vec{R}, t) \rangle$.

The full Hamiltonian of Eq. 6.4 is obtained by adding again the nuclear kinetic energy to the Born-Oppenheimer Hamiltonian

$$\hat{H} = \sum_{j=1}^M \frac{-\hbar^2}{2M_j} \nabla_{\vec{R}_j}^2 + \hat{H}^{BO} \quad (12.3)$$

In the second step, we determine the Born-Oppenheimer wave functions $|\Psi_n^{BO}(\vec{R})\rangle$ and the Born-Oppenheimer surfaces $E_n^{BO}(\vec{R})$ from

$$[\hat{H}^{BO}(\vec{R}) - E_n^{BO}(\vec{R})] |\Psi_n^{BO}(\vec{R})\rangle = 0 \quad (12.4)$$

Eq. 12.4 corresponds to a Schrödinger equation for the electrons feeling the static potential for frozen nuclear positions. The **Born-Oppenheimer surfaces** $E_n^{BO}(\vec{R})$ are simply the position-dependent energy eigenvalues of the Born-Oppenheimer Hamiltonian. For each atomic configuration we obtain a ground-state Born-Oppenheimer surface and infinitely many excited-state Born-Oppenheimer surfaces, which are labeled by the quantum number n . Similarly, the **Born-Oppenheimer wave functions** $\Psi_n^{BO}(\vec{x}_1, \dots, \vec{x}_N, \vec{R}_1, \dots, \vec{R}_M)$ depend parametrically on the nuclear positions \vec{R} .

The Born-Oppenheimer wave functions are orthogonal for each set of atomic positions, i.e.

$$\langle \Psi_m^{BO}(\vec{R}) | \Psi_n^{BO}(\vec{R}) \rangle = \int d^{4N}x \Psi_m^{BO*}(\vec{x}, \vec{R}) \Psi_n^{BO}(\vec{x}, \vec{R}) = \delta_{m,n} \quad (12.5)$$

Ansatz for the electronic-nuclear wave function

Now we are ready to write down the ansatz for the many-particle wave function of a system of electrons and nuclei: We express the many-particle wave function $\Phi(\vec{x}, \vec{R}, t)$ as a product of this Born-Oppenheimer wave function $\Psi_n^{BO}(\vec{x}, \vec{R})$ and a time-dependent nuclear wave function $\phi(\vec{R}, t)$, which is a time-dependent wave function $\phi_n(\vec{R}_1, \dots, \vec{R}_M, t)$ of the nuclear coordinates only.

BORN-HUANG EXPANSION

$$\Phi(\vec{x}, \vec{R}, t) = \sum_n \Psi_n^{BO}(\vec{x}, \vec{R}) \phi_n(\vec{R}, t) \quad (12.6)$$

The multi-valued nuclear wave function obeys the normalization condition

$$\sum_n \int d^{3M}R \phi_n^*(\vec{R}, t) \phi_n(\vec{R}, t) = 1 \quad (12.7)$$

It is important to realize that the Born-Huang expansion for the wave function is not an approximation. Every wave function can exactly be represented in this form.

Derivation of the Nuclear Schrödinger equation

When the Born-Huang expansion, Eq. 12.6, is inserted into the many-particle Schrödinger equation Eq. 6.1 with the full Hamiltonian Eq. 6.4, we obtain

$$\begin{aligned}
 & i\hbar\partial_t \left[\sum_n \Psi_n^{BO}(\vec{x}, \vec{R}) \phi_n(\vec{R}, t) \right] \stackrel{\text{Eq. 6.1}}{=} \hat{H} \left[\sum_n \Psi_n^{BO}(\vec{x}, \vec{R}) \phi_n(\vec{R}, t) \right] \\
 & \stackrel{\text{Eq. 12.3}}{=} \left[\sum_{i=1}^M \frac{-\hbar^2}{2M_i} \vec{\nabla}_{R_i}^2 + \hat{H}^{BO} \right] \left[\sum_n \Psi_n^{BO}(\vec{x}, \vec{R}) \phi_n(\vec{R}, t) \right] \\
 & \stackrel{\text{Eq. 12.4}}{=} \sum_n \Psi_n^{BO}(\vec{x}, \vec{R}) \left[\sum_{i=1}^M \frac{-\hbar^2}{2M_i} \vec{\nabla}_{R_i}^2 + E_n^{BO}(\vec{R}) \right] \phi_n(\vec{R}, t) \\
 & + \sum_n \left[\sum_{i=1}^M \frac{-\hbar^2}{M_i} \left(\vec{\nabla}_{R_i} \Psi_n^{BO}(\vec{x}, \vec{R}) \right) \vec{\nabla}_{R_i} + \sum_{i=1}^M \frac{-\hbar^2}{2M_i} \left(\vec{\nabla}_{R_i}^2 \Psi_n^{BO}(\vec{x}, \vec{R}) \right) \right] \phi_n(\vec{R}, t)
 \end{aligned} \tag{12.8}$$

Now we multiply Eq. 12.8 from the left by the complex conjugate Born-Oppenheimer wave function $\Psi_m^{BO*}(\vec{x}, \vec{R})$ and integrate over the electronic coordinates. Hereby, we exploit the orthonormality Eq. 12.5 of the Born-Oppenheimer wave functions.

As the result, we obtain an Schrödinger equation for the nuclear motion alone.

$$\begin{aligned}
 i\hbar\partial_t \phi_m(\vec{R}, t) & \stackrel{\text{Eqs. 12.8, 12.5}}{=} \left[\sum_{i=1}^M \frac{-\hbar^2}{2M_i} \vec{\nabla}_{R_i}^2 + E_m^{BO}(\vec{R}) \right] \phi_m(\vec{R}, t) \\
 & + \sum_n \left[\sum_{i=1}^M \frac{1}{M_i} \langle \Psi_m^{BO} | \frac{\hbar}{i} \vec{\nabla}_{R_i} | \Psi_n^{BO} \rangle \frac{\hbar}{i} \vec{\nabla}_{R_i} + \sum_{i=1}^M \frac{-\hbar^2}{2M_i} \langle \Psi_m^{BO} | \vec{\nabla}_{R_i}^2 | \Psi_n^{BO} \rangle \right] \phi_n(\vec{R}, t)
 \end{aligned} \tag{12.9}$$

Note, that the brackets $\langle \dots \rangle$ are evaluated by integrating over the electronic degrees of freedom only. Thus the matrix elements still depend explicitly on the nuclear coordinates. Note also, that the gradients $\vec{\nabla}_{R_i}$ in the parentheses act on the nuclear and not the electronic wave functions, which is easily overlooked.

Up to now, we did not introduce any approximations to arrive at the nuclear Schrödinger equation Eq. 12.9. We are still on solid ground.

Derivative couplings

In the following, we will discuss the individual terms of Eq. 12.9. Before we continue, however, let us simplify the notation again: The general structure of Eq. 12.9 is

$$i\hbar\partial_t \phi_m(\vec{R}, t) = \left[\sum_j \frac{\hat{P}_j^2}{2M_j} + E_m^{BO}(\vec{R}) \right] \phi_m(\vec{R}, t) + \sum_n \sum_{j=1}^M \frac{1}{M_j} \left[\vec{A}_{m,n,j}(\vec{R}) \hat{P}_j + B_{m,n}(\vec{R}) \right] \phi_n(\vec{R}, t) \tag{12.10}$$

where $\vec{P}_j = \frac{\hbar}{i} \vec{\nabla}_{R_j}$ is the momentum vector of the j -th particle and the first and second **derivative couplings** are defined by

$$\vec{A}_{m,n,j}(\vec{R}) := \langle \Psi_m^{BO}(\vec{R}) | \frac{\hbar}{i} \vec{\nabla}_{R_j} | \Psi_n^{BO}(\vec{R}) \rangle \tag{12.11}$$

$$B_{m,n,j}(\vec{R}) := \frac{1}{2} \langle \Psi_m^{BO}(\vec{R}) | \left(\frac{\hbar}{i} \vec{\nabla}_{R_j} \right)^2 | \Psi_n^{BO}(\vec{R}) \rangle \tag{12.12}$$

The first and the second derivative couplings are not independent from each other: The second derivative coupling B can be expressed by the first derivative couplings $\vec{A}_{m,n,j}(\vec{R})$. This is shown as follows (see in [139]):

$$\begin{aligned}
\frac{\hbar}{i} \vec{\nabla}_{R_j} \vec{A}_{m,n,j}(\vec{R}) &\stackrel{\text{Eq. 12.11}}{=} \frac{\hbar}{i} \vec{\nabla}_{R_j} \left\langle \Psi_m^{BO}(\vec{R}) \left| \frac{\hbar}{i} \vec{\nabla}_{R_j} \right| \Psi_n^{BO}(\vec{R}) \right\rangle \\
&= - \left\langle \frac{\hbar}{i} \vec{\nabla}_{R_j} \Psi_m^{BO}(\vec{R}) \left| \frac{\hbar}{i} \vec{\nabla}_{R_j} \right| \Psi_n^{BO}(\vec{R}) \right\rangle + \underbrace{\left\langle \Psi_m^{BO}(\vec{R}) \left| \left(\frac{\hbar}{i} \vec{\nabla}_{R_j} \right)^2 \right| \Psi_n^{BO}(\vec{R}) \right\rangle}_{2B_{m,n,j}(\vec{R})} \\
&= - \left\langle \frac{\hbar}{i} \vec{\nabla}_{R_j} \Psi_m^{BO}(\vec{R}) \left| \underbrace{\left(\sum_k \left| \Psi_k^{BO}(\vec{R}) \right\rangle \left\langle \Psi_k^{BO}(\vec{R}) \right| \right)}_{=\hat{1}} \right| \frac{\hbar}{i} \vec{\nabla}_{R_j} \Psi_n^{BO}(\vec{R}) \right\rangle + 2B_{m,n,j}(\vec{R}) \\
&= - \sum_k \left\langle \frac{\hbar}{i} \vec{\nabla}_{R_j} \Psi_m^{BO}(\vec{R}) \left| \Psi_k^{BO}(\vec{R}) \right\rangle \left\langle \Psi_k^{BO}(\vec{R}) \left| \frac{\hbar}{i} \vec{\nabla}_{R_j} \right| \Psi_n^{BO}(\vec{R}) \right\rangle + 2B_{m,n,j}(\vec{R}) \\
&= - \sum_k \left\langle \Psi_k^{BO}(\vec{R}) \left| \frac{\hbar}{i} \vec{\nabla}_{R_j} \right| \Psi_m^{BO}(\vec{R}) \right\rangle^* \left\langle \Psi_k^{BO}(\vec{R}) \left| \frac{\hbar}{i} \vec{\nabla}_{R_j} \right| \Psi_n^{BO}(\vec{R}) \right\rangle + 2B_{m,n,j}(\vec{R}) \\
&= - \sum_k \vec{A}_{k,m,j}^*(\vec{R}) \vec{A}_{k,n,j}(\vec{R}) + 2B_{m,n,j}(\vec{R})
\end{aligned}$$

Exploiting that is hermitean in the band indices, $\vec{A}_{m,n,j}(\vec{R}) = \vec{A}_{n,m,j}^*(\vec{R})$, which follows from the defining equation Eq. 12.11, we obtain

$$B_{m,n,j}(\vec{R}) = \frac{\hbar}{i} \vec{\nabla}_{R_j} \vec{A}_{m,n,j}(\vec{R}) + \sum_k \vec{A}_{m,k,j}(\vec{R}) \vec{A}_{k,n,j}(\vec{R}) \quad (12.13)$$

Thus, we only need the first derivative couplings, while the second derivative couplings can be obtained from the former via Eq. 12.13.

Final form for the nuclear Schrödinger equation

Here we will develop a relation (see in [139]), that will allow us to put the nuclear Schrödinger equation into a convenient form

$$\begin{aligned}
&\sum_k \left(\delta_{k,m} \frac{\hbar}{i} \vec{\nabla}_{R_j} + \vec{A}_{m,k,j}(\vec{R}) \right) \left(\delta_{k,n} \frac{\hbar}{i} \vec{\nabla}_{R_j} + \vec{A}_{k,n,j}(\vec{R}) \right) \\
&= \delta_{n,m} \left(\frac{\hbar}{i} \vec{\nabla}_{R_j} \right)^2 + \frac{\hbar}{i} \vec{\nabla}_{R_j} \vec{A}_{m,n,j}(\vec{R}) + \vec{A}_{m,n,j}(\vec{R}) \frac{\hbar}{i} \vec{\nabla}_{R_j} + \sum_k \vec{A}_{k,m,j}(\vec{R}) \vec{A}_{k,n,j}(\vec{R}) \\
&\stackrel{\text{Eq. 12.13}}{=} \left(\frac{\hbar}{i} \vec{\nabla}_{R_j} \right)^2 + \vec{A}_{m,n,j}(\vec{R}) \frac{\hbar}{i} \vec{\nabla}_{R_j} + B_{m,n,j}(\vec{R})
\end{aligned} \quad (12.14)$$

Comparison of this result, Eq. 12.14, with the nuclear Schrödinger equation Eq. 12.10, suggests another form of the nuclear Schrödinger equation, namely the one given below in Eq. 12.15.

SCHRÖDINGER EQUATION FOR THE NUCLEAR WAVE FUNCTIONS IN TERMS OF
BORN-OPPENHEIMER WAVE FUNCTIONS

$$i\hbar\partial_t\phi_m(\vec{R}, t) = \sum_n \left[\sum_{j=1}^M \frac{1}{2M_j} \sum_k \left(\delta_{m,k} \frac{\hbar}{i} \vec{\nabla}_{R_j} + \vec{A}_{m,k,j}(\vec{R}) \right) \left(\delta_{k,n} \frac{\hbar}{i} \vec{\nabla}_{R_j} + \vec{A}_{k,n,j}(\vec{R}) \right) + \delta_{m,n} E_m^{BO}(\vec{R}) \right] \phi_n(\vec{R}, t) \quad (12.15)$$

or, combining the components of the nuclear wave functions in a vector-matrix notation – denoting vectors by arrows and matrices by bold-face symbols –

$$i\hbar\partial_t\vec{\phi}(\vec{R}, t) = \left[\sum_{j=1}^M \frac{1}{2M_j} \left(\mathbf{1}\hat{P}_j + \vec{A}_j(\vec{R}) \right)^2 + \mathbf{E}^{BO}(\vec{R}) \right] \vec{\phi}(\vec{R}, t) \quad (12.16)$$

where \mathbf{E}^{BO} denotes the diagonal matrix with the Born-Oppenheimer energies as diagonal elements and $\hat{P}_j = \frac{\hbar}{i} \vec{\nabla}_{R_j}$ is the momentum operator of the j -th nucleus. The first-derivative couplings $\vec{A}_{m,k,j}(\vec{R})$ are defined in Eq. 12.11.

$$\vec{A}_{m,n,j}(\vec{R}) \stackrel{\text{Eq. 12.11}}{=} \langle \Psi_m^{BO}(\vec{R}) | \frac{\hbar}{i} \vec{\nabla}_{R_j} | \Psi_n^{BO}(\vec{R}) \rangle = \langle \Psi_m^{BO}(\vec{R}) | \hat{P}_j | \Psi_n^{BO}(\vec{R}) \rangle \quad (12.17)$$

The first-derivative couplings act similar to a vector potential in electrostatics.

We have not introduced any approximations to bring Eq. 12.16 into the new form given by Eq. 12.9. That is we are still on solid grounds.

12.2 Born-Oppenheimer approximation

The Born-Oppenheimer approximation amounts to ignoring the derivative couplings in Eq. 12.15

BORN-OPPENHEIMER APPROXIMATION FOR THE NUCLEAR WAVE FUNCTION

$$i\hbar\partial_t\phi_n(\vec{R}, t) = \left[\sum_{i=1}^M \frac{-\hbar^2}{2M_i} \vec{\nabla}_{R_i}^2 + E_n^{BO}(\vec{R}) \right] \phi_n(\vec{R}, t) \quad (12.18)$$

This equation describes nuclei that move on a given total energy surface $E_n^{BO}(\vec{R})$, which is called the **Born-Oppenheimer surface**. The Born-Oppenheimer surface may be an excited-state surface or the ground-state surface. The wave function may also have contributions simultaneously on different total energy surfaces. However, within the Born-Oppenheimer approximation, the contributions on different surfaces do not influence each other.

In other words, the system is with probability $P_n = \int d^3R \phi_n^*(\vec{R}) \phi_n(\vec{R})$ on the excited state surface $E_n(\vec{R})$.

The neglect of the non-adiabatic effects is the essence of the **Born-Oppenheimer approximation**. In the absence of the non-adiabatic effects, we could start the system in a particular eigenstate of the Born-Oppenheimer Hamiltonian, and the system would always evolve on the same total energy surface $E_n^{BO}(\vec{R})$. Thus, if we start the system in the electronic ground state, it will remain exactly in the instantaneous electronic ground state, while the nuclei are moving. Band crossings are the exceptions: Here the Born-Oppenheimer approximation does not give a unique answer.

The separation of nuclear and electronic degrees of freedom have already been in use before the original Born-Oppenheimer approximation[140]. Born and Oppenheimer [137] gave a justification for neglecting the non-adiabatic effects.

There is another approximation, the so-called **adiabatic approximation**, which goes beyond the Born-Oppenheimer approximation and includes all terms that do not connect different components of the nuclear wave function with each other. We will not discuss this approximation further.

12.3 Classical approximation

12.3.1 Classical approximation in the Born-Oppenheimer approximation

The most simple approach to the classical approximation is to take the Hamilton operator in the Born-Oppenheimer approximation from Eq. 12.18, constrain it to a particular total energy surface specified by n , and form the corresponding Hamilton function.

$$H_n(\vec{P}, \vec{R}) = \sum_j \frac{\vec{P}_j^2}{2M_j} + E_n^{BO}(\vec{R})$$

The Hamilton function defines the classical Hamilton equations of motion

$$\begin{aligned} \partial_t \vec{R}_j &= \vec{\nabla}_{\vec{P}_j} H_n(\vec{P}, \vec{R}, t) = \frac{1}{M_j} \vec{P}_j \\ \partial_t \vec{P}_j &= -\vec{\nabla}_{\vec{R}_j} H_n(\vec{P}, \vec{R}, t) = -\vec{\nabla}_{\vec{R}_j} E_n^{BO}(\vec{R}) \end{aligned}$$

This in turn leads to the Newton's equations of motion for the nuclei

$$M_j \partial_t^2 \vec{R}_j = -\vec{\nabla}_{\vec{R}_j} E_n^{BO}(\vec{R})$$

This is the approximation that is most widely used to study the dynamics of the atoms. A simulation of classical atoms using some kind of parameterized Born-Oppenheimer surface is called **molecular dynamics simulation**.

The Born-Oppenheimer surface $E_n^{BO}(\vec{R})$ acts just like a total energy surface for the motion of the nuclei. Once $E_n^{BO}(\vec{R})$ is known, the electrons are taken completely out of the picture. Within the Born-Oppenheimer approximation, no transitions between the ground-state and the excited-state surface take place. This implies not only that a system in the electronic ground state remains in the ground state. It also implies that a system in the excited state will remain there for ever. Transitions between different sheets $E_n^{BO}(\vec{R})$ of the Born-Oppenheimer energy are only possible when non-adiabatic effects are included.

12.4 Nonadiabatic correction

This section is under construction! proceed to the classical approximation...

12.4.1 Derivative couplings

In the appendix F.1 on p 191, we rewrite the off-diagonal elements of the first-derivative couplings in Eq. F.5 in the form

$$\vec{A}_{m,n,j} \stackrel{\text{Eq. F.5}}{=} \frac{\langle \Psi_m^{BO} | [\hat{P}_j, \hat{H}^{BO}(\vec{R})]_- | \Psi_n^{BO} \rangle}{E_n^{BO}(\vec{R}) - E_m^{BO}(\vec{R})} \quad \text{for } E_m^{BO} \neq E_n^{BO}$$

where $\hat{p}_j = \frac{\hbar}{i} \vec{\nabla}_{R_j}$ is the momentum operator for the j -th nucleus. $\hat{H}^{BO}(\vec{R})$ is a Hamiltonian acting on the electronic degrees of freedom.

This expression makes it evident that non-adiabatic effects are not negligible when two Born-Oppenheimer surfaces become degenerate.

12.4.2 Crossing of Born-Oppenheimer surfaces

The non-adiabatic effects become important when the different Born-Oppenheimer surfaces come close or even cross. Let us therefore inspect what happens at a crossing of two Born-Oppenheimer surfaces. We will see that the character of the wave function changes suddenly, as one passes through a crossing, but remains on the same Born-Oppenheimer surface. As a result, the non-adiabatic term suddenly increases, which induces transitions between the different sheets of the Born-Oppenheimer surface.

If the Born-Oppenheimer surfaces cross, this crossing can be changed into an **avoided crossing**.

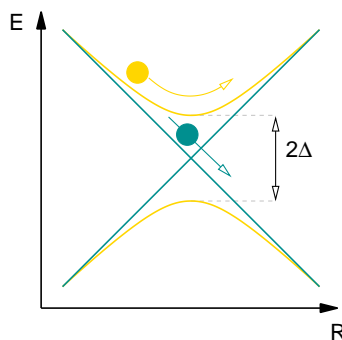
What is an avoided crossing? Let us start with a position-dependent Hamiltonian for a one-dimensional nuclear coordinate R , for which the energy levels cross for a certain position $R_0 = 0$. In addition we add non-diagonal terms Δ to the Hamiltonian in order to explore the role of the coupling terms.

$$H = \begin{pmatrix} E_0 + aR & \Delta \\ \Delta & E_0 - aR \end{pmatrix}$$

We obtain the eigenvalues as

$$E_{\pm} = E_0 \pm \sqrt{a^2 R^2 - \Delta^2}$$

The case $\Delta = 0$ describes the situation in the Born-Oppenheimer approximation. Here the two energy levels touch. A nonzero value of Δ describes the situation with adiabatic effects. Here the energy levels are split by 2Δ . Thus at the crossing, the off-diagonal term has a qualitative effect, while farther away from the crossing the effect of Δ is minor.



If a system starts on the excited state surface, such as a molecule in a photochemical reaction, it will be able to drop from the excited state surface only, if it can get rid of the energy 2Δ , by creating another excitation such as a vibration or a photon. The smaller the band gap at the avoided crossing, the more likely is it that the molecule falls into the ground state.

12.4.3 Landau-Zener Formula

not finished!!!

The transition between two adiabatic total energy surfaces has been analyzed by Landau and Zener¹ [142, ?, 141]. for a one-dimensional model. Here we follow the analysis of Wittig[141].

¹According to Wittig[141] the result of Landau[?] has an error of 2π

The model of Landau and Zener considers two crossing Born-Oppenheimer surfaces in only one dimension X .

$$\mathbf{H}^{BO}(X) = \begin{pmatrix} -F_1 X & 0 \\ 0 & -F_2 X \end{pmatrix}$$

The Born-Oppenheimer surfaces are assumed to depend linearly on the atomic coordinate X .

The non-adiabatic effects are approximated by non-diagonal elements of the Hamiltonian, that are considered independent of the atomix position. Thus the full Hamiltonian has the form

$$\mathbf{H}(X) = \begin{pmatrix} -F_1 X & H_{12} \\ H_{12}^* & -F_2 X \end{pmatrix}$$

The nuclear dynamics is considered classical, and with a constant velocity $\partial_t X(t) = V$, that is $X(t) = Vt$. This turns the position-dependent Hamiltonian into an effectively time-dependent Hamiltonian.

$$\mathbf{H}(t) = \begin{pmatrix} -F_1 Vt & H_{12} \\ H_{12}^* & -F_2 Vt \end{pmatrix}$$

The time dependent electronic Hamiltonian is described by the following Ansatz

$$\begin{pmatrix} \Phi_1 \\ \Phi_2 \end{pmatrix} = \begin{pmatrix} A(t)e^{-\frac{i}{\hbar} \int dt E_1^{BO}(X(t))} \\ B(t)e^{-\frac{i}{\hbar} \int dt E_2^{BO}(X(t))} \end{pmatrix} = \begin{pmatrix} A(t)e^{+\frac{i}{\hbar} \int dt F_1 Vt} \\ B(t)e^{+\frac{i}{\hbar} \int dt F_2 Vt} \end{pmatrix} = \begin{pmatrix} A(t)e^{+\frac{i}{\hbar} \frac{F_1 V}{2} t^2} \\ B(t)e^{+\frac{i}{\hbar} \frac{F_2 V}{2} t^2} \end{pmatrix}$$

The lower bound of the time integral has been ignored because they are a multiplicative factor, that can be absorbed in the initial conditions.

Insertion into the time dependent Schrödinger equation yield

$$\begin{aligned} i\hbar \partial_t \begin{pmatrix} A(t)e^{iF_1 Vt^2/(2\hbar)} \\ B(t)e^{iF_2 Vt^2/(2\hbar)} \end{pmatrix} &= \begin{pmatrix} -F_1 Vt & H_{12} \\ H_{12}^* & -F_2 Vt \end{pmatrix} \begin{pmatrix} A(t)e^{iF_1 Vt^2/(2\hbar)} \\ B(t)e^{iF_2 Vt^2/(2\hbar)} \end{pmatrix} \\ \begin{pmatrix} \partial_t A(t) \\ \partial_t B(t) \end{pmatrix} &= \begin{pmatrix} -\frac{i}{\hbar} H_{12} B(t)e^{i(F_2 - F_1)Vt^2/(2\hbar)} \\ -\frac{i}{\hbar} H_{12}^* A(t)e^{-i(F_2 - F_1)Vt^2/(2\hbar)} \end{pmatrix} \end{aligned}$$

thus

$$\begin{aligned} \partial_t A(t) &= -\frac{i}{\hbar} H_{12} B(t)e^{i(F_2 - F_1)Vt^2/(2\hbar)} \\ \partial_t B(t) &= -\frac{i}{\hbar} H_{12}^* A(t)e^{-i(F_2 - F_1)Vt^2/(2\hbar)} \quad \Rightarrow \quad A(t) = -\frac{\hbar}{i} \underbrace{\frac{H_{12}}{|H_{12}|^2}}_{1/H_{12}^*} e^{i(F_2 - F_1)Vt^2/(2\hbar)} \partial_t B(t) \end{aligned}$$

Insertion of the second equation into the first yields a differential equation for $B(t)$.

$$\begin{aligned} \partial_t \left(\underbrace{-\frac{\hbar}{i} \frac{H_{12}}{|H_{12}|^2} e^{i(F_2 - F_1)Vt^2/(2\hbar)} \partial_t B(t)}_{A(t)} \right) &= -\frac{i}{\hbar} H_{12} B(t)e^{i(F_2 - F_1)Vt^2/(2\hbar)} \\ -\frac{H_{12}}{|H_{12}|^2} (F_2 - F_1)Vt e^{i(F_2 - F_1)Vt^2/(2\hbar)} \partial_t B(t) &+ \left(-\frac{\hbar}{i} \frac{H_{12}}{|H_{12}|^2} e^{i(F_2 - F_1)Vt^2/(2\hbar)} \partial_t^2 B(t) \right) = -\frac{i}{\hbar} H_{12} B(t)e^{i\frac{(F_2 - F_1)V}{2\hbar} t^2} \\ -\frac{1}{|H_{12}|^2} (F_2 - F_1)Vt \partial_t B(t) &+ \left(-\frac{\hbar}{i} \frac{1}{|H_{12}|^2} \partial_t^2 B(t) \right) = -\frac{i}{\hbar} B(t) \\ \frac{i}{\hbar} (F_2 - F_1)Vt \partial_t B(t) &+ \partial_t^2 B(t) = -\frac{1}{\hbar^2} |H_{12}|^2 B(t) \\ \partial_t^2 B(t) + \frac{i}{\hbar} (F_2 - F_1)Vt \partial_t B(t) &+ \frac{1}{\hbar^2} |H_{12}|^2 B(t) = 0 \end{aligned}$$

Thus we have a differential equation for the probability amplitude on the second sheet. We now look for a solution of this differential equation, respectively its value $B(t = +\infty)$ with the initial condition $B(-\infty) = \partial_t B(-\infty) = 0$.

This is a differential equation of the form

$$\ddot{x} + i\alpha t \dot{x} + \beta x = 0$$

So far, the derivation is standard. Wittig showed a solution to the problem using contour integrals.

$$\begin{aligned} \frac{1}{t} \frac{\ddot{x}}{x} + i\alpha \frac{\dot{x}}{x} + \frac{\beta}{t} &= 0 \\ i\alpha \int_{B_i}^{B_f} dB \frac{1}{B} &= -\beta \int_{t_i}^{t_f} dt \frac{1}{t} - \int_{t_i}^{t_f} dt \frac{1}{t} \frac{\ddot{x}}{x} \\ i\alpha \ln\left[\frac{B_f}{B_i}\right] &= -\beta \int_{-\infty}^{\infty} dt \frac{1}{t} - \int_{-\infty}^{\infty} dt \frac{1}{t} \frac{\ddot{x}}{x} \end{aligned}$$

The integral of the first term on the right hand side yields

$$\int_{-\infty}^{\infty} dt \frac{1}{t} = \pm i\pi$$

depending on whether the integration is performed in the upper or lower half plane.

Thus we obtain

$$\begin{aligned} \ln[x_f] &= \ln[x_i] \mp \pi \frac{\beta}{\alpha} + \frac{i}{\alpha} \int_{-\infty}^{\infty} dt \frac{1}{t} \frac{\ddot{x}}{x} \\ x_f &= x_i e^{\pi\beta/\alpha} \exp\left(\frac{i}{\alpha} \int_{-\infty}^{\infty} dt \frac{1}{t} \frac{\ddot{x}}{x}\right) \end{aligned}$$

The rest of the derivation should go on here...

LANDAU ZENER ESTIMATE FOR THE TRANSITION PROBABILITY AT A BAND CROSSING

The transition probability is (Eq. 16 of Wittig)

$$P = \exp\left(2\pi \underbrace{\frac{|H_{12}|}{\hbar}}_{\text{Rabi frequency}} \underbrace{\frac{|H_{12}|}{V|F_1 - F_2|}}_{\tau}\right)$$

τ is of order of the time it takes to cross the region where the Born-Oppenheimer surfaces are closer than the avoided crossing surface.

=====

The result of their analysis is the **Landau-Zener formula**, which gives the probability for a transition for a one-dimensional model

$$P = e^{-2\pi\omega_{12}\tau} \quad \text{with } \omega_{12} = \frac{H_{12}}{\hbar} \text{ and } \tau = \frac{|H_{12}|}{v|F_1 - F_2|} \quad (12.19)$$

where v is the velocity and H_{12} is the coupling between the two crossing total energy surfaces. ω_{12} is the **Rabi frequency** at the crossing point and τ is a measure for the duration of the interaction between the surfaces. The model hamiltonian underlying the Landau Zener formula has the form

12.4.4 Phase relations

For a good introduction on the subject of conical intersections and the geometric phase see the article of Child[143].

When we determine the adiabatic or Born-Oppenheimer states, we only have to fulfill an eigenvalue equation. An eigenvalue equation determines the states only up to a unitary transformation. One such unitary transformation is the multiplication of a phase factor $e^{i\phi}$ to any of the states. Another is the interchange of two states. This unitary transformation can be chosen independently for each atomic configuration \vec{R} .

Such a unitary transformation by a position dependent unitary matrix $U(\vec{R})$,

$$\begin{aligned}\Phi'_j(\vec{x}, \vec{R}) &= \sum_m \Phi_m(\vec{x}, \vec{R}) U_{m,j}(\vec{R}) \\ \phi'_j(\vec{R}, t) &= \sum_n \phi_n(\vec{R}, t) U_{n,j}(\vec{R}),\end{aligned}$$

leaves the final wave function intact, if we similarly transform the nuclear wave function. This is shown as follows:

$$\begin{aligned}\Phi(\vec{x}, \vec{R}, t) &= \sum_n \Psi_n(\vec{x}, \vec{R}) \phi_n(\vec{R}, t) = \sum_{m,n} \Psi_m(\vec{x}, \vec{R}) \underbrace{\left(\sum_j U_{m,j} U_{j,n}^\dagger \right)}_{\delta_{m,n}} \phi_n(\vec{R}, t) \\ &= \sum_j \left(\sum_m \Psi_m(\vec{x}, \vec{R}) U_{m,j} \right) \left(\sum_n \phi_n(\vec{R}, t) U_{n,j} \right) = \sum_j \Psi'_j(\vec{x}, \vec{R}) \phi'_j(\vec{R}, t)\end{aligned}$$

While the nuclear wave function $\phi_n(\vec{R}, t)$ is completely changed by the transformation, it still obeys the same differential equation in the adiabatic or the Born-Oppenheimer approximation.

This apparent paradox is resolved by taking the non-adiabatic effects into account. The term $\vec{B}_{m,n,j}$ depends strongly on this position dependent unitary matrix. Taking this into account the differential equation changes, so that the entire description becomes invariant with respect to the unitary approximation.

This provides us with an additional requirement for the Born-Oppenheimer approximation. We need to fix the unitary transformation for the Born-Oppenheimer states such that the term $\vec{A}_{m,n,j}$ is as small as possible. Thus we should choose the Born-Oppenheimer states such that they change as little as possible from one atomic configuration to the next. However, also this choice is not unique.

It can be shown that in certain situations, it is not even possible to select a set of Born-Oppenheimer wave functions, that is continuous in configuration space. This leads to the so-called **geometrical phase** or called **Berry phase**. [144] (For the role of the Berry phase in chemical reactions see D.C. Clary, Science 309, 1195 (2005))

Here, a few reviews related to non-adiabatic effects [145]. Interesting is also the PhD thesis of Florian Dufey [140]. I have not read them carefully yet. A good introduction is the special volume of the Journal "Advances in Chemical Physics" from 2002 [146].

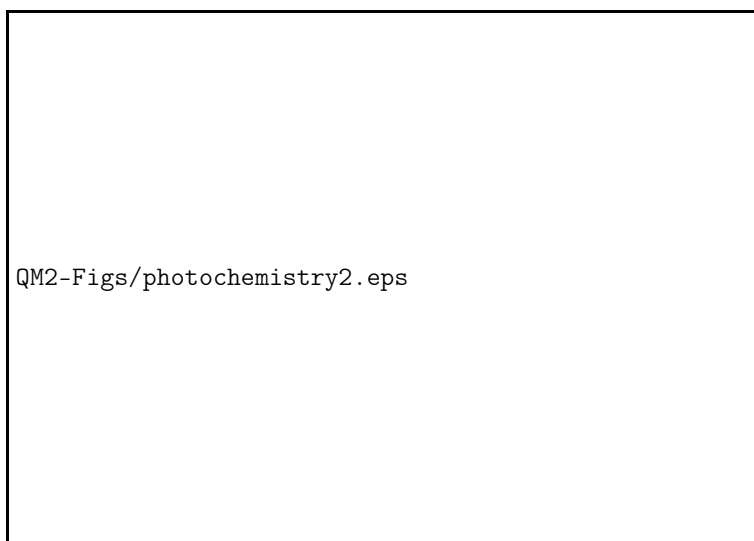


Fig. 12.1: Schematics of a photochemical reaction. An optical excitation raises the system from the ground-state total energy sheet to the excited state total energy surface. At a conical intersection the system can change to the lower sheet. At this point, non-adiabatic effects are important. (From a lecture “Molecular dynamics” by John Tully, Park City 2005)

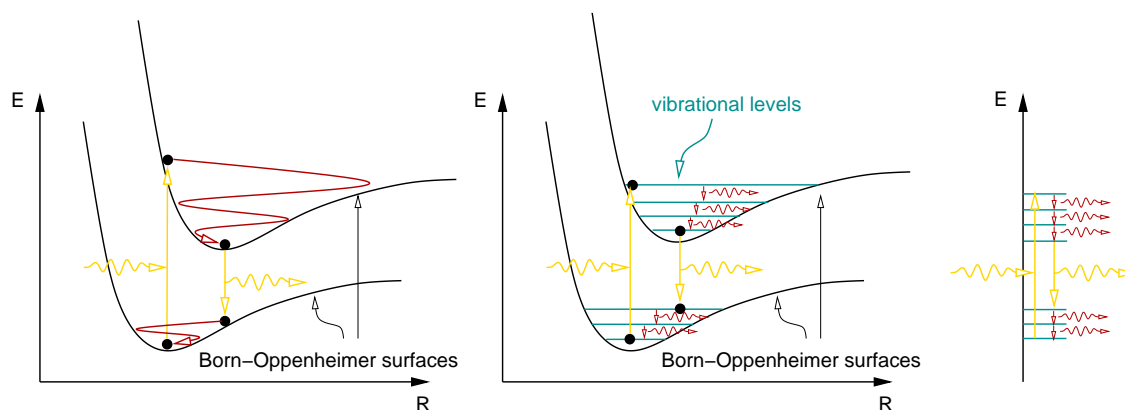


Fig. 12.2: Schematic for the optical absorption and desorption of a photon. Let R be one spatial coordinate for the nuclei, such as a bond distance. A photon excites an electron from the ground state sheet of the total energy surface to an excited state sheet. The atoms vibrate around the equilibrium structure of the excited energy surface. During that process the system dissipates energy. In other words, it thermalizes by emitting phonons. At some point the electron drops again on the ground state energy surface, while emitting a photon. The emitted photon has a lower energy than the absorbed photon, because some of the energy has been lost by creating for example phonons, i.e. heat. The system vibrates again about the equilibrium structure until it has dissipated its energy. Note that the transition proceeds between different energy levels of the total energy, which also include the vibrational levels. Thus vibrations or phonons are excited as well. Thus to determine the absorption probability not only the optical transition matrix elements of the electronic subsystem must be considered, but also the overlap of the nuclear part of the wave function. Note that the figure describes the case at zero temperature. At finite temperature, the system can be initially already in a excited vibrational level. The left figure is appropriate for a classical description of the nuclear motion, while the right figure is an abstract energy level diagram appropriate for a quantum description.

Part II

Appendices

Appendix A

Notation for spin indices

We use a notation that combines the continuous spatial indices \vec{r} with the discrete spin indices into a four dimensional vector \vec{x} . This shortcut notation has a more rigorous basis[147], which we will show here.

We introduce an artificial spin coordinate q . This is not a spatial coordinate, but it is a coordinate in some other abstract one-dimensional space. On this space, we assume that there is a complete¹ and orthonormal basis with only two functions, namely $\alpha(q)$ and $\beta(q)$. They obey

$$\begin{aligned}\int dq \alpha^*(q)\alpha(q) &= 1 \\ \int dq \beta^*(q)\beta(q) &= 1 \\ \int dq \alpha^*(q)\beta(q) &= 0\end{aligned}$$

A wave function may now depend on a spatial coordinate and this fictitious spin variable q . They form together a four dimensional vector

$$\vec{x} \stackrel{\text{def}}{=} (\vec{r}, q)$$

An electronic wave function depends on all these variables:

$$\langle \vec{x} | \psi \rangle = \langle \vec{r}, q | \psi \rangle = \psi(\vec{r}, q)$$

We can now decompose this vector into its components

$$\begin{aligned}\psi(\vec{r}, \uparrow) &\stackrel{\text{def}}{=} \int dq \alpha^*(q) \psi(\vec{r}, q) \\ \psi(\vec{r}, \downarrow) &\stackrel{\text{def}}{=} \int dq \beta^*(q) \psi(\vec{r}, q)\end{aligned}$$

¹This is where the argument is weak: a complete set of functions on a finite interval is always infinite. Probably one needs Grassman variables

Appendix B

Time-inversion symmetry

Time inversion symmetry says that it is not possible from a conservative classical trajectory to find out if time is running forward or backward in time. If take a physical trajectory and let the time run backwards, it still fulfills the equations of motion.

Electrodynamics and gravitation obey time inversion symmetry exactly. Time inversion alone is however not a fundamental symmetry of nature. The weak interaction, which is for example responsible for the β decay of nuclei, violates it. Time inversion must be replaced by the weaker CPT-inversion symmetry. This is the so-called **CPT-theorem** posed by Wolfgang Pauli. The CPT theorem says that the fundamental laws of nature must obey a symmetry under simultaneous application of three operations:

- charge inversion (C)
- space inversion (P for Parity)
- time inversion (T)

The CPT theorem is based on the assumptions of Lorentz invariance, causality, locality and the existence of a Hamilton operator that is bounded by below. Electrodynamics and gravitation are symmetric under the three symmetry operations individually.

As we are not concerned with weak interactions we can assume exact time inversion symmetry.

B.1 Schrödinger equation

Let us now investigate what time inversion symmetry implies in quantum mechanics:

Let us consider the Schrödinger equation in a magnetic field

$$i\hbar\partial_t\Psi(\vec{r}, t) = \left[\frac{(\frac{\hbar}{i}\vec{\nabla} - q\vec{A})^2}{2m} + q\Phi \right] \Psi(\vec{r}, t) \quad (\text{B.1})$$

Let us take the complex conjugate of the Eq. B.1

$$-i\hbar\partial_t\Psi^*(\vec{r}, t) = \left[\frac{(-\frac{\hbar}{i}\vec{\nabla} - q\vec{A})^2}{2m} + q\Phi \right] \Psi^*(\vec{r}, t) = \left[\frac{(\frac{\hbar}{i}\vec{\nabla} + q\vec{A})^2}{2m} + q\Phi \right] \Psi^*(\vec{r}, t) \quad (\text{B.2})$$

Next we look for the equation obeyed by $\psi(\vec{r}, -t)$, if Eq. B.2 holds

$$i\hbar\partial_t\Psi^*(\vec{r}, -t) = \left[\frac{(\frac{\hbar}{i}\vec{\nabla} + q\vec{A}(\vec{r}, -t))^2}{2m} + q\Phi(\vec{r}, -t) \right] \Psi^*(\vec{r}, -t) \quad (\text{B.3})$$

One can see immediately that Eq. B.3 is identical to Eq. B.1 if we revert the sign of the vector potential \vec{A} , when we invert the time. Thus the Schrödinger equation is symmetric under the time inversion symmetry as stated below:

TIME-INVERSION
$\begin{aligned}\vec{A}(\vec{r}, t) &\rightarrow -\vec{A}(\vec{r}, -t) \\ \Phi(\vec{r}, t) &\rightarrow \Phi(\vec{r}, -t) \\ \Psi(\vec{r}, t) &\rightarrow \Psi^*(\vec{r}, -t)\end{aligned}$

For the time-independent Schrödinger equation we obtain

$$\Psi(\vec{r}, t) = \Psi_\epsilon(\vec{r})e^{-\frac{i}{\hbar}\epsilon t}$$

so that

$$\Psi^*(\vec{r}, -t) = \Psi_\epsilon^*(\vec{r})e^{-\frac{i}{\hbar}\epsilon t}$$

Thus, the time inversion symmetry applied to energy eigenstates has the effect that the wave function is turned into its complex conjugate.

Let us look at the problem from stationary Schrödinger equation.

$$\left[\frac{(\frac{\hbar}{i}\vec{\nabla} - q\vec{A})^2}{2m} + q\Phi - \epsilon \right] \Psi_\epsilon(\vec{r}) = 0$$

We take the complex conjugate of this equation

$$\left[\frac{(\frac{\hbar}{i}\vec{\nabla} + q\vec{A})^2}{2m} + q\Phi - \epsilon \right] \Psi_\epsilon^*(\vec{r}) = 0$$

Thus, we see that the complex conjugate of the wave function solves the same Schrödinger equation with the magnetic field reversed. If there is no magnetic field, the complex conjugate is also a solution of the original wave function. Thus, we can superimpose the two solutions to obtain two real solutions, namely the real part and the imaginary part. Thus, in the absence of a magnetic field the wave functions can be assumed to be purely real.

B.2 Pauli equation

The proper theory of electrons is the **Dirac equation**, which describes electrons by a four component spinor, that describes spin up and spin-down electrons as well as their antiparticles, the positrons. In the non-relativistic limit electrons and positrons become independent. Now electrons and positrons obey the so-called Pauli equation.

The **Pauli equation** has the form

$$i\hbar\partial_t|\psi(t)\rangle = \left[\frac{(\vec{p} - q\vec{A})^2}{2m_0} + q\Phi - \frac{q}{m_0}\hat{\vec{S}}\vec{B} \right] |\psi\rangle \quad (\text{B.4})$$

The wave function is now a two-component spinor with a spin-up and a spin-down component. The spin-operator is represented by the Pauli matrices

$$\vec{S} \stackrel{\text{Eq. 7.1}}{=} \frac{\hbar}{2} (\hat{\sigma}_x, \hat{\sigma}_y, \hat{\sigma}_z)$$

The Pauli matrices are given in Eq. 7.2 on 90. The magnetic field is related to the vector potential via $\vec{B} = \vec{\nabla} \times \vec{A}$.

Expressed with explicit spinor components, the Pauli equation has the form

$$i\hbar\partial_t\psi(\vec{r}, \sigma, t) = \sum_{\sigma'} \left[\underbrace{\left(\frac{(\frac{\hbar}{i}\vec{\nabla} - q\vec{A})^2}{2m_0} + q\Phi \right)}_{\hat{H}_0} \delta_{\sigma,\sigma'} - \frac{q}{m_0} \vec{B} \vec{S}_{\sigma,\sigma'} \right] \psi(\vec{r}, \sigma', t) \quad (\text{B.5})$$

We proceed as we did for the Schrödinger equation by taking the complex conjugate of the Pauli equation Eq. B.5

$$-i\hbar\partial_t\psi^*(\vec{r}, \sigma, t) = \sum_{\sigma'} \left[\left(\frac{(-\frac{\hbar}{i}\vec{\nabla} - q\vec{A})^2}{2m_0} + q\Phi \right) \delta_{\sigma,\sigma'} - \frac{q}{m_0} \vec{B} \vec{S}_{\sigma,\sigma'}^* \right] \psi^*(\vec{r}, \sigma', t) \quad (\text{B.6})$$

Now we revert the time argument in Eq. B.6 and perform the transformation of the potentials $\vec{A}'(\vec{r}, t) = -\vec{A}(\vec{r}, -t)$ and $\Phi'(\vec{r}, t) = \Phi(\vec{r}, -t)$:

$$i\hbar\partial_t\psi^*(\vec{r}, \sigma, -t) = \sum_{\sigma'} \left[\underbrace{\left(\frac{(\frac{\hbar}{i}\vec{\nabla} - q\vec{A}'(\vec{r}, t))^2}{2m_0} + q\Phi'(\vec{r}, t) \right)}_{\hat{H}_0'} \delta_{\sigma,\sigma'} + \frac{q}{m_0} \vec{B}'(\vec{r}, t) \vec{S}_{\sigma,\sigma'}^* \right] \psi^*(\vec{r}, \sigma', -t) \quad (\text{B.7})$$

We observe that it is no more sufficient to replace the wave function by its complex conjugate of the time-reverted function as in the Schrödinger equation.

In order to find the transformation of the wave functions let us rewrite the equation in components. The original equation Eq. B.5 written in components looks like

$$\begin{pmatrix} (i\hbar\partial_t - \hat{H}_0)\psi(\vec{r}, \uparrow, t) \\ (i\hbar\partial_t - \hat{H}_0)\psi(\vec{r}, \downarrow, t) \end{pmatrix} \stackrel{\text{Eq. B.5}}{=} -\frac{\hbar q}{2m_0} \begin{pmatrix} B_z & B_x - iB_y \\ B_x + iB_y & -B_z \end{pmatrix} \begin{pmatrix} \psi(\vec{r}, \uparrow, t) \\ \psi(\vec{r}, \downarrow, t) \end{pmatrix} \quad (\text{B.8})$$

which is the original Pauli equation Eq. B.5, with the symbols replaced by the primed, that is the transformed, variables.

So far we arrived at Eq. B.7, which in component notation, looks like

$$\begin{pmatrix} (i\hbar\partial_t - \hat{H}_0')\psi^*(\vec{r}, \uparrow, -t) \\ (i\hbar\partial_t - \hat{H}_0')\psi^*(\vec{r}, \downarrow, -t) \end{pmatrix} \stackrel{\text{Eq. B.7}}{=} \underbrace{-\frac{\hbar q}{2m_0} \begin{pmatrix} -B'_z & -B'_x - iB'_y \\ -B'_x + iB'_y & B'_z \end{pmatrix}}_{+\frac{q}{m_0} \vec{B} \vec{S}^*} \begin{pmatrix} \psi^*(\vec{r}, \uparrow, -t) \\ \psi^*(\vec{r}, \downarrow, -t) \end{pmatrix} \quad (\text{B.9})$$

In order to get an idea on how to proceed let us consider the special case $B'_x = B'_y = 0$. In this case the diagonal elements of the equation could be brought into the form of Eq. B.8 by interchanging the spin indices of the wave functions. Interchanging the spin indices of Eq. B.9 yields

$$\begin{pmatrix} (i\hbar\partial_t - \hat{H}_0')\psi^*(\vec{r}, \downarrow, -t) \\ (i\hbar\partial_t - \hat{H}_0')\psi^*(\vec{r}, \uparrow, -t) \end{pmatrix} = -\frac{\hbar q}{2m_0} \begin{pmatrix} B'_z & -B'_x + iB'_y \\ -B'_x - iB'_y & -B'_z \end{pmatrix} \begin{pmatrix} \psi^*(\vec{r}, \downarrow, -t) \\ \psi^*(\vec{r}, \uparrow, -t) \end{pmatrix}$$

However, the off-diagonal elements of the equation would still differ by the sign. This problem can be remedied by flipping the sign of one of the wave function components.

$$\begin{pmatrix} (i\hbar\partial_t - \hat{H}_0')[-\psi^*(\vec{r}, \downarrow, -t)] \\ (i\hbar\partial_t - \hat{H}_0')\psi^*(\vec{r}, \uparrow, -t) \end{pmatrix} = -\frac{\hbar q}{2m_0} \begin{pmatrix} B'_z & B'_x - iB'_y \\ B'_x + iB'_y & -B'_z \end{pmatrix} \begin{pmatrix} [-\psi^*(\vec{r}, \downarrow, -t)] \\ \psi^*(\vec{r}, \uparrow, -t) \end{pmatrix}$$

which leads to the desired form Eq. B.8.

The time inversion for two-component spinors and electromagnetic fields is therefore

TIME-INVERSION FOR TWO-COMPONENT SPINORS

$$\psi'(\vec{r}, \uparrow, t) = -\psi^*(\vec{r}, \downarrow, -t)$$

$$\psi'(\vec{r}, \downarrow, t) = +\psi^*(\vec{r}, \uparrow, -t)$$

$$\vec{A}'(\vec{r}, t) = -\vec{A}(\vec{r}, -t)$$

$$\Phi'(\vec{r}, t) = \Phi(\vec{r}, -t)$$

If we investigate the resulting transformation of the spin expectation values, we see that the spin is inverted. This is expected under time inversion symmetry, if we interpret the spin as a angular momentum. If we invert the time, the particle is spinning in the opposite direction.

Appendix C

Slater determinants for parallel and antiparallel spins

Why can spin-up and spin-down electrons be treated as non-identical particles, even though they are only spinor-components of identical particles.

Here we try to give an answer by showing that a one-particle orbital can be occupied independently of each other with one spin-up and one spin-down electron. That is for each placement of the two electrons into one-particle orbitals there is a Slater determinant. For two spin-up electrons or for two spin-down electrons, the same one-particle orbital can only be occupied once.

This implies that the statistics of spin up and spin-down electrons is such that spin up electrons are treated as a class of identical particles and spin-down electrons are treated as a different class of independent particles.

Let us consider two spatial one-particle orbitals $\chi_a(\vec{r})$ and $\chi_b(\vec{r})$. The two orbitals shall be orthonormal. Out of these two orbitals, we construct four spin orbitals, namely

$$\begin{aligned}\phi_{a\uparrow}(\vec{r}, \sigma) &= \chi_a(\vec{r})\delta_{\sigma,\uparrow} \\ \phi_{a\downarrow}(\vec{r}, \sigma) &= \chi_a(\vec{r})\delta_{\sigma,\downarrow} \\ \phi_{b\uparrow}(\vec{r}, \sigma) &= \chi_b(\vec{r})\delta_{\sigma,\uparrow} \\ \phi_{b\downarrow}(\vec{r}, \sigma) &= \chi_b(\vec{r})\delta_{\sigma,\downarrow}\end{aligned}$$

or using $\alpha \in \{a, b\}$ and $s \in \{\uparrow, \downarrow\}$.

$$\phi_{\alpha,s}(\vec{r}, \sigma) = \chi_\alpha(\vec{r})\delta_{s,\sigma}$$

Out of these one-particle spin orbitals, we construct the Slater determinants

$$\begin{aligned}\Phi_{\alpha,\beta,s,s'}(\vec{r}, \sigma, \vec{r}', \sigma') &= \frac{1}{\sqrt{2}} \left(\phi_{\alpha,s}(\vec{r}, \sigma) \phi_{\beta,s'}(\vec{r}', \sigma') - \phi_{\beta,s'}(\vec{r}, \sigma) \phi_{\alpha,s}(\vec{r}', \sigma') \right) \\ &= \frac{1}{\sqrt{2}} \left(\chi_\alpha(\vec{r}) \chi_\beta(\vec{r}') \delta_{s,\sigma} \delta_{s',\sigma'} - \chi_\beta(\vec{r}) \chi_\alpha(\vec{r}') \delta_{s,\sigma'} \delta_{s',\sigma} \right)\end{aligned}$$

Some of these Slater determinants are zero states, but that does not matter at the moment.

These Slater determinants are products of a spatial two-particle wave function and a two-particle wave function in the spin space. It will be convenient to introduce such two particle states that are

symmetric and antisymmetric under particle exchange. (Exchange of the arguments.) These are

$$\begin{aligned}\Psi_{\alpha,\beta}^+(\vec{r}, \vec{r}') &\stackrel{\text{def}}{=} \frac{1}{\sqrt{2}} \left(\chi_{\alpha}(\vec{r})\chi_{\beta}(\vec{r}') + \chi_{\beta}(\vec{r})\chi_{\alpha}(\vec{r}') \right) \\ \Psi_{\alpha,\beta}^-(\vec{r}, \vec{r}') &\stackrel{\text{def}}{=} \frac{1}{\sqrt{2}} \left(\chi_{\alpha}(\vec{r})\chi_{\beta}(\vec{r}') - \chi_{\beta}(\vec{r})\chi_{\alpha}(\vec{r}') \right) \\ G_{s,s'}^+(\sigma, \sigma') &\stackrel{\text{def}}{=} \frac{1}{\sqrt{2}} \left(\delta_{s,\sigma}\delta_{s',\sigma'} + \delta_{s',\sigma}\delta_{s,\sigma'} \right) \\ G_{s,s'}^-(\sigma, \sigma') &\stackrel{\text{def}}{=} \frac{1}{\sqrt{2}} \left(\delta_{s,\sigma}\delta_{s',\sigma'} - \delta_{s',\sigma}\delta_{s,\sigma'} \right)\end{aligned}$$

The Slater determinants have the form

$$\begin{aligned}\Phi_{\alpha,\beta,s,s'}(\vec{r}, \sigma, \vec{r}', \sigma') &= \frac{1}{\sqrt{2}} \left[\frac{1}{2} \left(\Psi_{\alpha,\beta}^+ + \Psi_{\alpha,\beta}^- \right) \left(G_{s,s'}^+ + G_{s,s'}^- \right) - \frac{1}{2} \left(\Psi_{\alpha,\beta}^+ - \Psi_{\alpha,\beta}^- \right) \left(G_{s,s'}^+ - G_{s,s'}^- \right) \right] \\ &= \frac{1}{\sqrt{2}} \left[\Psi_{\alpha,\beta}^+(\vec{r}, \vec{r}') G_{s,s'}^-(\sigma, \sigma') + \Psi_{\alpha,\beta}^-(\vec{r}, \vec{r}') G_{s,s'}^+(\sigma, \sigma') \right] \quad (\text{C.1})\end{aligned}$$

Now we can analyze the result using

$$\begin{aligned}G_{s,s'}^-(\sigma, \sigma') &\equiv 0 & \text{for } s = s' \\ \Psi_{\alpha,\beta}^-(\vec{r}, \vec{r}') &\equiv 0 & \text{for } \alpha = \beta\end{aligned}$$

Let us now consider two spin up electrons. Because of Eq. C.1 and $G_{\uparrow,\uparrow}^- = 0$, there is only a single non-zero Slater determinant, namely

$$|\Phi_{a,b,\uparrow,\uparrow}\rangle = \Psi_{a,b}^- \left(\frac{1}{\sqrt{2}} G_{s,s'}^+ \right)$$

The Slater-determinant $|\Phi_{b,a,\uparrow,\uparrow}\rangle$ differs from $|\Phi_{a,b,\uparrow,\uparrow}\rangle$ only by a sign change. Thus we see that the spatial wave function is antisymmetric. Hence, the Pauli principle exists in the spatial coordinates.

To show the difference let us investigate the states with different spin.

$$\begin{aligned}|\Phi_{a,a,\uparrow,\downarrow}\rangle &= \left(\frac{1}{\sqrt{2}} \Psi_{a,a}^+ \right) G_{\uparrow,\downarrow}^- \\ |\Phi_{a,b,\uparrow,\downarrow}\rangle &= \frac{1}{\sqrt{2}} \left(\Psi_{a,b}^+ G_{\uparrow,\downarrow}^- + \Psi_{a,b}^- G_{\uparrow,\downarrow}^+ \right) \\ |\Phi_{b,a,\uparrow,\downarrow}\rangle &= \frac{1}{\sqrt{2}} \left(\Psi_{a,b}^+ G_{\uparrow,\downarrow}^- - \Psi_{a,b}^- G_{\uparrow,\downarrow}^+ \right) \\ |\Phi_{b,b,\uparrow,\downarrow}\rangle &= \left(\frac{1}{\sqrt{2}} \Psi_{b,b}^+ \right) G_{\uparrow,\downarrow}^-\end{aligned}$$

We see that the two electrons with different spin can be placed without restriction into the two spatial one-particle orbitals.

This indicates that the statistics of electrons with different spin is identical to that of two non-identical particles. The statistics of electrons with like spin is like identical particles.

C.0.1 Spatial symmetry for parallel and antiparallel spins

Here we show that

- the spatial wave functions for two electrons with parallel spin is antisymmetric
- the spatial wave functions for two electrons with anti-parallel spin is symmetric

under exchange of the coordinates.

A common misconception is that the Slater determinant of two one-particle spin-orbitals with opposite spin describes two electrons with anti-parallel spin. For such a state the z-component of the spin vanishes, but it is a superposition of a two states with $S_z = 0$, namely one with antiparallel spin and the other with parallel spin with a total spin lying in the xy-plane.

In order to determine states with parallel and antiparallel spin, we need to determine the spin eigenstates and eigenvalues. If the eigenvalue for $\hat{S}_{tot}^2 = (\hat{S}_1 + \hat{S}_2)^2$ vanishes, the wave function has antiparallel spin. If the eigenvalue is $2\hbar^2$ the spins are parallel.

Using the ladder operators \hat{S}_{\pm} we write the total spin as

$$\begin{aligned}\hat{S}_{tot}^2 &= (\hat{S}_1 + \hat{S}_2)^2 \\ &= \hat{S}_1^2 + \hat{S}_2^2 + 2\hat{S}_1\hat{S}_2 \\ &= \hat{S}_1^2 + \hat{S}_2^2 + 2\left[\frac{1}{2}\hat{S}_{1,+}\hat{S}_{2,-} + \frac{1}{2}\hat{S}_{1,-}\hat{S}_{2,+} + \hat{S}_{1,z}\hat{S}_{2,z}\right] \\ &= \hat{S}_1^2 + \hat{S}_2^2 + \hat{S}_{1,+}\hat{S}_{2,-} + \hat{S}_{1,-}\hat{S}_{2,+} + 2\hat{S}_{1,z}\hat{S}_{2,z}\end{aligned}$$

The ladder operators are defined as

$$\begin{aligned}\hat{S}_+ &= \hat{S}_x + i\hat{S}_y \\ \hat{S}_- &= \hat{S}_x - i\hat{S}_y\end{aligned}$$

and obey

$$\begin{aligned}\hat{S}_-|\uparrow\rangle &= |\downarrow\rangle\hbar & \text{and} & & \hat{S}_-|\downarrow\rangle &= |\emptyset\rangle \\ \hat{S}_+|\uparrow\rangle &= |\emptyset\rangle & \text{and} & & \hat{S}_+|\downarrow\rangle &= |\uparrow\rangle\hbar\end{aligned}$$

Thus

$$\begin{aligned}(\hat{S}_{1+}\hat{S}_{2-} + \hat{S}_{1-}\hat{S}_{2+})|G_{\uparrow,\downarrow}^{\pm}\rangle &= (\hat{S}_{1+}\hat{S}_{2-} + \hat{S}_{1-}\hat{S}_{2+})\frac{1}{\sqrt{2}}(|\uparrow,\downarrow\rangle \pm |\downarrow,\uparrow\rangle) \\ &= \frac{1}{\sqrt{2}}(|\downarrow,\uparrow\rangle \pm |\uparrow,\downarrow\rangle)\hbar^2 \\ &= |G_{\uparrow,\downarrow}^{\pm}\rangle(\pm\hbar^2) \\ (\hat{S}_{1+}\hat{S}_{2-} + \hat{S}_{1-}\hat{S}_{2+})|G_{\uparrow,\uparrow}^{\pm}\rangle &= |\emptyset\rangle \\ (\hat{S}_{1+}\hat{S}_{2-} + \hat{S}_{1-}\hat{S}_{2+})|G_{\downarrow,\downarrow}^{\pm}\rangle &= |\emptyset\rangle \\ \hat{S}_{1,z}\hat{S}_{2,z}|G_{\uparrow,\downarrow}^{\pm}\rangle &= |G_{\uparrow,\downarrow}^{\pm}\rangle\left(-\frac{\hbar^2}{4}\right) \\ \hat{S}_{1,z}\hat{S}_{2,z}|G_{\uparrow,\uparrow}^{\pm}\rangle &= |G_{\uparrow,\uparrow}^{\pm}\rangle\left(+\frac{\hbar^2}{4}\right) \\ \hat{S}_{1,z}\hat{S}_{2,z}|G_{\downarrow,\downarrow}^{\pm}\rangle &= |G_{\downarrow,\downarrow}^{\pm}\rangle\left(+\frac{\hbar^2}{4}\right) \\ \hat{S}_i^2|G_{s,s'}^{\pm}\rangle &= |G_{s,s'}^{\pm}\rangle\frac{3\hbar^2}{4}\end{aligned}$$

$$\begin{aligned}\hat{S}_{tot}^2|G_{\uparrow,\downarrow}^{\pm}\rangle &= |G_{\uparrow,\downarrow}^{\pm}\rangle\left[\frac{3\hbar^2}{4} + \frac{3\hbar^2}{4} \pm \hbar^2 - \frac{\hbar^2}{2}\right] = |G_{\uparrow,\downarrow}^{\pm}\rangle(1 \pm 1)\hbar^2 \\ \hat{S}_{tot}^2|G_{\uparrow,\uparrow}^{\pm}\rangle &= |G_{\uparrow,\uparrow}^{\pm}\rangle\left[\frac{3\hbar^2}{4} + \frac{3\hbar^2}{4} + \frac{\hbar^2}{2}\right] = |G_{\uparrow,\uparrow}^{\pm}\rangle 2\hbar^2 \\ \hat{S}_{tot}^2|G_{\downarrow,\downarrow}^{\pm}\rangle &= |G_{\downarrow,\downarrow}^{\pm}\rangle\left[\frac{3\hbar^2}{4} + \frac{3\hbar^2}{4} + \frac{\hbar^2}{2}\right] = |G_{\downarrow,\downarrow}^{\pm}\rangle 2\hbar^2\end{aligned}$$

Thus we see that $|G_{\uparrow,\downarrow}^+\rangle$, $|G_{\uparrow,\uparrow}^+\rangle$ and $|G_{\downarrow,\downarrow}^+\rangle$ describe two electrons with parallel spin. Note that $|G_{s,s'}^-\rangle$ vanishes for parallel spin.

The only solution with antiparallel spin is $|G_{\uparrow,\downarrow}^-\rangle$.

From Eq. C.1 we know that the antisymmetric spin wave function is always combined with the symmetric spatial orbital and vice versa. Hence, the wave functions describing two electrons with anti-parallel spin are symmetric in their spatial coordinates, while the ones with parallel spin have an antisymmetric spatial wave function.

C.0.2 An intuitive analogy for particle with spin

Consider balls that are painted on the one side green and on the other side red.

If we place two such balls on a table with the green side up, turn around and look at them again, we cannot tell if the two balls have been interchanged.

No we place them with opposite colors up. If we only allow that the positions of the two balls are interchanged, but exclude that they are turned around, we can tell the two spheres apart from their orientation. Hence we can treat them as non-identical spheres.

However, if we consider exchanges of position *and* orientation, we are again unable to tell, whether the spheres have been interchanged or not.

Thus, if we can exclude that the spins of the particles –or the orientation of our spheres– change, we can divide electrons into two classes of particles, namely spin-up and spin-down electrons. Particles within each class are undistinguishable, but spin-up and spin-down electrons can be distinguished. When the spin is preserved, the Hamiltonian is invariant with respect to spin-rotation, and spin is a good quantum number.

However, if there is a magnetic field, which can cause a rotation of the spin direction, the division into spin-up and spin-down particles is no more a useful concept. In our model, if the orientation of the spheres can change with time, we cannot use it as distinguishing feature.

Appendix D

Hartree-Fock of the free-electron gas

Here, we derive the changes in the dispersion relation $\epsilon(\vec{k})$ of the free-electron gas due to the exchange potential discussed in section 9.6 on p. 114.

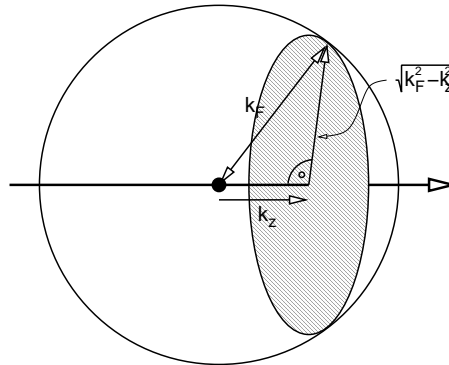
Because of the translational symmetry, we can assume that the charge density is spatially constant.¹ Since the problem is translationally invariant, we can furthermore deduce that the eigenstates are plane waves.

D.1 Exchange potential as non-local potential

Let us evaluate the non-local potential as defined in Eq. 9.17 using plane waves as defined in Eq. 4.1 as basis functions.

$$\begin{aligned}
 V_x(\vec{x}, \vec{x}') &\stackrel{\text{Eq. 9.17}}{=} - \left[\sum_j \frac{e^2 \phi_j^*(\vec{x}) \phi_j(\vec{x}')}{4\pi\epsilon_0 |\vec{r} - \vec{r}'|} \right] \\
 &\stackrel{\text{Eq. 4.1}}{=} \frac{-e^2}{4\pi\epsilon_0 \Omega} \left[\sum_{\vec{k}} \theta(k_F - |\vec{k}|) \underbrace{\frac{(2\pi)^3}{\Omega}}_1 \underbrace{\frac{\Omega}{(2\pi)^3}}_{\rightarrow d^3k} \frac{e^{i\vec{k}(\vec{r}-\vec{r}')} \delta_{\sigma,\sigma'}}{|\vec{r} - \vec{r}'|} \right] \\
 &= \frac{-e^2}{4\pi\epsilon_0 |\vec{r} - \vec{r}'|} \frac{\delta_{\sigma,\sigma'}}{(2\pi)^3} \int d^3k \theta(k_F - |\vec{k}|) e^{i\vec{k}(\vec{r}-\vec{r}')} \quad (\text{D.1})
 \end{aligned}$$

We see that the integral is isotropic in $\vec{r}' - \vec{r}$. Thus, we can assume, without loss of generality, that the distance vector points in z-direction, that is $\vec{r}' - \vec{r} = \vec{e}_z s$.



¹We assume here that there is no symmetry breaking, which is not guaranteed.

$$\begin{aligned}
\int_{\vec{k} \leq k_F} d^3k e^{ik_z s} &= \int_{-k_F}^{k_F} dk_z e^{ik_z s} \underbrace{\int_{k_x^2 + k_y^2 < k_F^2 - k_z^2} dk_x dk_y}_{\pi(k_F^2 - k_z^2)} \\
&= \int_{-k_F}^{k_F} dk_z (\pi(k_F^2 - k_z^2)) e^{ik_z s} \\
&= \pi k_F^2 \int_{-k_F}^{k_F} dk_z e^{ik_z s} - \pi \int_{-k_F}^{k_F} dk_z k_z^2 e^{ik_z s} \\
&= \pi k_F^2 \int_{-k_F}^{k_F} dk_z e^{ik_z s} + \pi \frac{d^2}{ds^2} \int_{-k_F}^{k_F} dk_z e^{ik_z s} \\
&= \pi \left[k_F^2 + \frac{d^2}{ds^2} \right] \left[\frac{1}{is} e^{ik_z s} \right]_{-k_F}^{k_F} \\
&= \pi \left[k_F^2 + \frac{d^2}{ds^2} \right] \frac{e^{ik_F s} - e^{-ik_F s}}{is} \\
&= 2\pi k_F^3 \left[1 + \frac{d^2}{d(k_F s)^2} \right] \frac{\sin(k_F s)}{k_F s} \\
&= 2\pi k_F^3 \left[\left(1 + \frac{d^2}{dx^2} \right) \frac{\sin(x)}{x} \right]_{x=k_F s} \\
&= 2\pi k_F^3 \left[\frac{\sin(x)}{x} - \frac{\sin(x)}{x} - \frac{2 \cos(x)}{x^2} + \frac{2 \sin(x)}{x^3} \right]_{x=k_F s} \\
&= \frac{4\pi}{3} k_F^3 \left[-3 \frac{\cos(k_F s)}{(k_F s)^2} + 3 \frac{\sin(k_F s)}{(k_F s)^3} \right]
\end{aligned} \tag{D.2}$$

Now we insert the result of the integral into the expression for the nonlocal potential.

$$\begin{aligned}
V_x(s, \sigma, \sigma') &\stackrel{\text{Eqs. D.1, D.2}}{=} \frac{-e^2 \delta_{\sigma, \sigma'}}{4\pi \epsilon_0 s} \frac{1}{(2\pi)^3} \underbrace{4\pi k_F^3 \left[-\frac{\cos(k_F s)}{(k_F s)^2} + \frac{\sin(k_F s)}{(k_F s)^3} \right]}_{\int d^3k \theta(k_F - |\vec{k}|) e^{i\vec{k}(\vec{r}' - \vec{r})}} \\
&= \frac{e^2 \delta_{\sigma, \sigma'}}{4\pi \epsilon_0 s} \frac{1}{(2\pi)^3} \frac{4\pi}{3} k_F^3 \left[3 \frac{(k_F s) \cos(k_F s) - \sin(k_F s)}{(k_F s)^3} \right]
\end{aligned} \tag{D.3}$$

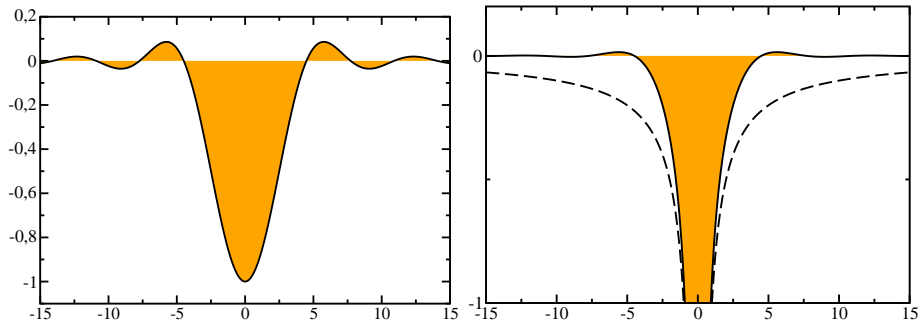


Fig. D.1: The shape of the non-local exchange potential (right) for a free electron gas as calculated in the Hartree Fock method. The dashed line corresponds to a Coulomb interaction. The function $3 \frac{x \cos(x) - \sin(x)}{x^3}$ is shown on the left-hand side.

D.2 Energy level shifts by the Exchange potential

Now we need to evaluate the expectation values of this potential in order to obtain the energy shifts:

$$\begin{aligned} d\epsilon_{\vec{k},\sigma} &= \frac{1}{\Omega} \int d^3r \int d^3r' V_x(|\vec{r}-\vec{r}'|, \sigma, \sigma') e^{i\vec{k}(\vec{r}-\vec{r}')} \\ &\stackrel{s \stackrel{\text{def}}{=} \vec{r}-\vec{r}'}{=} \underbrace{\frac{1}{\Omega} \int d^3r \int d^3s}_{1} V_x(|\vec{s}|, \sigma, \sigma') e^{i\vec{k}\vec{s}} \end{aligned}$$

Now we decompose the plane wave into spherical harmonics (see appendix "Distributionen, d-Funktionen und Fourier transformationen in the text book of Messiah[148])

$$e^{i\vec{k}\vec{r}} = 4\pi \sum_{\ell=1}^{\infty} \sum_{m=-\ell}^{\ell} i^{\ell} j_{\ell}(|\vec{k}||\vec{r}|) Y_{\ell,m}^*(\vec{k}) Y_{\ell,m}(\vec{r})$$

Thus, we obtain

$$\begin{aligned} d\epsilon_{\vec{k},\sigma} &= \int d^3s V_x(|\vec{s}|, \sigma, \sigma') 4\pi \sum_{\ell=1}^{\infty} \sum_{m=-\ell}^{\ell} i^{\ell} j_{\ell}(|\vec{k}||\vec{s}|) Y_{\ell,m}^*(\vec{k}) Y_{\ell,m}(\vec{s}) \\ &= 4\pi \sum_{\ell=1}^{\infty} \sum_{m=-\ell}^{\ell} i^{\ell} Y_{\ell,m}^*(\vec{k}) \int d^3s V_x(|\vec{s}|, \sigma, \sigma') j_{\ell}(|\vec{k}||\vec{s}|) Y_{\ell,m}(\vec{s}) \end{aligned}$$

Because the non-local potential is isotropic only the term with $\ell = 0$ contributes.

$$\begin{aligned} d\epsilon_{\vec{k},\sigma} &= 4\pi \underbrace{Y_{0,0}^*(\vec{k})}_{\frac{1}{\sqrt{4\pi}}} \int d^3s V_x(|\vec{s}|, \sigma, \sigma) \underbrace{j_0(|\vec{k}||\vec{s}|)}_{j_0(x) = \frac{\sin(x)}{x}} \underbrace{Y_{0,0}(\vec{s})}_{\frac{1}{\sqrt{4\pi}}} \\ &= \int d^3s V_x(|\vec{s}|, \sigma, \sigma) \frac{\sin(|\vec{k}||\vec{s}|)}{|\vec{k}||\vec{s}|} \\ &\stackrel{s \stackrel{\text{def}}{=} |\vec{s}|}{=} 4\pi \int ds s^2 V_x(s, \sigma, \sigma) \frac{\sin(|\vec{k}|s)}{|\vec{k}|s} \\ &= \frac{4\pi}{|\vec{k}|} \int ds V_x(s, \sigma, \sigma) s \sin(|\vec{k}|s) \\ &\stackrel{Eq. 9.19}{=} \frac{4\pi}{|\vec{k}|} \int ds \frac{e^2}{4\pi\epsilon_0} \frac{1}{(2\pi)^2} \frac{4\pi}{3} k_F^3 \left[3 \frac{k_F s \cos(k_F s) - \sin(k_F s)}{(k_F s)^3} \right] s \sin(|\vec{k}|s) \\ &= \frac{4\pi}{|\vec{k}|} \frac{e^2}{4\pi\epsilon_0} \frac{1}{(2\pi)^2} \frac{4\pi}{3} k_F^3 \int ds \left[3 \frac{k_F s \cos(k_F s) - \sin(k_F s)}{(k_F s)^3} \right] \sin(|\vec{k}|s) \\ &\stackrel{r \stackrel{\text{def}}{=} k_F s}{=} \frac{4\pi}{k_F |\vec{k}|} \frac{e^2}{4\pi\epsilon_0} \frac{1}{(2\pi)^2} \frac{4\pi}{3} k_F^3 \int_0^{\infty} dr \left[3 \frac{r \cos(r) - \sin(r)}{r^3} \right] \sin\left(\frac{|\vec{k}|}{k_F} r\right) \end{aligned}$$

Now we need to solve the integral

$$I = \int_0^{\infty} dx \left[3 \frac{x \cos(x) - \sin(x)}{x^3} \right] \sin(ax)$$

where $a = |\vec{k}|/k_F$. The difficulty with this integral is that we cannot take the two terms apart, because the individual parts of the integrand diverge at the origin. Thus, during the derivation, we have to deal with divergent expressions.

$$\begin{aligned}\partial_x \frac{\sin(x)}{x^{n-1}} &= -(n-1) \frac{\sin(x)}{x^n} + \frac{\cos(x)}{x^{n-1}} \\ \Rightarrow \frac{\sin(x)}{x^n} &= \frac{1}{(n-1)} \left[\frac{\cos(x)}{x^{n-1}} - \partial_x \frac{\sin(x)}{x^{n-1}} \right]\end{aligned}\quad (D.4)$$

$$\begin{aligned}Eq. D.4 \quad \int_0^\infty dx \frac{\sin(x)}{x^3} \sin(ax) &= \frac{1}{2} \int_0^\infty dx \frac{\cos(x)}{x^2} \sin(ax) - \frac{1}{2} \int_0^\infty dx \sin(ax) \partial_x \frac{\sin(x)}{x^2} \\ &= \frac{1}{2} \int_0^\infty dx \frac{\cos(x)}{x^2} \sin(ax) \\ &\quad - \frac{1}{2} \left[\sin(ax) \frac{\sin(x)}{x^2} \right]_0^\infty + \frac{a}{2} \int_0^\infty dx \frac{\sin(x)}{x^2} \cos(ax) \\ &= \frac{a}{2} + \frac{1}{2} \int_0^\infty dx \frac{\cos(x) \sin(ax) + a \sin(x) \cos(ax)}{x^2}\end{aligned}\quad (D.5)$$

$$\begin{aligned}Eq. D.4 \quad \int_0^\infty dx \frac{\sin(x)}{x^2} \cos(ax) &= \int_0^\infty dx \frac{\cos(x)}{x} \cos(ax) - \int_0^\infty dx \cos(ax) \partial_x \frac{\sin(x)}{x} \\ &= \int_0^\infty dx \frac{\cos(x)}{x} \cos(ax) \\ &\quad - \left[\cos(ax) \frac{\sin(x)}{x} \right]_0^\infty - a \int_0^\infty dx \frac{\sin(x)}{x} \sin(ax) \\ &= 1 + \int_0^\infty dx \frac{\cos(x) \cos(ax) - a \sin(x) \sin(ax)}{x}\end{aligned}\quad (D.6)$$

Thus, we obtain

$$\begin{aligned}I &= 3 \int_0^\infty dx \frac{x \cos(x) - \sin(x)}{x^3} \sin(ax) \\ &= 3 \int_0^\infty dx \frac{\cos(x) \sin(ax)}{x^2} - 3 \int_0^\infty dx \frac{\sin(x) \sin(ax)}{x^3} \\ Eq. D.5 \quad &= 3 \int_0^\infty dx \frac{\cos(x) \sin(ax)}{x^2} - \frac{3a}{2} - \frac{3}{2} \int_0^\infty dx \frac{\cos(x) \sin(ax) + a \sin(x) \cos(ax)}{x^2} \\ &= -\frac{3a}{2} + \frac{3}{2} \int_0^\infty dx \frac{\cos(x) \sin(ax)}{x^2} - \frac{3a}{2} \int_0^\infty dx \frac{\sin(x) \cos(ax)}{x^2} \\ &= -\frac{3a}{2} + \frac{3a}{2} \int_0^\infty dy \frac{\cos(\frac{1}{a}y) \sin(y)}{y^2} - \frac{3a}{2} \int_0^\infty dx \frac{\sin(x) \cos(ax)}{x^2} \\ Eq. D.6 \quad &= -\frac{3a}{2} + \frac{3a}{2} \left[1 + \int_0^\infty dy \frac{\cos(\frac{1}{a}y) \cos(y) - \frac{1}{a} \sin(\frac{1}{a}y) \sin(y)}{y} \right] \\ &\quad - \frac{3a}{2} \left[1 + \int_0^\infty dx \frac{\cos(ax) \cos(x) - a \sin(ax) \sin(x)}{x} \right] \\ &= -\frac{3a}{2} + \frac{3a}{2} \left[\int_0^\infty dx \frac{\cos(x) \cos(ax) - \frac{1}{a} \sin(x) \sin(ax)}{x} \right] \\ &\quad - \frac{3a}{2} \left[\int_0^\infty dx \frac{\cos(ax) \cos(x) - a \sin(ax) \sin(x)}{x} \right] \\ &= -\frac{3a}{2} + \frac{3a}{2} \left(-\frac{1}{a} + a \right) \left[\int_0^\infty dx \frac{\sin(x) \sin(ax)}{x} \right] \\ &= -\frac{3a}{2} + \frac{3}{2} (a^2 - 1) \left[\int_0^\infty dx \frac{\sin(x) \sin(ax)}{x} \right]\end{aligned}$$

We recognize that the integral is the fourier transform of $\frac{\sin(x)}{x}$. From the Fourier transform tables

of Bronstein[149] we take

$$\begin{aligned} \sqrt{\frac{2}{\pi}} \int_0^\infty dx \sin(xy) \frac{\sin(ax)}{x} &\stackrel{\text{Bronstein}}{=} \frac{1}{\sqrt{2\pi}} \ln \left| \frac{y+a}{y-a} \right| \\ \xrightarrow{a \rightarrow 1; y \rightarrow a} \int_0^\infty dx \sin(ax) \frac{\sin(x)}{x} &= \frac{1}{2} \ln \left| \frac{a+1}{a-1} \right| = \frac{1}{2} \ln \left| \frac{1+a}{1-a} \right| \end{aligned}$$

Thus, we obtain

$$I = -\frac{3a}{2} + \frac{3}{4}(a^2 - 1) \ln \left| \frac{1+a}{1-a} \right|$$

Now we are done with the Integral. We need to insert the result in the correction for the energy eigenvalues

$$\begin{aligned} d\epsilon_{\vec{k},\sigma} &= \frac{4\pi}{k_F |\vec{k}|} \frac{e^2}{4\pi\epsilon_0} \frac{1}{(2\pi)^2} \frac{4\pi}{3} k_F^3 \left[-\frac{3a}{2} + \frac{3(a^2 - 1)}{4} \ln \left| \frac{a+1}{a-1} \right| \right] \\ &= \frac{4\pi}{k_F^2} \frac{e^2}{4\pi\epsilon_0} \frac{1}{(2\pi)^2} \frac{4\pi}{3} k_F^3 \left[-\frac{3}{2} + \frac{3(a^2 - 1)}{4a} \ln \left| \frac{a+1}{a-1} \right| \right] \\ &= -\frac{e^2}{4\pi\epsilon_0} \frac{2k_F}{\pi} \left[\frac{1}{2} + \frac{1-a^2}{4a} \ln \left| \frac{1+a}{1-a} \right| \right] \end{aligned}$$

The function in parenthesis is shown in Fig. D.2 and the resulting dispersion relation is discussed in section 9.6 on p. 114.

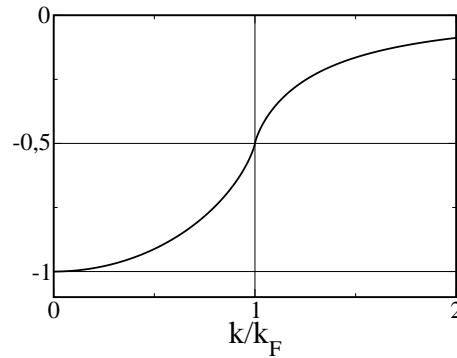


Fig. D.2: The function $f(a) = -\left(\frac{1}{2} + \frac{1-a^2}{4a} \ln \left| \frac{1+a}{1-a} \right| \right)$ as function of $a = k/k_F$. Note that the slope for $k = k_F$ is infinite. For $k \gg k_F$ the function approaches zero.

Appendix E

Slater-Condon rules

In this section we derive the Slater-Condon rules spelled out in section ?? on p. ??.

We assume that the Slater determinants are in maximum coincidence spelled out on p ?? The principle of maximum coincidence can be used to place the one-particle orbitals that differ between the two Slater determinants to the front. The other one-particle orbitals, which are identical in both Slater determinants are placed in the identical position of both determinants.

E.1 Matrix elements between identical Slater determinants

The result has already been obtained when we worked out the equations for the Hartree Fock method, where we obtained Eq. 9.6 and Eq. 9.13 on p. 106ff. They are identical to the first Slater-Condon rule Eq. ?? given above.

E.2 Matrix element of a one-particle operator with Slater determinants differing by 1 one-particle orbital

First we consider Slater determinants that differ by exactly one one-particle orbital. Due to the form of maximum coincidence we can place these two orbitals in the first position. Hence, $|\psi_1\rangle \neq |\phi_1\rangle$, but $|\psi_i\rangle = |\phi_i\rangle$ for $i \neq 1$. Thus, $\langle\psi_i|\phi_j\rangle = \delta_{i,j}(1 - \delta_{i,1})$.

$$\begin{aligned}\langle\psi|\hat{A}_1|\phi\rangle &= \frac{1}{N!} \sum_{i_1, \dots, i_N=1}^N \sum_{j_1, \dots, j_N=1}^N \epsilon_{i_1, i_2, \dots, i_N} \epsilon_{j_1, j_2, \dots, j_N} \\ &\quad \cdot \langle\psi_{i_1}|\hat{A}|\phi_{j_1}\rangle \underbrace{\langle\psi_{i_2}|\phi_{j_2}\rangle}_{\delta_{i_2, j_2}(1-\delta_{i_2, 1})} \dots \underbrace{\langle\psi_{i_N}|\phi_{j_N}\rangle}_{\delta_{i_N, j_N}(1-\delta_{i_N, 1})} \\ &= \frac{1}{N!} \sum_{i_1, \dots, i_N=1}^N \sum_{j_1=1}^N \epsilon_{i_1, i_2, \dots, i_N} \epsilon_{j_1, i_2, \dots, i_N} \\ &\quad \cdot \langle\psi_{i_1}|\hat{A}|\phi_{j_1}\rangle (1 - \delta_{i_2, 1}) \dots (1 - \delta_{i_N, 1})\end{aligned}$$

Because the Levi-Civita symbol is only non-zero if all indices differ, the product of the two Levi-Civita symbols can only be non-zero if their first index is identical.

$$\langle\psi|\hat{A}_1|\phi\rangle = \frac{1}{N!} \sum_{i_1, \dots, i_N=1}^N (\epsilon_{i_1, i_2, \dots, i_N})^2 \langle\psi_{i_1}|\hat{A}|\phi_{i_1}\rangle (1 - \delta_{i_2, 1}) \dots (1 - \delta_{i_N, 1})$$

Furthermore there is a contribution only if the first index i_1 has the value 1. If that is not the case there is a term $(1 - \delta_{i_1,1})$ that vanishes.

$$\langle \Psi | \hat{A}_1 | \Phi \rangle = \frac{1}{N!} \sum_{i_2, \dots, i_N=1}^N (\epsilon_{1, i_2, \dots, i_N})^2 \langle \psi_1 | \hat{A} | \phi_1 \rangle$$

The Levi-Civita symbols contribute, if all indices are different, This happens $(N-1)!$ times, which corresponds to the number of permutations of the indices $2, \dots, N$. Thus, we obtain

$$\langle \Psi | \hat{A}_1 | \Phi \rangle = \frac{1}{N} \langle \psi_1 | \hat{A} | \phi_1 \rangle$$

Since the operator has the form $\hat{A} = \sum_{i=1}^N \hat{A}_i$, and since all operators \hat{A}_i contribute the same result, we obtain

$$\langle \Psi | \hat{A} | \Phi \rangle = \langle \psi_1 | \hat{A} | \phi_1 \rangle$$

which corresponds to the first line in the second Slater-Condon rule Eq. ??.

E.3 Matrix element of a two-particle operator with Slater determinants differing by one one-particle orbital

We consider the matrix element between two Slater determinants

$$\begin{aligned} \langle \vec{x}_1, \dots, \vec{x}_N | \Psi \rangle &= \frac{1}{\sqrt{N!}} \sum_{i_1, \dots, i_N=1}^N \epsilon_{i_1, \dots, i_N} \langle \vec{x}_1 | \psi_{i_1} \rangle \cdots \langle \vec{x}_N | \psi_{i_N} \rangle \\ \langle \vec{x}_1, \dots, \vec{x}_N | \Phi \rangle &= \frac{1}{\sqrt{N!}} \sum_{j_1, \dots, j_N=1}^N \epsilon_{j_1, \dots, j_N} \langle \vec{x}_1 | \phi_{j_1} \rangle \cdots \langle \vec{x}_N | \phi_{j_N} \rangle \end{aligned}$$

with all one-particle orbitals equal, except the two first orbitals, that is

$$\langle \psi_i | \phi_j \rangle = \begin{cases} \delta_{ij} & \text{for } i, j \in 2, \dots, N \\ 0 & \text{for } i = 1 \text{ and/or } j = 1 \end{cases} = \delta_{ij}(1 - \delta_{i,1})$$

Note that we the Slater determinants are in maximum coincidence, as required, because the two orbitals that are present in only one of the two Slater determinants stand at the same position, namely the first. The orbitals which are identical for both Slater determinants are in the same position.

Now we can work out the matrix element of the interaction operator $\hat{W}_{1,2}$ that acts exclusively on the first two particle coordinates. Later we will see that the result is the same for each pair of coordinates, so that the sum over pairs is done easily at the end of the calculation.

$$\begin{aligned} \langle \Psi | \hat{W}_{1,2} | \Phi \rangle &= \frac{1}{N!} \sum_{i_1, \dots, i_N=1}^N \sum_{j_1, \dots, j_N=1}^N \epsilon_{i_1, i_2, \dots, i_N} \epsilon_{j_1, j_2, \dots, j_N} \\ &\quad \cdot \langle \psi_{i_1} \psi_{i_2} | \hat{W}_{1,2} | \phi_{j_1} \phi_{j_2} \rangle \underbrace{\langle \psi_{i_3} | \phi_{j_3} \rangle}_{\delta_{i_3, j_3}(1 - \delta_{i_3, 1})} \cdots \underbrace{\langle \psi_{i_N} | \phi_{j_N} \rangle}_{\delta_{i_N, j_N}(1 - \delta_{i_N, 1})} \\ &= \frac{1}{N!} \sum_{i_1, \dots, i_N=1}^N \sum_{j_1, j_2=1}^N \epsilon_{i_1, i_2, i_3, \dots, i_N} \epsilon_{j_1, j_2, i_3, \dots, i_N} \\ &\quad \cdot \langle \psi_{i_1} \psi_{i_2} | \hat{W} | \phi_{j_1} \phi_{j_2} \rangle (1 - \delta_{i_3, 1}) \cdots (1 - \delta_{i_N, 1}) \end{aligned}$$

Now we can work out the sum over the indices j_1, j_2 . Because the antisymmetric tensor vanishes, whenever two indices are equal, the indices j_1, j_2 must be in the set $j_1, j_2 \in \{i_1, i_2\}$. Furthermore the two indices j_1, j_2 must differ, again to avoid that the antisymmetric tensor vanishes. Hence only two terms from the second sum survive, namely the one with $(j_1, j_2) = (i_1, i_2)$ and the one where the two indices are interchanged $(j_1, j_2) = (i_2, i_1)$.

$$\begin{aligned} \langle \Psi | \hat{W}_{1,2} | \Phi \rangle &= \frac{1}{N!} \sum_{i_1, \dots, i_N=1}^N \left[(\epsilon_{i_1, i_2, \dots, i_N})^2 \langle \psi_{i_1} \psi_{i_2} | \hat{W}_{1,2} | \phi_{i_1} \phi_{i_2} \rangle \right. \\ &\quad \left. + \epsilon_{i_1, i_2, i_3, \dots, i_N} \epsilon_{i_2, i_1, i_3, \dots, i_N} \langle \psi_{i_1} \psi_{i_2} | \hat{W}_{1,2} | \phi_{i_2} \phi_{i_1} \rangle \right] \\ &\quad \cdot (1 - \delta_{i_3,1}) \dots (1 - \delta_{i_N,1}) \\ &= \frac{1}{N!} \sum_{i_1, \dots, i_N=1}^N (\epsilon_{i_1, i_2, \dots, i_N})^2 \left(\langle \psi_{i_1} \psi_{i_2} | \hat{W}_{1,2} | \phi_{i_1} \phi_{i_2} \rangle - \langle \psi_{i_1} \psi_{i_2} | \hat{W}_{1,2} | \phi_{i_2} \phi_{i_1} \rangle \right) \\ &\quad \cdot (1 - \delta_{i_3,1}) \dots (1 - \delta_{i_N,1}) \end{aligned}$$

Furthermore there is a contribution only if one of the first two indices i_1, i_2 has the value 1. If that is not the case, there is a term $(1 - \delta_{i_1,1})$ that vanishes.

$$\begin{aligned} \langle \Psi | \hat{W}_{1,2} | \Phi \rangle &= \frac{1}{N!} \sum_{i_2, i_3, \dots, i_N=1}^N (\epsilon_{1, i_2, \dots, i_N})^2 \left(\langle \psi_1 \psi_{i_2} | \hat{W}_{1,2} | \phi_1 \phi_{i_2} \rangle - \langle \psi_1 \psi_{i_2} | \hat{W}_{1,2} | \phi_{i_2} \phi_1 \rangle \right) \\ &\quad + \frac{1}{N!} \sum_{i_1, i_3, \dots, i_N=1}^N (\epsilon_{i_1, 1, i_3, \dots, i_N})^2 \left(\langle \psi_{i_1} \psi_1 | \hat{W}_{1,2} | \phi_{i_1} \phi_1 \rangle - \langle \psi_{i_1} \psi_1 | \hat{W}_{1,2} | \phi_1 \phi_{i_1} \rangle \right) \\ &= \frac{2}{N!} \sum_{n=2}^N \left(\langle \psi_1 \psi_n | \hat{W}_{1,2} | \phi_1 \phi_n \rangle - \langle \psi_1 \psi_n | \hat{W}_{1,2} | \phi_n \phi_1 \rangle \right) \underbrace{\sum_{i_3, \dots, i_N=1}^N (\epsilon_{1, n, \dots, i_N})^2}_{(N-2)!} \\ &= \underbrace{\frac{2(N-2)!}{N!}}_{\frac{2}{N(N-1)}} \sum_{n=2}^N \left(\langle \psi_1 \psi_n | \hat{W}_{1,2} | \phi_1 \phi_n \rangle - \langle \psi_1 \psi_n | \hat{W}_{1,2} | \phi_n \phi_1 \rangle \right) \end{aligned}$$

Since the operator has the form $\hat{W} = \frac{1}{2} \sum_{i \neq j}^N \hat{W}_{ij}$. Each pair contributes the same result. As there are $N(N-1)$ distinct pairs in the double-sum, we obtain

$$\langle \Psi | \hat{W} | \Phi \rangle = \sum_{n=1}^N \left(\langle \psi_1 \psi_n | \hat{W}_{1,2} | \phi_1 \phi_n \rangle - \langle \psi_1 \psi_n | \hat{W}_{1,2} | \phi_n \phi_1 \rangle \right)$$

This result corresponds to the second line in the second Slater-Condon rule Eq. ???. The sum runs now over all terms because the element with $n = 1$ cancels anyway.

E.4 Matrix element of a one-particle operator with Slater determinants differing by 2 one-particle orbitals

$$\begin{aligned} \langle \Psi | \hat{A}_1 | \Phi \rangle &= \frac{1}{N!} \sum_{i_1, \dots, i_N=1}^N \sum_{j_1, \dots, j_N=1}^N \epsilon_{i_1, i_2, \dots, i_N} \epsilon_{j_1, j_2, \dots, j_N} \\ &\quad \cdot \langle \psi_{i_1} | \hat{A} | \phi_{j_1} \rangle \underbrace{\langle \psi_{i_2} | \phi_{j_2} \rangle}_{\delta_{i_2, j_2} (1 - \delta_{i_2, 1}) (1 - \delta_{i_2, 2})} \dots \underbrace{\langle \psi_{i_N} | \phi_{j_N} \rangle}_{\delta_{i_N, j_N} (1 - \delta_{i_N, 1}) (1 - \delta_{i_N, 2})} \end{aligned}$$

It is evident that this matrix element vanishes, because in each term there is at least one scalar product between orbitals that differ in the two Slater determinants.

This result corresponds to the first line in the third Slater-Condon rule Eq. ??.

E.5 Matrix element of a two-particle operator with Slater determinants differing by 2 one-particle orbitals

$$\begin{aligned}
 \langle \Psi | \hat{W}_{x_1, x_2} | \Phi \rangle &= \frac{1}{N!} \sum_{i_1, \dots, i_N} \sum_{j_1, \dots, j_N} \epsilon_{i_1, i_2, \dots, i_N} \epsilon_{j_1, j_2, \dots, j_N} \\
 &\quad \cdot \langle \psi_{i_1} \psi_{i_2} | \hat{A} | \phi_{j_1} \phi_{j_2} \rangle \underbrace{\langle \psi_{i_3} | \phi_{j_3} \rangle}_{\delta_{i_3, j_3} (1 - \delta_{i_3, 1}) (1 - \delta_{i_3, 2})} \dots \underbrace{\langle \psi_{i_N} | \phi_{j_N} \rangle}_{\delta_{i_N, j_N} (1 - \delta_{i_N, 1}) (1 - \delta_{i_N, 2})} \\
 &= \frac{1}{N!} \sum_{i_1, i_2=1}^2 \sum_{j_1, j_2=1}^2 \langle \psi_{i_1} \psi_{i_2} | \hat{A} | \phi_{j_1} \phi_{j_2} \rangle \sum_{i_3, \dots, i_N} \epsilon_{i_1, i_2, i_3, \dots, i_N} \epsilon_{j_1, j_2, i_3, \dots, i_N} \\
 &= \frac{1}{N!} \sum_{i_1, i_2=1}^2 \sum_{j_1, j_2=1}^2 \langle \psi_{i_1} \psi_{i_2} | \hat{A} | \phi_{j_1} \phi_{j_2} \rangle (N-2)! (\delta_{i_1, j_1} \delta_{i_2, j_2} - \delta_{i_1, j_2} \delta_{i_2, j_1}) \\
 &= \frac{2}{N(N-1)} (\langle \psi_1 \psi_2 | \hat{A} | \phi_1 \phi_2 \rangle - \langle \psi_1 \psi_2 | \hat{A} | \phi_2 \phi_1 \rangle)
 \end{aligned}$$

With the interaction $\hat{W} = \frac{1}{2} \sum_{i \neq j}^N \hat{W}_{ij}$ we obtain with $\langle \Psi | W_{ij} | \Phi \rangle = \langle \Psi | W_{1,2} | \Phi \rangle$

$$\langle \Psi | \hat{W} | \Phi \rangle = \langle \psi_1 \psi_2 | \hat{A} | \phi_1 \phi_2 \rangle - \langle \psi_1 \psi_2 | \hat{A} | \phi_2 \phi_1 \rangle$$

This result corresponds to the second line in the third Slater-Condon rule Eq. ??.

E.6 Matrix elements between Slater determinants differing by more than two one-particle orbitals

The result vanishes. The argument is analogous to that about in Section E.4

Appendix F

Non-adiabatic effects

This section contains some derivations to which we refer in the section on non-adiabatic effects.

F.1 The off-diagonal terms of the first-derivative couplings $\vec{A}_{n,m,j}$

The non-Born-Oppenheimer terms are related to the derivative couplings defined in Eq. 12.17 p. 161

$$\vec{A}_{m,n,j} \stackrel{\text{Eq. 12.17}}{:=} \langle \Psi_m^{BO} | \frac{\hbar}{i} \vec{\nabla}_{R_j} | \Psi_n^{BO} \rangle = \langle \Psi_m^{BO} | \hat{P}_j | \Psi_n^{BO} \rangle \quad (\text{F.1})$$

Here we relate the first-derivative couplings to the derivatives of the Born-Oppenheimer Hamiltonian and the Born-Oppenheimer surfaces.

FIRST-DERIVATIVE COUPLINGS

The first-derivative couplings can be expressed as

$$\vec{A}_{m,n,j}(\vec{R}) \stackrel{\text{Eq. F.4}}{=} \frac{\langle \Psi_m^{BO}(\vec{R}) | [\hat{P}_j, \hat{H}^{BO}(\vec{R})]_- | \Psi_n^{BO}(\vec{R}) \rangle}{\hat{E}_n^{BO}(\vec{R}) - E_m^{BO}(\vec{R})} \quad \text{for } E_n \neq E_m \quad (\text{F.2})$$

where $\hat{P}_j = \frac{\hbar}{i} \vec{\nabla}_{R_j}$ is the momentum operator for the j -th nucleus.

The matrix of first-derivative couplings is hermitean, that is

$$A_{m,n,j} \stackrel{\text{Eq. F.5}}{=} A_{n,m,j}^* \quad (\text{F.3})$$

This will make it evident that non-adiabatic effects will be dominant, when two Born-Oppenheimer surfaces become degenerate.

The off-diagonal term of $\vec{A}_{n,m,j}(\vec{r})$ of the first non-adiabatic term is obtained as follows: We begin with the Schrödinger equation for the Born-Oppenheimer wave function

$$\left(\hat{H}^{BO}(\vec{R}) - E_n^{BO}(\vec{R}) \right) | \Psi_n^{BO}(\vec{R}) \rangle = 0$$

Because this equation is valid for all atomic positions, also the gradient of the above expression vanishes.

$$\begin{aligned} 0 &= \vec{\nabla}_R \left(\hat{H}^{BO}(\vec{R}) - E_n^{BO}(\vec{R}) \right) | \Psi_n^{BO}(\vec{R}) \rangle \\ &= \left[\vec{\nabla}_R, \hat{H}^{BO}(\vec{R}) \right] | \Psi_n^{BO}(\vec{R}) \rangle - | \Psi_n^{BO}(\vec{R}) \rangle \vec{\nabla}_R E_n^{BO}(\vec{R}) + \left(\hat{H}^{BO}(\vec{R}) - E_n^{BO}(\vec{R}) \right) \vec{\nabla}_R | \Psi_n^{BO}(\vec{R}) \rangle \end{aligned}$$

Now we multiply from the left with the bra $\langle \Psi_m^{BO} |$ and form the scalar products in the electronic Hilbert space.

$$\begin{aligned}
0 &= \langle \Psi_m^{BO} | \left[\vec{\nabla}_R, \hat{H}^{BO}(\vec{R}) \right] | \Psi_n^{BO}(\vec{R}) \rangle - \langle \Psi_m^{BO} | \Psi_n^{BO}(\vec{R}) \rangle \vec{\nabla}_R E_n^{BO}(\vec{R}) + \langle \Psi_m^{BO} | \left(\hat{H}^{BO}(\vec{R}) - E_n^{BO}(\vec{R}) \right) \vec{\nabla}_R | \Psi_n^{BO}(\vec{R}) \rangle \\
&= \langle \Psi_m^{BO} | \left[\vec{\nabla}_R, \hat{H}^{BO}(\vec{R}) \right] | \Psi_n^{BO}(\vec{R}) \rangle - \langle \Psi_m^{BO} | \Psi_n^{BO} \rangle \vec{\nabla}_R E_n^{BO}(\vec{R}) + \langle \Psi_m^{BO} | \left(\hat{H}^{BO}(\vec{R}) - E_n^{BO}(\vec{R}) \right) \vec{\nabla}_R | \Psi_n^{BO} \rangle \\
&= \langle \Psi_m^{BO} | \left[\vec{\nabla}_R, \hat{H}^{BO}(\vec{R}) \right] | \Psi_n^{BO} \rangle - \delta_{m,n} \vec{\nabla}_R E_n^{BO}(\vec{R}) + \left(\hat{E}_m^{BO}(\vec{R}) - E_n^{BO}(\vec{R}) \right) \langle \Psi_m^{BO} | \vec{\nabla}_R | \Psi_n^{BO} \rangle
\end{aligned}$$

Thus we obtain

$$\begin{aligned}
\vec{A}_{m,n,j} &= \langle \Psi_m^{BO} | \frac{\hbar}{i} \vec{\nabla}_{R_j} | \Psi_n^{BO} \rangle = \frac{\langle \Psi_m^{BO} | \left[\frac{\hbar}{i} \vec{\nabla}_{R_j}, \hat{H}^{BO}(\vec{R}) \right] | \Psi_n^{BO} \rangle}{\hat{E}_n^{BO}(\vec{R}) - E_m^{BO}(\vec{R})} \\
&= \frac{\langle \Psi_m^{BO} | \left[\hat{P}_j, \hat{H}^{BO}(\vec{R}) \right] | \Psi_n^{BO} \rangle}{\hat{E}_n^{BO}(\vec{R}) - E_m^{BO}(\vec{R})} \quad \text{for } E_n \neq E_m \quad (\text{F.4})
\end{aligned}$$

This is the proof for Eq. F.2 given above.

One can furthermore show that the first-derivative couplings are purely real. For this purpose, we investigate the derivatives of the overlap matrix elements of the Born-Oppenheimer states.

$$\begin{aligned}
\langle \Psi_m^{BO} | \Psi_n^{BO} \rangle &= \delta_{m,n} \\
0 &= \vec{\nabla}_{R_j} \langle \Psi_m^{BO} | \Psi_n^{BO} \rangle \\
&= \langle \vec{\nabla}_{R_j} \Psi_m^{BO} | \Psi_n^{BO} \rangle + \langle \Psi_m^{BO} | \vec{\nabla}_{R_j} \Psi_n^{BO} \rangle \\
&= \langle \Psi_n^{BO} | \vec{\nabla}_{R_j} \Psi_m^{BO} \rangle^* + \langle \Psi_m^{BO} | \vec{\nabla}_{R_j} \Psi_n^{BO} \rangle \\
0 &= -\langle \Psi_n^{BO} | \hat{P}_j \Psi_m^{BO} \rangle^* + \langle \Psi_m^{BO} | \hat{P}_j \Psi_n^{BO} \rangle \\
\Rightarrow \quad A_{m,n,j}(\vec{R}) &= A_{n,m,j}^*(\vec{R}) \quad (\text{F.5})
\end{aligned}$$

This tells us that the first derivative couplings are an Hermitean matrix, which proves Eq. F.3.

This argument Eq. F.5 has been used to argue that the diagonal derivative couplings vanish, if the wave functions are purely real. Because the momentum operator is an imaginary, the diagonal operator matrix element $A_{n,n,j}$ are purely imaginary. Because the $A_{n,m,j}$ is hermitean, the diagonal element $A_{n,n,j}$ must be purely real. From this contradiction follows that $A_{n,n,j} = 0$ for real wave functions.

Appendix G

Non-crossing rule

The **non-crossing rule** has been derived by von Neumann and Wigner[150]. The noncrossing rule has been criticized, but the criticism has been refuted.(see discussion in [151])

NON-CROSSING RULE

In general, i.e. without symmetries, a band crossing of two bands is a $m - 3$ -dimensional manifold in the m -dimensional parameter space of a Hamiltonian.
If the Hamiltonian is real, for example due to time-inversion symmetry, a band crossing is a $m - 2$ -dimensional manifold.

Consider a Hamiltonian in an n -dimensional Hilbert space with elements $H_{ij}(x_1, \dots, x_m)$, that depend on a set (x_1, \dots, x_m) of m parameters. The parameters may be atomic positions. The condition that two eigenvalues cross, determines a sub-manifold in the parameter space of dimension $m - 3$ or of dimension $m - 2$ if the Hamiltonian is chosen real. Thus the condition of a double degeneracy fixes three parameters of a complex Hamiltonian and two parameters of a real Hamiltonian.

Thus, if the (real) Hamiltonian depends on a three coordinates, the degeneracy is limited to a line, which is one condition for a **conical intersection**(for a review see the paper of Yarkony[151]).

The complex case is required, for example, in the presence of magnetic fields, because magnetic fields break the time inversion symmetry of the wave function.

General case: complex Hamiltonians

The argument depends on counting the number of free variables in a Hamiltonian with a given set of eigenvalues. The Hamiltonian is specified uniquely by its eigenvalues and eigenvectors

$$H_{ij} = \sum_k U_{i,k}^\dagger E_k U_{k,j} \quad (\text{G.1})$$

It takes n conditions to fix the eigenvalues, and n^2 conditions to fix a unitary matrix.

To show that a unitary matrix is determined by n^2 conditions, we start from a general complex matrix, which has $(2n)^2$ real parameters. A complex matrix is unitary, if its column vectors are orthonormal, i.e. $\mathbf{U}^\dagger \mathbf{U} = \mathbf{1}$. Orthonormality consists of n^2 conditions, that is $n(n-1)/2$ double-valued conditions (real and imaginary part) for orthogonality and n real conditions for the normalization. Thus a general unitary is determined by n^2 real parameters.

However, the unitary matrix in Eq. G.1 is not unique, because any additional unitary transformation \mathbf{V} , that does not change the diagonal matrix of the eigenvalues, can be multiplied to the already existing unitary matrix \mathbf{U} .

$$H_{ij} = \sum_k U_{i,k}^\dagger E_k U_{k,j} = \sum_{k,m,n} U_{i,m}^\dagger V_{m,k}^\dagger E_k V_{k,n} U_{n,j} \quad \text{if} \quad \sum_k V_{m,k}^\dagger E_k V_{k,n} = E_m \delta_{m,n}$$

For each singly degenerate state, the unitary matrix \mathbf{V} , i.e. the subblock referring only to this state, is a complex phase factor. That is there is one degree of freedom. For a doubly degenerate state, \mathbf{V} can be a unitary matrix in this two-dimensional subspace. A unitary matrix in two dimensions has $2^2 = 4$ degrees of freedom. Continuing this argument we find that, if the states have degeneracies g_1, g_2, \dots, g_ℓ , the number of degrees of freedom of \mathbf{V} is $v := \sum_{j=1}^{\ell} g_j^2$. Here ℓ is the number of degenerate multiplets and $\sum_{j=1}^{\ell} g_j = n$.

Thus, the Hamiltonian is fixed by

$$\ell + n^2 - \sum_{j=1}^{\ell} g_j^2$$

ℓ conditions fix the eigenvalues and $n^2 - \sum_{j=1}^{\ell} g_j^2$ is the number of conditions fixing the unitary matrix up to factors that do not affect the eigenvalues.

Example: Consider a Hamiltonian with n non-degenerate states: It takes $n + n^2 - n = n^2$ parameters to determine a Hamiltonian without degeneracies and $(n-1) + n^2 - 2^2 - (n-2) = n^2 - 3$ parameters to fix the Hamiltonian with a double degeneracy. Thus the condition that one point is degenerate introduces $n^2 - (n^2 - 3) = 3$ conditions on the parameter set. As a consequence two bands in three dimensions can cross in a point, but not along a line.

Consider a Hamiltonian $H(\vec{R})$ that depends parametrically on the coordinates of one atom. The condition of a doubly degenerate state determines all three parameters. Hence the degeneracy will be a single point. This is one condition for a conical intersection.

Real Hamiltonians

If we exploit time-inversion symmetry, we can choose the wave functions to be real. In this case the count is different: Instead of unitary matrices, we need to use real, orthogonal matrices.

A real, orthogonal matrix of dimension n has $\frac{1}{2}n(n-1)$ independent parameters. This is obtained as follows: A general real matrix has n^2 real parameters. The conditions for orthonormality of the eigenvectors are no more all independent, but an interchange of two indices in $\sum_k U_{k,i} U_{k,j} = \delta_{i,j}$ leads to the same condition. Thus the orthonormality imposes $n(n+1)/2$ conditions. Hence a real orthonormal matrix has $n^2 - n(n+1)/2 = n(n-1)/2$ degrees of freedom.

Thus the number of degrees of freedom for a real hermitean matrix is

$$\ell + \frac{n(n-1)}{2} - \sum_{j=1}^{\ell} \frac{g_j(g_j-1)}{2}$$

Let us now analyze the case where two band cross: The non-degenerate Hamiltonian has $n + \frac{n(n-1)}{2} = \frac{n(n+1)}{2}$ degrees of freedom. A matrix with two degenerate states has $(n-1) + \frac{n(n-1)}{2} - 1 = \frac{n(n+1)}{2} - 2$ degrees of freedom. Thus a band crossing of a real Hamiltonian fixes two dimensions. Hence, a conical intersection of real Hamiltonians in a three dimensional space form a line.

Bibliography

- [1] Über die Quantenmechanik der Elektronen in Kristallgittern: F. Bloch *Zeitschr. Phys.* **52**, 555 (1929).
- [2] Simplified LCAO method for the periodic potential problem: J.C. Slater and G.F. Koster *Phys. Rev.* **94**, 1498 (1954).
- [3] M. Wolfsberg and L. Helmholz *J. Chem. Phys.* **20**, 837 (1952).
- [4] *The role of frontier orbitals in chemical reactions* in Nobel Lectures Chemistry, 1981-1990 : World Scientific, Singapore K. Fukui (1982).
- [5] Hydrogen Electrochemistry and Stress-Induced Leakage Current in Silica: P.E. Bloechl and J.H. Stathis *Phys. Rev. Lett* **83**, 372 (1999).
- [6] First-Principles calculations of defects in oxygen-deficient silica exposed to hydrogen: P.E. Blöchl *Phys. Rev. B* **62**, 6158 (2000).
- [7] Elementary prediction of linear combination of atomic orbital matrix elements: S. Froyen and W.A. Harrison *Phys. Rev. B* **20**, 2420 (1979).
- [8] Theory of the two-center bond: W.A. Harrison *Phys. Rev. B* **27**, 3592 (1983).
- [9] Theory of the Multicenter Bond: M. van Schilfgaarde and W.A. Harrison *Phys. Rev. B* **33**, 2653 (1986).
- [10] Crystal Orbital Hamilton Populations (COHP). Energy-Resolved Visualization of Chemical Bonding in Solids Based on Density-Functional Calculations: R. Dronskowski and P.E. Blöchl *J. Phys. Chem.* **97**, 8617 (1993).
- [11] A New Electroaffinity Scale; Together with Data on Valence States and on Valence Ionization Potentials and Electron Affinities: R.S. Mulliken *J. Chem. Phys.* **2**, 782 (1934).
- [12] Simple Approach to the Band-Structure Problem: O.K. Andersen *Sol. St. Commun.* **13**, 113 (1973).
- [13] Linear Methods in band theory: O. K. Andersen *Phys. Rev. B* **12**, 3060 (1975).
- [14] Magnetic ground state properties of transition metals: O.K. Andersen, J. Madsen, U.K. Poulsen, O. Jepsen, and J. Kollar *Physica* **86-88B**, 249 (1977).
- [15] The Occurrence of Singularities in the Elastic Fretluency Distribution of a Crystal: Léon van Hove *Phys. Rev.* **89**, 1189 (1953).
- [16] The positive electron: Carl D. Anderson *Phys. Rev.* **43**, 491 (1933).
- [17] The theory of complex spectra: J.C. Slater *Phys. Rev.* **34**, 1293 (1929).
- [18] Cohesion in Monovalent Metals: J.C. Slater *Phys. Rev.* **35**, 509 (1930).

- [19] Näherungsmethode zur Lösung des quantenmechanischen Mehrkörperproblems: V. Fock *Zeitschr. Phys.* **61**, 126 (1930).
- [20] "Selfconsistent field" mit Austausch für Natrium: V. Fock *Zeitschr. Phys.* **62**, 795 (1930).
- [21] The Wave Mechanics of an Atom with a Non-Coulomb Central Field. Part I-Theory and Methods: D.R. Hartree *Proc. Cam. Phil. Soc.* **24**, 89 (1928).
- [22] The Wave Mechanics of an Atom with a Non-Coulomb Central Field. Part II-Some Results and Discussion: D.R. Hartree *Proc. Cam. Phil. Soc.* **24**, 111 (1928).
- [23] Self interaction correction to density-functional approximations for many-electron systems: J.P. Perdew and A. Zunger *Phys. Rev. B* **23**, 5048 (1981).
- [24] Correlated Orbitals for the ground state of the hydrogen molecule: W. Kolos and C.C. Roothaan *Rev. Mod. Phys.* **32**, 205 (1960).
- [25] *Electronic Structure of Matter - Wave functions and Density Functionals* in Nobel Lectures, Chemistry, 1996-2000 : World Scientific, Singapore W. Kohn (2003).
- [26] Inhomogeneous electron gas: Pierre Hohenberg and Walter Kohn *Phys. Rev.* **136**, B864 (1964).
- [27] Self-consistent equations including exchange and correlation effects: Walter Kohn and Lu J. Sham *Phys. Rev.* **140**, A1133 (1965).
- [28] The density functional formalism, its applications and prospects: Robert O. Jones and Olle Gunnarsson *Rev. Mod. Phys.* **61**, 689 (1989).
- [29] A Quantum Chemical View of Density Functional Theory: Evert Jan Baerends and Oleg V. Gritsenko *J. Phys. Chem. A* **101**, 5383 (1997).
- [30] Basic density functional Theory: U. von Barth *Physica Scripta* **109**, 9 (2004).
- [31] Prescription for the design and selection of density functional approximations: More constraint satisfaction with fewer fits: J.P. Perdew, A. Ruzsinszky, J. Tao, V.N. Staroverov, G.E. Scuseria, and G.I. Csonka *J. Chem. Phys.* **123**, 62201 (2005).
- [32] Insights into Current Limitations of Density Functional Theory: Aron J. Cohen, Paula Mori-Sánchez, and Weitao Yang *Science* **321**, 792 (2008).
- [33] *Electronic Structure Methods: Augmented Waves, Pseudopotentials and the Projector augmented wave method* in Handbook for Materials Modeling : Springer Peter E. Blöchl, Clemens J. Först, and Johannes Kästner (2005).
- [34] Projector augmented wave method: Ab-initio molecular dynamics with full wave functions: P. E. Blöchl, C. J. Först, and J. Schimpl *Bull. Mater. Sci.* **26**, 33 (2003).
- [35] Quantum Theory of Many-Particle Systems. I. Physical Interpretations by Means of Density Matrices, Natural Spin-Orbitals, and Convergence Problems in the Method of Configurational Interaction: P.-O. Löwdin *Phys. Rev.* **97**, 1474 (1955).
- [36] Structure of Fermion Density Matrices: A.J. Coleman *Rev. Mod. Phys.* **35**, 668 (1963).
- [37] Electron correlation in semiconductors and insulators: Band gaps and quasiparticle energies: Mark S. Hybertsen and Steven G. Louie *Phys. Rev. B* **34**, 5390 (1986).
- [38] Why semilocal functionals work: Accuracy of the on-top pair density and importance of system averaging: Kieron Burke, John P. Perdew, and Matthias Ernzerhof *J. Chem. Phys.* **109**, 3760 (1998).

-
- [39] Comparison Shopping for a Gradient-Corrected Density Functional: John P. Perdew and Kieron Burke *Int. J. Quant. Chem.* **57**, 309 (1996).
- [40] Universal variational functionals of electron densities, first order density matrixes and natural spin-orbitals and solution of the v-representability problem: M. Levy *Proc. Nat'l Acad. Sci. USA* **76**, 6062 (1979).
- [41] Density functionals for Coulomb systems: E.H. Lieb *Int. J. Quant. Chem.* **24**, 243 (1983).
- [42] Jacob's ladder of density functional approximations for the exchange-correlation energy: John P. Perdew and Karla Schmidt *AIP Conf. Proc.* **577**, 1 (2001).
- [43] Analysis of the Electronic Exchange in Atoms: I. Lindgren and K. Schwarz *Phys. Rev. A* **5**, 542 (1972).
- [44] Ground state of the electron gas by a stochastic method: D.M. Ceperley and B.J. Alder *Phys. Rev. Lett.* **45**, 566 (1980).
- [45] Correlation Energy of an Electron Gas with a Slowly Varying High Density: Sh.-K. Ma and K.A. Brueckner *Phys. Rev.* **165**, 18 (1968).
- [46] A local exchange-correlation potential for the spin polarized case. I: U. von Barth and L. Hedin *J. Phys. C: Solid State Phys.* **5**, 1629 (1972).
- [47] Exchange and correlation in atoms, molecules, and solids by the spin-density-functional formalism: Olle Gunnarsson and Bengt I. Lundquist *Phys. Rev. B* **13**, 4274 (1976).
- [48] Accurate Density Functional for the Energy: Real-Space Cutoff of the Gradient Expansion for the Exchange Hole: John P. Perdew *Phys. Rev. Lett* **55**, 1665 (1985).
- [49] Beyond the local-density approximation in calculations of ground-state electronic properties: D.C. Langreth and M.J. Mehl *Phys. Rev. B* **28**, 1809 (1983).
- [50] Density-functional exchange energy with correct asymptotic behavior: A. D. Becke *Phys. Rev. A* **38**, 3098 (1988).
- [51] Generalized Gradient Approximation made simple: John P. Perdew, Kieron Burke, and Matthias Ernzerhof *Phys. Rev. Lett* **77**, 3865 (1996).
- [52] Determining and Extending the Domain of Exchange and Correlation Functionals: E.I. Proynov, E. Ruiz, A. Vela, and D. R. Salahub *Int. J. Quant. Chem.* **56**, S29, 61 (1995).
- [53] A novel form for the exchange-correlation energy functional: T. Van Voorhis and G.E. Scuseria *J. Chem. Phys.* **109**, 400 (1998).
- [54] A new inhomogeneity parameter in density-functional theory: Axel D. Becke *J. Chem. Phys.* **109**, 2092 (1998).
- [55] Climbing the Density Functional Ladder: Nonempirical Meta-Å Generalized Gradient Approximation Designed for Molecules and Solids: Jianmin Tao, John P. Perdew, Viktor N. Staroverov, and Gustavo E. Scuseria *Phys. Rev. Lett* **91**, 146401 (2003).
- [56] A New Mixing of Hartree-Fock and Local Density-Functional Theories: Axel D. Becke *J. Chem. Phys.* **98**, 1372 (1993).
- [57] Density Functional Thermochemistry. III. The Role of Exact Exchange: Axel D. Becke *J. Chem. Phys* **98**, 5648 (1993).
- [58] The surface energy of a bounded electron gas: J. Harris and R.O. Jones *J. Phys. F: Met. Phys.* **4**, 1170 (1974).

- [59] The exchange-correlation energy of a metallic surface: David C. Langreth and John P. Perdew *Sol. St. Commun.* **17**, 1425 (1975).
- [60] Rationale for mixing exact exchange with density functional approximations: John P. Perdew, Matthias Ernzerhof, and Kieron Burke *J. Chem. Phys.* **105**, 9982 (1996).
- [61] Hybrid functionals based on a screened Coulomb potential: J. Heyd, G.E. Scuseria, and M. Ernzerhof *J. Chem. Phys.* **118**, 8207 (2003).
- [62] Hybrid functionals applied to extended systems: M. Marsman, J. Paier, A. Stroppa, and G. Kresse *J. Phys. Chem.* **20**, 64201 (2008).
- [63] Ab-Initio calculation of vibrational adsorption and circular dichroism spectra using density-functional force fields: P.J. Stephens, F.J. Devlin, C.F. Chabalowski, and M.J. Frisch *J. Phys. Chem* **98**, 11623 (1994).
- [64] Assessment of the Perdew-Ernzerhof Exchange-Correlation Functional: M. Ernzerhof and G.E. Scuseria *J. Chem. Phys.* **110**, 5029 (99).
- [65] Toward reliable density functional methods without adjustable parameters: The PBE0 model: C. Adamo and V. Barone *J. Chem. Phys.* **110**, 6158 (1999).
- [66] Band Theory and Mott Insulators: Hubbard U instead of Stoner I: Vladimir I. Anisimov, Jan Zaanen, and Ole Krogh Andersen *Phys. Rev. B* **44**, 943 (1991).
- [67] Density-functional theory and strong interactions: Orbital ordering in Mott-Hubbard insulators: A. I. Liechtenstein, V. I. Anisimov, and J. Zaanen *Phys. Rev. B* **52**, 5467 (1995).
- [68] Exact Exchange for Correlated Electrons: Pavel Novak, Jan Kunes, Laurent Chaput, and Warren E. Pickett *Phys. Stat. Sol. B* **243**, 563 (2006).
- [69] Hybrid Exchange-Correlation Energy Functionals for Strongly Correlated Electrons: Applications to Transition-metal Monoxides: Fabien Tran, Peter Blaha, Karlheinz Schwarz, and Pavel Novák *Phys. Rev. B* **74**, 155108 (2006).
- [70] Van der Waals Density Functional for General Geometries: M. Dion, H. Rydberg, E. Schröder, D. C. Langreth, and B. I. Lundqvist *Phys. Rev. Lett* **92**, 246401 (2004).
- [71] Van der Waals density functional: Self-consistent potential and the nature of the van der Waals bond: T. Thonhauser, Valentino R. Cooper, Shen Li, Aaron Puzder, P. Hyldgaard, and D.C. Langreth *Phys. Rev. B* **76**, 125112 (2007).
- [72] Higher-accuracy van der Waals density functional: Kyuho Lee, Éamonn D. Murray, Lingzhu Kong, Bengt I. Lundqvist, and David C. Langreth *Phys. Rev. B* **82**, 81101 (2010).
- [73] Gaussian-1 theory: A general procedure for prediction of molecular energies: John A. Pople, Martin Head-Gordon, Douglas J. Fox, Krishnan Raghavachari, and Larry A. Curtiss *J. Chem. Phys.* **90**, 5622 (1989).
- [74] Gaussian-1 theory of molecular energies for second-row compounds: Larry A. Curtiss, Christopher Jones, Gary W. Trucks, Krishnan Raghavachari, and John A. Pople *J. Chem. Phys.* **93**, 2537 (1990).
- [75] Assessment of Gaussian-2 and density functional theories for the computation of enthalpies of formation: Larry A. Curtiss, Krishnan Raghavachari, Paul C. Redfern, and John A. Pople *J. Chem. Phys.* **106**, 1063 (1997).
- [76] Assessment of Gaussian-2 and density functional theories for the computation of ionization potentials and electron affinities: Larry A. Curtiss, Paul C. Redfern, Krishnan Raghavachari, and John A. Pople *J. Chem. Phys.* **109**, 42 (1998).

-
- [77] Density-functional thermochemistry. I. The effect of the exchange-only gradient correction: A. D. Becke *J. Chem. Phys.* **96**, 2155 (1992).
- [78] Density-functional thermochemistry. II. The effect of the Perdew-Wang generalized-gradient correlation correction: A. D. Becke *J. Chem. Phys.* **97**, 9173 (1992).
- [79] Density-functional thermochemistry. IV. A new dynamical correlation functional and implications for exact-exchange mixing: Axel D. Becke *J. Chem. Phys.* **104**, 1040 (1996).
- [80] Density-functional thermochemistry. V. Systematic optimization of exchange-correlation functionals: Axel D. Becke *J. Chem. Phys.* **107**, 8554 (1997).
- [81] The perdew-burke-ernzerhof exchange-correlation functional applied to the G2-1 test set using a plane-wave basis set: J. Paier, R. Hirschl, M. Marsman, and G. Kresse *J. Chem. Phys.* **122**, 234102 (2005).
- [82] Screened hybrid density functionals applied to solids: J. Paier, M. Marsman, K. Hummer, G. Kresse, I.C. Gerber, and J.G. Ángyán *J. Chem. Phys.* **124**, 154709 (2006).
- [83] Erratum: "Screened hybrid density functionals applied to solids" [*J. Chem. Phys.* **124**, 154709 (2006)]: J. Paier, M. Marsman, K. Hummer, G. Kresse, I. C. Gerber, and J. G. Ángyán *J. Chem. Phys.* **125**, 249901 (2006).
- [84] Projector Augmented-Wave Method: Peter E. Blöchl *Phys. Rev. B* **50**, 17953 (1994).
- [85] Wave Functions in a Periodic Potential: J.C. Slater *Phys. Rev.* **51**, 846 (1937).
- [86] On the calculation of the energy of a Bloch wave in a metal: J. Korryng *Physica* **13**, 392 (1947).
- [87] Solution of the Schrödinger Equation in Periodic Lattices with an Application to Metallic Lithium: W. Kohn and N. Rostocker *Phys. Rev.* **94**, 1111 (1954).
- [88] Linearized augmented plane-wave method for the electronic band structure of thin films: H. Krakauer, M. Posternak, and A. J. Freeman *Phys. Rev. B* **19**, 1706 (1979).
- [89] Planewaves, pseudopotentials and the LAPW method David J. Singh Kluwer (1994).
- [90] Simple formula for the atomic forces in the augmented-plane-wave method: J.M. Soler and A.R. Williams *Phys. Rev. B* **40**, 1560 (1989).
- [91] Ground-state properties of lanthanum: Treatment of extended-core states: David Singh *Phys. Rev. B* **43**, 6388 (1991).
- [92] An alternative way of linearizing the augmented plane-wave method: E. Sjöstedt, L. Nordström, and D. J. Singh *Solid State Commun.* **114**, 15 (2000).
- [93] Efficient linearization of the augmented plane-wave method: Georg K. H. Madsen, Peter Blaha, Karlheinz Schwarz, Elisabeth Sjöstedt, and Lars Nordstroem *Phys. Rev. B* **64**, 195134 (2001).
- [94] The LMTO method: muffin-tin orbitals and electronic structure Hans L. Skriver Springer (1984).
- [95] Explicit, First-principles Tight-Binding Theory: Ole K. Andersen and Ove Jepsen *Phys. Rev. Lett* **53**, 2571 (1984).
- [96] Third-generation muffin-tin orbitals: O. K. Andersen, T. Saha-Dasgupta, and S. Ezhof *Bull. Mater. Sci.* **26**, 19 (2003).

- [97] The LDA+DMFT Approach to Materials with Strong Electronic Correlations: Karsten Held, Igor A. Nekrasov, Georg Keller, Volker Eyert, Nils Blümer, Andrew K. McMahan, Richard T. Scalettar, Thomas Pruschke, Vladimir I. Anisimov, and Dieter Vollhardt *NIC Series (John von Neumann Institute for Computing)* **10**, 175 (2002).
- [98] A New Method for Calculating Wave Functions in Crystals: C. Herring *Phys. Rev.* **57**, 1169 (1940).
- [99] New Method for Calculating Wave Functions in Crystals and Molecules: J.C. Phillips and L. Kleinman *Phys. Rev.* **116**, 287 (1959).
- [100] Approximate formulation of the orthogonalized plane-wave method: E. Antoncik *J. Phys. Chem. Solids* **10**, 314 (1959).
- [101] Norm-Conserving Pseudopotentials: D. R. Hamann, M. Schlüter, and C. Chiang *Phys. Rev. Lett* **43**, 1494 (1979).
- [102] First-principles nonlocal-pseudopotential approach in the density-functional formalism: Development and application to atoms: Alex Zunger and Marvin L. Cohen *Phys. Rev. B* **18**, 5449 (1978).
- [103] Non-singular atomic pseudopotentials for solid state applications: G.P. Kerker *J. Phys. C: Solid State Phys.* **13**, L189 (1980).
- [104] Pseudopotentials that work: From H to Pu: Giovanni B. Bachelet, Don R. Hamann, and Michael Schlüter *Phys. Rev. B* **26**, 4199 (1982).
- [105] Efficient pseudopotentials for plane-wave calculations: N. Troullier and J.L. Martins *Phys. Rev. B* **43**, 1993 (1991).
- [106] Optimized and transferable nonlocal separable ab initio pseudopotentials: J.S. Lin, A. Qteish, M.C. Payne, and V. Heine *Phys. Rev. B* **47**, 4174 (1993).
- [107] Ab initio pseudopotentials for electronic structure calculations of poly-atomic systems using density-functional theory: M. Fuchs and M. Scheffler *Comp. Phys. Comm.* **119**, 67 (1998).
- [108] Efficient Form for Model Pseudopotentials: Leonard Kleinman and D. M. Bylander *Phys. Rev. Lett* **48**, 1425 (1982).
- [109] Generalized separable potentials for electronic-structure calculations: Peter E. Blöchl *Phys. Rev. B* **41**, 5414 (1990).
- [110] Soft self-consistent pseudopotentials in a generalized eigenvalue formalism: D. Vanderbilt *Phys. Rev. B* **41**, 7892 (1990).
- [111] Nonlinear ionic pseudopotentials in spin-density-functional calculations: S. G. Louie, S. Froyen, and M. L. Cohen *Phys. Rev. B* **26**, 1738 (1982).
- [112] Analysis of separable potentials: Xavier Gonze, Roland Stumpf, and Matthias Scheffler *Phys. Rev. B* **44**, 8503 (1991).
- [113] First-principles calculations of hyperfine parameters: C.G. Van de Walle and P.E. Blöchl *Phys. Rev. B* **47**, 4244 (1993).
- [114] Unified Approach for Molecular Dynamics and Density-Functional Theory: Roberto Car and Michele Parrinello *Phys. Rev. Lett* **55**, 2471 (1985).
- [115] A unified formulation of the constant temperature molecular dynamics methods: S. Nose *J. Chem. Phys.* **81**, 511 (1984).

-
- [116] Canonical dynamics: Equilibrium phase space distributions: William G. Hoover *Phys. Rev. A* **31**, 1695 (1985).
- [117] Adiabaticity in First-Principles Molecular Dynamics: Peter E. Blöchl and Michele Parrinello *Phys. Rev. B* **45**, 9413 (1992).
- [118] Second-Generation Wave-Function Thermostat for Ab-Initio Molecular Dynamics: Peter E. Blöchl *Phys. Rev. B* **65**, 104303 (2002).
- [119] From ultrasoft pseudopotentials to the projector augmented-wave method: Georg Kresse and D. Joubert *Phys. Rev. B* **59**, 1758 (1999).
- [120] Orthogonal polynomial projectors for the projector augmented wave method of electronic structure calculations: N. A. W. Holzwarth, G. E. Matthews, A. R. Tackett, and R. B. Dunning *Phys. Rev. B* **57**, 11827 (1998).
- [121] A Projector Augmented Wave (PAW) code for electronic structure calculations, Part I: atom-paw for generating atom-centered functions: N.A.W. Holzwarth, A.R. Tackett, and G.E. Matthews *Comp. Phys. Comm.* **135**, 329 (2001).
- [122] A Projector Augmented Wave (PAW) code for electronic structure calculations, Part II: pwpaw for periodic solids in a plane wave basis: A.R. Tackett, N.A.W. Holzwarth, and G.E. Matthews *Comp. Phys. Comm.* **135**, 348 (2001).
- [123] ABINIT: First-principles approach to material and nanosystem properties: X. Gonze, B. Amadon, P. M. Anglade, J. M. Beuken, F. Bottin, P. Boulanger, F. Bruneval, D. Caliste, R. Caracas, M. Cote, T. Deutsch, L. Genovese, Ph. Ghosez, M. Giantomassi, S. Goedecker, D. R. Hamann, P. Hermet, F. Jollet, G. Jomard, S. Leroux, M. Mancini, S. Mazevet, M. J. T. Oliveira, G. Onida, Y. Pouillon, T. Rangel, G. M. Rignanese, D. Sangalli, R. Shaltaf, M. Torrent, M. J. Verstraete, G. Zerah, and J. W. Zwanziger *Computer Physics Communications* **180**(12), 2582–2615 (2009).
- [124] Implementation of the projector augmented-wave method in the ABINIT code: Application to the study of iron under pressure: Marc Torrent, Francois Jollet, Francois Bottin, Gilles Zerah, and Xavier Gonze *Comp. Mat. Sci.* **42**, 337 (2008).
- [125] NWChem: New Functionality: J. Bylaska, Michel Dupuis, So Hirata, Lisa Pollack, Dayle M. Smith, Tjerk P. Straatsma, and Edoardo Aprà *Lecture Notes in Computer Science* **2660**, 168 (2003).
- [126] NWChem: A comprehensive and scalable open-source solution for large scale molecular simulations: M. Valiev, E. J. Bylaska, N. Govind, K. Kowalski, T. P. Straatsma and H. J. J. Van Dam, D. Wang, J. Nieplocha, E. Apra, T. L. Windus, and W. A. de Jong *Computer Physics Communications* **181**, 1477–1489 (2010).
- [127] Die Projector Augmented Wave-Methode: Ein schnelles Allelektronenverfahren für die ab-initio-Molekulardynamik Winfried Kromen PhD thesis RWTH Aachen (2001).
- [128] QUANTUM ESPRESSO: a modular and open-source software project for quantum simulations of materials: Paolo Giannozzi, Stefano Baroni, Nicola Bonini, Matteo Calandra, Roberto Car, Carlo Cavazzoni, Davide Ceresoli, Guido L Chiarotti, Matteo Cococcioni, Ismaila Dabo, Andrea Dal Corso, Stefano Fabris Stefano de Gironcoli and, Guido Fratesi, Ralph Gebauer, Uwe Gerstmann, Anton Kokalj Christos Gougousis5, Michele Lazzeri, Layla Martin-Samos, Nicola Marzari, Francesco Mauri, Riccardo Mazzarello, Stefano Paolini, Alfredo Pasquarello, Lorenzo Paulatto, Carlo Sbraccia, Sandro Scandolo, Gabriele Sclauszero, Ari P Seitsonen, Alexander Smogunov, Paolo Umari, and Renata M Wentzcovitch *J. Phys.: Condens. Matter* **21**, 395502 (2009).

- [129] Real-space grid implementation of the projector augmented wave method: J. J. Mortensen, L. B. Hansen, and K. W. Jacobsen *Phys. Rev. B* **71**, 35109 (2005).
- [130] Electronic structure packages: Two implementations of the projector augmented wave (PAW) formalism: Marc Torrent, N.A.W. Holzwarth, Francois Jollet, David Harris, Nicholas Lepley, and Xiao Xu *Comp. Phys. Comm.* **181**, 1862 (2010).
- [131] Electrostatic decoupling of periodic images of plane wave expanded densities and derived atomic point charges: P.E. Blöchl *J. Chem. Phys.* **103**, 7422 (1995).
- [132] A Combined Car-Parrinello QM/MM Implementation for ab Initio Molecular Dynamics Simulations of Extended Systems: Application to Transition Metal Catalysis: T.K. Woo, P.M. Margl, P.E. Blöchl, and T. Ziegler *J. Phys. Chem. B* **101**, 7877 (1997).
- [133] Implementation of the Projector Augmented-Wave LDA+U Method: Application to the Electronic Structure of NiO: O. Bengone, M. Alouani, P. Blöchl, and J. Hugel *Phys. Rev. B* **62**, 16392 (2000).
- [134] Electric-Field Gradient Calculations using the Projector Augmented Wave Method: H.M. Petrilli, P.E. Blöchl, P. Blaha, and K. Schwarz *Phys. Rev. B* **57**, 14690 (1998).
- [135] All-electron magnetic response with pseudopotentials: NMR chemical shifts: Chris J. Pickard and Francesco Mauri *Phys. Rev. B* **63**, 245101 (2001).
- [136] Ab initio theory of nmr chemical shifts in solids and liquids: F. Mauri, B.G. Pfommer, and S.G. Louie *Phys. Rev. Lett.*, 5300 (1996).
- [137] Zur Quantentheorie der Molekeln: M. Born and R. Oppenheimer *Ann. Phys.* **84**, 457 (1927).
- [138] Dynamical Theory of Crystal Lattices M. Born and K. Huang Oxford University Press, Oxford (1954).
- [139] Applying direct molecular dynamics to non-adiabatic systems: G.A. Worth and M.A. Robb *Adv. Chem. Phys.* **124**, 355 (2002).
- [140] Störungsreihen für die nichtadiabatische Kopplung mit durchschneidenden Potentialflächen F. Dufey PhD thesis Technische Universität München (2002).
- [141] The Landau-Zener Formula: C. Wittig *J. Phys. Chem.* **109**, 8428 (2005).
- [142] Non-adiabatic Crossing of Energy Levels: C. Zener *Proc. Roy. Soc. A* **137**, 696 (1932).
- [143] Early perspectives on geometric phase: M.S. Child *Adv. Chem. Phys.* **124**, 1 (2002).
- [144] Quantal phase factors accompanying adiabatic changes: M.V. Berry *Proc. Roy. Soc. A* **392**, 45 (1984).
- [145] Chemical Reaction dynamics beyond the Born-Oppenheimer approximation: L. Butler *Annu. Rev. Phys. Chem.* **49**, 124 (1998).
- [146] The role of degenerate states in chemistry M. Baer and G.D. Billing, editors volume 124 of *Adv. Chem. Phys.* John Wiley and Sons (2002).
- [147] Modern Quantum Chemistry: Introduction to Advanced Electronic Structure Theory A. Szabo and N.S. Ostlund.
- [148] Quantum Mechanics A. Messiah Dover (2000).
- [149] Taschenbuch der Mathematik I.N. Bronstein and K.A. Semendjajew BSB B.G. eubner Verlagsgesellschaft, Leipzig (1983).

- [150] Über das Verhalten von Eigenwerten bei adiabatischen Prozessen: J. v. Neumann and E.P. Wigner *Phys. Z* **30**, 467 (1929).
- [151] Diabolical conical intersections: D.R. Yarkony *Rev. Mod. Phys.* **68**, 985 (1996).

Index

- adiabatic approximation, 162
- adiabatic connection, 135
- anti-bonding state, 16
- antisymmetric tensor, 95
- APW, 141
- ASA, 142
- atomic spheres approximation, 142
- augmented plane wave method, 141
- augmented-wave method, 141
- avoided crossing, 163
- band structure, 58
- Berry phase, 166
- Bloch theorem, 58
- block diagonal, 29
- Bohr magneton, 92
- bonding state, 16
- Born-Huang expansion, 158
- Born-Oppenheimer Approximation, 161
- Born-Oppenheimer approximation, 157
- Born-Oppenheimer surfaces, 158
- Born-Oppenheimer surface, 161
- Born-Oppenheimer wave functions, 158
- Born-Oppenheimer wave functions, 157
- Boson, 98
- Brillouin zone, 69
- canonical band theory, 82
- Car-Parrinello method, 146
- characteristic polynomial, 14
- charge transferability, 145
- COHP, 57
- commutating operations, 48
- complete neglect of overlap, 13
- conical intersection, 193
- COOP, 57
- core repulsion, 77
- correlation energy, 125
- Crystal Orbital Hamilton Population, 57
- Crystal Orbital Overlap Population, 57
- density
 - conditional, 121
 - two-particle, 120
- density of states
 - total, 57
- density functional theory, 11
- density matrix
 - one-particle, 120
- Density of States, 22
- density of states
 - projected, 57
- Density of states
 - per volume, 60
- derivative coupling, 159
- dimensional bottle-neck, 87
- Dirac equation, 92
- Dirac equation, 174
- dispersion relation
 - linear chain, 21
- double bond, 44
- eigenvectors, 12
- electron affinity, 78
- electronegativity, 79
- electrophile, 19
- energy transferability, 145
- ethene, 44
- exchange and correlation energy, 125
- exchange and correlation
 - potential energy, 122
- exchange energy, 110, 125
- exponential wall, 119
- extended zone scheme, 68
- Fermi-level, 18
- Fermion, 98
- ferromagnetism, 111
- Fock Operator, 114
- free electron gas, 55
- fully antisymmetric tensor, 95
- functional, 123
- generalized gradient approximation, 133
- GGA, 133
- Hartree method, 103
- Hartree Energy, 110
- Hartree energy, 109, 122
- Hartree-Fock method, 103
- Hartree-Fock equations, 112

- hole function, 122
- HOMO, 19
- hopping matrix element, 12
- Hund's rule, 111
- hybrid functional, 134
- ionization potential, 78
- Jacob's ladder, 130
- jellium model, 55
- kinetic energy functional, 124
- KKR method, 141
- Kohn-Sham energy, 126
- Kohn-Sham orbitals, 124
- LAPACK, 12
- Laplace-Runge-Lenz vector, 75
- lattice constant, 63
- lattice vector
 - general, 63
 - primitive, 63
 - reciprocal, 63
- LDA, 132
- Levi-Civita symbol, 95
- linear augmented-wave method, 142
- linear muffin-tin-orbital method, 142
- LMTO, 142
- local density approximation, 132
- local operator, 113
- local potential, 113
- local spin density approximation, 132
- LSD, 132
- LUMO, 19
- magnetic anisotropy, 86
- meta GGA, 134
- methane, 48
- molecular dynamics, 162
- muffin-tin potential, 141
- natural orbital, 121
- node plane, 16
- non-crossing rule, 193
- non-local potential, 113
- nucleophile, 19
- number of states, 58
- occupation, 121
- one-particle operator, 104
- one-particle wave function, 99
- oxidation state, 80
- Pauli equation, 92, 174
- Pauli matrix, 90
- Pauli principle, 86
- periodic, 63
- periodic boundary condition, 20
- periodic zone scheme, 68
- permutation operator, 98
- phase
 - geometrical, 166
- positions
 - relative, 63
- positron, 92
- projector augmented-wave method, 141
- projector augmented-wave method, 146
- pseudopotential, 140, 143
- quantum numbers, 32, 98
- Rabi frequency, 165
- radical, 19
- rank, 95
- Reciprocal lattice vectors, 64
- reduced zone scheme, 68
- self interaction, 110
- self-interaction energy, 110
- semi-local form, 144
- separable form, 145
- Slater determinant, 101
- Slater-Koster tables, 39
- spin-orbitals, 89
- spinor, 89
- standard model, 85
- star, 39
- stray fields, 87
- symmetry, 29, 30, 96
- tensor
 - fully antisymmetric, 95
- three-center bond, 44
- tight-binding method, 39
- tight-binding model, 36
- time-inversion symmetry, 174
 - for spinors, 176
- transformation operator, 29, 96
- triple bond, 44
- two-particle operator, 104
- unit cell
 - primitive, 63
- unscreening, 144
- Wigner Seitz cell, 69
- Wirtinger derivatives, 112
- Wolfsberg-Helmholtz formula, 13